Towards an Economical Ionic Liquid Based Biorefinery

A thesis submitted for the degree of

Doctor of Philosophy

by

Florence Joséfine Virginia Gschwend

Supervised by Dr Jason P. Hallett, Prof. Paul S. Fennell and Dr Anthe George

Imperial College London

Department of Chemical Engineering

Grantham Institute for Climate Change

Climate-KIC

Declaration of Originality

The entirety of the work described in this thesis was carried out at Imperial College London between October 2013 and May 2017. Unless otherwise stated the work is my own and has not been submitted previously for a degree at this or another university.

Copyright

The copyright of this thesis rests with the author and is made available under a Creative Commons Attribution Non-Commercial No Derivatives licence. Researchers are free to copy, distribute or transmit the thesis on the condition that they attribute it, that they do not use it for commercial purposes and that they do not alter, transform or build upon it. For any reuse or redistribution, researchers must make clear to others the licence terms of this work.

Publications and Awards

The pretreatment method used for the majority of experiments in this thesis has been published as a video in a peer-reviewed journal. Some of the results presented in this thesis have resulted in a patent or been published in the peer-reviewed literature. Furthermore the technology is currently being scaled-up and commercialised and has won several awards.

F. J. V. Gschwend, A. Brandt, C. L. Chambon, W.-C. Tu, L. Weigand and J. P. Hallett, *J. Vis. Exp.*, 2016.

A. Brandt, F. Gschwend, P. Fennell, T. Lammens, B. Tan, J. Weale and J. Hallett, *Green Chem.*, 2017.

A. Brandt, F. Gschwend, P. Fennell, J. Hallett, G. Kelsall, Deconstruction of biomass and extraction of copper in various ionic liquids; GB1520453.0, filed on 20.11.2015

Royal Society Translation Award, April 2017

Althea Imperial Prize, Runner-up, May 2016

Abstract

Lignocellulosic biomass has the potential to be used as feedstock for the sustainable and carbon-neutral production of fuels, materials and chemicals. For the realisation of this potential, cost-effective fractionation of the biomass in different product streams is necessary.

The work presented in this thesis focuses on the use of protic ionic liquids for the fractionation of various types of lignocellulosic biomass with the aim of achieving process improvements leading to a potential cost reduction at industrial scale. Firstly, the use of triethylammonium hydrogensulfate as a lower-cost alternative to more commonly used aprotic ionic liquids for the fractionation of the grass *Miscanthus x giganteus* has been shown. A cellulose enriched pulp giving high enzymatic saccharification yields was recovered after pretreatment under mild conditions. Subsequent process intensification showed that high saccharification yields can be obtained after as little as 15 min of pretreatment time.

Secondly, the more easily grown yet more recalcitrant softwood pine was used as a feedstock. *N,N*-dimethylbutylammonium hydrogensulfate was found to be effective at producing a highly digestible cellulose pulp. Thirdly, waste wood from construction and demolition as well as pre-consumer construction wood containing various heavy metals (as preservatives and contaminants) were successfully fractionated. The biocide copper was quantitatively extracted from copper azole treated wood, allowing for the production of bioethanol via fermentation. The copper was shown to be recoverable via electrodeposition. The use of contaminated waste wood as a feedstock for the production of materials, fuels and chemicals not only eliminates an unresolved waste management problem but also increases the economic viability of the bioeconomy. The ionic liquid was shown to be recyclable at least six times without losing performance. Alongside the pulp, the obtained lignin was analysed using ^{31}P and 2D HSQC NMR, gel permeation chromatography and elemental analysis in order to elucidate the lignin extraction mechanism.

Acknowledgements

I first want to thank Clem, yes, before I thank my supervisors. I've recently seen more and more posts on Facebook and other social media about mental health problems amongst PhD students, typically posted *by* PhD students. As I am writing this, exhausted, yes, but mentally healthy, I think back to those days in the Lab Without Windows, aka the Dungeon, and the countless late nights and weekends in the lab and office, and if there was one single thing that prevented me from going insane, then it was probably Clem, who suffered, listened to horrible Eurovision songs, and laughed, with me. *Then*, I'd like to thank Jason and Paul, for their supervision, general life advice and for waiting for me at the Imperial College Health Centre after I ingested ionic liquid. I'd also like to thank Anthe, who welcomed me to California for two great months and offered her support from afar. I'm also grateful for having been part of the Hallett Research Group, aka the Empire, which became to a large extent my family, and would like to thank its past and current members for having made this PhD experience so much more enjoyable.

Special thanks go to Agi, who spent hours and hours training me and many other PhD students on all her protocols and always offered advice. I'd also like to thank Karen, for carrying out fermentations, and Geoff and Franky, for their advice and help with electrochemistry. Furthermore I'd like to acknowledge all the help I received from various members of staff from Imperial and especially the Department: Patricia and Andrew from the analytical services, Vito who helped with SEM, Yingqi who always managed to get the 600 MHz NMR machine to work by typing the exact same thing I typed already, Pete for measuring ^{31}P NMRs, and the various members of the Hallett and Fennell research groups who helped me out with various pieces of equipment. I'd like to specially mention Louis, Leila and Marius, MRes students I've supervised during my PhD who all were great to work with and have produced data that also went into this thesis. Danke au an mini liebe Eltere wo mi immr hän lo wagse und mi die letschte 5 Joor au us dr Färni unterstützt.

Thanks also to Sophie and Pippa for proofreading my thesis and especially to Pippa for not expecting any conversation in the last few weeks when, in the evenings, I sat at the kitchen table, staring into blank space, trying to pick up an olive for about 3 minutes. Lastly, I'd like to thank Sia, who provided much of the soundtrack to this PhD, with songs such as "Cheap Thrills" (a PhD student is always on a budget), "Unstoppable" (when you're really in desperate need of some sleep, but instead you work and turn into a liability), "Titanium" (when you drop that sample and just shrug), "Angel by the Wings" (when you pick up the spilled sample and start again), and "The Greatest" (when it's Friday 6 pm and you know you'll be working another 5 hours, and the next day, and the day after).

Glossary

[C_2C_1im]	1-ethyl-3-methylimidazolium
[C_4C_1im]	1-butyl-3-methylimidazolium
[ABS]	alkylbenzenesulfonate
[DMBA]	*N,N*-dimethylbutylammonium
[HC_4im]	*N*-butylimidazolium
[HC_1im]	*N*-methylimidazolium
[NTf_2]	*bis*(trifluoromethanesulfonyl)imide
[TEA]	triethylammonium
AFEX	ammonia fibre expansion
AIL	acid insoluble lignin
AIR	acid insoluble residue
APIL	aprotic ionic liquid
ASL	acid soluble lignin
CA	copper azole
CCA	chromatvisoed copper arsenate
COSLIF	cellulose solvent- and organic solvent-based lignocellulose fractionation
CV	cyclic voltammetry
DA	dilute acid
DFRC	derivatisation followed by reductive cleavage
DMSO	dimethylsulfoxide
F	ferulate
G	guaiacyl
GC	glassy carbon
GHG	greenhouse gases
H	*p*-hydroxyphenyl
HMBC	heteronuclear multiple bond coherence
HMF	5-hydroxymethylfurfural
HMQC	heteronuclear multiple quantum coherence
HPLC	high performance liquid chromatography
HSQC	heteronuclear single quantum coherence
ICP-OES	inductively coupled plasma optical emission spectrometry
IL	ionic liquid
IR	infrared spectroscopy
LA	levulinic acid

LCC	lignin-carbohydrate complex
LHW	liquid hot water
M	molar
MESP	minimum ethanol selling price
M_n	number average molecular weight
MS	mass spectrometry
M_w	weight average molecular weight
NMR	nuclear magnetic resonance spectroscopy
NREL	National Renewable Energy Laboratory
ODW	oven-dried weight
*p*CA	*p*-coumarate
PDI	polydispersity index
PIL	protic ionic liquid
ppm	parts per million
S	syringyl
SE	steam explosion
TGA	thermogravimetric analysis
TOCSY	total correlation spectroscopy
TT	tanalised or treated timber
UV	ultraviolet spectroscopy
VP	virgin pine
wt%	weight percent
α	Kamlet-Taft acidity
β	Kamlet-Taft basicity
δ	chemical shift (ppm)
π*	Kamlet-Taft polarizability

Contents

List of Figures

List of Tables

Introduction

At present most of our fuels and chemicals come from fossil feedstocks which need to be extracted, transported and refined into final products. Extraction is becoming more difficult, resulting in environmental destruction, e.g. the conversion of boreal forests to open-pit oil sand mines,[1] and contamination of the surrounding environment and water ways.[2] During transportation of crude oil, spills occur, causing long-term damage to the environment[3] and contaminating soil and water,[4] ultimately resulting in the death of wildlife[5] and causing diseases and health problems to human populations in affected areas.[6] Burning of fossil fuels produces CO_2 which results in a net increase of the CO_2 concentration in the atmosphere, with oil won from tar sands (an increasingly relied on energy source), having an especially high CO_2 footprint.[7] There is little disagreement amongst responsible scientists that this human activity is causing global warming which will potentially displace a large numbers of people affected by sea level rise[8] and an increase in land surface temperature.

Therefore a more sustainable, carbon-neutral alternative is needed. Biomass offers such an alternative, being bio-renewable and potentially carbon-neutral or even carbon-negative.[9,10] To achieve this, technical challenges need to be overcome and value chains critically assessed in order to provide a truly sustainable alternative.

Whilst biodiesel can only be isolated directly from oily plants,[11] bio-ethanol is the prominent biomass derived fuel and can be obtained from any kind of plant.[12] Sucrose or starch derived ethanol is relatively easily produced; however its negative impacts on land usage, such as deforestation, have raised some concern.[13] Lignocellulosic biomass on the other hand is the most abundant plant material on earth[14] with an extensive geographical availability,[15] has higher yields per land area[16] and can be grown at a lower cost with less fertilizer inputs than plants that mainly contain sucrose and starch.[17] The use of lignocellulosic biomass is thus preferential from a socio-economic as well as an environmental point of view.[18] Lignocellulose however is highly recalcitrant towards chemical and biological attack and thus requires a pretreatment step before the cellulose contained in the biomass can be converted into ethanol.[13] There are different chemical and physical pretreatment methods, some of which use ionic liquids (ILs),[19,20] a class of organic salts with melting points below 100°C.[21] Whilst IL based pretreatment is one of the most effective to date,[22,23] its successful commercialisation has been hindered by several factors: the best performing ionic liquids from a deconstruction point of view are made from expensive starting materials,[24] difficult to purify and not very stable under the pretreatment conditions.[25] There is thus a need for a more inexpensive and stable alternative.

Construction wood is typically treated with a metal-containing preservative in order to prolong its lifetime. However, these metals leach out and contaminate the environment long after the use of the

wood if not contained.[26] Furthermore, this type of waste wood cannot be used for combustion, pyrolysis or gasification due to the release of metal containing fly ash[27] and/or gaseous emissions[28,29] and the disposal of treated timber thus still constitutes an unresolved waste management problem. Some ionic liquids have been found to strongly coordinate to metals.[30] Combined with their ability to disrupt biomass, this opens up the possibility to use the pretreatment step with a concomitant extraction. Additionally, while the feedstock costs currently constitute one third of the production costs of cellulosic ethanol,[31] the use of waste wood helps to decrease production costs of lignocellulosic ethanol, thus making it more competitive with traditional bio-ethanol and fossil fuels.

This project aims at overcoming two different environmental challenges: the disposal of treated timber and the enhancement of the sustainability and competitiveness of lignocellulosic ethanol. The use of thermally stable, low-cost ionic liquids will be investigated for pretreatment of a variety of feedstocks and concomitant metal extraction. The ultimate goal is to demonstrate the use of waste wood as an inexpensive feedstock for bio-ethanol production.

Part I of this thesis reviews existing literature around the topics of ionic liquids, biomass and biomass processing and waste wood in order to identify gaps. Part II gives the experimental details for the results discussed in Part III. Part IV summarises the most important conclusions. Raw spectra can be found in the Appendix.

Part I. Background

1. Ionic Liquids

1.1. General

Ionic liquids are defined as organic salts with melting points below 100°C.[32] First generation ILs are typically comprised of chloroaluminate anions (e.g. $[AlCl_4]^-$) and alkyl substituted pyridines or imidazoles.[32] The following generations of ILs however, which are in the focus of this thesis, are often comprised of nitrogen-compound based cations, such as amines,[24] imidazoles[33–35] or pyridines,[36] with a wide range of possible anions, some of which are displayed in Figure I-1. In addition, task specific ionic liquids which are highly functionalised are currently being researched.[37,38] The range of applications of ionic liquids is wide, from the use as solvents and catalysts in organic reactions,[39–41] electrochemistry[42] or the pretreatment of biomass for biofuel production[13,15,34,38] to CO_2 capture[37] and as sensors.[43,44] Their use is mostly justified due to their favourable properties, such as their low vapour pressure[45] and wide liquid range, their recyclability and the possibility to tune their properties to one's needs.[46] Nevertheless, their synthesis and purification is often challenging and expensive, which undermines the frequency of their application on an industrial scale.[47] One prominent successful example for the use of an ionic liquid in an industrial process is BASF's BASIL process which is 80,000 times (!!!) more productive than their conventional process for the production of their alkoxyphenylphosphine.[48] Ionic liquids are also used as the stationary phase in gas chromatography,[49] to break azeotropes, for the isomerisation of 3,4-epoxybut-1-ene to 2,5-dihydrofuran, the dimerization of alkenes and as paint additives.[47]

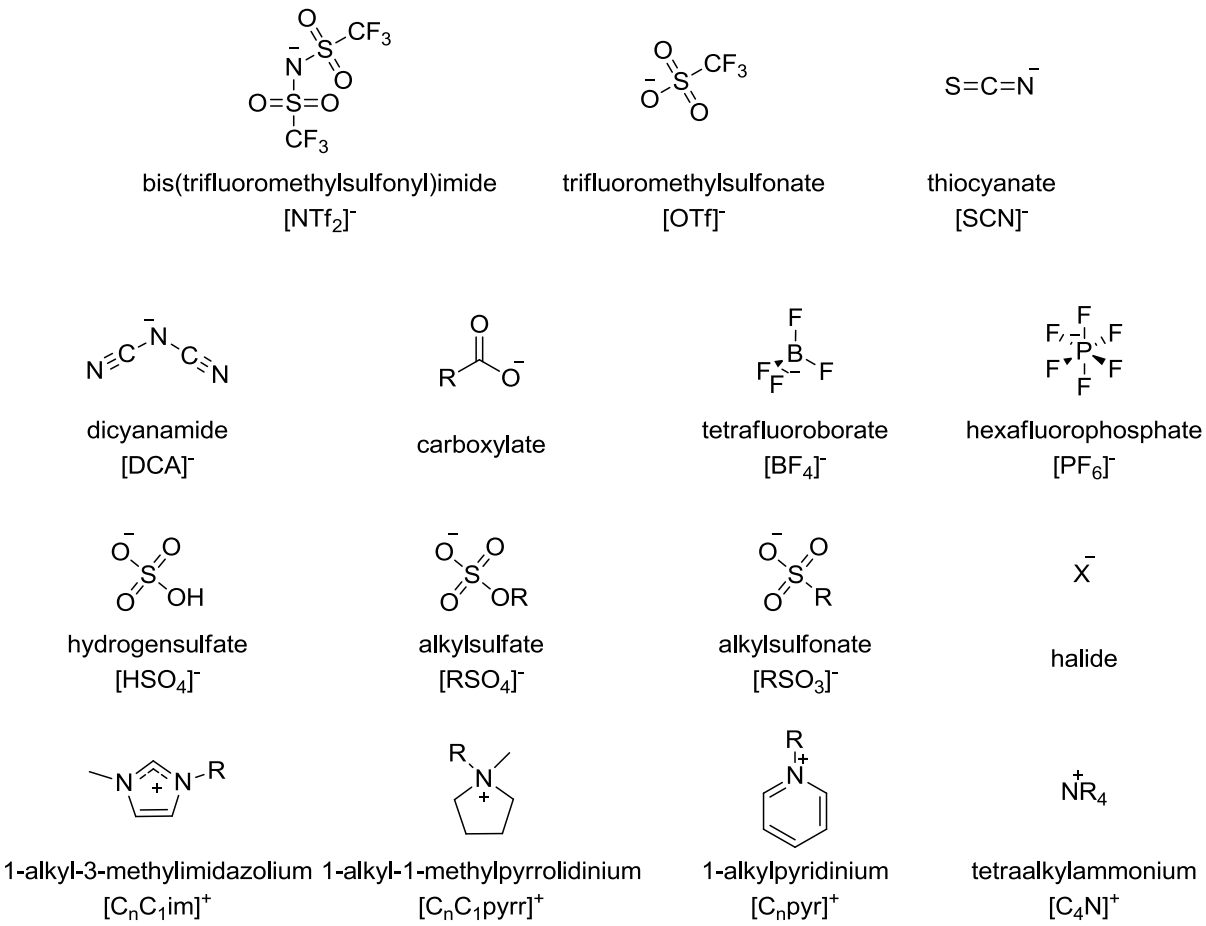

Figure I-1 Common anions and cations of ILs.

1.2. Physicochemical Properties

Ionic liquids have a melting point lower than 100°C, however certain ILs, including a few 1-alkyl-3-methylimidazolium based ones[50] and some with formate anions,[51] are found to melt at temperatures well below 0°C.[32] While for common organic solvents and water the higher end of the liquid range is governed by boiling, most ionic liquids will decompose before reaching their evaporation temperature.[32] Maximum decomposition temperatures of around 500°C have been found, e.g. for 1,2-dimethyl-3-ethylimidazolium hexafluorophosphate.[52] However, both melting and decomposition temperatures are sensitive to impurities.[32] Higher melting points are obtained for ILs with symmetric cations, e.g. $[C_4C_4im]^+$ vs. $[C_4C_1im]$[52] or diethylammonium ([DEA]) vs. methylbutylammonium ([MBA]) and triethylammonium ([TEA]) vs. dimethylethylammonium ([DMEA]).[51]

IL viscosities at room temperature are generally high and range from 10 mPa·s to over 1000 mPa·s.[32] They are influenced by the nature of both cation and anion and the extent of their van der Waals and hydrogen bonding interactions. Viscosities for ILs with a given anion increase with increasing length of alkyl chains or total number of carbons for quaternary ammonium salts[52] as well as 1-alkyl-3-

methylimidazolium ILs.[50] High melting points and viscosities can also be the result of incorporation of certain functional groups[53] and fluorination of the anion has been found to lead to an increase of the viscosity due to increased van der Waals interactions.[54] Branching of alkyl side chains also results in higher viscosities, as a result of less rotational freedom.[52] Similar to melting points, lower viscosities can be obtained by asymmetrical substitution due to less efficient packing of the ions. As a result of high symmetry, [BF_4] and [PF_6] ionic liquids tend to have high viscosities.[50]

Just like melting and decomposition temperatures, IL viscosities are sensitive to impurities but also the presence of water and often a range of values for the same ionic liquid is reported in the literature due to very small differences in one of the parameters during measurement.[32] As little as 1.5-6wt% of chloride present in a non-haloaluminate alkylimidazolium ionic liquid can raise its viscosity by 30-600%.[32] Similarly, the viscosity of [C_4C_1im][BF_4] decreases by 50% upon absorption of 2wt% of water.[32] Also the addition of a co-solvent can lower the viscosity. An exponential decrease in the viscosity of three ILs was observed with the addition of dimethylformamide or 3-picoline as co-solvents.[55] Viscosities of ILs have been found to exhibit an unusually high temperature dependence and viscosities similar to water can be achieved upon heating.[51] Equally, lowering the temperature results in an increase of viscosity, e.g. in the case of [C_4C_1im][PF_6] where lowering the temperature by 5 K from 298 K to 293 K resulted in an increase in viscosity of 27%.[32] As a result of the high viscosity, diffusion in ILs is generally slow, exhibited by small diffusion coefficients.[42,55–57] As opposed to viscosity and phase transition points, the density of ionic liquids has been found to be rather insensitive to impurities and ranges from 0.90 g cm^{-3} for [bis(bis-hexyl-amino)-methylene] dimethylammonium chloride[52] to 2.4 g cm^{-1} for [SMe_3][Al_2Br_7].[32]

The properties of ionic liquids as solvents vary depending on the exact nature and polarity of the ionic liquid. In a general solvent system, the polarity of a solvent is defined as the sum of all its interactions with a solute, such as coulombic, permanent and induced dipole-dipole, hydrogen bonding and electron pair donor and acceptor interactions.[58] In order to quantify these interactions, Kamlet and Taft developed three empirical polarity scales: the hydrogen bond acidity α, the hydrogen bond basicity β and the dipolarity/polarizability π*.[59,60] These are measured by the solvatochromic effect on the wavelengths of absorption of a set of dyes. For ionic liquids, π* values are generally close to 1, independent of the cation or anion.[58] This is similar to e.g. DMSO (1.00), nitrobenzene (1.01) and water (1.09).[61] In comparison, aliphatic hydrocarbons have π* values close to 0.[61] While the anion mainly influences the β value, which ranges from around 0 to 1.61, the cation affects the α value, ranging from 0.2 to 1.2.[58] In comparison, water has an α value of 1.17 and a β of around 0.18 pyridines and amines, often used in IL synthesis, have a β value of 0 and α values between 0.5 and 0.9.[61]

1.2.1. Stability

First generation ionic liquids, based on chloroaluminates, are air and moisture sensitive which imposes the need for handling under an inert atmosphere.[32] The following generations of ionic liquids with anions such as $[NO_2]^-$, $[NO_3]^-$ and $[OAc]^-$ on the other hand show improved stability towards moisture,[62] which allows handling them in an open atmosphere. ILs comprising anions such as $[BF_4]^-$, $[PF_6]^-$ and $[SbF_6]^-$ however still undergo hydrolysis in the presence of water, releasing the highly toxic and corrosive HF and other species.[21,50]

Independent of their stability towards moisture, some ionic liquids have shown very good electrochemical stability.[63] For most electrochemical applications, the potential window is the decisive property, determining the potential range in which a solvent can be used without electrochemical degradation. ILs have gained wide interest in the electrochemical community due to their wide potential windows of up to 6 V with imidazolium based ionic liquids typically having one of around 4 V. The width of the potential window is not only governed by the molecular structure of the electrolyte material but is also strongly affected by the electrode materials used and impurities present in the ionic liquid, including, once again, water.[63]

As mentioned earlier, the upper limit of the liquid range of ILs is typically governed by their decomposition temperature and many ILs have excellent thermal stability, some up to around 500°C.[52] Most commonly, thermal stability of ionic liquids is measured by thermogravimetric analysis.[25,35,64] The experimental set-up used most frequently is a ramping experiment where the temperature is constantly increased and the sample weight percentage recorded as a function of the temperature.[25] The T_{onset}, which is the intersection of the tangent at the steepest point of the thermogravimetric curve with the baseline weight, has been reported for various ionic liquids in the literature.[33] However, T_{onset} depends strongly on the experimental set up, including heating rate and pan material,[25,65,66] and is often considerably higher than the temperature at which the IL is stable over a long time period[67,68] and therefore the temperature where the IL can be used in a process without significant loss. $[C_nC_1im]Cl$ ILs have been found to slowly decompose under isothermal conditions well below the T_{onset} as measured by fast scan TGA experiments.[67] Recently, triarylsulfonium ILs which are stable in air at 300°C for 90 days have been reported.[69]

Although TGA is widely used for the determination of the decomposition temperature of ionic liquids, it suffers from only being able to detect decomposition resulting in weight loss.[63] A different way of determining the long-term stability of imidazolium based ionic liquids is the potentiometric acid-base titration to detect imidazoles, one of the major degradation products of such ionic liquids.[68] It has been shown that $[C_4C_1im]$ and $[C_2C_1im]Cl$ already age at temperatures as low as 140°C while having a

decomposition temperature of around 200°C.[68] Surprisingly it was found that $[C_4C_1im][PF_6]$ degrades twice as much as $[C_4C_1im]Cl$ at 140°C while $[C_4C_1im][BF_4]$ is completely stable at this temperature. However, TGA results imply that $[C_4C_1im][PF_6]$ is more thermally stable than $[C_4C_1im]Cl$.[68] $[C_2C_1im]$ and $[C_4C_1im][EtSO_3]$ only degrade slightly at 200°C and $[C_4C_1im][NTf_2]$ did not show any signs of decomposition even after 10 days at 250°C.[68] Electrospray ionization mass spectrometry (ESI-MS) measurements have shown that the main decomposition pathways are the elimination of the side-chain, transalkylation and retroalkylation, by a nucleophilic attack from the anion.[21,68] As halogen anions are a lot more nucleophilic than complex anions such as $[PF_6]^-$, $[BF_4]^-$ or $[NTf_2]^-$, halogen containing ionic liquids are significantly more prone to degradation.[35,68] Studies with varying alkyl chain lengths only showed a minor dependence with longer alkyl chains decreasing the decomposition temperature slightly.[35,63]

1.3. Protic Ionic Liquids

Recently, less expensive and more easily synthesised protic ILs (PILs) have gained increased attention, especially for biomass applications, such as the dissolution and regeneration of Kraft lignin,[36] pretreatment of cashew apple bagasse,[70] delignification of corn stover[71] and the production of biodiesel from microalgae,[72] but also in electrochemistry.[73] Their synthesis is a one step process where a Brønsted acid, such as carboxylic[70,71] and mineral acids,[24,74] and a Brønsted base, such as alkanolamines,[70] alkylamines,[24,74] imidazoles[75] or morpholine,[76] are mixed together (Figure I-2). An extensive literature review on the properties and applications of PILs can be found elsewhere.[76] By varying the acid to base ratio, the properties of the ionic liquid can be altered and adjusted depending on the application.[75] Unlike aprotic ILs (APILs), some PILs will undergo boiling rather than decomposition upon heating by reversing the proton transfer from the base back to the acid.[51] PILs are in equilibrium with their underlying acid and base, resulting in vapour pressures which will in some cases reach 1 atm, when boiling starts. The boiling point can be predicted by the difference in pK_a values of the acid and base of which the ionic liquid was made, where a larger difference results in a higher boiling point.[21] For example, acetic or formic acid-based PILs tend to lose weight at temperatures exceeding just 25°C.[77] The need to remove a substantial amount of water after PIL synthesis involving aqueous acids sometimes leads to the involuntary formation of non-stoichiometric acid-base mixtures.[77] PILs that do not boil are those with strong proton transfer, which tend to decompose before reaching the boiling point,[51,76] PILs with carboxyl anions, which are susceptible to amide formation,[76] and nitrate anions, which decompose in a very exothermic fashion, i.e. an explosion.[51,76] $[HSO_4]^-$ ILs such as triethylammonium hydrogensulfate ($[TEA][HSO_4]$), 1-methylimidazolium hydrogensulfate ($[HC_1im][HSO_4]$) and trimethylammonium hydrogensulfate are reported to decompose rather than distil and to be thermally stable up to around 260-310°C.[76]

The electrochemical windows of PILs are narrower than those of corresponding APILs, which has been attributed to the availability of the dissociable proton on the cation which is expected to withdraw electrons more readily and reduce the cation at more positive potentials than the aprotic analogue.[78] Yet PILs are promising electrolytes in many applications. The electrochemical window of a PIL is affected by many factors in a complicated way[79] and also depends on the electrode material. The largest electrochemical windows for PILs are typically found with glassy carbon (GC) electrodes.[77,79] For different electrode materials the potential window magnitudes may follow different orders for a given selection of ionic liquids. Diethanolammonium hydrogensulfate, for example, has a wider electrochemical window than diethanolammonium chloride when using a boron-doped diamond electrode, while the order is reversed at a gold or GC electrode.[77] While the conductivity of PILs is generally low due to high viscosity, adding water increases conductivity significantly by reducing the viscosity, but also narrows the potential window.[77]

Arguably the most important advantage that PILs have over APILs is their much lower production cost.[72,80] The cost reduction compared to APILs comes mainly from a much shorter synthesis route requiring fewer synthetic steps; [TEA][HSO_4] requires 7 steps starting from oil, N_2, H_2, S_8 and O_2, vs. 29 steps in the case of [C_2C_1im][OAc].[80] As a result of the exothermic reactions involved in PIL synthesis, energy costs are typically negligible and excess heat can in some cases even be used for other processes.[72] Furthermore no purification step is required.[24] Hallett *et al.* estimated the production cost of [TEA][HSO_4] at \$1.24/kg and [HC_1im][HSO_4] is expected to cost \$2.96/kg.[80] Chiappe *et al*. used the same methodology to estimate the cost of several other PILs and calculated a price of \$1.94/kg and \$1.84/kg for two tetramethylguanidinium based PILs.[72] The cost of a PIL are dominated by the raw material costs[80] and, since mineral acids are generally inexpensive, depend mainly on the cost of the organic base involved.[24] Additionally, PIL have a smaller environmental footprint due to their facile synthesis which uses less organic solvents and results in less waste than APIL synthesis.[80]

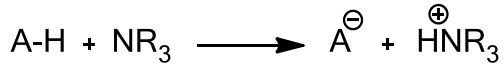

Figure I-2 Acid base reaction yielding a trialkylammonium PIL.

1.4. Toxicity

There has been evidence that certain ILs have greater (eco)toxicity than molecular solvents[81] and there is therefore concern about the environmental benefits of using ILs over traditional solvents. The cytotoxicity of ILs has shown a strong dependency on the nature of the biological system that is tested. A given IL may be found to be benign for a particular type of cells[82] or organisms,[83] but then demonstrate high toxicity towards others. General trends can however be observed. In the case of

[$C_nC_1$im] ILs, the toxicity increases with longer alkyl chains.[81,83] Incorporation of hydroxyl or methoxy groups on the side chain results in lower toxicity.[82] For a given cation, certain anions have been found to be more toxic than others although there has not been a very wide range studied. Generally chloride ILs show relatively low toxicity and ILs with fluorinated anions, such as [NTf_2], show higher toxicity.[82] A study has found that [$C_nC_1$im]Cl IL toxicity on unicellular organisms is due to a swelling of the cell membrane.[81] In line with what was observed for other organisms, cytotoxicity increases with increasing alkyl chain length of the cation and suggested that cation insertion into the cell membrane is responsible for the toxicity. Longer alkyl chains are therefore more easily embedded in the cell membrane, which leads to its rupture.[81]

PILs have been found to be less toxic than aprotic imidazolium based ones[83] and much less than phosphonium ILs.[82] Accidental ingestion of [HC_4im][HSO_4] by the author has so far not shown noticeable oral or dermal toxicity of [HC_4im][HSO_4]. A study that analysed PILs based on amines and organic acids showed no toxicity in the performed aquatic toxicity tests with the exception of three PILs with butyric or iso-butyric acid anions.[83] The analysed PILs are around 60 times more biodegradable than the APILs, and most PILs in the study fall into the category of "readily biodegradable". Contrarily a study analysing four PILs based on the N-methyl-2-hydroxyethylammonium cation with acetate, propionate, butyrate or pentanoate anions found these PILs to have low biodegradability.[84] Again the length of the alkyl chain, this time on the anion though, was found to negatively impact the effect of the PILs on the organism studied. In a study on the mutagenic and carcinogenic effects of 16 PILs, 15 were found to be non-mutagenic or carcinogenic.[85] The analysed PILs were composed of various alkanolamines and carboxylates or chloride anions. An increase of mutagenicity by an increasing number of carbon atoms on various alkyl chains could be counteracted by introducing more OH groups. Since some secondary amines are found to readily undergo transformation to highly carcinogenic N-nitrosamine compounds, the lack of mutagenic and carcinogenic effect of the corresponding PILs deemed them less harmful than their constituting amines.[85]

1.5. Electrochemistry and Electrodeposition

Electrodeposition from ionic liquids has been shown to be possible for many different metals and some metal alloys[86,87] and various review articles[63,88] as well as one very recent review about electrodeposition in ILs[89] are available. The use of ILs offers certain advantages over electrodeposition from aqueous or organic solutions, such as the possibility to use them in an open atmosphere and at elevated temperatures due to their low vapour pressure.[63] Furthermore it is possible to use ionic liquids for the electrodeposition of reactive metals such as Ti, Al and Mg which cannot be

electrodeposited from aqueous solutions.[87,90] As stated repeatedly, ILs are tunable and different cations and anions will give different surface morphologies of the deposited substance, such as dense and smooth, nanocrystalline or polycrystalline aluminium.[89] Adding an organic solvent to an ionic liquid increases its conductivity, not only by lowering the viscosity and thus increasing diffusion, but also by breaking up ion pairs, which is important for electrochemical applications.[55]

While most electrochemical applications make use of aprotic ionic liquids, protic ionic liquids have been studied to a minor extent. Their ionic conductivity is in many cases low due to their high viscosity[77] and their potential window is smaller than for APILs although still larger than for molecular protic sovents.[77] Their reductive stability is thought to be affected mainly by the proton reduction reaction.[91] However, they often show higher solubility of metal salts than their aprotic analogues and have successfully been used for electrodeposition of different metals[92,93] and organic polymers.[74] Similar to their aprotic analogues, tuning of the deposition parameters and the anion and cation used can result in different structures of the deposited metal (e.g. nano- and microstructured Ag films).[89]

Ni deposition has been achieved in PILs based on lactate and glycolate with imidazolium derived cations (2-methylimidazolium and 1-ethyl and 1-butylimidazolium).[94] 2-methylimidazolium ILs showed higher cathodic stability due to the replacement of the C-2 acidic proton with a methyl group. Furthermore, a higher Ni concentration made the deposition easier. Chromium deposition from aqueous solutions is typically achieved from hexavalent chromium, which is very toxic.[95] Trivalent chromium, although less toxic, is not typically used for chromium plating. This is due to the high stability of the hexaaquachromium (III) complex formed in aqueous solutions which makes plating impossible. Chromium deposition from imidazolium based ILs ($[C_2C_1im]Cl$, $[C_4C_1im]Cl$ and $[C_6C_1im]Cl$) from chromium (III), even in the presence of up to 18 equivalents of water, was however shown to be possible.[96] Chromium deposition as nanocrystalline chromium was also shown possible from the PIL $[C_4C_1im][HSO_4]$.[95] Copper deposition from ionic liquids has been widely studied and was shown to be possible in imidazolium, ammonium and pyrrolidinium[90] based aprotic ionic liquids.[63] Additionally, copper deposition has also been shown possible in the PILs ethylammonium nitrate and $[TEA][MeSO_3]$.[93]

1.6. Conclusions

The up-take of ILs in industrial processes has been slow. In order to overcome economic barriers to IL use, IL production cost needs to be decreased. PILs are promising candidates to overcome this challenge since their synthesis is facile and many PILs can be obtained from readily available and inexpensive bulk chemicals. PILs bear the further advantage of having lower toxicity and better biodegradability than their aprotic counterparts, potentially further facilitating their wider up-take by

industry. The high viscosity of many ILs, both protic and aprotic, at room temperature may potentially be overcome by carrying out the processing steps, including separations, at elevated temperatures or in the presence of a suitable co-solvent. Although literature data about PILs is currently limited, PILs hold great potential to be employed in industrial processes including biomass processing and electrochemistry.

2. Biorefinery

A biorefinery, analogous to a petroleum refinery, produces fuel, heat, electricity and/or chemicals from biomass.[9] The predominant biomass derived fuels are biodiesel, obtained from oily plants such as rapeseed and oil palm,[97] and ethanol, which can be obtained from any kind of plant.[98–100] The ease of production of bio-ethanol strongly depends on the type of biomass used. Ethanol is obtained directly by microbial fermentation from sucrose containing plants (e.g. sugar cane), via enzymatic or chemical hydrolysis and subsequent fermentation from starch (e.g. corn) or from lignocellulosic biomass (trees, grasses), requiring a pre-treatment step prior to hydrolysis and fermentation (Figure I-3).[13]

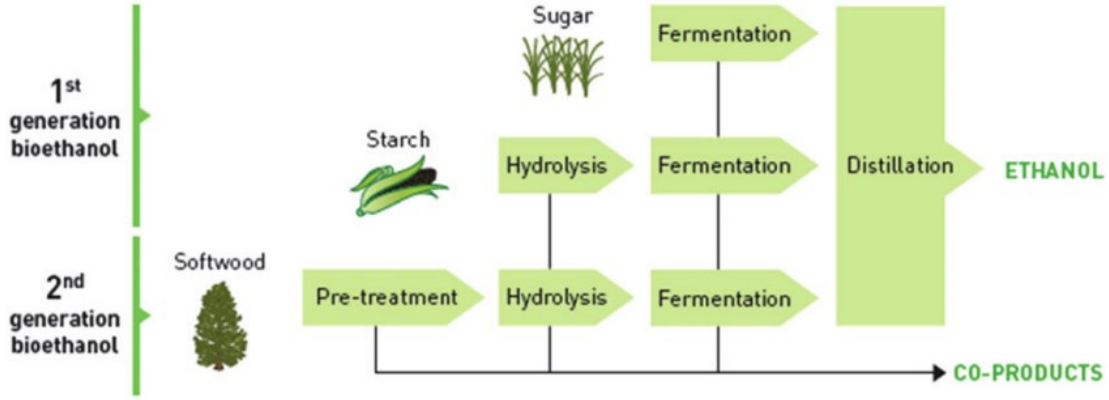

Figure I-3 First and second generation bio-ethanol.[13] 1st generation bio-ethanol from sugary plants only requires fermentation and in the case of starchy plants a hydrolysis step while 2nd generation bio-ethanol requires a pretreatment step.

While the production of first generation biofuels, such as bio-diesel from rapeseed or bio-ethanol from sugar beets, can afford CO_2 savings, their production can result in an increase in the release of nitrous oxide of over 600% compared to traditional fuels due to the use of fertilisers.[101] Additionally, their cultivation may result in land-use change, promoting a decrease in soil carbon when changing, e.g. forest land into agricultural land, thus negating any CO_2 savings afforded from replacing petroleum.[102] Perennial lignocellulosic crops, such as *Miscanthus,* conversely have low fertilizer requirements and do not deplete soil carbon.[103] Furthermore the cultivation of perennial biomass crops can have

beneficial effects on biodiversity compared to conventional agriculture.[104] Additionally lignocellulose is more abundant, grown faster with greater ease, and less limited by the local climate than agricultural plants.[15] The use of lignocellulosic biomass as a biorefinery feedstock is therefore environmentally and socioeconomically preferential.[18] However, the high recalcitrance of lignocellulose makes a pretreatment step necessary. Various pretreatment methods are currently under development, such as steam explosion (SE),[105] ammonia fibre expansion (AFEX),[106] concentrated acid,[107] dilute acid (DA),[108] hot water,[109] organosolv[110,111] and ionic liquid pretreatments,[15,112,113] including ionoSolv pretreatments,[19,114] some of which are discussed in more detail later on. While the main goal of most pretreatment technologies is the isolation of a highly digestible cellulose pulp for enzymatic hydrolysis, various factors need to be taken into consideration for a successful industrial application. The process's energy requirement,[12] recyclability of chemicals or solvents involved,[14] the solid to liquid ratio[113] during the process as well as the residence time[115] are features which need to be considered, as they all influence capital and/or operating costs.[116] In order to add value to the process and thus making it more competitive with traditional fossil fuel based refineries, full utilisation of all biomass components is required, setting a new focus on the valorisation of the lignin fraction.[117]

2.1. Lignocellulose

Lignocellulose is made from three biopolymers, namely lignin, a heterogeneous polymer containing aromatic subunits, cellulose, a highly crystalline form of polymeric glucose, and hemicellulose, an amorphous polymer consisting of a mixture of pentoses and hexoses.[118,119] Together these three components account for ca. 90% of the dry weight of biomass. Figure I-4 shows the structure of lignocellulose; linear cellulose fibres (yellow) are surrounded by hemicellulose (blue) which in turn is interconnected with lignin (orange).[13] Further, lignocellulosic biomass contains smaller amounts of pectins, inorganics, proteins and extractives such as waxes and lipids.[5] Lignocellulosic biomass contains up to 70% of carbohydrates, but the composition varies depending on species,[118] plant tissue[118,121] and growth conditions and stage.[122] Lignocellulosic biomass can be split in three types, namely softwoods, hardwoods and grasses, which all differ not only in their carbohydrate content but also in the composition of their substructures lignin and hemicellulose.[13,118] Although mildly disputed, there is general agreement on the existence of covalent bonds between the lignin and hemicellulose fractions, but not between the lignin and cellulose fractions.[123] These linkages between lignin and hemicellulose are thought to be mainly ester and in some cases ether bonds giving rise to lignin-carbohydrate complexes (LCCs).[64]

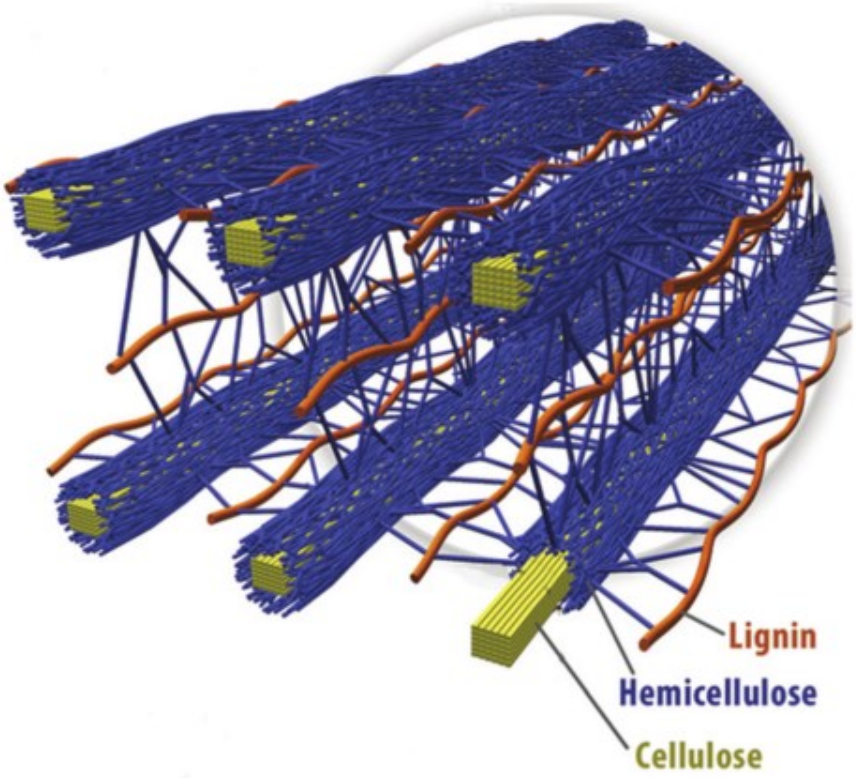

Figure I-4 Structure of lignocellulosic biomass.[13]

2.1.1. Cellulose

Cellulose is the largest component of lignocellulosic biomass and accounts for 35-50 wt% of the dry biomass.[13] It is a linear polymer made of glucose units which are linked to each other by 1-4-β glycosidic bonds (Figure I-5, left) forming microfibrils.[119] It is the β-configuration that is responsible for the linearity of the polymer, opposed to the α-configuration (Figure I-5, right), which instead gives rise to a helical structure, like in starch.[13] Further, two intramolecular hydrogen bonds between neighbouring glucose units and one intermolecular hydrogen bond link the chains into flat sheets.[118] These sheets mostly interact with each other through van der Waals interactions which lead to a stabilisation of the cellulose fibrils. While native cellulose (cellulose I) contains two intramolecular and one intermolecular hydrogen bonds, it can be converted into cellulose II which is thermodynamically more stable and contains hydrogen bonds between different sheets. Cellulose is insoluble in water and most solvents.[118] Solvents and solvent systems able to dissolve cellulose include *N,N*-dimethylacetamide/LiCl,[124] *N*-methylmorpholine-*N*-oxide,[125] concentrated phosphoric acid,[126–128] a range of ionic liquids[126,129–131] and ionic liquids mixed with organic solvents.[132] Swelling, dissolving[18] and regenerating native cellulose[13] can be used to convert cellulose I to cellulose II. Native cellulose is thermally stable up to around 250°C, where it starts to degrade through depolymerisation, dehydration and decomposition.[133,134] Rapid decomposition is observed at temperatures above 300-

350°C.[135] Cellulose modification, for example by the introduction of sulfonic acid groups, can reduce the thermal stability.[136] Cellulose depolymerisation to glucose is possible using Brønsted acids[137–139] or metal chlorides[131] as well as enzymes.[34,140–142]

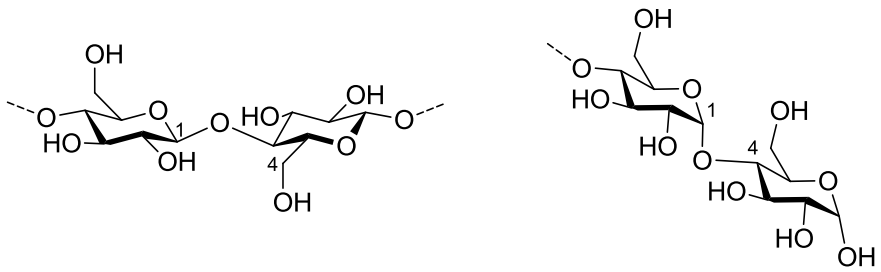

Figure I-5 1-4-β glycosidic bond found in cellulose (left) and 1-4-α glycosidic bond found in starch (right).

Cellulose itself represents a useful material for several applications. So-called dissolving pulp is composed of more than 90% cellulose and is used to produce rayon, cellophane and cellulose esters such as cellulose acetate.[143] Microcrystalline cellulose is widely used as a filler or binder in tablets.[134] Microfibrillated cellulose can be used for the production of self-healing hydrogels, a promising new material used in biomedical and pharmaceutical fields.[144] Nanocellulose, a cellulosic material with a cellulose fibril width of up to 100 nm, has been shown to form aerogels used amongst others as oil sorbents.[145] Carboxymethylcellulose has been used as a green jellifying agent for the production of renewable aqueous dye sensitized solar cells.[146] Cellulose films can be produced from azide modified cellulose.[147]

Alternatively cellulose can be hydrolysed to glucose which in turn can be converted into a multitude of products such as ethanol,[148,149] levulinic acid,[150,151] lactic acid,[38] HMF,[152,153] sorbitol[154] and gluconic acid.[155] Lactic acid is a commodity chemical widely used in the food and pharmaceutical industries as well as the production of the biodegradable plastic poly-lactic acid (PLA).[150] Furthermore PLA can be spun into fibres for biomedical applications.[156] Gluconic acid and its derivatives are widely used food additives.[155] Production of HMF from fructose[157] and glucose[152] (shown in Figure I-6) in certain ionic liquids with metal catalysts was shown to be possible with near quantitative yields. One-pot conversion of cellulose to HMF was shown to be possible using $[C_4C_1im][HSO_4]$ in combination with $CrCl_3$ as a catalyst.[153] HMF can be oxidised to furan-2,5-dicarboxylic acid (FDCA) which can be used as a substitute for terephthalic acid in the production of poly(ethylene terephthalate) PET and poly(butylene terephthalate) PBT (resulting in the production of PEF and PBF instead).[158] PEF and PBF have improved thermo-mechanical characteristics compared to PET and PBT and FDCA is therefore a promising bio-derived value-added chemical. Under slightly different conditions 2,5-diformylfuran

(DFF) rather than FDCA is obtained, a versatile compound used as a precursor for the synthesis of various polymers and resins.[159] Another product derived from HMF is levulinic acid[160] which can again be turned into a variety of products including fuel additives (γ-valerolactone, levulinic acid esters), food flavouring agents, pharmaceutical compounds,[151] herbicides (δ-aminolevulinic acid), solvents (THF, *N*-alkylpyrrolidone) and polymers (diphenolic acid).[161] Alternatively HMF can be converted into 5-hydroxymethyl-2-vinylfuran, an adhesive which can bond to metal, glass, plastics and rubber.[162] The unwanted formation of humins however remains a challenge in the production of value added chemicals from cellulose via HMF.[160] The production of low-volume but high value products from biomass in addition to biofuels is expected to help achieve a higher return on investment of biorefineries.[163]

Cellulose thus represents an important platform for the production of not only bio-ethanol, but also other fuels, materials and chemicals, some of which have an established market and use, while others are still being developed and/or in the search of a market. For many applications which currently rely on the use of a fossil feedstock, the production cost and quality of the cellulose derived alternative will be essential and therefore a low-cost route to cellulose and cellulosic sugars of the required purity and specifications will be necessary.

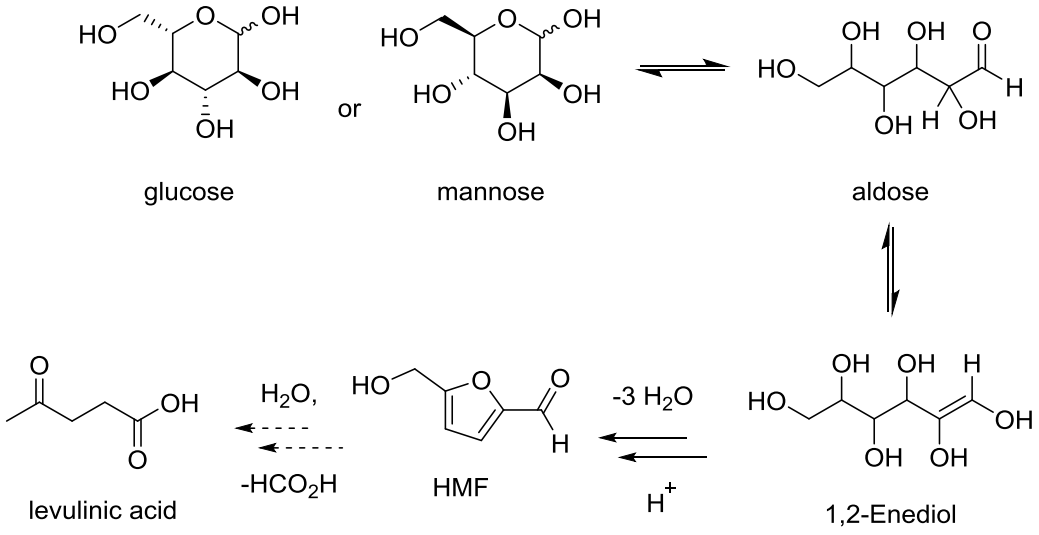

Figure I-6 Suggested acid catalysed mechanism for the formation of HMF and levulinic acid from hexoses via acyclic intermediates.[164]

2.1.2. Hemicellulose

Hemicellulose, like cellulose, is a polysaccharide; however with a polymerisation degree of 100-200 it has a much lower molecular weight than cellulose.[13] It makes up around 25 wt% of the dry biomass and contains hexose (glucose, mannose and galactose) and pentose (xylose and arabinose) sugars, the

exact abundance of which is largely dependent on the plant species.[119] Unlike cellulose, hemicellulose is branched and contains functionalised groups, such as acetyl and methyl groups and cinnamic, glucuronic and galacturonic acids.[165,166] Some hardwood species further contain traces of rhamnose.[118] Hemicellulose is an amorphous matrix material which is suspected to bind covalently to cellulose fibrils.[118] The substitution with hydrophobic acetyl and methyl groups enhances its affinity for lignin, creating a linkage between the lignin and cellulose. As hemicellulose is non-crystalline it is more susceptible to depolymerisation, especially under acidic conditions.[118] Alternatively, enzymes[167] and alkali[119] can be used for hemicellulose hydrolysis. Furthermore, hemicellulose also has a lower thermal stability than both lignin and cellulose, which is suspected to be a result of the presence of acetyl groups.[136]

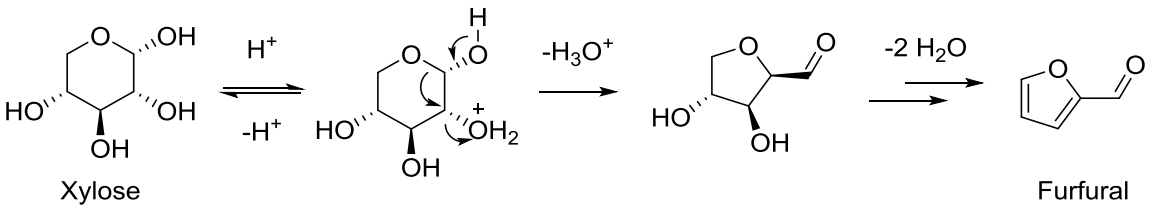

Figure I-7 Proposed acid catalysed formation of furfural from xylose.[168]

Hemicellulose C6 sugars, or hexoses, can undergo the same transformations to HMF as glucose,[164,169] which has been described above. C5 sugars, or pentoses, however readily dehydrate to furfural in acidic media[170] or in the presence of metal chlorides.[171,172] The mechanism for furfural formation is not entirely clear,[172] one proposed mechanism is displayed in Figure I-7. Furfural is an extremely versatile platform chemical and a promising candidate for the replacement of the production of many petro-chemicals. An extensive review on furfural and its transformation to a large range of compounds has been published in 2016 and a scheme of the products obtainable is presented in Figure I-8.[161] Amongst others, furfural can be converted to levulinic acid for which uses have been described in the above section. Furfural can, similar to HMF, form humins through self-coupling or resinification reactions with itself or other biomass components, or fragment to smaller molecules such as formic acid, formaldehyde and lactic acid.[170] These consumption reactions can limit furfural yields.[172] Yields can be improved by continuous removal of formed furfural, e.g. through distillation, which makes acidic ionic liquids an extremely favourable solvent and catalyst system for furfural production.[170] In addition to furfural, xylitol can be obtained from xylose via hydrogenation.[173] Xylitol in return is also an important platform chemical potentially used for the production of 1,3-pentadiene, used in the production of resins and a building block in organic synthesis.[173]

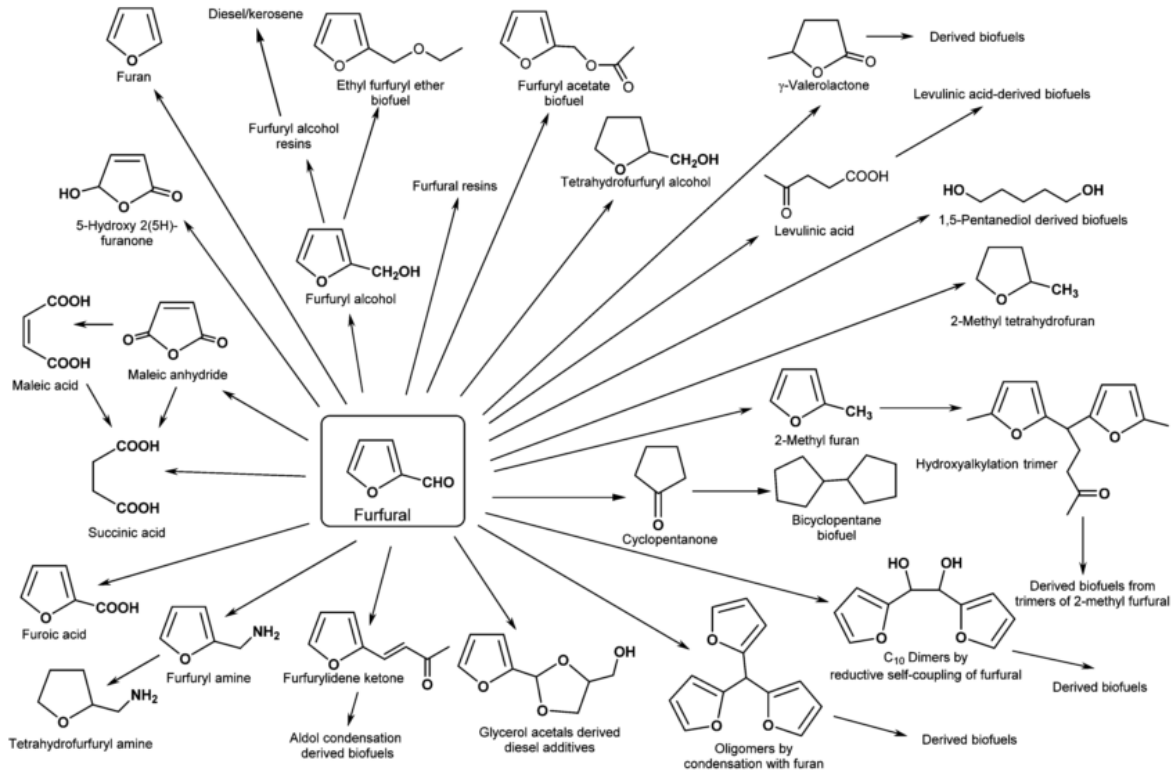

Figure I-8 Products obtained from furfural.[161]

2.1.3. Lignin

Lignin is the component of biomass containing aromatic units, built up at a mature state of plant growth.[13,119] It is water insoluble, therefore adding to water resistance, has an irregular structure and serves as a structural reinforcement.[119] It is resilient to biological and physical attack and thus functions as a shield for the polysaccharides.[5] Its biosynthesis proceeds via radical polymerisation of three monomers: coniferyl, sinapyl and *p*-coumaryl alcohol, which, once integrated in the polymeric structure, are referred to as guaiacyl (G), syringyl (S) and p-hydroxyphenyl (H) units respectively (Figure I-9, bottom row). Around half of the linkage bonds between these monomeric units are β-*O*-4' ether bonds, other C-O and C-C linkages are also present but to a lesser extent (Figure I-9, rows 1 and 2).[13] As a result of the radical polymerisation of three monomers, lignin is a heterogeneous polymer with varying physicochemical characteristics. Its properties depend on a variety of factors including plant species,[174] growth conditions and stage[175] and plant tissue.[121,176] Genetically engineering plants in order to obtain a more homogeneous lignin stream, with the aim to more easily valorise it, has been proposed.[174] However, this will not be discussed in detail since the focus of the here presented studies are around the use of waste streams from naturally occurring biomass.

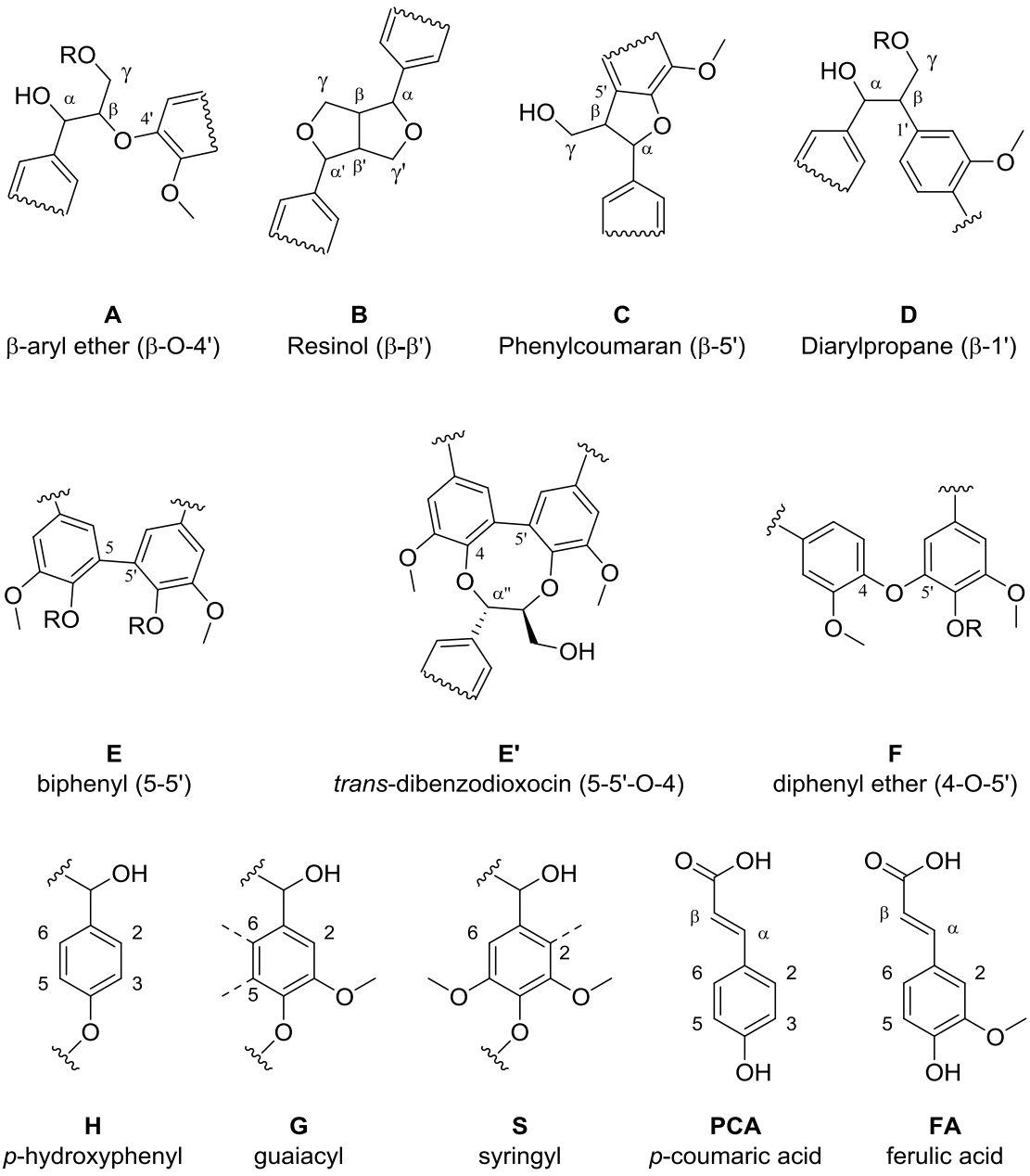

Figure I-9 Common lignin subunits and linkages.

The relative abundance of the three monomers depends on the type of biomass and impacts the reactivity of lignin and therefore the ease of the delignification process.[5] C-C cross-linkages are found extensively between the C-5' positions of guaiacyl units, which are formed during the lignification and delignification of mainly softwoods (structures C, E and E' in Figure I-9).[118] Such C-C crosslinks are not readily hydrolysed with acid or base and as a consequence the delignification process becomes more challenging.[177] In contrast, syringyl units, present in a significant number in hardwoods, are substituted in the C-5 position, making such crosslinks impossible. Therefore hardwoods are more easily delignfied than softwoods.[13] Depending on the type of biomass, lignin may also contain significant amounts of ferulates (F) and *p*-coumarates (*p*CA) (Figure I-9) which are involved in cross-coupling with lignin

monomers and the formation of LCCs.[178] Softwood, which is typically used as construction wood, only contains traces of F and *p*CA but more bi-phenyls (E and E' in Figure I-9) and di-phenyl ethers (F in Figure I-9)[5] and direct ester linkages between lignin and hemicelluloses are present.[13]

2.1.3.1.1. Lignin Valorisation

As explained earlier, lignin is responsible for the recalcitrance of lignocellulosic biomass and poses a barrier to the hydrolysis of the carbohydrates, making the pretreatment step necessary. Depending on the nature of this pretreatment step, the lignin can undergo different chemical modifications.[179–183] Challenges in the use of lignin for the production of value-added products are its heterogeneity, generally leading to a mixture of products, and poor reactivity especially of highly condensed lignins typically obtained after very harsh pretreatments.[184] However, the valorisation of lignin is critical to make a biorefinery economically viable.[185] A report for the United States Department of Energy suggests that lignin valorisation could increase the value of lignin by a factor of four and possible product classes are displayed in Figure I-10.[186]

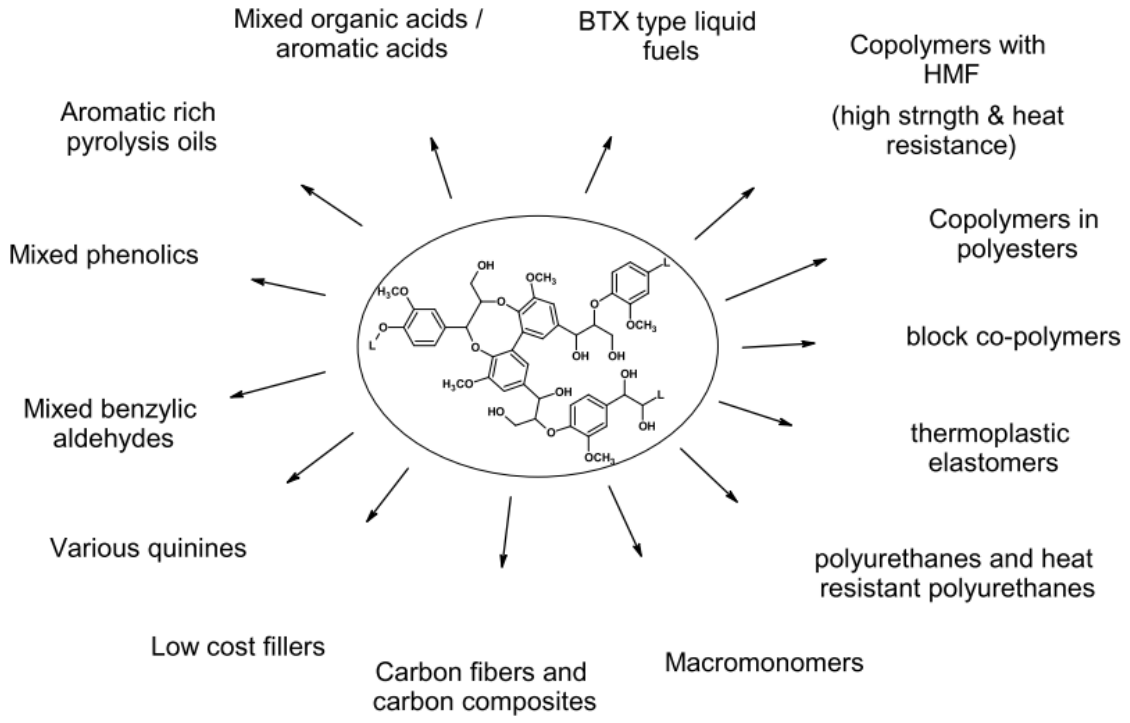

Figure I-10 Product classes potentially available from Lignin.[186]

While combustion of solid biomass and biomass components is used for heat and energy production, biomass suffers from low volumetric energy density.[9] The conversion of biomass and biomass components into liquid fuels with higher energy density is thus favourable. There are various strategies for the conversion of lignin into fuels and products of higher value in the form of small, low-molecular weight molecules. Thermochemical processes, such as pyrolysis and hydrogenolysis, are

able to yield bio-oils from lignin.[187,188] The pyrolysis of lignin generally leads to a mixture of phenolic compounds as well as a significant amount of char.[189] Hydrogenolysis, a process where the presence of hydrogen aids the cleavage of various bonds, similarly yields a mixture of alkylphenols and further hydrodeoxygenation leads to the formation of cyclic hydrocarbons.[190] Oxidative depolymerisation of lignin can afford a mixture of phenolic compounds under mild conditions.[191,192] These include aromatics which are difficult to synthesise conventionally from fossil feedstocks with structures closely related to the building blocks of lignin,[186] such as vanillic acid using TiO_2 and H_2O_2 as an oxidant,[193] guaiacol and vanillin using electorchemical depolymerisation[194] and hydroxyl-aromatic benzaldehydes and carboxylic acids using aerobic oxidation in the presence of catalysts.[192] Solid base catalysed depolymerisation of lignin results in the formation of low molecular weight products including esters and phenols.[195]

However, the wider application of these technologies faces many barriers. Often many steps are required before a useful product is obtained. Pyrolysis oil from lignin is typically oxygen rich, making it acidic and reactive, forming high viscosity and corrosive oils, impeding its direct use as a fuel.[196] Pyrolysis oil upgrading is therefore required and can be achieved by catalytic hydrodeoxygenation[197] where the challenge remains to use as little hydrogen from an external source as possible.[198] The production of bio-diesel from alkaline lignin required a three step process involving a transfer hydrogenolysis of lignin using 2-propanol as hydrogen donor, followed by transesterification of the hydroxylgroups followed by hydrotreatment where hydrogen is used to produce the fully deoxygenated bio-diesel.[199] Another challenge for successful industrial application of depolymerisation technologies for lignin is selective cleavage of C-C and C-O bonds. Research is being conducted in the area of catalytic lignin depolymerisation and copper doped porous metal oxides have been found to nearly completely convert lignin into methanol soluble mono- and oligomers for the production of bio-oils via deoxygenation under super-critical conditions but there are still problems associated with over-reduction of the aromatic moieties.[200] Catalysts can also directly be used during pyrolysis, such as Lewis-acids, so higher bio-oil yields can be obtained.[201] Using fast pyrolysis over a zirconium silica catalyst at 600°C yielded 49% BTX (benzene, toluene, xylene) from alkaline lignin.[202] Torrefaction (i.e. heating to around 200-400°C in the absence of air) of lignin previous to catalytic fast pyrolysis showed to increase the selectivity to BTX but lowering the overall aromatic hydrocarbon yield.[203]

Some of these lignin conversion technologies can be applied directly to the lignin containing biomass. Direct processing of birch wood *via* hydrogenolysis using a Ru/C catalyst was shown to yield a lignin oil while leaving behind a cellulose rich pulp.[204] Similarly, reductive depolymerisation of lignin using

metal triflates and Pd/C catalysts resulted in the formation of alkylmethoxyphenols directly from biomass, again leaving behind a cellulose rich solid.[205] More marginal strategies for lignin conversion into higher value products include lignin fermentation using enzymes and microbes.[206–208]

Alternatively, lignin can be used as a polymer directly as obtained or with small modifications for a range of applications, for example as a building block for thermoplastics,[209,210] a sorbent for heavy metals,[211] to stabilize urea in slow-release fertilizers,[212] an active ingredient of suncream,[213] as UV filter in cellulose films,[147] an antioxidant and thermal stabilizer,[214,215] flame retardant,[216] for the production of biocompatible nanofibres,[215] or to replace phenol in phenol-formaldehyde resins.[217] Different characteristics of lignin are important for the various applications, such as the presence of sulfonic acid groups and a large surface area for heavy metal adsorption,[211] high degree of condensation for an increased thermal stability,[218] absence of carbohydrate impurities and sulfur for successful blending to form suncream,[213] low PDI for blending with polyethylene,[219] and high phenolic –OH content for thermal stabilisation and antioxidant properties,[214] as well as for the replacement of phenol.[217] Obtaining a consistent lignin stream with the desired chemical properties is therefore important and requires a good understanding of the effects of the biomass type and isolation method on the lignin characteristics. Additionally, lignin isolation methods that allow for the isolation of different fractions with a more narrow distribution of molecular weights and functionalities are being investigated in order to facilitate lignin valorisation. Lignin can either be fractionated and/or purified after its isolation using a variety of lignin solvents[36,220,221] or the isolation method can be altered in order to directly isolate different fractions.[222]

2.1.3.1.2. Lignin Characterisation

Signal overlap and low detectability associated with the heterogeneous polymeric structure of lignin make quantitative structural analysis very challenging. There are several wet chemistry and degradation methods available for the quantification of main functionalities within the lignin structure, such as the thioacidolysis for the determination of lignin aromatic units,[128] alkaline nitrobenzene oxidation for the degree of condensation,[223] aminolysis for the detection of Phe-OH and OMe and derivatisation followed by reductive cleavage (DFRC) for β-*O*-4 linkage frequency.[224] However, they all only allow the detection of a specific functionality and fail to create a complete picture. Furthermore interpretation after derivatisation is more ambiguous and prone to systematic errors.[225] Other destructive methods include thermogravimetric analysis (TGA),[209,220] certain NMR techniques,[226,227] pyrolysis–gas chromatography–mass spectrometry (py-GC/MS)[218] and elemental analysis.[228] Py-GC/MS is used to gain insight into the subunit composition of lignin and can give information on the S/G ratio.[193] Elemental analysis can be used to test for impurities through the

isolation method (e.g. sulfite pulping or IL pretreatment) and to assess fuel value.[179] Non-destructive techniques include NMR,[179,229,230] IR[231] and UV spectroscopy[147] and gel permeation chromatography (GPC).[220,231]

The advantage of NMR spectroscopy over the optical methods is the higher resolution, giving access to more detailed information.[225] Several NMR techniques offer structural analysis, some of which are quantitative.[227,230,232] Solid state as well as solution state NMR has been applied to lignin characterisation where ionic liquids such as $[C_2C_1im][OAc]$ as additives can improve lignin solubility.[31] Alternatively, acetylation can improve the solubility of lignin.[223] Phosphitylation and subsequent ^{31}P NMR spectroscopy offers the quantitative detection of aromatic groups with free phenolic hydroxyls such as *p*-hydroxyphenyl, catechols, guaiacyl units and condensed and uncondensed phenolics as well as carboxylic acid groups.[226] The aliphatic, phenolic and carboxylic acid hydroxyl groups react with a phosphitylation agent and an internal standard is added to the mixture for quantitative integration. A database with spectral information of various model compounds is available for comparison and identification of subunits present in lignin.[226] Similarly ^{19}F NMR spectroscopy can be used for the detection and quantification of carbonyl groups via a trifluoromethylation.[233] Again, some data of model compounds are available for comparison and identification,[234] however this technique has not received much attention recently.

2D NMR techniques are used due to less spectral overlap of signals. Heteronuclear single and multiple quantum coherence (HSQC and HMQC) spectroscopy give signals for $C\text{-}H_x$ groups and can be used to distinguish between aliphatic and aromatic components.[235] Changes in the structural characteristics can be determined by volume integration of the HSQC peaks with an accuracy with less than 10% error.[31] Although NMR techniques typically suffer from high detection limits, the detection limit for HMQC has been estimated to be below 0.3 per 100 aromatic units.[230] A HSQC and HMQC spectrum can be divided into two areas of interest; the aliphatic oxygenated region can be used to estimate the relative abundance of the different interunit linkages[223] while the S/G ratio is estimated from the signals in the aromatic region. However, not all interunit linkages are detectable by these 2D NMR techniques: while β-*O*-4', β-β', β-1', β-5' and 5-5'-*O*-4 linkages are easily detected through one of the $C\text{-}H_n$ groups on the aliphatic side chain, 4-*O*-5' and 5-5' bonds cannot be detected. Further 2D techniques used include HMBC (heteronuclear multiple bond correlation),[236] where signals are obtained for hydrogens and carbons separated by 2-4 bonds, and TOCSY (TOtal Correlation SpectroscopY),[237] where all hydrogens in one spin system (i.e. linked by H-C and C-C bonds) give cross peaks. These are mostly used for the confirmation of findings from other techniques.[230] HMBC can also be used for the detection of hydroxyl groups after acetylation thereof and carbonyl groups, which

is not possible with HSQC.[238] HSQC-TOCSY 3D NMR spectroscopy has been used for the more reliable assignment of cross-peaks and giving access to information on subunits and connectivities which have not been investigated via corresponding model compounds.[236] A more comprehensive picture of the lignin structure is drawn by ^{13}C NMR spectroscopy.[223] However low natural abundance of the ^{13}C nucleus make long measuring times necessary which can be decreased by a factor of four by adding a relaxation agent[225] but still remain significantly longer (around 24 hours) than for other NMR techniques.[239] ^{1}H NMR spectroscopy is used in many cases but is insufficient by itself due to the extensive overlap of signals.

IR spectroscopy offers the qualitative detection of various structural units, such as carbonyl groups in various systems.[240] The content of S groups can be estimated as well as the amount of residual carbohydrates present. Furthermore structural changes can be monitored inexpensively and fast.[223] Gel permeation chromatography (GPC) or size exclusion chromatography (SEC) is used to determine the weight-average (M_w) and number-average molecular weights (M_n) as well as the polydispersity of the lignin polymers.[239,241] Thermogravimetric analysis (TGA) measures weight loss over a time period or as a function of increasing temperature, or a combination of the two.[36,220] It is used to assess the thermal stability,[242] thermal oxidation stability[216] of lignin as well as its ash content[218] and char-forming capability.[216] Similarly, differential scanning calorimetry (DSC) can be used to study the thermal behaviour of lignin and its derivatives, e.g. to determine the glass transition temperature T_g,[209,218] the melting temperature T_m, cold crystallization temperature T_{cc}, melt enthalpy ΔH_m and crystallinity.[215] Thermal properties of lignin are especially important for its application in materials, such as thermoplastics,[209] or as an additive to improve thermal stability of plastics.[214,242]

In order to obtain a comprehensive picture of lignin, often a combination of techniques is used.[179,183,210,221,243] The degree of polymerisation and branching for example was determined by an end-group titration approach consisting of a quantitative HSQC, ^{31}P NMR and DFRC.[243] This highlights the importance of finding a set of analytical techniques that complement each other in order to obtain conclusive insights into the properties of an isolated lignin and the lignin chemistry occurring during a given isolation process.

2.2. Deconstruction of Lignocellulose

The deconstruction of lignocellulosic biomass has been known for over a century for the production of paper with improved strength. During the so called Kraft process, the biomass is heated in an aqueous mixture of NaOH and NaHS or Na_2S at 130-180°C for several hours, dissolving part of the hemicellulose and most of the lignin by fragmentation and formation of water soluble lignothiols. The liquor is burnt afterwards for energy generation and regeneration of the sulfide.[125] This and other

processes for paper production are optimised for high cellulose yield and fibre strength. However, the biorefinery requires an inexpensive route to sugars that are easily fermented and a by-product stream that yields value added chemicals to increase the economic viability of the process.[13]

The initial focus of the deconstruction process in the context of the biorefinery is providing glucose for fermentation.[13] Hereby, different strategies are followed, from disrupting the lignocellulosic structure,[121,128,244,245] decrystallizing the cellulose[107,129,246] to selectively removing lignin and/or hemicelluloses.[75,112,247] Several review articles are available discussing these different strategies.[248,249] In a second step, the saccharification, the glycosidic bonds are hydrolysed, usually catalysed by either enzymes[245,250] or chemicals.[107,251] A barrier for enzymatic hydrolysis is that native cellulose exhibits a high degree of crystallinity which limits the substrate accessibility. Lignocellulose pretreatments based on cellulose-dissolving solvents have been shown to be more effective than traditional pretreatments in terms of overcoming this problem; the regenerated cellulose is amorphous and has a larger and more accessible surface area, increasing enzymatic hydrolysis rates.[126] Although it was found that substrate accessibility and therefore the crystallinity of the cellulose is the most important factor affecting the enzymatic hydrolysis rate,[252] removal of lignin and lignin derived compounds is also important to avoid deactivation of the enzymes as some lignin derived compounds (e.g. syringyl aldehyde and vanillic acid) inhibit hydrolases and fermentative organisms completely.[128] In the following paragraphs, the most important pretreatment technologies are briefly discussed.

Examples for water based lignocellulose disruption include liquid hot water (LHW)[253,254] or autohydrolysis,[109,255,256] high-temperature saturated steam[257] and steam explosion.[258–260] These methods differ slightly from each other in temperature and pressure and some of the terms are used interchangeably, especially for LHW and autohydrolysis, sometimes also referred to as hydrothermal pretreatment.[261] Some authors refer to autohydrolysis as a steam pretreatment with typical operating temperatures of above 170°C and reaction times of a few minutes to hours[262] where the general working principle is that hemicelluloses are hydrolysed and form acids, which in turn further catalyse the hydrolysis of hemicellulose oligomers.[248] High-temperature saturated steam requires even higher temperatures and pressures of up to 260°C and 67 bar.[257] Rapid release of the pressure results in a small explosion within the wet cell walls which additionally disrupts the biomass and is referred to as steam explosion (SE) pretreatment.[259] Using liquid hot water rather than steam allows the extraction of hemicellulose mainly in the form of oligomers, with only a few sugar monomers formed. This consequently results in a lower amount of sugar degradation products, such as furfural, and therefore a more limited amount of inhibitors formed.[254] All of these pretreatments typically result in the removal of hemicelluloses and redistribution of lignin, thus leaving behind a cellulose- and lignin-rich

solid with an enlarged surface area and an increased porosity.[100,262] The exact outcome depends on the severity, i.e. a factor calculated from the residence time and reaction temperature.[263] Addition of catalysts, e.g. dilute sulfuric acid for dilute acid (DA)[108,263] or dilute acid steam explosion (DA-SE) pretreatment,[258,260] further improves hemicellulose hydrolysis while lowering the required temperatures and/or shortening reaction times.[264]

While avoiding the use of expensive chemicals and catalysts and not requiring complex separations of solvents and solids, these processes suffer from the formation of inhibitors which negatively impact enzymatic hydrolysis of the cellulose pulp, including 5-HMF and furfural,[263,265] modified lignin[128] as well as pseudo-lignin,[121,245] making high enzyme loadings necessary[128] and further impeding subsequent fermentation.[263] Additionally, high pressure withstanding and corrosion resistant equipment ensured results with comparatively high capital cost, especially for dilute acid pretreatment.[115]

A similar effect of increased cell wall porosity is achieved by the ammonia fibre expansion (AFEX) process without negatively affecting the lignin structure.[256] AFEX pretreatment is further characterised as a "dry-to-dry" process: typically, the biomass is loaded into a reactor and liquid or gaseous ammonia added (1:1 ammonia to biomass ratio), the temperature raised to around 135°C (resulting in a pressure of between 35 and 50 bar) for 45 min and then released to allow the ammonia to evaporate, yielding dry, pretreated biomass.[266] The overall biomass composition therefore remains unchanged, however hemicellulose depolymerisation and de-acetylation occurs while the cellulose crystallinity is lowered. Partial hemicellulose and lignin removal, as well as a reduction in the crystallinity index of the cellulose can also be achieved by electron beam irradiation.[267] These pretreatment techniques which mostly result in hemicellulose removal and/or disruption of the biomass are mainly effective for herbaceous biomass[106,253] and agricultural residues,[182,256,261,267] somewhat effective with hardwoods[268,269] and hardly effective with softwoods.[177] A combination of these treatments, e.g. saturated steam followed by ball-milling can however improve yields, also from softwoods.[257]

Simple ball-milling of biomass has been shown to decrease the crystallinity of the cellulose and result in higher enzymatic hydrolysis yields while otherwise not changing the biomass composition.[167] Its high energy consumption however impedes the wider use of this technology.[126] Decrystallizing cellulose to a larger extent is possible using cellulose solvents, for example during the cellulose solvent and organic solvent lignocellulose fractionation (COSLIF) process. Biomass is dissolved in a cellulose solvent, typically phosphoric acid,[128] or using ionic liquids with a sufficiently high hydrogen bond basicity β, such as $[C_2C_1im][OAc]$ or $[C_4C_1im]Cl$, in the absence of water.[20,31,246,247,256,270] Subsequently, the cellulose is regenerated as an amorphous solid by adding an antisolvent, typically ethanol or water, while hemicelluloses and lignin are removed to some extent. The regenerated cellulose exhibits better

digestibility (ca. 50 times higher enzymatic hydrolysis rate) due to lower crystallinty[117,271] and enlarged surface area.[128] One of the drawbacks of the dissolution process using ionic liquids is the limited thermal stability of these types of salts[25,272] as well as the energy requirement to remove moisture, allowing full cellulose dissolution to occur. Compared to the aforementioned pretreatment methods which rely mainly on the removal of hemicelluloses and are effective for herbaceous biomass, decrystallizing the cellulose has been shown to be fairly effective with a wider range of biomass feedstocks including hard- and softwoods.[273]

However, complete dissolution of biomass is not crucial for the successful outcome of a pretreatment and rather the removal of lignin and increasing the accessible area of cellulose are the goals of other lignocellulose pretreatment techniques. Adding low concentrations of base to aqueous pretreatments can significantly improve lignin removal and enhance enzymatic hydrolysis of the recovered cellulose.[173] Soaking lignocellulosic biomass in lime in the presence of water removes large amounts of lignin. The reaction time is strongly dependent on the temperature used and can range from weeks at room temperature to a few hours if heated to 130°C.[274] Adding air or oxygen to the pretreatment system further aids lignin removal, making this type of pretreatment suitable for more recalcitrant biomass types.[274] Treatment with alkaline solutions of hydrogen peroxide at high temperatures is able to make part of the lignin soluble while decreasing the cellulose crystallinity slightly, resulting in a highly digestible pulp even from softwoods.[275,276] Similarly, sulfites can be added to dilute acid, hot water or steam explosion pretreatment in order to form water soluble lignosulfonates, resulting in higher hydrolysis yields of the partially delignified pulps and making it also possible to treat softwoods.[259,277,278] For agricultural residues and herbaceous biomass, soaking in aqueous ammonia for a few hours at temperatures of up to 90°C is highly effective.[279,280] Around 60% of the lignin is removed[281] and the recovered cellulose is highly digestible, yet not decrystallized.[282] Another successful example for processing grasses and hardwoods is the organosolv process where the biomass is pretreated in hot aqueous alcohol with a low concentration of acid catalyst (around 1-2%),[111,283,284] or concentrated organic acids,[285] leaving the cellulose undissolved in the pulp while removing the lignin and hydrolysed hemicellulose sugars which can be recovered from the liquid fraction and separated by precipitation of the lignin upon addition of additional water. Alternatively, a base catalyst can be used in order to preserve the hemicellulose sugars.[286] Very similarly to the acid catalysed organosolv treatment, certain ionic liquid-water mixtures have been found to effectively remove hemicelluloses and lignin from lignocellulosic biomass.[19] This process, termed ionoSolv process in analogy to the organosolv process, is discussed in more detail in the following section.

2.2.1. IonoSolv Pretreatment

During the ionoSolv process, similar to the organosolv process, not full but partial dissolution of the biomass is aimed for. Different to the basic acetate or chloride ionic liquids capable of dissolving biomass, the ionic liquids used in the ionoSolv process are typically composed of a hydrogensulfate or alkylsulfate anion and an imidazole or amine derived cation. Unlike the process of biomass dissolution, which is only achieved in the absence of water, the ionoSolv process requires 10-40wt% of water; after the pretreatment of *Miscanthus* with $[HC_4im][HSO_4]$ with 20wt% water for example a maximum of around 90% of the glucose was released compared to less than 20% in the absence of water.[75] Further, a low water content enhances carbohydrate degradation and pseudo-lignin formation.[19]

During ionoSolv pretreatment the lignin and hemicellulose are partly or fully dissolved, leading to a cellulose-rich material which is recovered after the pretreatment. Lignin can be precipitated from the ionic liquid liquor by adding more water as an anti-solvent. Almost full delignification of *Miscanthus* was reported using $[C_4C_1im][MeSO_4]$, $[HC_4im][HSO_4]$ or $[C_4C_1im][HSO_4]$[13] which was attributed to the somewhat nucleophilic character of the neutral or acidic anions which can act as catalysts or reactants during the delignification.[19] Although the undissolved cellulose is still crystalline, saccharification is accelerated about 30 times compared to untreated biomass. This acceleration is attributed to the enlarged surface area of the cellulose and the removal of lignin. Diedericks *et al.*[252] reported incomplete lignin removal from sugar cane bagasse with dry $[C_4C_1im][MeSO_4]$, however fully digestible cellulose was obtained after 2 hours at 150°C without additional water. Adding H_2SO_4 as an acid catalyst did not increase the cellulose digestibility but led to the enhanced formation of byproducts such as acetic acid, 5-HMF and furfural. Similarly, in a recent publication from our group, Verdia *et al.*[75] employed the less expensive protic ionic liquid, $[HC_4im][HSO_4]$ with different acid to base ratios. The findings show that a higher acid concentration results in lower saccharification yields due to the degradation of the carbohydrates. Higher base concentrations however decreased the effectiveness of the pretreatment. Already small differences in acid to base ratios have shown to strongly affect the outcome of the pretreatment (0.99:1 vs. 1.01:1), making accurate measuring of the starting materials for ionic liquid synthesis critical.

During pretreatment, lignin is partially to fully solubilised into the ionic liquid and can be partially re-precipitated upon addition of water. Higher molecular weight lignin precipitates readily while lower molecular weight fragments and oligomers stay in solution due to strong π-π interactions between aromatic lignin mono- and oligomers and the ionic liquid cation.[187]

2.3. Technoeconomic and Life Cycle Considerations of Bioenergy Value Chains

In order to produce fuels, materials and chemicals from biomass in a sustainable way, life cycle and economic considerations of the entire value chain are crucial. Bioenergy systems, although sometimes considered to be carbon neutral, often require non-renewable energy inputs for production of the feedstock, transportation and conversion, which all need to be taken into consideration.[103] The environmental and economic sustainability of current and future biofuels have often been questioned and studied, with titles of publications ranging from "Use of U.S. Croplands for Biofuels Increases Greenhouse Gases Through Emissions from Land-Use Change"[102] and "2nd Generation biofuels a sure bet? A life cycle assessment of how things could go wrong"[287] to "Take a Closer Look: Biofuels Can Support Environmental, Economic and Social Goals".[288] Life-cycle greenhouse gas (GHG) emissions of biofuels and other bioenergy systems are very challenging to estimate[289] since they depend on a variety of factors. They originate from a variety of processes including land-use change,[102] fertilizer use and N_2O emissions from crop cultivation[101] and production of the fuel.[290] As a result, life cycle analyses of apparently similar bioenergy systems can have surprisingly different outcomes for several reasons, such as type and management of the feedstock used, the conversion technology applied and the end-use technology.[291]

Also system boundaries, e.g. allocation of by-products, and the reference energy system with which the bioenergy chain is compared are very important,[103,292] with direct and indirect land-use change often being a major decisive factor.[102,293] Hoefnagels *et al.* studied GHG footprints of different biofuel production systems and found that land-use change can have a positive or negative effect on GHG emissions and could result in credits, depending on what the reference land is.[294] They found that the carbon content of cropland may be increased through the cultivation of energy crops, e.g. in the case of degraded land from palm fruit cultivation in South-East Asia or logged over woodland in Tanzania. Land-use change may however result in the release of large quantities of carbon if carbon intensive land such as natural rainforest is converted into cropland for biodiesel from palm fruit, resulting in GHG emissions more than three times higher than from fossil diesel.[294] GHG emissions from land-use change are one-off emissions which, as more biofuels are produced from the land, are slowly off-set.[102] Searchinger *et al.* estimated that GHG emissions from land-use change for the production of US corn ethanol take 167 years to pay back while ethanol from Brazilian sugarcane can pay back its carbon debt from land-use change in around 4 years if only tropical grazing land is used and 45 years if rainforest land is converted.[102] It is therefore important to critically assess biofuel supply chains and manage them sustainably in order to achieve a positive environmental impact from their use. Dale *et al.* reported that sustainable biofuel systems can be achieved when integrated with sustainable agriculture and forestry systems.[288] They argue that, if implemented correctly, the production of

biofuels can increase the sustainability of the agricultural system. Especially the use of perennial feedstocks generally provides an opportunity for the integration of bioenergy production and agricultural systems by reducing soil erosion, retaining nutrients and increasing organic matter while breaking pest and disease cycles.[288,295] In general, second generation biofuels, such as cellulosic ethanol e.g. from perennial feedstocks, renewable diesel from biomass and bio-methane, have lower well-to-wheel emissions compared to their first generation counterparts and appear to have the best long-term potential to provide sustainable, low life-cycle GHG fuels.[296]

Other than land-use change, allocation of by-products and the reference energy system with which the bioenergy chain is compared are important factors in the LCA of biofuel systems. There are several examples where co-product allocation outweighs the primary goal, i.e. CO_2 savings from displacing fossil fuels with bio-ethanol. A study comparing AFEX and DA pretreatment of switchgrass and corn stover for the production of bio-ethanol found that, despite AFEX pretreatment resulting in higher sugar and hence higher ethanol yields, higher CO_2 savings are achieved by the DA process. This is due to credits for electricity production from the burning of the non-fermented lignin and residual carbohydrate fraction, which was larger for the DA process as a result of the poorer hydrolysis yields.[290] The study, from 2010, used the American electricity mix as reference which is coal and therefore CO_2 heavy, and CO_2 savings ranged from 1380 to 50 gCO_2e/L of ethanol, depending on the model used. The importance of the reference system is highlighted by a study looking at the use of sugarcane bagasse in South Africa. While diversion of the currently burnt bagasse to produce cellulosic ethanol appeared economically attractive, the study found that from an environmental perspective the status-quo outperformed the studied scenarios as a result of the coal-heavy electricity that is replaced by bioenergy if the bagasse is burnt, but not if it is used as a biofuel feedstock.[287] Utilization of other renewable sources for electricity production could however drastically change this.[14] In a more recent study (2016) Prasad *et al.* compared LHW, DA, SE and organosolv pretreatments of corn stover on CO_2 emissions, water depletion, acidification potential and eutrophication. LHW performed best overall with the highest sugar yields and significantly lower CO_2 emissions of 0.94 $kgCO_2e$/kg fermentable sugar while DA clearly performed worst of the technologies studied(385 $kgCO_2e$/kg fermentable sugar), mainly due to long reaction times in a second reaction step that included soaking in lime for 12 hours at 60°C.[297]

According to Hamelinck *et al.* lignocellulosic bio-ethanol has an efficiency of around 35% based on the higher heating value (HHV) from biomass to ethanol which rises to about 60% if electricity is co-generated from burning the lignin.[298] The exergy efficiency (i.e. the maximum useful work which can be obtained from a system), as calculated by Kang and Tan, of bio-ethanol produced from corn and

only accounting for the total non-renewable energy input needed, ranged from 0.78 to 1.75, depending on the assumptions made and the model in use.[299] Taken into consideration were seeds, fertilizers and herbicides for cultivation, fuel for transport of the corn, energy required for all steps from biomass delivery to anhydrous ethanol and fuel for ethanol distribution.

Techno-economic analysis of bio-ethanol production from switchgrass using AFEX, DA, lime, LHW, soaking in aqueous ammonia and SO_2 SE showed that there were only small differences in direct capital cost, although distributed differently over reactor cost, chemical recovery systems and influence on downstream processing cost.[115] The capital cost of the pretreatment units depended on processing conditions, such as temperature, residence time, solids loading as well as chemicals and their recovery strategies. The pretreatment, enzymatic hydrolysis, fermentation and ethanol recovery accounted for around 50% of the total direct fixed capital with the boiler for the recovery of heat from lignin and residual biomass accounting for another third. Feedstock cost was found to be 45-53% of the final minimum ethanol selling price (MESP) for the six investigated technologies, with switchgrass costing around $79/dry tonne. MESP was found to be lowest for AFEX pretreatment and the differences between the different technologies was mainly attributed to a large fraction of oligomeric hemicelluloses which are currently impossible to ferment, extracted by some of the treatments and especially LHW. In a scenario where oligomeric sugars can be fermented these differences in MESP can be reduced and MESP would be around $2.5/gal ethanol for all studied technologies except for soaking in dilute ammonia, which has a higher MESP due to an expensive chemical recovery system. In a different study, MESP for IL pretreatment via dissolution of the biomass followed by acid hydrolysis was found to lie above $8/gal ethanol but the authors concluded that the price could be lowered to $4/gal if hydrolysis yields and sugar recovery were improved.[116] George *et al.* on the other hand reported carefully designed low-cost ionic liquids with which the MESP could be lowered to $3.22/gal ethanol,[24] and, not quite incidentally, one of the ionic liquids reported has been the focus of some of the experimental work during this PhD project.

2.4. Conclusions

In a viable biorefinery, both the carbohydrate and lignin platforms will need to be considered. The production of bulk chemicals, materials and fuels from lignin or cellulose requires in some cases more research, while other routes are well established. In both cases however, large quantities of low-cost lignin and cellulose will be required. This in turn necessitates a lignocellulose fractionation process with low operating and capital cost which is robust and effective on a variety of feedstocks and can produce both products with consistent quality. The properties of especially the lignin will need to be well-understood and match the requirements of the targeted application. Last but not least, feedstock

sourcing will need to be considered carefully if an overall benefit for the environment is to be achieved.

3. Waste Wood

Wood is a naturally occurring waste from forestry but also a building material useful in the construction of houses[300] and furniture and the raw material in the paper making process.[301] While there are ca. 1.3m tonnes of forestry residues arising in the UK every year,[302] larger volumes of waste wood are produced in the form of pre- and post-consumer waste wood from the construction and demolition industries. Exact numbers or up-to-date estimates are difficult to obtain but a DEFRA projection from 2012 estimates around 4.3m tonnes of waste wood being generated annually in the UK.[303] Of these, the construction and demolition industries are producing 1.2 and 1.1m tonnes respectively, giving rise to 1.9m tonnes of solid treated wood alongside clean wood.[304] The largest market for waste wood is thought to be the panel board market, using around 1.1m tonnes of waste wood every year.[303] Numbers on how much wood goes to landfill vary between different reports and are generally very poorly reported but are thought to lie in the vicinity of 1m tonnes annually.[303] A 2015 report by the European Parliamentary Research Service (EPRS) suggests that the EU collects 52.9m tonnes of waste wood every year of which 46% is being recycled while the majority of the rest is sent to incineration.[305] US numbers are even more poorly reported, however the construction and demolition industries alone are thought to produce 40.2m tonnes of waste wood annually of which 48% are "still available for recovery".[306]

3.1. Treated Timber

In order to prolong the lifetime of construction wood and protect it from microbial and chemical degradation, the wood is treated with copper containing preservatives. Different preservatives are available, such as alkaline copper quaternary (ACQ), copper azole (CA, Tanalith E) and micronized copper quaternary (MCQ) which all contain large amounts of copper (up to 3700 ppm).[307] Also chromated copper arsenate (CCA, Tanalith C) has been used extensively in the past but is not in use any more in Europe,[308] the US,[309] or Japan.[310] It is still used in Africa and Asia.[311] Three different formulations, A, B and C, were, or still are, used with C being the most common one consisting of 47.5% chromium (VI) oxide (CrO_3), 34.0% arsenic (V) oxide (As_2O_5) and 18.5% copper (II) oxide (CuO),[312] generally traded under the name Tanalith C (Lonza).[311] Such treated timber can contain over 5000 mg kg^{-1} of arsenic and chromium.[313] The liquid formulation is applied by first putting the cut timber in big tanks which are evacuated. The cylindrical tank is then flooded with the wood preservative solution and a hydraulic pressure applied to force the preservative deep into the structure of the timber. Thereafter, the solution is pumped back out of the cylinder into a storage tank and a final vacuum

extracts excess preservative solution which is also pumped back to storage. Fixation of the CCA treatment formulation within the wood structure is not fully understood but it is suspected that the reduction of Cr(VI) to Cr(III), which results in the formation of insoluble complexes from the reactive and mobile form of Cr(VI), is at least partly responsible.[300]

All of the above preservatives increase the lifetime of the wood by 20-50 years making it non-biodegradable. They ultimately pose a problem at the end of the service life of the wood as the metals start leaking into the environment when taken to landfill.[26] Chromium and copper compounds are classified as non-volatile and thus only a small percentage escapes into the atmosphere upon combustion, gasification or pyrolysis of the contaminated biomass (less than 7%) while the remains are found in the ash and can simply be filtered off.[27] Arsenic on the other hand forms very volatile compounds that are partially released into the atmosphere upon combustion, pyrolysis or gasification.[27] Arsenic and hexavalent chromium are known to be very toxic to human life[313] and carcinogenic[310,314] and thus need to be contained.

Copper can be recovered from the treated wood by leaching with sulfuric acid which makes the copper soluble. 90-93% of the copper can be recovered with this method at a cost of ca. $180 per ton of treated wood.[307] 99% arsenic and 91% of chromium can be extracted from CCA treated wood with a similar method, reducing the amount of arsenic leaching into the environment by 86% at an estimated cost of $115 per ton of treated wood.[313] It is therefore important not only from an ecological but also economical point of view to find an inexpensive way for the extraction and recycling of copper and chromium and the appropriate disposal of arsenic.

3.1.1. Extraction and Recovery of Metals from Wood

Extraction of the metal preservatives usually involves one or several leaching steps using different acids such as acetic acid, oxalic acid[315] or sulfuric acid,[307] chelating agents such as EDTA,[26] bacteria or hydrogen peroxide.[313] Almost complete removal of all three elements from CCA treated wood with oxalic acid in a first leaching step and sodium oxalate under acidic conditions in a second step was achieved accompanied by decomposition of wood.[316] However, challenges remain such as the extraction and recycling of the chromium and copper from the extract and discarding of As, as well as recycling of the acidic water.[313] A problem of arsenic reduction as a recovery strategy is the formation of toxic arsine gas AsH_3.[317] As(III) and As(V) can be reduced to As(0) under the right conditions with negligible arsine evolution. Alternatively, arsenic can be extracted electrochemically from acidic washing solutions by concomitant reduction of copper to form Cu_3As and Cu_5As_2 deposits without the formation of arsine gas.[318]

3.2. Waste and Treated Wood in Pyrolysis, Gasification and Combustion

Studies with model compounds have demonstrated that As_2O_3 is very volatile and mass loss occurs at temperatures well below 200°C. As_2O_5 on the other hand is not volatile below 600°C but can be reduced in the presence of H_2 at temperatures of around 425°C. Copper(II) oxide thermally decomposes at 775°C in a nitrogen atmosphere and at 1050°C if H_2 is present while chromium(III) oxide does not react under pyrolysis, gasification or combustion conditions. However, arsenic(V) oxide volatilises in the presence of Cr(III) oxide or forms chromium arsenate ($CrAsO_5$) which is also very volatile. Furthermore, the decomposition of arsenic(V) oxide is accelerated in the presence of glucose, char, wood and pyrolysis vapours which make a reducing environment.[319]

During pyrolysis of contaminated wood, most of the copper and chromium is found in the ashes, however the exact partitioning depends on the type of furnace and the oxygen content of the atmosphere as oxides are less volatile than e.g. chlorides.[27] Arsenic however is partially released into the environment; 16.4% was released during pyrolysis for one hour at 275°C and 24.8% during 30 min at 350°C. The presence of CCA in wood also has an impact on partitioning of pyrolysis products.[320] During gasification, arsenic removal from the product gas requires a hot filter.[28] A Swedish study has found that incineration of CCA treated wood together with non-hazardous waste results in the formation of arsenic contaminated slag and fly ashes which prevents their further use for e.g. spreading on the forest floor.[321] But also other types of waste wood cause problems upon combustion. Burning of furniture waste has been found to result in emission of hazardous pollutants, such as polycyclic aromatic hydrocarbons and dioxin-like polychlorinated biphenyls (PCBs).[29] The latter pollutant is thought to be formed through a reaction of pentachlorophenol, a widely used wood preservative, but also from carbon, oxygen and chlorine at temperatures between 200 and 400°C, catalysed by copper.[29]

3.3. Conclusions

The disposal of treated wood waste is an environmental problem as well as a wasted resource and an economical solution still needs to be developed. Especially CCA treated wood is of concern but also other types of waste wood need to be considered. Strategies for the metal extraction and recovery as well as the use of the wood material beyond its heating value therefore need to be developed.

4. References

1 R. C. Rooney, S. E. Bayley and D. W. Schindler, *Proc. Natl. Acad. Sci. U. S. A.*, 2012, **109**, 4933–4937.

2 K. P. Timoney and P. Lee, *Open Conserv. Biol. J.*, 2009, **3**, 65–81.

3 D. Irons, S. Kendall, W. Erickson and L. McDonald, *Condor*, 2000, **102**, 723–737.

4 C. H. Peterson, S. D. Rice, J. W. Short and B. E. B. and D. B. I. Daniel Esler, James L. Bodkin,

Science (80-.)., 2003, **302**, 2082–2086.
5 J. F. Piatt and G. R. Ford, *Am. Fish. Soc. Symp.*, 1996, 18, 712–719.
6 G. M. Solomon and S. Janssen, *J. Am. Med. Assoc.*, 2010, **304**, 1118.
7 A. D. Charpentier, J. A. Bergerson and H. L. MacLean, *Environ. Res. Lett.*, 2009, **4**, 14005.
8 R. J. Nicholls and A. Cazenave, *Science (80-.).*, 2010, **328**, 1517–1520.
9 M. Stöcker, *Angew. Chem. Int. Ed. Engl.*, 2008, **47**, 9200–11.
10 K. Tokimatsu, R. Yasuoka and M. Nishio, *Appl. Energy*, 2015, **185**, 1899–1906.
11 Z. Qiu, L. Zhao and L. Weatherley, *Chem. Eng. Process. Process Intensif.*, 2010, **49**, 323–330.
12 S. Macrelli, J. Mogensen and G. Zacchi, *Biotechnol. Biofuels*, 2012, **5**, 22.
13 A. Brandt, J. Gräsvik, J. P. Hallett and T. Welton, *Green Chem.*, 2013, **15**, 550.
14 N. R. Baral and A. Shah, *Biofuels, Bioprod. Biorefining*, 2016, **10**, 70–88.
15 J. Shi, J. M. Gladden, N. Sathitsuksanoh, P. Kambam, L. Sandoval, D. Mitra, S. Zhang, A. George, S. W. Singer, B. a. Simmons and S. Singh, *Green Chem.*, 2013, **15**, 2579.
16 H. Lou, Q. Hu, X. Qiu, X. Li and X. Lin, *BioEnergy Res.*, 2016, **9**, 335–343.
17 N. Brosse, A. Dufour, X. Meng, Q. Sun and A. Ragauskas, *Biofuels, Bioprod. Biorefining*, 2012, **6**, 580–598.
18 N. Sathitsuksanoh, A. George and Y.-H. P. Zhang, *J. Chem. Technol. Biotechnol.*, 2013, **88**, 169–180.
19 A. Brandt, M. J. Ray, T. Q. To, D. J. Leak, R. J. Murphy and T. Welton, *Green Chem.*, 2011, **13**, 2489.
20 D. Groff, A. George, N. Sun, N. Sathitsuksanoh, G. Bokinsky, B. A. Simmons, B. M. Holmes and J. D. Keasling, *Green Chem.*, 2013, **15**, 1264.
21 J. P. Hallett and T. Welton, *Chem. Rev.*, 2011, **111**, 3508–76.
22 K. Shill, S. Padmanabhan, Q. Xin, J. M. Prausnitz, D. S. Clark and H. W. Blanch, *Biotechnol. Bioeng.*, 2011, **108**, 511–520.
23 B. Simmons, *Enhanced Mixed Feedstock Processing Using Ionic Liquids*, 2016.
24 A. George, A. Brandt, K. Tran, S. M. S. N. S. Zahari, D. Klein-Marcuschamer, N. Sun, N. Sathitsuksanoh, J. Shi, V. Stavila, R. Parthasarathi, S. Singh, B. M. Holmes, T. Welton, B. a. Simmons and J. P. Hallett, *Green Chem.*, 2015, **17**, 1728–1734.
25 M. T. Clough, K. Geyer, P. a Hunt, J. Mertes and T. Welton, *Phys. Chem. Chem. Phys.*, 2013, **15**, 20480–95.
26 F.-C. C. Chang, Y.-N. N. Wang, P.-J. J. Chen and C.-H. H. Ko, *J. Environ. Manage.*, 2013, **122**, 42–6.
27 A. Nzihou and B. Stanmore, *J. Hazard. Mater.*, 2013, **256–257**, 56–66.
28 J. Kramb, J. Konttinen, R. Backman, K. Salo and M. Roberts, *Fuel*, 2016, **181**, 319–324.
29 A. I. Moreno, R. Font and J. A. Conesa, *Waste Manag.*, 2016, **58**, 299–308.
30 A. Stojanovic and B. K. Keppler, *Sep. Sci. Technol.*, 2012, **47**, 189–203.
31 N. Sathitsuksanoh, K. M. Holtman, D. J. Yelle, T. Morgan, V. Stavila, J. Pelton, H. Blanch, B. a. Simmons and A. George, *Green Chem.*, 2014, **16**, 1236.
32 P. Wasserscheid and T. Welton, *Ionic liquids in synthesis*, John Wiley & Sons, 2008.
33 C. P. Fredlake, J. M. Crosthwaite, D. G. Hert, S. N. V. K. Aki and J. F. Brennecke, *J. Chem. Eng. Data*, 2004, **49**, 954–964.
34 S. H. Lee, T. V Doherty, R. J. Linhardt and J. S. Dordick, *Biotechnol. Bioeng.*, 2009, **102**, 1368–76.
35 W. H. Awad, J. W. Gilman, M. Nyden, R. H. Harris, T. E. Sutto, J. Callahan, P. C. Trulove, H. C. DeLong and D. M. Fox, *Thermochim. Acta*, 2004, **409**, 3–11.
36 T. Rashid, C. F. Kait, I. Regupathi and T. Murugesan, *Ind. Crops Prod.*, 2016, **84**, 284–293.
37 Y. Zhao, X. Zhang, Y. Zhen, H. Dong, G. Zhao, S. Zeng, X. Tian and S. Zhang, *Int. J. Greenh. Gas Control*, 2011, **5**, 367–373.
38 K. L. Luska, P. Migowski and W. Leitner, *Green Chem.*, 2015, **17**, 3195–3206.
39 V. Misuk, D. Breuch and H. Löwe, *Chem. Eng. J.*, 2011, **173**, 536–540.

40 C. Lin, H. Zhan, M. Liu, S. Fu and L. Lucia, *Chem. Res. Chinese Univ.*, 2013, **29**, 159–165.
41 S. Zhou, L. Liu, B. Wang, F. Xu and R. C. Sun, *Chinese Chem. Lett.*, 2012, **23**, 379–382.
42 R. G. Evans, O. V Klymenko, P. D. Price, S. G. Davies, C. Hardacre and R. G. Compton, *Chemphyschem*, 2005, **6**, 526–33.
43 F. Loe-Mie, G. Marchand, J. Berthier, N. Sarrut, M. Pucheault, M. Blanchard-Desce, F. Vinet and M. Vaultier, *Angew. Chem. Int. Ed. Engl.*, 2010, **49**, 424–7.
44 C.-Y. Wu, W.-H. Liao and Y.-C. Tung, *Lab Chip*, 2011, **11**, 1740–6.
45 P. Dubois, G. Marchand, Y. Fouillet, J. Berthier, T. Douki, F. Hassine, S. Gmouh and M. Vaultier, *Anal. Chem.*, 2006, **78**, 4909–17.
46 M. Shahid, T. Xiong, M. Castrec-Rouelle, T. Leveque and C. Dumat, *J. Environ. Sci. (China)*, 2013, **25**, 2451–2459.
47 N. V Plechkova and K. R. Seddon, *Chem Soc Rev*, 2008, **37**, 123–150.
48 R. D. Rogers and K. R. Seddon, *Science (80-.).*, 2003, **302**, 792–793.
49 M. D. Buchanan, *Report. Chromatogr. Appl. Newsl.*, **59**, 1–24.
50 J. G. Huddleston, A. E. Visser, W. M. Reichert, H. D. Willauer, G. a. Broker and R. D. Rogers, *Green Chem.*, 2001, **3**, 156–164.
51 J.-P. Belieres and C. A. Angell, *J. Phys. Chem. B*, 2007, **111**, 4926–4937.
52 S. Zhang, N. Sun, X. He, X. Lu and X. Zhang, *J. Phys. Chem. Ref. Data*, 2006, **35**, 1475–1517.
53 A. Messadi, A. Mohamadou, S. Boudesocque, L. Dupont and E. Guillon, *Sep. Purif. Technol.*, 2013, **107**, 172–178.
54 R. Fareghi-Alamdari and R. Hatefipour, *Thermochim. Acta*, 2015, **617**, 172–178.
55 C. Comminges, R. Barhdadi, M. Laurent and M. Troupel, *J. Chem. Eng. Data*, 2006, **51**, 680–685.
56 A. Noda, K. Hayamizu and M. Watanabe, *J. Phys. Chem. B*, 2001, **105**, 4603–4610.
57 H. Tokuda, K. Hayamizu, K. Ishii, M. A. B. H. Susan and M. Watanabe, *J. Phys. Chem. B*, 2005, **109**, 6103–6110.
58 M. A. Ab Rani, A. Brant, L. Crowhurst, A. Dolan, M. Lui, N. H. Hassan, J. P. Hallett, P. A. Hunt, H. Niedermeyer, J. M. Perez-Arlandis, M. Schrems, T. Welton and R. Wilding, *Phys. Chem. Chem. Phys.*, 2011, **13**, 16831–40.
59 L. Crowhurst, P. R. Mawdsley, J. M. Perez-Arlandis, P. a. Salter and T. Welton, *Phys. Chem. Chem. Phys.*, 2003, **5**, 2790–2794.
60 M. J. Kamlet and R. W. Taft, *J. Am. Chem. Soc.*, 1976, **98**, 377–383.
61 M. J. Kamlet, J.-L. M. Abboud, M. H. Abraham and R. W. Taft, *J. Org. Chem*, 1983, **48**, 2877–2887.
62 J. Wilkes and M. Zaworotko, *J. Chem. Soc. Chem. Commun.*, 1992, 965–967.
63 F. Endres, D. MacFarlane and A. Abbott, *Electrodeposition from ionic liquids*, 2008.
64 A. W. T. King, A. Parviainen, P. Karhunen, J. Matikainen, L. K. J. Hauru, H. Sixta and I. Kilpeläinen, *RSC Adv.*, 2012, **2**, 8020.
65 K. J. Baranyai, G. B. Deacon, D. R. MacFarlane, J. M. Pringle and J. L. Scott, *Aust. J. Chem.*, 2004, **57**, 145.
66 H. L. Ngo, K. LeCompte, L. Hargens and A. B. McEwen, *Thermochim. Acta*, 2000, **357–358**, 97–102.
67 V. Kamavaram and R. G. Reddy, *Int. J. Therm. Sci.*, 2008, **47**, 773–777.
68 N. Meine, F. Benedito and R. Rinaldi, *Green Chem.*, 2010, **12**, 1711.
69 B. Siu, C. G. Cassity, A. Benchea, T. Hamby, J. Hendrich, K. J. Strickland, A. Wierzbicki, R. E. Sykora, E. A. Salter, R. A. O'Brien, K. N. West and J. H. Davis, *RSC Adv.*, 2017, **7**, 7623–7630.
70 C. L. B. Reis, L. M. A. e Silva, T. H. S. Rodrigues, A. K. N. Félix, R. S. de Santiago-Aguiar, K. M. Canuto and M. V. P. Rocha, *Bioresour. Technol.*, 2017, **224**, 694–701.
71 E. C. Achinivu, R. M. Howard, G. Li, H. Gracz and W. A. Henderson, *Green Chem.*, 2014, **16**, 1114.
72 C. Chiappe, A. Mezzetta, C. S. Pomelli, G. Iaquaniello, A. Gentile and B. Masciocchi, *Green*

Chem., 2016, **18**, 4982–4989.
73 C. H. C. Janssen, N. A. Macías-Ruvalcaba, M. Aguilar-Martínez and M. N. Kobrak, *Sep. Purif. Technol.*, 2016, **168**, 275–283.
74 G. a. Snook, T. L. Greaves and A. S. Best, *J. Mater. Chem.*, 2011, **21**, 7622.
75 P. Verdía, A. Brandt, J. P. Hallett, M. J. Ray and T. Welton, *Green Chem.*, 2014, **16**, 1617.
76 T. L. Greaves and C. J. Drummond, *Chem. Rev.*, 2008, **108**, 206–237.
77 C. Zhao, G. Burrell, A. a J. Torriero, F. Separovic, N. F. Dunlop, D. R. MacFarlane and A. M. Bond, *J. Phys. Chem. B*, 2008, **112**, 6923–6936.
78 B. Dilasari, Y. Jung and K. Kwon, *Electrochem. commun.*, 2016, **73**, 20–23.
79 X. Lu, G. Burrell, F. Separovic and C. Zhao, *J. Phys. Chem. B*, 2012, **116**, 9160–70.
80 L. Chen, M. Sharifzadeh, N. Mac Dowell, T. Welton, N. Shah and J. P. Hallett, *Green Chem.*, 2014, **16**, 3098.
81 B. Yoo, B. Jing, S. E. Jones, G. A. Lamberti, Y. Zhu, J. K. Shah and E. J. Maginn, *Sci. Rep.*, 2016, **6**, 19889.
82 K. S. Egorova and V. P. Ananikov, *ChemSusChem*, 2014, **7**, 336–60.
83 B. Peric, J. Sierra, E. Martí, R. Cruañas, M. A. Garau, J. Arning, U. Bottin-Weber and S. Stolte, *J. Hazard. Mater.*, 2013, **261**, 99–105.
84 M. V. S. Oliveira, B. T. Vidal, C. M. Melo, R. de C. M. de Miranda, C. M. F. Soares, J. A. P. Coutinho, S. P. M. Ventura, S. Mattedi and Á. S. Lima, *Chemosphere*, 2016, **147**, 460–466.
85 J. E. S. J. Reid, N. Sullivan, L. Swift, G. A. Hembury, S. Shimizu and A. J. Walker, *Sustain. Chem. Process.*, 2015, **3**, 17.
86 R. Bomparola, S. Caporali, A. Lavacchi and U. Bardi, *Surf. Coatings Technol.*, 2007, **201**, 9485–9490.
87 J. Vaughan, *Miner. Process. Extr. Metall.*, 2008, **117**, 113–117.
88 F. Endres, *Chemphyschem*, 2002, **3**, 145–54.
89 Q. Zhang, Q. Wang, S. Zhang, X. Lu and X. Zhang, *ChemPhysChem*, 2016, **17**, 335–351.
90 S. Z. El Abedin, M. Pölleth, S. A. Meiss, J. Janek and F. Endres, *Green Chem.*, 2007, **9**, 549–553.
91 A. L. Chong, M. Forsyth and D. R. MacFarlane, *Electrochim. Acta*, 2015, **159**, 219–226.
92 B. H. R. Suryanto, C. a. Gunawan, X. Lu and C. Zhao, *Electrochim. Acta*, 2012, **81**, 98–105.
93 C. a. Gunawan, B. H. R. Suryanto and C. Zhao, *J. Electrochem. Soc.*, 2012, **159**, D611–D615.
94 B. Meenatchi, V. Renuga and A. Manikandan, *J. Inorg. Organomet. Polym. Mater.*, 2016, **26**, 423–430.
95 X. He, Q. Zhu, B. Hou, C. Li, Y. Jiang, C. Zhang and L. Wu, *Surf. Coatings Technol.*, 2015, **262**, 148–153.
96 L. Sun and J. F. Brennecke, *Ind. Eng. Chem. Res.*, 2015, **54**, 4879–4890.
97 A. M. Hennecke, M. Faist, J. Reinhardt, V. Junquera, J. Neeft and H. Fehrenbach, *Appl. Energy*, 2013, **102**, 55–62.
98 T. H. Kim, F. Taylor and K. B. Hicks, *Bioresour. Technol.*, 2008, **99**, 5694–5702.
99 P. Kaparaju, M. Serrano, A. B. Thomsen, P. Kongjan and I. Angelidaki, *Bioresour. Technol.*, 2009, **100**, 2562–8.
100 X. Zhuang, W. Wang, Q. Yu, W. Qi, Q. Wang, X. Tan, G. Zhou and Z. Yuan, *Bioresour. Technol.*, 2016, **199**, 68–75.
101 G. P. Hammond, S. Kallu and M. C. McManus, *Appl. Energy*, 2008, **85**, 506–515.
102 T. Searchinger, R. Heimlich, R. A. Houghton, F. Dong, A. Elobeid, J. Fabiosa, S. Tokgoz, D. Hayes and T.-H. Yu, *Science (80-.).*, 2008, **319**, 1238–1240.
103 F. Cherubini, N. D. Bird, A. Cowie, G. Jungmeier, B. Schlamadinger and S. Woess-Gallasch, *Resour. Conserv. Recycl.*, 2009, **53**, 434–447.
104 A. J. Haughton, A. J. Bond, A. A. Lovett, T. Dockerty, G. Sünnenberg, S. J. Clark, D. A. Bohan, R. B. Sage, M. D. Mallott, V. E. Mallott, M. D. Cunningham, A. B. Riche, I. F. Shield, J. W. Finch, M. M. Turner and A. Karp, *J. Appl. Ecol.*, 2009, **46**, 315–322.
105 F. Cotana, G. Cavalaglio, M. Gelosia, A. Nicolini, V. Coccia and A. Petrozzi, *Energy Procedia*,

2014, **45**, 42–51.
106 H. Alizadeh, F. Teymouri, T. I. Gilbert and B. E. Dale, *Appl. Biochem. Biotechnol.*, 2005, **121–124**, 1133–1141.
107 Y. P. Wijaya, R. D. D. Putra, V. T. Widyaya, J. M. Ha, D. J. Suh and C. S. Kim, *Bioresour. Technol.*, 2014, **164**, 221–231.
108 F. Hu and A. Ragauskas, *RSC Adv.*, 2014, **4**, 4317.
109 T. Pielhop, G. O. Larrazábal and P. Rudolf von Rohr, *Green Chem.*, 2016, **18**, 5239–5247.
110 Y. Xu, K. Li and M. Zhang, *Colloids Surfaces A Physicochem. Eng. Asp.*, 2007, **301**, 255–263.
111 M. Li, M. Tu, D. Cao, P. Bass and S. Adhikari, *J. Agric. Food Chem.*, 2013, **61**, 646–54.
112 A. M. Socha, R. Parthasarathi, J. Shi, S. Pattathil and D. Whyte, 2014, 1–9.
113 F. Xu, J. Sun, N. V. S. N. M. Konda, J. Shi, T. Dutta, C. D. Scown, B. A. Simmons and S. Singh, *Energy Environ. Sci.*, 2016, **9**, 1042–1049.
114 B. J. Cox and J. G. Ekerdt, *Bioresour. Technol.*, 2013, **134**, 59–65.
115 L. Tao, A. Aden, R. T. Elander, V. R. Pallapolu, Y. Y. Lee, R. J. Garlock, V. Balan, B. E. Dale, Y. Kim, N. S. Mosier, M. R. Ladisch, M. Falls, M. T. Holtzapple, R. Sierra, J. Shi, M. a. Ebrik, T. Redmond, B. Yang, C. E. Wyman, B. Hames, S. Thomas and R. E. Warner, *Bioresour. Technol.*, 2011, **102**, 11105–11114.
116 P. Oleskowicz-Popiel, D. Klein-Marcuschamer, B. a. Simmons and H. W. Blanch, *Bioresour. Technol.*, 2014, **158**, 294–299.
117 N. Labbé, L. M. Kline, L. Moens, K. Kim, P. C. Kim and D. G. Hayes, *Bioresour. Technol.*, 2012, **104**, 701–7.
118 R. Pettersen, *The Chemistry of Solid Wood*, American Chemical Society, Washington, DC, 1984, vol. 207.
119 T. E. Timell, *Wood Sci. Technol.*, 1967, **1**, 45–70.
120 N. Sathitsuksanoh, K. M. Holtman, D. J. Yelle, T. Morgan, J. Pelton, H. Blanch, B. A. Simmons and A. George, 1–4.
121 M. Normark, S. Winestrand, T. a Lestander and L. J. Jönsson, *BMC Biotechnol.*, 2014, **14**, 20.
122 E. M. Hodgson, D. J. Nowakowski, I. Shield, A. Riche, A. V. Bridgwater, J. C. Clifton-Brown and I. S. Donnison, *Bioresour. Technol.*, 2011, **102**, 3411–3418.
123 L. Kyllönen, A. Parviainen, S. Deb, M. Lawoko, M. Gorlov, I. Kilpeläinen and A. W. T. King, *Green Chem.*, 2013, **15**, 2374.
124 E. Togawa and T. Kondo, *J. Polym. Sci. Part B Polym. Phys.*, 2007, **45**, 2850–2859.
125 D. J. G. P. van Osch, L. J. B. M. Kollau, A. van den Bruinhorst, S. Asikainen, M. A. A. Rocha and M. C. Kroon, *Phys. Chem. Chem. Phys.*, 2017, **19**, 2636–2665.
126 N. Sathitsuksanoh, Z. Zhu and Y. Zhang, *Cellulose*, 2012, 1161–1172.
127 X. Du, L. A. Lucia and R. A. Ghiladi, *ACS Sustain. Chem. Eng.*, 2016, **4**, 3669–3678.
128 N. Sathitsuksanoh, B. Xu, B. Zhao and Y.-H. P. Zhang, *PLoS One*, 2013, **8**, e73523.
129 N. Sun, M. Rahman, Y. Qin, M. L. Maxim, H. Rodríguez and R. D. Rogers, *Green Chem.*, 2009, **11**, 646.
130 A. Hufendiek, V. Trouillet, M. A. R. Meier and C. Barner-Kowollik, *Biomacromolecules*, 2014, **15**, 2563–2572.
131 Y. Su, H. M. Brown, G. Li, X. D. Zhou, J. E. Amonette, J. L. Fulton, D. M. Camaioni and Z. C. Zhang, *Appl. Catal. A Gen.*, 2011, **391**, 436–442.
132 X.-F. Tian, Z. Fang, D. Jiang and X.-Y. Sun, *Biotechnol. Biofuels*, 2011, **4**, 53.
133 M. Roman and W. T. Winter, *Biomacromolecules*, 2004, **5**, 1671–1677.
134 M. El-Sakhawy and M. L. Hassan, *Carbohydr. Polym.*, 2007, **67**, 1–10.
135 S. Ouajai and R. A. Shanks, *Polym. Degrad. Stab.*, 2005, **89**, 327–335.
136 H. Kargarzadeh, I. Ahmad, I. Abdullah, A. Dufresne, S. Y. Zainudin and R. M. Sheltami, *Cellulose*, 2012, **19**, 855–866.
137 C. Zhang, Z. Fu, Y. C. Liu, B. Dai, Y. Zou, X. Gong, Y. Wang, X. Deng, H. Wu, Q. Xu, K. R. Steven and D. Yin, *Green Chem.*, 2012, **14**, 1928.

138 J. F. Saeman, *Ind. Eng. Chem.*, 1945, **37**, 43–52.
139 C. Li, Q. Wang and Z. K. Zhao, *Green Chem.*, 2008, **10**, 177.
140 H. Li, Y. Pu, R. Kumar, A. J. Ragauskas and C. E. Wyman, *Biotechnol. Bioeng.*, 2014, **111**, 485–492.
141 X. L. Luo, J. Y. Zhu, R. Gleisner and H. Y. Zhan, *Cellulose*, 2011, **18**, 1055–1062.
142 M. Tu, R. P. Chandra and J. N. Saddler, *Biotechnol. Prog.*, 2007, **23**, 1130–1137.
143 A. Higson, *Cellulose: Renewable Chemicals factsheet*, 2011.
144 B. Lu, F. Lin, X. Jiang, J. Cheng, Q. Lu, J. Song, C. Chen and B. Huang, *ACS Sustain. Chem. Eng.*, 2017, **5**, 948–956.
145 H. Liu, B. Geng, Y. Chen and H. Wang, *ACS Sustain. Chem. Eng.*, 2017, **5**, 49–66.
146 F. Bella, S. Galliano, M. Falco, G. Viscardi, C. Barolo, M. Grätzel and C. Gerbaldi, *Green Chem.*, 2017.
147 H. Sadeghifar, R. Venditti, J. Jur, R. E. Gorga and J. J. Pawlak, *ACS Sustain. Chem. Eng.*, 2017, **5**, 625–631.
148 X. Li, T. H. Kim and N. P. Nghiem, *Bioresour. Technol.*, 2010, **101**, 5910–5916.
149 S. Macrelli, PhD Thesis, Lund University, 2014.
150 Z. Zhang, J. Song and B. Han, *Chem. Rev.*, 2016, acs.chemrev.6b00457.
151 N. A. S. Ramli and N. A. S. Amin, *BioEnergy Res.*, 2017, **10**, 50–63.
152 S. Eminov, A. Brandt, J. D. E. T. Wilton-Ely and J. P. Hallett, *PLoS One*, 2016, **11**, e0163835.
153 S. Eminov, P. Filippousi, A. Brandt, J. Wilton-Ely and J. Hallett, *Inorganics*, 2016, **4**, 32.
154 A. Romero, E. Alonso, Á. Sastre and A. Nieto-Márquez, *Microporous Mesoporous Mater.*, 2016, **224**, 1–8.
155 A. M. Cañete-Rodríguez, I. M. Santos-Dueñas, J. E. Jiménez-Hornero, A. Ehrenreich, W. Liebl and I. García-García, *Process Biochem.*, 2016, **51**, 1891–1903.
156 T. A. M. Valente, D. M. Silva, P. S. Gomes, M. H. Fernandes, J. D. Santos and V. Sencadas, *ACS Appl. Mater. Interfaces*, 2016, **8**, 3241–3249.
157 S. Eminov, J. D. E. T. Wilton-Ely and J. P. Hallett, *ACS Sustain. Chem. Eng.*, 2014, **2**, 978–981.
158 J. Carlos Morales-Huerta, A. Martínez de Ilarduya and S. Muñoz-Guerra, *Polymer (Guildf).*, 2016, **87**, 148–158.
159 Z. Yang, W. Qi, R. Su and Z. He, *Energy & Fuels*, 2017, **31**, 533–541.
160 F. Yu, R. Zhong, H. Chong, M. Smet, W. Dehaen and B. F. Sels, *Green Chem.*, 2017, **19**, 153–163.
161 R. Mariscal, P. Maireles-Torres, M. Ojeda, I. Sádaba and M. López Granados, *Energy Environ. Sci.*, 2016, **9**, 1144–1189.
162 M. Han, X. Liu, X. Zhang, Y. Pang, P. Xu, J. Guo, Y. Liu, S. Zhang and S. Ji, *Green Chem.*, 2017, **19**, 722–728.
163 J. J. Bozell and G. R. Petersen, *Green Chem.*, 2010, **12**, 539.
164 R. J. Van Putten, J. N. M. Soetedjo, E. A. Pidko, J. C. Van Der Waal, E. J. M. Hensen, E. De Jong and H. J. Heeres, *ChemSusChem*, 2013, **6**, 1681–1687.
165 K. Wang, H. Yang, X. Yao, F. Xu and R.-C. Sun, *Bioresour. Technol.*, 2012, **116**, 99–106.
166 A. Khoddami, M. a Wilkes and T. H. Roberts, *Molecules*, 2013, **18**, 2328–75.
167 M. Yoshida, Y. Liu, S. Uchida, K. Kawarada, Y. Ukagami, H. Ichinose, S. Kaneko and K. Fukuda, *Biosci. Biotechnol. Biochem.*, 2008, **72**, 805–810.
168 J. B. Binder, J. J. Blank, A. V. Cefali and R. T. Raines, *ChemSusChem*, 2010, **3**, 1268–1272.
169 J. B. Binder, A. V. Cefali, J. J. Blank and R. T. Raines, *Energy Environ. Sci.*, 2010, **3**, 765.
170 S. Peleteiro, S. Rivas, J. L. Alonso, V. Santos and J. C. Parajó, *Bioresour. Technol.*, 2016, **202**, 181–191.
171 L. Mao, L. Zhang, N. Gao and A. Li, *Green Chem.*, 2013, **15**, 727.
172 B. Danon, G. Marcotullio and W. de Jong, *Green Chem.*, 2014, **16**, 39–54.
173 R. Sun, M. Zheng, X. Li, J. Pang, A. Wang, X. Wang and T. Zhang, *Green Chem.*, 2017, **19**, 638–642.

174 Y. Mottiar, R. Vanholme, W. Boerjan, J. Ralph and S. D. Mansfield, *Curr. Opin. Biotechnol.*, 2016, **37**, 190–200.
175 B.-C. Zhao, B.-Y. Chen, S. Yang, T.-Q. Yuan, A. Charlton and R.-C. Sun, *ACS Sustain. Chem. Eng.*, 2017, **5**, 1113–1122.
176 B. Jiang, T. Cao, F. Gu, W. Wu and Y. Jin, *ACS Sustain. Chem. Eng.*, 2017, **5**, 342–349.
177 L. Kumar, V. Arantes, R. Chandra and J. Saddler, *Bioresour. Technol.*, 2012, **103**, 201–208.
178 H. Kim and J. Ralph, *Org. Biomol. Chem.*, 2010, **8**, 576–91.
179 A. Brandt, L. Chen, B. E. van Dongen, T. Welton and J. P. Hallett, *Green Chem.*, 2015, **17**, 5019–5034.
180 B. Nanayakkara, M. Manley-Harris and I. D. Suckling, *J. Agric. Food Chem.*, 2011, **59**, 12514–12519.
181 T. M. Jarrell, C. L. Marcum, H. Sheng, B. C. Owen, C. J. O'Lenick, H. Maraun, J. J. Bozell and H. I. Kenttämaa, *Green Chem.*, 2014.
182 C. Krishnan, L. da C. Sousa, M. Jin, L. Chang, B. E. Dale and V. Balan, *Biotechnol. Bioeng.*, 2010, **107**, 441–450.
183 H. Yang, Y. Xie, X. Zheng, Y. Pu, F. Huang, X. Meng, W. Wu, A. Ragauskas and L. Yao, *Bioresour. Technol.*, 2016, **207**, 361–369.
184 R. H. Narron, H. Kim, H. Chang, H. Jameel and S. Park, *Curr. Opin. Biotechnol.*, 2016, **38**, 39–46.
185 Y.-H. P. Zhang, *J. Ind. Microbiol. Biotechnol.*, 2008, **35**, 367–75.
186 J. E. Holladay, J. F. White, J. J. Bozell and D. Johnson, *Top Value-Added Chemicals from Biomass Volume II — Results of Screening for Potential Candidates from Biorefinery Lignin*, 2007, vol. II.
187 J. Zakzeski, P. C. a Bruijnincx, A. L. Jongerius and B. M. Weckhuysen, *Chem. Rev.*, 2010, **110**, 3552–99.
188 M. P. Pandey and C. S. Kim, *Chem. Eng. Technol.*, 2011, **34**, 29–41.
189 F.-X. Collard and J. Blin, *Renew. Sustain. Energy Rev.*, 2014, **38**, 594–608.
190 H. Wang, L. Zhang, T. Deng, H. Ruan, X. Hou, J. R. Cort and B. Yang, *Green Chem.*, 2016, **18**, 2802–2810.
191 E. Reichert, R. Wintringer, D. a. Volmer and R. Hempelmann, *Phys. Chem. Chem. Phys.*, 2012, **14**, 5214.
192 W. Partenheimer, *Adv. Synth. Catal.*, 2009, **351**, 456–466.
193 R. Prado, X. Erdocia, G. F. De Gregorio, J. Labidi and T. Welton, *ACS Sustain. Chem. Eng.*, 2016, **4**, 5277–5288.
194 D. Di Marino, D. Stöckmann, S. Kriescher, S. Stiefel and M. Wessling, *Green Chem.*, 2016.
195 C. Division and C. Division, 2016, 19–22.
196 H. Ben, W. Mu, Y. Deng and A. J. Ragauskas, *Fuel*, 2013, **103**, 1148–1153.
197 R. N. Olcese, G. Lardier, M. Bettahar, J. Ghanbaja, S. Fontana, V. Carré, F. Aubriet, D. Petitjean and A. Dufour, *ChemSusChem*, 2013, **6**, 1490–9.
198 D. M. Alonso, J. Q. Bond and J. a. Dumesic, *Green Chem.*, 2010, **12**, 1493.
199 J. Löfstedt, C. Dahlstrand, A. Orebom, G. Meuzelaar, S. Sawadjoon, M. V. Galkin, P. Agback, M. Wimby, E. Corresa, Y. Mathieu, L. Sauvanaud, S. Eriksson, A. Corma and J. S. M. Samec, *ChemSusChem*, 2016, **9**, 1392–1396.
200 G. Warner, T. S. Hansen, A. Riisager, E. S. Beach, K. Barta and P. T. Anastas, *Bioresour. Technol.*, 2014, **161C**, 78–83.
201 N. Rajić, N. Z. Logar, A. Rečnik, M. El-Roz, F. Thibault-Starzyk, P. Sprenger, L. Hannevold, A. Andersen and M. Stöcker, *Microporous Mesoporous Mater.*, 2013, **176**, 162–167.
202 A. M. Elfadly, I. F. Zeid, F. Z. Yehia, A. M. Rabie, M. M. aboualala and S. E. Park, *Int. J. Biol. Macromol.*, 2016, **91**, 278–293.
203 R. Mahadevan, S. Adhikari, R. Shakya, K. Wang, D. C. Dayton, M. Li, Y. Pu and A. J. Ragauskas, *J. Anal. Appl. Pyrolysis*, 2016, **122**, 95–105.

204 S. Van den Bosch, W. Schutyser, S.-F. Koelewijn, T. Renders, C. M. Courtin and B. F. Sels, *Chem. Commun.*, 2015, **51**, 13158–13161.
205 O. Morales Gonzalez, J. Zhu, X. Huang, T. I. Korányi, M. Boot and E. J. M. Hensen, *Green Chem.*, 2016.
206 C. Zhao, S. Xie, Y. Pu, R. Zhang, F. Huang, A. J. Ragauskas and J. S. Yuan, *Green Chem.*, 2016, 1306–1312.
207 L. Lin, Y. Cheng, Y. Pu, S. Sun, X. Li, M. Jin, E. A. Pierson, D. C. Gross, B. E. Dale, S. Y. Dai, A. J. Ragauskas and J. S. Yuan, *Green Chem.*, 2016, **18**, 5536–5547.
208 C. Crestini and D. S. Argyropoulos, *Bioorg. Med. Chem.*, 1998, **6**, 2161–2169.
209 T. Bova, C. D. Tran, M. Y. Balakshin, J. Chen, E. A. Capanema and A. K. Naskar, *Green Chem.*, 2016, **18**, 5423–5437.
210 K. A. Y. Koivu, H. Sadeghifar, P. A. Nousiainen, D. S. Argyropoulos and J. Sipil?, *ACS Sustain. Chem. Eng.*, 2016, **4**, 5238–5247.
211 F. Xu, T.-T. Zhu, Q.-Q. Rao, S.-W. Shui, W.-W. Li, H.-B. He and R.-S. Yao, *J. Environ. Sci.*, 2016, 1–9.
212 M. H. Sipponen, O. J. Rojas, V. Pihlajaniemi, K. S. Lintinen and M. Österberg, *ACS Sustain. Chem. Eng.*, 2016, acssuschemeng.6b02348.
213 Y. Qian, X. Qiu and S. Zhu, *ACS Sustain. Chem. Eng.*, 2016, **4**, 4029–4035.
214 D. Ye, S. Li, X. Lu, X. Zhang and O. J. Rojas, *ACS Sustain. Chem. Eng.*, 2016, **4**, 5248–5257.
215 D. Kai, W. Ren, L. Tian, P. L. Chee, Y. Liu, S. Ramakrishna and X. J. Loh, *ACS Sustain. Chem. Eng.*, 2016, **4**, 5268–5276.
216 L. Liu, G. Huang, P. Song, Y. Yu and S. Fu, *ACS Sustain. Chem. Eng.*, 2016, acssuschemeng.6b00955.
217 N. Tachon, B. Benjelloun-mlayah and M. Delmas, *BioResources*, 2016, **11**, 5797–5815.
218 O. Gordobil, R. Moriana, L. Zhang, J. Labidi and O. Sevastyanova, *Ind. Crops Prod.*, 2016, **83**, 155–165.
219 H. Sadeghifar and D. S. Argyropoulos, *ACS Sustain. Chem. Eng.*, 2016, **4**, 5160–5166.
220 M. F. Li, S. N. Sun, F. Xu and R. C. Sun, *Sep. Purif. Technol.*, 2012, **101**, 18–25.
221 M. Lauberts, O. Sevastyanova, J. Ponomarenko, T. Dizhbite, G. Dobele, A. Volperts, L. Lauberte and G. Telysheva, *Ind. Crops Prod.*, 2016, **392**, 124–130.
222 L. da Costa Sousa, M. Foston, V. Bokade, A. Azarpira, F. Lu, A. J. Ragauskas, J. Ralph, B. Dale and V. Balan, *Green Chem.*, 2016, **18**, 4205–4215.
223 T.-Q. Yuan, S.-N. Sun, F. Xu and R.-C. Sun, *J. Agric. Food Chem.*, 2011, **59**, 6605–15.
224 J.-Y. Kim, S. Oh, H. Hwang, U.-J. Kim and J. W. Choi, *Polym. Degrad. Stab.*, 2013, **98**, 1671–1678.
225 E. a Capanema, M. Y. Balakshin and J. F. Kadla, *J. Agric. Food Chem.*, 2004, **52**, 1850–60.
226 Y. Pu, S. Cao and A. J. Ragauskas, *Energy Environ. Sci.*, 2011, **4**, 3154.
227 B. R. M. Sevillano, G. Mortha, M. Barrelle, D. Lachenal, D. Universitaire and S. Martin, *Holzforschung*, 2001, **55**, 286–295.
228 N. E. El Mansouri and J. Salvadó, *Ind. Crops Prod.*, 2006, **24**, 8–16.
229 S. Constant, H. L. J. Wienk, A. E. Frissen, P. de Peinder, R. Boelens, D. S. van Es, R. J. H. Grisel, B. M. Weckhuysen, W. J. J. Huijgen, R. J. A. Gosselink and P. C. A. Bruijnincx, *Green Chem.*, 2016, **18**, 2651–2665.
230 E. a Capanema, M. Y. Balakshin and J. F. Kadla, *J. Agric. Food Chem.*, 2005, **53**, 9639–9649.
231 L. Yang, D. Wang, D. Zhou and Y. Zhang, *Int. J. Biol. Macromol.*, 2016, **85**, 417–424.
232 M. Sette, R. Wechselberger and C. Crestini, *Chemistry*, 2011, **17**, 9529–35.
233 B. C. Ahvazi, C. Crestini and D. S. Argyropoulos, *J. Agric. Food Chem.*, 1999, **47**, 190–201.
234 B. C. Ahvazi and D. S. Argyropoulos, *J. Agric. Food Chem.*, 1996, **44**, 2167–2175.
235 J. Ralph and L. Landucci, in *Lignin and Lignans*, CRC Press, 2010, pp. 137–243.
236 T. M. Liitiä, S. L. Maunu, B. Hortling, M. Toikka and I. Kilpeläinen, *J. Agric. Food Chem.*, 2003, **51**, 2136–43.

237 P. Nolis and T. Parella, *J. Magn. Reson.*, 2005, **176**, 15–26.
238 D. J. Yelle, D. Wei, J. Ralph and K. E. Hammel, *Environ. Microbiol.*, 2011, **13**, 1091–100.
239 C. Vanderghem, A. Richel, N. Jacquet, C. Blecker and M. Paquot, *Polym. Degrad. Stab.*, 2011, **96**, 1761–1770.
240 T. Yuan, S. Sun, F. Xu and R. Sun, *BioResources*, 2011, **6**, 414–433.
241 S. S. Y. Tan, D. R. MacFarlane, J. Upfal, L. a. Edye, W. O. S. Doherty, A. F. Patti, J. M. Pringle and J. L. Scott, *Green Chem.*, 2009, **11**, 339.
242 L. Llovera, B. Benjelloun-Mlayah and M. Delmas, *BioResources*, 2016, **11**, 6320–6334.
243 C. Crestini, F. Melone, M. Sette and R. Saladino, *Biomacromolecules*, 2011, **12**, 3928–3935.
244 P. Langan, L. Petridis, H. M. O'Neill, S. V. Pingali, M. Foston, Y. Nishiyama, R. Schulz, B. Lindner, B. L. Hanson, S. Harton, W. T. Heller, V. Urban, B. R. Evans, S. Gnanakaran, A. J. Ragauskas, J. C. Smith and B. H. Davison, *Green Chem.*, 2014, **16**, 63.
245 F. Hu, S. Jung and A. Ragauskas, *ACS Sustain. Chem. Eng.*, 2013, **1**, 62–65.
246 G. Cheng, P. Varanasi, R. Arora, V. Stavila, B. a. Simmons, M. S. Kent and S. Singh, *J. Phys. Chem. B*, 2012, **116**, 10049–10054.
247 H. Wang, M. L. Maxim, G. Gurau and R. D. Rogers, *Bioresour. Technol.*, 2013, **136**, 739–42.
248 A. T. W. M. Hendriks and G. Zeeman, *Bioresour. Technol.*, 2009, **100**, 10–18.
249 S. Sun, S. Sun, X. Cao and R. Sun, *Bioresour. Technol.*, 2016, **199**, 49–58.
250 X. Lin, X. Qiu, L. Yuan, Z. Li, H. Lou, M. Zhou and D. Yang, *Bioresour. Technol.*, 2015, **185**, 165–170.
251 J. B. Binder and R. T. Raines, *Proc. Natl. Acad. Sci. U. S. A.*, 2010, **107**, 4516–21.
252 D. Diedericks, E. van Rensburg, M. D. P. García-Aparicio and J. F. Görgens, *Biotechnol. Prog.*, 2011, **28**, 76–84.
253 Q. Yu, J. Liu, X. Zhuang, Z. Yuan, W. Wang, W. Qi, Q. Wang, X. Tan and X. Kong, *Bioresour. Technol.*, 2016, **199**, 265–270.
254 N. Mosier, R. Hendrickson, N. Ho, M. Sedlak and M. R. Ladisch, *Bioresour. Technol.*, 2005, **96**, 1986–1993.
255 H. Amiri and K. Karimi, *Ind. Eng. Chem. Res.*, 2016, **55**, 4836–4845.
256 J. A. Perez-Pimienta, C. A. Flores-Gómez, H. A. Ruiz, N. Sathitsuksanoh, V. Balan, L. da Costa Sousa, B. E. Dale, S. Singh and B. A. Simmons, *Bioresour. Technol.*, 2016, **211**, 216–223.
257 C. Asada, C. Sasaki, T. Hirano and Y. Nakamura, *Bioresour. Technol.*, 2015, **182**, 245–250.
258 X. Zhang, Q. Yuan and G. Cheng, *Carbohydr. Polym.*, 2017, **156**, 351–356.
259 R. P. Chandra, Q. L. Chu, J. Hu, N. Zhong, M. Lin, J. S. Lee and J. Saddler, *Bioresour. Technol.*, 2016, **199**, 135–141.
260 J. Zhang, Y. Song, B. Wang, X. Zhang and T. Tan, *Renew. Energy*, 2016, **88**, 164–170.
261 M. Michelin and J. A. Teixeira, *Bioresour. Technol.*, 2016, **216**, 862–869.
262 B. Yang and C. E. Wyman, in *Biofuels: Methods and Protocols*, ed. J. R. Mielenz, Humana Press, Totowa, NJ, NJ, 2009, vol. 581, pp. 103–114.
263 S. Larsson, E. Palmqvist, B. Hahn-Hägerdal, C. Tengborg, K. Stenberg, G. Zacchi and N.-O. Nilvebrant, *Enzyme Microb. Technol.*, 1999, **24**, 151–159.
264 Q. Sun, M. Foston, X. Meng, D. Sawada, S. V. Pingali, H. M. O'Neill, H. Li, C. E. Wyman, P. Langan, A. J. Ragauskas and R. Kumar, *Biotechnol. Biofuels*, 2014, **7**, 150.
265 B. Du, L. N. Sharma, C. Becker, S.-F. Chen, R. A. Mowery, G. P. van Walsum and C. K. Chambliss, *Biotechnol. Bioeng.*, 2010, **107**, 430–440.
266 P. M. Abdul, J. M. Jahim, S. Harun, M. Markom, N. A. Lutpi, O. Hassan, V. Balan, B. E. Dale and M. T. Mohd Nor, *Bioresour. Technol.*, 2016, **211**, 200–208.
267 X. Guo, T. Zhang, S. Shu, W. Zheng and M. Gao, *ACS Sustain. Chem. Eng.*, 2017, **5**, 420–425.
268 S. V. Pingali, V. S. Urban, W. T. Heller, J. McGaughey, H. O'Neill, M. B. Foston, H. Li, C. E. Wyman, D. A. Myles, P. Langan, A. Ragauskas, B. Davison and B. R. Evans, *ACS Sustain. Chem. Eng.*, 2017, **5**, 426–435.
269 X. Jiang, Q. Hou, W. Liu, H. Zhang and Q. Qin, *Bioresour. Technol.*, 2016, **222**, 361–366.

270 A. M. D. C. Lopes, K. G. João, E. Bogel-Łukasik, L. B. Roseiro, R. Bogel-Łukasik and A. M. da Costa Lopes, *J. Agric. Food Chem.*, 2013, **61**, 7874–82.
271 C.-Z. Liu, F. Wang, A. R. Stiles and C. Guo, *Appl. Energy*, 2012, **92**, 406–414.
272 W. Li, N. Sun, B. Stoner, X. Jiang, X. Lu and R. D. Rogers, *Green Chem.*, 2011, **13**, 2038.
273 J. Shi, V. S. Thompson, N. A. Yancey, V. Stavila, B. A. Simmons and S. Singh, *Biofuels*, 2013, **4**, 63–72.
274 C. E. Wyman, B. E. Dale, R. T. Elander, M. Holtzapple, M. R. Ladisch and Y. Y. Lee, *Bioresour. Technol.*, 2005, **96**, 1959–1966.
275 P. Martel and J. M. Gould, *J. Appl. Polym. Sci.*, 1990, **39**, 707–714.
276 C. Alvarez-Vasco and X. Zhang, *Biomass and Bioenergy*, 2017, **96**, 96–102.
277 J. Y. Zhu, W. Zhu, P. Obryan, B. S. Dien, S. Tian, R. Gleisner and X. J. Pan, *Appl. Microbiol. Biotechnol.*, 2010, **86**, 1355–1365.
278 H. Zhou, S.-Y. Leu, X. Wu, J. Y. Zhu, R. Gleisner, D. Yang, X. Qiu and E. Horn, *RSC Adv.*, 2014, **4**, 27030.
279 C. G. Yoo, H. Kim, F. Lu, A. Azarpira, X. Pan, K. K. Oh, J. S. Kim, J. Ralph and T. H. Kim, *Bioenergy Res.*, 2016, **9**, 67–76.
280 J. Domanski, S. Borowski, O. Marchut-Mikolajczyk and P. Kubacki, *Biomass and Bioenergy*, 2016, **91**, 91–97.
281 T. H. Kim and Y. Y. Lee, *Appl. Biochem. Biotechnol.*, 2007, **137–140**, 81–92.
282 J. Wang, D. Xin, X. Hou, J. Wu, X. Fan, K. Li and J. Zhang, *Bioresour. Technol.*, 2016, **199**, 211–219.
283 X. Pan, N. Gilkes, J. Kadla, K. Pye, S. Saka, D. Gregg, K. Ehara, D. Xie, D. Lam and J. Saddler, *Biotechnol. Bioeng.*, 2006, **94**, 851–61.
284 M.-Q. Zhu, J.-L. Wen, Y.-Q. Su, Q. Wei and R.-C. Sun, *Bioresour. Technol.*, 2015, **185**, 378–385.
285 M.-F. Li, S. Yang and R.-C. Sun, *Bioresour. Technol.*, 2016, **200**, 971–980.
286 Y. N. Guragain, K. P. Bastola, R. L. Madl and P. V. Vadlani, *BioEnergy Res.*, 2016, **9**, 643–655.
287 R. Melamu and H. Von Blottnitz, *J. Clean. Prod.*, 2011, **19**, 138–144.
288 B. E. Dale, J. E. Anderson, R. C. Brown, S. Csonka, V. H. Dale, G. Herwick, R. D. Jackson, N. Jordan, S. Kaffka, K. L. Kline, L. R. Lynd, C. Malmstrom, R. G. Ong, T. L. Richard, C. Taylor and M. Q. Wang, *Environ. Sci. Technol.*, 2014, **48**, 7200–7203.
289 T. E. McKone, W. W. Nazaroff, P. Berck, M. Auffhammer, T. Lipman, M. S. Torn, E. Masanet, A. Lobscheid, N. Santero, U. Mishra, A. Barrett, M. Bomberg, K. Fingerman, C. Scown, B. Strogen and A. Horvath, *Environ. Sci. Technol.*, 2011, **45**, 1751–1756.
290 S. Spatari, D. M. Bagley and H. L. MacLean, *Bioresour. Technol.*, 2010, **101**, 654–667.
291 F. Cherubini and A. H. Strømman, *Bioresour. Technol.*, 2011, **102**, 437–451.
292 V. Menon and M. Rao, *Prog. Energy Combust. Sci.*, 2012, **38**, 522–550.
293 H. Cai, J. Wang, Y. Feng, M. Wang, Z. Qin and J. B. Dunn, *Energy Environ. Sci.*, 2016, **9**, 2855–2867.
294 R. Hoefnagels, E. Smeets and A. Faaij, *Renew. Sustain. Energy Rev.*, 2010, **14**, 1661–1694.
295 F. Cherubini and G. Jungmeier, *Int. J. Life Cycle Assess.*, 2010, **15**, 53–66.
296 International Energy agency (IEA), *Transport, Energy and CO2*, 2009.
297 A. Prasad, M. Sotenko, T. Blenkinsopp and S. R. Coles, *Int. J. Life Cycle Assess.*, 2016, **21**, 44–50.
298 C. N. Hamelinck, G. Van Hooijdonk and A. P. C. Faaij, *Biomass and Bioenergy*, 2005, **28**, 384–410.
299 Q. Kang and T. Tan, *Sustainability*, 2016, **8**, 76.
300 J. A. Hingston, C. D. Collins, R. J. Murphy and J. N. Lester, *Environ. Pollut.*, 2001, **111**, 53–66.
301 M. Fresse, I. Schmidt and K. Fischer, *Macromol. Symp.*, 2006, **232**, 13–18.
302 D. Di Maio, D. Turley and L. Hopwood, *Lignocellulosic feedstock in the UK*, 2014.
303 DEFRA, *Wood waste : A short review of recent research*, 2012.
304 H. Dick, A. Hennig and P. Scholes, *Gate fees Report 2015/16: Comparing the cost of*

alternative waste treatment options, 2016.
305 Didier Bourguignon (EPRS), *Understanding waste streams Treatment of specific waste*, 2015.
306 S. Cratkovich, J. Howe, J. Bowyer, E. Pepke, M. Frank and K. Fernholz, *Municipal solid waste (MSW) and construction and demolition (C&D) wood waste generation and recovery in the United States*, 2014.
307 L. Coudert, J. Blais and G. Mercier, *J. Environ. Eng.*, 2013, **139**, 576–587.
308 T. G. Mercer and L. E. Frostick, *Sci. Total Environ.*, 2012, **427**–**428**, 165–174.
309 J. Jambeck, K. Weitz, H. Solo-Gabriele, T. Townsend and S. Thorneloe, *Waste Manag.*, 2007, **27**, 21–28.
310 N. Ohgami, O. Yamanoshita, N. D. Thang, I. Yajima, C. Nakano, W. Wenting, S. Ohnuma and M. Kato, *Environ. Pollut.*, 2015, **206**, 456–460.
311 Lonza, https://www.lonzawoodprotection.com/eu/tanalith-family/, (accessed March 2017).
312 L. Coudert, J.-F. Blais, G. Mercier, P. Cooper, A. Janin and L. Gastonguay, *J. Environ. Manage.*, 2014, **132**, 197–206.
313 A. Janin, J.-F. Blais, G. Mercier and P. Drogui, *J. Hazard. Mater.*, 2009, **169**, 136–45.
314 A. Arita and M. Costa, *Metallomics*, 2009, **1**, 222–228.
315 B. Yu, C. Y. Hse and T. F. Shupe, *41st Annu. Meet. Biarritz, Fr.*, 2010.
316 T. Kakitani, T. Hata, T. Kajimoto and Y. Imamura, *Waste Manag.*, 2006, **26**, 453–8.
317 F. Brusciotti and P. Duby, *Electrochem. commun.*, 2008, **10**, 572–576.
318 C.-P. Nanseu-Njiki, V. Alonzo, D. Bartak, E. Ngameni and A. Darchen, *Sci. Total Environ.*, 2007, **384**, 48–54.
319 L. Helsen and E. Van den Bulck, *Environ. Pollut.*, 2005, **134**, 301–14.
320 Q. Fu, D. S. Argyropoulos, D. C. Tilotta and L. A. Lucia, *Ind. Eng. Chem. Res.*, 2007, **46**, 5258–5264.
321 A. Augustsson, L. Sörme, A. Karlsson and J. Amneklev, *J. Ind. Ecol.*, 2016, **0**, 1–11.

Research Gap and Objectives

From the reviewed literature we can see that, in order to replace the petrochemical industry and shift towards a bio-economy, there is a need for a biomass pretreatment process with low operating and capital cost, while being effective on a variety of abundant and low-cost biomass feedstocks.

Ionic liquid based pretreatment potentially offers such a process due to some of the ILs' favourable properties: their low vapour pressure means that they can be used at elevated temperature without the need for expensive, pressure resistant equipment while also allowing for quantitative solvent recovery with no losses to atmosphere. Furthermore various ILs have already been shown to be effective for pretreatment of a variety of feedstocks. There is, however, an unavoidable requirement for improvement before IL based pretreatment can be a viable option. Many ILs suffer from prohibitively high production costs and therefore an effective, low-cost alternative is required. Additionally, performance and throughput of the processes using them still needs to be improved and solvent recycling tested. There is an additional need for a deeper understanding of the lignin chemistry occurring during this IL based process since holistic use of the biomass will be crucial in order to make any biorefinery viable. Therefore, lignin yields and properties will need to be investigated in more detail, requiring thorough characterisation.

Another technical challenge society faces is the disposal of waste, especially when the waste is mixed with a significant quantity of foreign matter, which makes recycling difficult. Many valuable resources are lost on a continual basis due to the difficulty of recycling them economically. One of those lost resources is waste wood from construction and demolition, often not recycled as a result of the heavy metal based preservatives used for wood treatment and other contaminants present at its end of life. Again, ILs appear to be a potential solution to the problem, having been utilised for their applications in electrochemistry and metal extraction.

This opens up the exciting possibility to tackle two seemingly unrelated problems and use each of them to solve the other one. The IL pretreatment process, competing with other pretreatment processes and the petrochemical industry, benefits from using an unwanted and hence very low-cost feedstock, therefore potentially drastically improving its economic viability. At the same time, a waste problem is solved and usable products are obtained. The challenge in making this possibility a reality is the fact that the ILs used for electrochemical applications tend to not perform very well during biomass processing. It is therefore necessary to find an IL and suitable conditions that tick all the boxes.

The objectives of this project were therefore to investigate whether it was possible to:

- Find one or several low-cost IL(s) suitable for processing of a variety of lignocellulosic feedstocks, including softwoods
- Find one or several low-cost IL(s) suitable for the extraction of various heavy metals from biomass, including copper, chromium and arsenic
- Investigate the recovery of the extracted metals
- Find at least one IL which is capable of both, successfully processing softwoods and extracting said metals, and from which the metals can be recovered
- Modify process parameters to improve throughput while maintaining a high performance of the ionoSolv process
- Demonstrate that bio-derived products, specifically ethanol, can be obtained from wood after the ionoSolv process
- Gain a thorough understanding of the lignin chemistry occurring during the ionoSolv pretreatment
- Overall, by combination of the above, to make the ionoSolv process economically viable
- Identify the remaining challenges for successful industrial implementation

The pretreatment process used here was initially developed by Dr Agi Brandt and has since been adjusted. A video showing the key steps and explaining the entire process in detail can be found here.[1] An outline of the process is given in Figure I-11 and details of the procedure discussed here, which will help the reader to follow the results discussed in the subsequent chapters. Furthermore, Figure I-12 shows the liquid and solid streams throughout the process and the analytical methods used to analyse the various components at the different stages.

The biomass used in the experiments is prepared according to standard operating procedures given by the National Renewable Energy Laboratory (NREL) and includes chopping and sieving it to a specified particle size (details given in experimental section). Ionic liquids were

In a pressure tube, the biomass is mixed with an ionic liquid (typically already containing some water) and more water is added to achieve a final water content of 20wt%. The components are mixed well, using a vortex mixer, and the sealed tubes placed into a preheated fan assisted oven. At elevated temperature, the lignin and hemicellulose start to dissolve into the IL, leaving behind a pulp. At this point the IL contains dissolved lignin and hemicelluloses and/or products derived thereof and is referred to as the black liquor. In our protocol, ethanol is added to facilitate the separation of the pulp from the black liquor once the reaction mixture has cooled to room temperature. The pulp is washed

several times with ethanol and the wash ethanol added back to the black liquor, from where it is removed by evaporation.

Upon water addition to the black liquor, lignin precipitates out, which can then be separated from the now diluted IL. The lignin is washed with water and the wash water combined with the IL, from which it is removed by evaporation in order to obtain the recycled IL, referred to as the brown liquor.

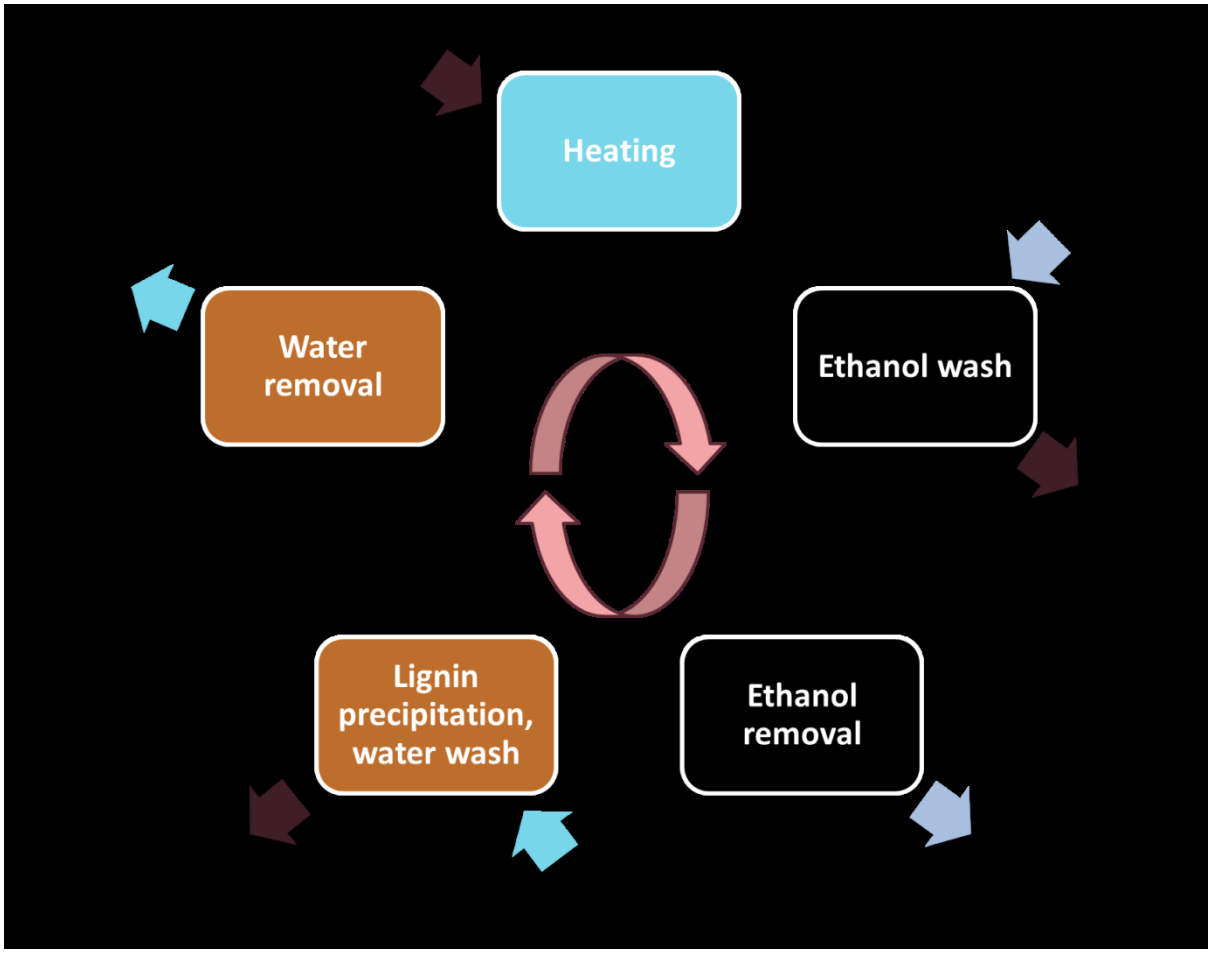

Figure I-11 ionoSolv pretreatment process.

As will be shown repeatedly throughout this thesis, the pulp isolated under different conditions will contain different components, such as the cellulose, residual lignin and hemicelluloses, but also reprecipitated lignin and humins. Therefore, the pulp is typically subjected to compositional analysis, using a standard protocol by the NREL. Since bioethanol and many other bio-derived products are obtained from glucose, the pulps are used in enzymatic hydrolysis and the sugar yields determined as a key performance indicator.

The lignin which is isolated as a precipitate is typically a modified version of the native lignin of the biomass, potentially containing some carbohydrate degradation products also. It has been

characterised by HSQC NMR, GPC and elemental analysis and modified with a phosphitylating agent for ^{31}P NMR.

The black liquor, typically containing the dissolved lignin and hemicelluloses as well as their degradation products has been analysed by HPLC on some of the solutes. Equally, the brown liquor, containing water soluble lignin and hemicellulose derived products, has also been analysed for some of these solutes.

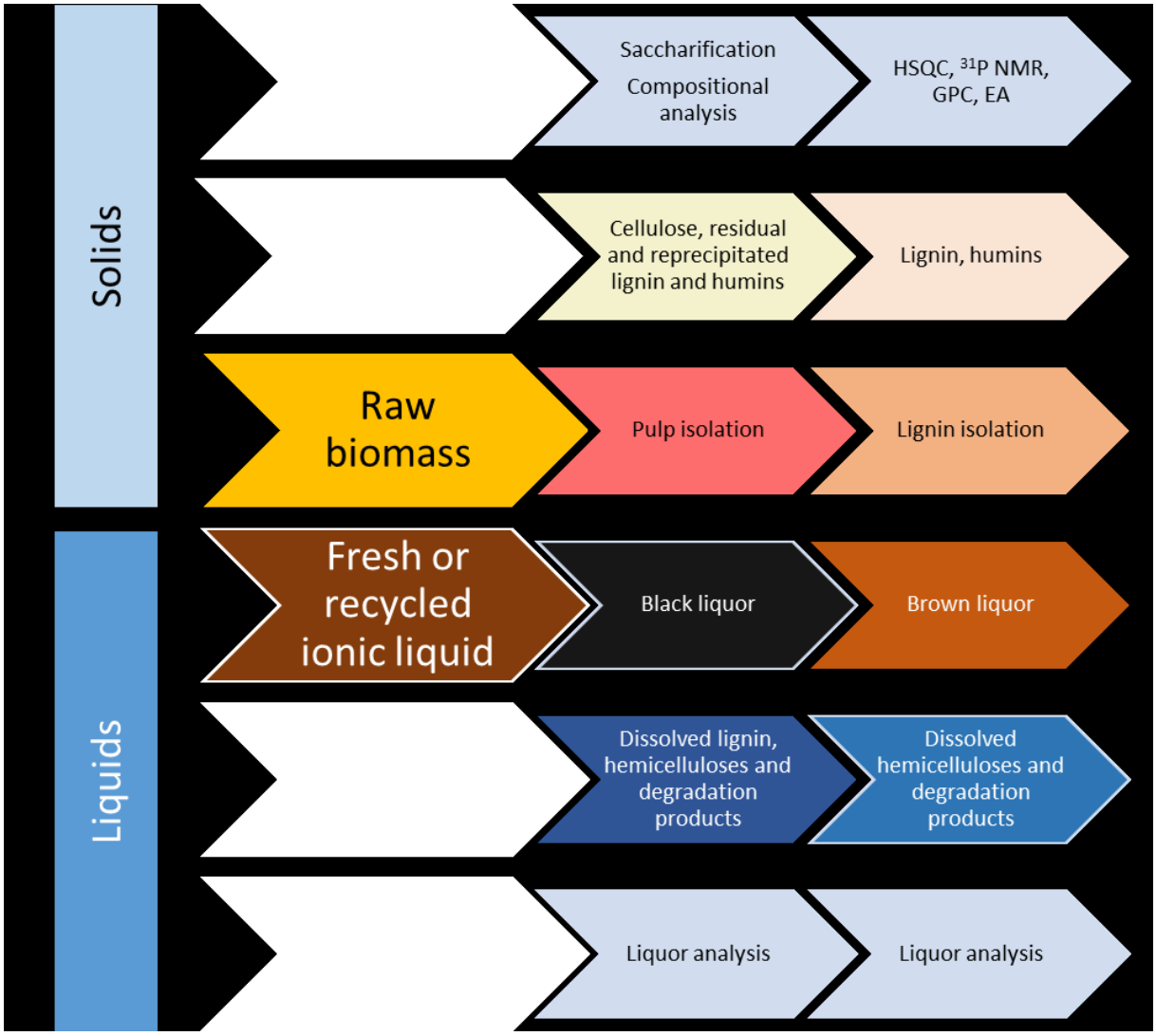

Figure I-12 Composition of the various components during the different stages of the process and the analytical techniques used for analysis.

Thesis Outline

Firstly, the experimental methods are reported, in order to allow the reader to better understand the results discussed in the following results chapters. These are structured as follows and include a short literature review at the beginning, summarising the most relevant information for the respective chapter. An initial study was conducted to examine the use of triethylammonium hydrogensulfate,

[TEA][HSO_4], for the pretreatment of *Miscanthus*. After a first study at 120°C, higher temperatures were tested. These results are discussed in the first results chapter. I then went on to pretreating other feedstocks. In Chapter 2, several ILs are investigated, examining the pretreatment of pine and many of the trends found for *Miscanthus* are observed again. I subsequently performed some process iterations in order to improve yields and throughput. The most important and exciting chapter is the third results chapter where metal containing construction wood is pretreated, as well as real mixed waste wood. Here I not only investigate the pretreatment from the perspective of the production of highly digestible pulps, but also the metal extraction and recovery. Finally, the production of ethanol via fermentation of the hydrolysed sugars is attempted. The fourth results chapter includes a more in depth analysis of the obtained lignins and a briefer analysis of the ionic liquid liquors and their solutes. Many of the observations from the first three chapters can only be explained and understood if lignin and hemicellulose chemistry is taken into account. Lastly, the most important results are summarised and discussed in the Conclusions.

Part II.Experimental Methods

General Materials and Equipment

Reagents and solvents were purchased from Sigma Aldrich and, unless stated otherwise, used as received. Sugars used for calibrations were at least 99% pure. The Karl-Fischer titrator used in this work was a V20 volumetric Titrator (Mettler-Toledo), the vortex shaker a VWR International REAX TOP and the analytical balance a Sartorius CPA 1003 S balance (±0.001 g).

Ionic Liquids

Starting materials for ionic liquid synthesis were purchased from Sigma Aldrich and, unless stated otherwise, used as received. The minimum purity of the starting materials was as follows: triethylamine ≥99%, *N,N*-dimethylbutylamine 99%, diethylamine ≥99.5%, 1-methylimidazole 99%, 1-butylimidazole 98%. HCl was obtained as a concentrate containing 1 mole (FIXANAL Fluka Analytical). Sulfuric acid was obtained from Sigma Aldrich as a 5M solution. Toluene was ACS, Reag. Ph. Eur., barium hydroxide was ≥98% and silver acetate 99.99% pure.

Protic ILs were synthesised according to the standard operating procedure of our laboratory.[1] In brief, the required amine or imidazole was weighed into a round-bottom flask and cooled with an ice bath. Under stirring, an equimolar amount of the required acid, typically as a 1 to 5M aqueous solution, was added dropwise. Excess water was removed first using a rotary evaporator (Büchi) and the product further dried using a Schlenk line at 40-70°C overnight. Since no work-up was involved, all yields were assumed to be quantitative. Aprotic ILs were synthesised according to a published procedure.[2]

1-ethyl-3-methylimidazolium chloride [C_2C_1im]Cl, 1-ethyl-3-methylimidazolium trifluoromethane-sulfonate [C_2C_1im][OTf] and diethanolammonium chloride [DEtOHA]Cl were purchased from Sigma Aldrich.

^{1}H, ^{13}C and HMQC NMRs were recorded on a Bruker 400 MHz spectrometer and can be found in the Appendix. Chemical shifts (δ) are reported in ppm, referenced to the DMSO signal at 2.500 (^{1}H dimension) and 39.520 (^{13}C dimension). Mass spectrometry was measure by Dr. Lisa Haigh (Imperial College London, Chemistry Department) on a Micromass Premier spectrometer.

Synthesis of triethylammonium hydrogensulfate [TEA][HSO_4]

Triethylamine (75.9 g, 750 mmol) was cooled with an ice bath in a 500 mL round-bottom flask. Under stirring, 150 mL of 5 M H_2SO_4 (750 mmol) were added dropwise. The water was removed using a rotary evaporator and the product dried using a Schlenk line at 40°C overnight. The ionic liquid was recovered as a white, hygroscopic solid.

^{1}H NMR: δH (400 MHz, DMSO-d^{6})/ppm: 3.39 (s (br), *H*SO_4^-, N-*H*$^+$), 3.10 (q, J = 7.3 Hz, 6H, N-C*H*$_2$), 1.20 (t, J=7.3 Hz, 9H, N-CH$_2$-C*H*$_3$). ^{13}C NMR: δC (101 MHz, DMSO-d^{6})/ppm: 46.21 (N-*C*H$_2$), 9.15 (N-CH$_2$-*C*H$_3$).

MS (Magnet FB$^+$) m/z: 102 ([TEA]$^+$, 100%), (Magnet FB$^-$) m/z: 79 ([HSO_4]$^-$, 100%).

Synthesis of *N,N*-dimethylbutylammonium hydrogensulfate [DMBA][HSO_4]

N,N-dimethylbutylamine (75.9 g, 750 mmol) was cooled with an ice bath in a 500 mL round-bottom flask. Under stirring, 150 mL of 5 M H_2SO_4 (750 mmol) were added dropwise. The water was removed initially using a rotary evaporator and the product further dried using a Schlenk line at 70°C overnight. The ionic liquid was recovered as a colourless, viscous liquid.

^{1}H NMR: δH (400 MHz, DMSO-d^{6})/ppm: 9.24 (s, 1H, N-*H*), 3.02 (dt, *J* = 12.9, 5.0 Hz, 2H, N-C*H*$_2$), 2.76 (d, *J* = 4.3 Hz, 6H, N-(C*H*$_3$)$_2$), 1.64 – 1.51 (m, 2H, N-CH$_2$-C*H*$_2$), 1.29 (h, *J* = 7.4 Hz, 2H, N-CH$_2$-CH$_2$-C*H*$_2$), 0.89 (t, *J* = 7.4 Hz, 3H, N-CH$_2$-CH$_2$-CH$_2$-C*H*$_3$). ^{13}C NMR δC (101 MHz, DMSO-d^{6})/ppm: 56.62 (N-*C*H$_2$), 42.48 (N-*C*H$_3$), 25.82 (N-CH$_2$-*C*H$_2$), 19.40 (N-CH$_2$-CH$_2$-*C*H$_2$), 13.71 (N-CH$_2$-CH$_2$-CH$_2$-*C*H$_3$).

MS (Magnet FB$^+$) m/z: 102 ([DMBA]$^+$, 100%), (Magnet FB$^-$) m/z: 79 ([HSO_4]$^-$, 100%).

Synthesis of diethylammonium hydrogensulfate [DEA][HSO_4]

Diethylamine (54.8 g, 750 mmol) was cooled with an ice bath in a 500 mL round-bottom flask. Under stirring, 150 mL of 5 M H_2SO_4 (750 mmol) were added dropwise. Excess water was removed using a rotary evaporator until a water content of below 20wt% was obtained. The ionic liquid water mixture was recovered as a colourless liquid.

^{1}H NMR: δH (400 MHz, DMSO-d^{6})/ppm: 8.27 (s, 2H, N*H*$_2$), 4.36 (s (br), *H*$_2$O, *H*SO_4), 2.91 (dt, *J* = 12.7, 6.6 Hz, 4H, N-(C*H*$_2$)$_2$), 1.15 (t, *J* = 7.3 Hz, 6H, N-(CH$_2$-C*H*$_3$)$_2$). ^{13}C NMR δC (101 MHz, DMSO-d^{6})/ppm: 41.77 (N-*C*H$_2$), 11.19 (N-CH$_2$-*C*H$_3$).

Synthesis of 1-butylimidazolium hydrogensulfate [HC_4im][HSO_4]

200 g of freshly distilled *N*-butylimidazole (1.61 mol) was cooled with an ice bath in a 1 L round-bottom flask. Under stirring, 322 mL of 5M H_2SO_4 (1.61 mol) were added dropwise. The water was removed initially using a rotary evaporator and the product further dried using a Schlenk line at 50°C overnight. The ionic liquid was recovered as a slightly pink, viscous liquid which changed colour over time to orange, golden and finally colourless.

^{1}H NMR: δH (400 MHz, DMSO-d^{6})/ppm: 9.14 (s, 1H, N-C*H*-N), 7.79 (s, 1H, N-C*H*), 7.68 (s, 1H, N-C*H*), 4.26 (br, N-*H*, *H*SO_4^-), 4.19 (t, J = 7.2 Hz, 2H, N-C*H*$_2$), 1.77 (m, 2H, N-CH$_2$-C*H*$_2$), 1.23 (m, 2H, N-CH$_2$-CH$_2$-C*H*$_2$), 0.88 (t, J = 7.4 Hz, 3H, N-CH$_2$-CH$_2$-CH$_2$-C*H*$_3$). ^{13}C NMR: δC (101 MHz, DMSO-d^{6})/ppm: 135.72 (N-*C*H-N*)*, 122.46 (N-*C*H*)*, 120.45 (N-*C*H*)*, 48.68 (N-*C*H$_2$), 31.90 (N-CH$_2$-*C*H$_2$), 19.29 (N-CH$_2$-CH$_2$-*C*H$_2$), 13.75 (N-CH$_2$-CH$_2$-CH$_2$-*C*H$_3$).

MS (Magnet FB^+) m/z: 125 ($[HC_4im]^+$, 100%), (Magnet FB^-) m/z: 79 ($[HSO_4]^-$, 100%).

Synthesis of 1-methylimidazolium hydrogensulfate [HC_1im][HSO_4]

1-Methylimidazole (102.6g, 1.25 mol) was cooled with an ice bath in a 1 L round-bottom flask. Under stirring, 250 ml of 5M H_2SO_4 (1.25 mol) were added dropwise. The water was removed initially using a rotary evaporator and the product further dried using a Schlenk line at 40°C overnight. The ionic liquid was recovered as a viscous colourless liquid.

^{1}H NMR: δ_H (400 MHz, DMSO-d^6)/ppm: 9.03 (s, 1H, H-2), 7.68 (s, 1H, H-4/5), 7.64 (s, 1H, H4/5), 4.70 (br, *H*SO_4^-, N-*H*$^+$), 3.87 (s, 3H, N-C*H*$_3$). HMQC: δ_C (101 MHz, DMSO-d^6)/ppm: 136.28 (C-2), 123.59 (C-4/5), 120.30 (C-4/5), 35.82 (N-*C*H_3).

MS (Magnet FB^+) m/z: 83 ($[C_1Him]^+$, 100%), (Magnet FB^-) m/z: 79 ($[HSO_4]^-$, 100%).

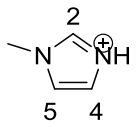

Synthesis of 1-methylimidazolium chloride [HC_1im]Cl

1-Methylimidazole (82.1g, 1.0 mol) was cooled with an ice bath in a 500 mL round-bottom flask. Under stirring, 1 mole of aqueous HCl was added dropwise. Excess water was removed using a rotary evaporator until a water content of below 20wt% was obtained. The ionic liquid water mixture was recovered as a yellowish liquid.

^{1}H NMR: δ_H (400 MHz, DMSO-d^6)/ppm: 9.16 (s, 1H, H-2), 7.71 (s, 1H, H-4/5), 7.64 (s, 1H, H4/5), 4.5-3.5 (br, *H*$_2$O, N-*H*$^+$), 3.87 (s, 3H, N-C*H*$_3$). ^{13}C NMR: δC (101 MHz, DMSO-d^6)/ppm: 135.63 (C-2), 123.21 (C-4/5), 119.55 (C-4/5), 35.48 (N-*C*H_3).

Synthesis of 1-ethyl-3-methylimidazolium acetate [C_2C_1im][OAc]

Synthesis of 1-ethyl-3-methylimidazolium bromide [C_2C_1im]Br

1-Methylimidazole was dried over KOH for 1 week under a nitrogen atmosphere and subsequently distilled under vacuum. Bromoethane was dried over P_2O_5 overnight under a nitrogen atmosphere and subsequently distilled.

1-methylimidazole (45 mL, 565 mmol) in toluene (200 mL) was cooled in an ice bath and bromoethane (70 mL, 938 mmol, 1.66 eq) was added dropwise over 1 hour. The reaction mixture was allowed to warm to room temperature and stirred for 3 days which lead to the formation of a white solid. Another 30 mL of bromoethane (402 mmol, 0.71 eq) were added and the mixture stirred for another 7 days. The solvent was removed via cannula filtration and the white solid washed with anhydrous ethyl acetate (50 mL). The white crystalline solid was dried in vacuum overnight (98.7 g, 92%).

^{1}H NMR: δ_H (400 MHz, DMSO-d^6)/ppm: 9.22 (s, 1H, H-2), 7.82 (t, J = 1.9 Hz, 1H, H-4/H-5), 7.73 (t, J = 1.7 Hz, 1H, H-4/H-5), 4.21 (q, J = 7.3 Hz, 2H, N-C*H*$_2$), 3.86 (s, 3H, N-Me), 1.42 (t, J = 7.3 Hz, 3H, CH$_2$-C*H*$_3$). ^{13}C NMR: δ_C (101 MHz, DMSO-d^6)/ppm: 136.73 (C-2), 124.03(C-4/5), 122.44(C-4/5), 44.58 (N-*C*), 36.19 (N-*C*), 15.61 (CH$_2$-*C*H$_3$).

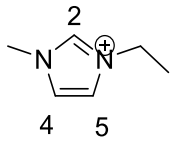

MS (Magnet FB$^+$) m/z: 111 ([C$_2$C$_1$im]$^+$, 100%), (Magnet FB$^-$) m/z: 79/81 ([Br]$^-$, 100%).

Synthesis of 1-ethyl-3-methylimidazolium acetate [C$_2$C$_1$im][OAc]

1-ethyl-3-methylimidazolium bromide (88.5 g, 463 mmol) was dissolved in 300 mL of water in an aluminium foil covered 500 mL flask. Silver acetate (77.8 g, 464 mmol, 1.00 eq) was added to the flask and the reaction mixture stirred at room temperature overnight. The precipitate was filtered off and the aqueous solution tested for silver and bromide ions by removing an aliquot and adding a 1M solution of 1-ethyl-3-methylimidazolium bromide and silver nitrate respectively. The deficient reactant was added until both tests were negative. The water was removed under reduced pressure and the product dried in vacuum overnight. 1-ethyl-3-methylimidazolium acetate was obtained as a colourless, free-flowing liquid (71.7 g, 91 %).

^{1}H NMR: δ_H (400 MHz, DMSO-d^6)/ppm: 9.46 (s, 1H, H-2), 7.80 (m, 1H, H-5), 7.72 (m, 1H, H-4), 4.20 (q, J = 7.3 Hz, 2H, N-C*H*$_2$), 3.86 (s, 3H, N-C*H*$_3$), 1.51 (s, 3H, CO$_2$-C*H*$_3$), 1.42 (t, J = 7.3 Hz, 3H, CH$_2$-C*H*$_3$). HMBC: δ_C (101 MHz, DMSO-d^6)/ppm: 173.03 (*C*O$_2$Me), 137.23, (C-2), 123.85 (C-4), 122.41 (C-5), 44.51 (N-*C*H$_2$), 36.09(N-*C*H$_3$), 26.83 (CO$_2$-*C*H$_3$), 15.62 (CH$_2$-*C*H$_3$).

MS (Magnet FB$^+$) m/z: 111 ([C$_2$C$_1$im]$^+$, 100%), (Magnet FB$^-$) m/z: 59 ([Acetate]$^-$, 100%).

Biomass Feedstock

Pinus sylvestris was obtained from Metla (Finish Forest Research Institute). *Miscanthus x giganteus* was obtained from Silwood Park campus (Imperial College London, UK). Beech wood chips were obtained from Rettenmaier & Söhne GmbH (DE). Infeed and processed waste wood was received from Sita UK (now Suez, UK). CCA treated wood was received from 天津市东丽区艺林木材防腐加工厂 (Tianjin Dongli District Yilin wood preservative processing plant, CN). Copper treated timber was purchased from Travis Perkins (UK). All biomass was air-dried, chopped (Retch SM 2000) and sieved (Retsch AS 200) (180-850 µm, -20 + 80 US mesh scale) prior to use and stored in plastic bags at room temperature in the dark.

Fractionation of Biomass

During pretreatment experiments, all weights were recorded using an A&D GH-252 with an accuracy of ±0.1 mg. Pretreatments were run in a Thermo Scientific HERA THERM convection oven, which was also used for the determination of oven dried weights. Lignin was dried in a Binder VD 23 vacuum oven. A C-28 centrifuge from Boeco, Germany was used.

For all types of biomass and recovered pulp the oven-dried weight (ODW) was determined by weighing out approximately 100 mg of biomass/pulp onto a preweighed piece of aluminium foil and recording the weight. The foil with the biomass/pulp was folded and oven dried (T=105°C) overnight. The next day, the hot packets were taken out of the oven and placed in a desiccator to allow cooling to room temperature. The new weight was recorded immediately afterwards and the moisture content calculated. This was done in triplicates for untreated biomass and once per sample for recovered pulp.

Pretreatments, determination of oven dried weight and ionic liquid water content measurements were conducted according to the standard operating procedure from our laboratory[3] in triplicates. An ionic liquid/water mix was prepared and its water content analysed by Karl-Fischer titration in triplicates.

A biomass to solvent ratio of 1:20 to 1:2 g/g was used on an oven dried basis. Pretreatments were conducted with a final water content of 20wt% according to *Equation 1*:

$$\%water = \frac{m_{IL} \cdot wc_{IL} + m_{BM} \cdot mc_{BM} + m_{water}}{m_{IL} + m_{water}}$$

Equation 1

Where m_{IL} is the mass of the IL solution, $w_{IL}$is the water content of the IL solution, m_{BM} is the biomass weight, mc_{BM} is the moisture content of the biomass and m_{water} is the weight of the water added in order to reach 20wt%. The moisture content was taken into account in order to make experiments at different loading more comparable since the amount of moisture in the biomass becomes more significant at higher loadings.

A summary of the pretreatment process is shown in Figure II-1. The required amount ±0.05 g of ionic liquid/water mix was weighed into a glass pressure tube and the exact weight recorded. The required amount of biomass ±0.02 g was added together with the required amount of water (if any) which was added with an Eppendorf pipette. The vials were capped and the content mixed with a vortex shaker. They were then placed into a preheated convection oven. After the pretreatment period, they were taken out and allowed to cool to room temperature. Experiments were carried out in triplicates.

For experiments with added CuO, the prepared IL/water mix was weighed into the pressure tubes and 100±10 mg of CuO added to it. The mixture was shaken and left at room temperature overnight to allow the copper to partially dissolve into the ionic liquid. The biomass is added the next day and instructions followed as described above.

After the pretreatment, 40 mL of ethanol was added to the pretreatment mixture and the suspension transferred into a 50 mL Falcon tube. The tube was shaken for one minute and the mixture then left at room temperature for at least 1 hour. The tube was mixed again for 30 seconds and then centrifuged at 4000 rpm for 50 minutes. The supernatant was decanted carefully into a round bottom flask. The washing step was repeated three more times. The remaining pulp was then transferred into a cellulose thimble and further washed by Soxhlet extraction with refluxing ethanol (150 mL) for 22 hours. The thimbles were then left on the bench overnight to dry. The ethanol used for the Soxhlet extraction was combined with the previous washes and evaporated under reduced pressure at 40°C, leaving the dried ionic liquid/lignin mixture. To the dried ionic liquid/lignin mixture, 30 mL of water was added in order to precipitate the lignin. The suspension was transferred into a 50 mL falcon tube, shaken for one minute and then left at room temperature for at least 1 hour. The tube was centrifuged and the supernatant decanted and collected in a round bottom flask. This washing step is repeated twice more and the water washings combined.

The air-dried pulp yield was determined by weighing the recovered biomass from the cellulose thimbles. The oven-dried yield was determined as described for the untreated biomass. The lid of the Falcon tube containing the lignin was pierced and the tube put into a vacuum oven overnight to dry at 40°C under vacuum. The dried lignin was weighed the next day.

For experiments where pulps were saccharified without air-drying in order to avoid hornification, the procedure was followed unchanged until the Soxhlet extraction step. The pulp containing thimbles were removed from the Soxhlet adapter after completion of the extraction and put in 50 mL falcon tubes which were immediately filled with DI water. The pulp was left in the thimble inside the falcon tube for at least an hour. The thimble was then taken out of the falcon tube and the pulp transferred back to the falcon tube using a spatula. The tubes were centrifuged for 30 min at 3000 rpm or 2000xG and the supernatant decanted. The pulp was weighed, its moisture content determined immediately and saccharifications started the following day.

For recycling experiments, the ionic liquid containing the combined water washings after the lignin precipitation was concentrated by evaporation of the excess water under reduced pressure at 40°C. Samples of the concentrated recycled ionic liquid were taken for further analysis, including Karl Fischer titration. The remainder of the recycled ionic liquid was transferred into a clean glass pressure tube

and the exact weight recorded. The required amounts of biomass and water were added and the regular protocol resumed.

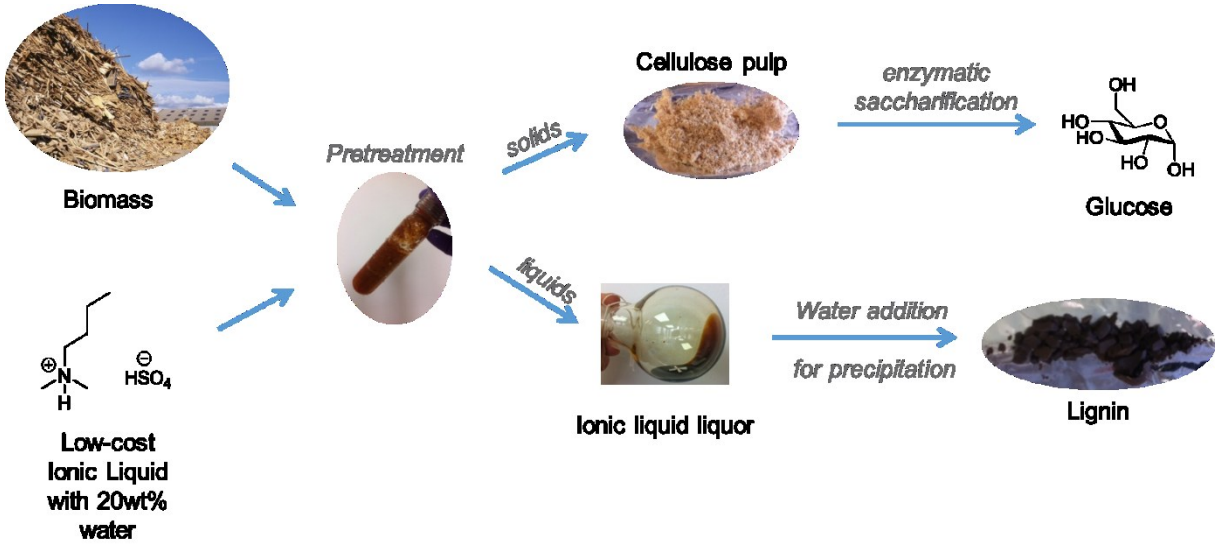

Figure II-1 Representation of one cycle of the ionoSolv process used. The IL and biomass shown are one example of several used in this thesis.

Pulp Analysis

Compositional Analysis

Compositional analysis was carried out according to a published procedure by the National Renewable Energy Laboratory (NREL).[4] 300 mg (calculated on ODW basis) of air-dry biomass or recovered pulp was weighed out into a pressure tube and the weight recorded. 3 mL of 72% sulfuric acid (Fluka) were added, the samples stirred with a Teflon stir rod and the pressure tubes placed into a preheated water bath at 30°C. The samples were stirred again every 15 min for one hour. They were then diluted with 84 mL distilled water and the lids closed. The samples were autoclaved (Sanyo Labo Autoclave ML5 3020 U) for 1 hour at 121°C and left to cool to close to ambient temperature. The samples were then filtered through filtering ceramic crucibles of a known weight. The filtrate was filled in two Falcon tubes and the remaining black solid washed with distilled water. The crucibles were placed into a convection oven (VWR Venti-Line 115) at 105°C for 24±2 hours to dry. They were then taken out and placed in a desiccator for 15 min before they were weighed and the weight recorded. They were then placed into a muffle oven (Nabertherm + controller P 330) and ashed to constant weight at 575°C. The weight after ashing was recorded. The content of acid insoluble lignin (AIL) was determined according to *Equation 2*. The content of one of the Falcon tubes was used for the determination of acid soluble lignin content (ASL) by UV analysis at 240 nm (*Equation 3*) (Perkin Elmer Lambda 650 UV/Vis spectrometer).

$$\%AIL = \frac{Weight_{crucible\ plus\ AIR} - Weight_{crucible\ plus\ ash}}{ODW_{sample}} \cdot 100$$

Equation 2

$$\%ASL = \frac{A}{l \cdot \varepsilon \cdot c} \cdot 100 = \frac{A \cdot V_{filtrate}}{l \cdot \varepsilon \cdot ODW_{sample}} \cdot 100$$

Equation 3

where $Weight_{crucibles\ plus\ AIR}$ is the weight of the oven-dried crucibles plus the acid insoluble residue, $Weight_{crucibles\ plus\ ash}$ is the weight of the crucibles after ashing to constant temperature at 575°C, A is the absorbance at 240 nm, l is the path length of the cuvette in cm (1 cm in this case), ε is the extinction coefficient (12 L/g cm), c is the concentration in mg/mL, ODW is the oven-dried weight of the sample in mg and $V_{filtrate}$ is the volume of the filtrate in mL and equal to 86.73 mL.

To the contents of the other Falcon tube, calcium carbonate was added until the pH reached 5. The liquid was passed through a 0.2 µm PTFE syringe filter and subsequently submitted to HPLC analysis (Shimadzu, Aminex HPX-97P from Bio rad, 300 x 7.8 mm, purified water as mobile phase at 0.6 ml/min, column temperature 85°C) for the determination of total sugar content. A representative chromatogram can be found in the Appendix. Calibration standards with concentrations of 0.1, 1, 2 and 4 mg/mL of glucose, xylose, mannose, arabinose and galactose were used. Sugar recovery standards were made as 10 mL aqueous solutions close to the expected sugar concentration of the samples and transferred to pressure tubes. 278 µL 72% sulfuric acid was added, the pressure tube closed and autoclaved and the sugar content determined as described above. The sugar recovery coefficient (SRC) was determined according to *Equation 4* and the sugar content of the analysed sample using *Equation 5*:

$$SRC = \frac{c_{HPLC} \cdot V}{initial\ weight}$$

Equation 4

$$\%Sugar = \frac{c_{HPLC} \cdot V \cdot corr_{anhydro}}{SRC \cdot ODW_{sample}} \cdot 100$$

Equation 5

where c_{HPLC} is the sugar concentration detected by HPLC, V is the initial volume of the solution in mL (10.00 mL for the sugar recovery standards and 86.73 mL for the samples), initial weight is the mass

of the sugars weighed in, $corr_{anhydro}$ is the correction for the mass increase during hydrolysis of polymeric sugars obtained by dividing the molecular weight of one polymeric sugar by its monomeric weight (0.90 for C6 sugars glucose, galactose and mannose and 0.88 for C5 sugars xylose and arabinose) and ODW is the oven-dried weight of the sample in mg.

Correlations between delignification and saccharification yields were calculated using least squares linear regression in Excel.

Saccharification Assay

Saccharification assays were carried out according to an adapted procedure by the NREL[5] in triplicates with blanks (also triplicates). All reagents were purchased from Sigma Aldrich.

For wet samples, moisture contents were determined again directly prior to saccharification. 100±10 mg (on and ODW basis) of air-dried or wet biomass were placed into a Sterilin tube and the weight recorded. Three blanks were run with 100 µL of purified water instead of biomass in order to correct for sugar residues present in the enzyme solutions. The water contained in the biomass sample was (calculated using its moisture content and the total sample mass) subtracted from 1.5 mL. The difference was added as water using a pipette. 8.4 mL solution consisting of 5 mL 1M sodium citrate buffer at pH 4.8, 40 µL tetracyline antibiotic solution (10 mg/mL in 70% ethanol), 30 µL cycloheximide antibiotic solution (10 mg/mL in purified water), 3.38-3.41 mL purified water and 20-50 µL of Novozymes experimental enzyme mixture NS-22201 (kindly provided directly by Novozymes) were added, the tubes closed and placed into an Stuart Orbital Incubator (S1500) for 7 days at 50°C and 250 rpm.

Saccharification yields were obtained by filtering 1 mL of the saccharification mixture through a PTFE syringe filter. Samples were run on Shimadzu HPLC with an AMINEX HPX-97P column (Bio rad, 300 x 7.8 mm) with purified water as mobile phase (0.6 mL/min). The column temperature was 85°C and acquisition was run for 20 min. A representative chromatogram can be found in the Appendix. Calibration standards with concentrations of 0.1, 1, 2 and 4 mg/mL of glucose, xylose, mannose, arabinose and galactose and 8 mg/mL of glucose were used.

Lignin characterisation

Elemental analysis was carried out by Stephen Atkin from Sheffield University.

HSQC NMR

For HSQC experiments of precipitated lignin, ca. 20 mg of lignin was dissolved in 0.25 mL of DMSO-d_6 and the solution transferred to a Shigemi tube. HSQC NMRs were recorded on a Bruker 600 MHz

spectrometer (pulse sequence hsqcetgpsi2, spectral width of 10 ppm in F2 (^{1}H) with 2048 data points and 160 ppm in F1 (^{13}C) with 256 data points, 16 scans and 1 s interscan delay).

Spectra were analysed using MestReNova (Version 8.0.0, Mestrelab Research 2012). All spectra were referenced to the DMSO peak at 2.500 ppm (^{1}H) and 39.520 ppm (^{13}C). Integrals were obtained for spectra of the same series of experiments simultaneously to ensure that the same areas were integrated by adding all relevant spectra to one file and selecting all of them while integrating the relevant area in one spectrum. Integration areas were selected visually according to peak assignments found in literature.[6] For ether linkages, the C-H_{α}-signals were integrated. Integrals are reported with respect to 100 (G_2+$G_{2,cond}$) signals. All spectra can be found in the Appendix.

^{31}P-NMR analysis

A solution of 1.6:1 (v/v) of anhydrous pyridine and deuterated chloroform was prepared. This 'stock solution' was used to prepare a further two mixtures: (1) a solution 20 mg/mL of the internal standard cyclohexanol (99%) dissolved in the stock solution, (2) a solution containing 5.6 mg/mL of chromium (III) acetylacetonate, a relaxation agent. The lignin was dried under vacuum (1 mbar) at 40-45°C for 24 hours. 10±2 mg dried lignin were weighed into a clean HPLC glass vial. To each lignin sample, the following reagents were added: 100 µL of anhydrous pyridine and deuterated chloroform solution, 50 µL of the cyclohexanol solution (1), 50 µL of the phosphitylating reagent 2-chloro-4,4,5,5-tetramethyl-1,3,2-dioxaphospholane (TMDP) and 50 µL of the relaxation agent solution (2). The sealed final mixture was vortex-mixed intensely for 5 minutes or until completely dissolved and transferred to a Shigemi tube. An inverse gated decoupling pulse sequence was used to obtain quantitative spectra on a Bruker Avance 500 MHz NMR machine using the following settings: 298 K (room temperature), Relaxation delay 25 s, 30° pulses, 127 scans. The quantity of the various hydroxyl group types was determined by integration using MestReNova relative to the concentration of the internal standard. The spectra can be found in the Appendix.

Gel permeation chromatography

GPC measurements were performed using an Agilent 1260 Infinity instrument equipped with a Viscotek column set (AGuard, A6000M and A3000M). The Agilent 1260 Infinity RID detector was used for detection. HPLC grade DMSO containing LiBr (1 g/L) was used as eluent at a flow rate of 0.4 mL/min at 60°C. Samples were prepared by dissolving 20 mg lignin in 1 ml eluent and filtering through a 0.2 µm syringe filter. Ten pullulan standards (Agilent calibration kit, 180 < Mp < 780,000) were used to calibrate the instrument.

Liquor characterisation

Ionic liquid solutions were analysed directly after pretreatment by removing ca. 200 mg of the solution with a pipette into an Eppendorf micro centrifuge tube. The exact weight was recorded, ca. 600 mg of water added and the exact weight recorded again. The tube was shaken and centrifuged with a VWR MICRO STAR 17R centrifuge at 4°C and 13.3 G for 10 min to remove any water-insoluble material. The supernatant was pipetted off into a HPLC vial and submitted for analysis on a Shimadzu HPLC system with RI and UV/Vis detector and an Aminex HPX-87H column (BioRad, 300 x 7.8 mm) with 0.01 M H_2SO_4 as mobile phase (0.6 mL/min). The column temperature was 55°C and acquisition was run for 55 min. A representative chromatogram can be found in the Appendix. Calibration was carried out using standards with concentrations of 0.01, 0.02, 0.1, 0.2 and 0.4, 1, 2 and 4 mg/mL of glucose, xylose, arabinose, furfural (99%), 5-HMF (99%), levulinic acid (≥98%), glacial acetic acid and formic acid (≥95%). Analyte concentrations in the HPLC sample were calculated using the resulting calibration curves (linear regression). The mass fraction w/w of analytes detected in the ionic liquid solution (in mg/g of dried biomass) was determined using *Equation 6*:

$$w/w = \frac{c_{HPLC} \cdot (m_{sample} + m_{water}) \cdot m_{IL}}{\rho_{HPLC} \cdot m_{sample} \cdot (1 - wc_{sample}) \cdot ODW_{BM}}$$

Equation 6

C_{HPLC}: analyte concentration as determined by HPLC analysis in mg/mL; m_{sample}: mass of ionic liquid solution sampled in mg; m_{water}: mass of water added in order to dilute IL sample in mg; m_{IL}: dry mass of ionic liquid used for pretreatment in g; ρ_{HPLC}: density of HPLC sample in g/mL (value used 1.045 g/mL); wc_{sample}: water content of the sample; ODW_{BM}: oven dried weight of the biomass used for pretreatment in g.

Trace Element Analysis

Inductively coupled plasma optical emission spectrometry (ICP-OES) measurements were performed on a Perkin Elmer Optima 2000. Standards were prepared using Multielement standard solution 4 for ICP in 10% nitric acid (TraceCERT). The standard solution was diluted with 5% nitric acid as required to obtain at least 3 different concentrations for calibration with no metal at a concentration higher than 25 ppm. Ionic liquid liquors were diluted to approximately 1wt% ionic liquid concentration with 5% nitric acid. In the case of IL liquors with high concentrations of metals, this solution was further diluted to obtain a maximum concentration of each metal of no more than 25 ppm. All solutions were filtered through a 0.4 µm syringe filter prior to analysis.

For analysis of solid samples (biomass, pulp and lignin) approximately 100 mg of sample was weighed out and the exact weight recorded (±0.1 mg, Mettler Toledo NewClassic MS). The samples were

digested in 1 mL 69% nitric acid in a closed PTFE vessel (MARSXpress vessels and microwave with power/time control by CEM with the following sequence: 300 W at 83% power for 5 min, 600 W at 66% power for 5 min and 1200 W at 58% power for 6 min). The obtained solution was cooled in a freezer for an hour before diluting to 10mL with 5% nitric acid and filtration through a 0.4 µm PTFE syringe filter.

Percentage recovery of metal M in the pulp was calculated according to *Equation 7*, in IL liquor according to *Equation 8*, and in lignin according to *Equation 9*:

$$\%M_{pulp} = \frac{c_{M,pulp}}{c_{M,BM} \cdot r_{pulp}}\%$$

Equation 7

$$\%M_{IL,n} = \frac{c_{M,IL,n}}{c_{M,BM} \cdot ODW_{BM}/(m_{IL} \cdot (1 - wc_{IL})) + c_{M,IL,n-1}}\%$$

Equation 8

$$\%M_{lignin} = \frac{c_{M,lignin}}{c_{M,BM} \cdot r_{lignin}}\%$$

Equation 9

Where $c_{M,x}$ is the concentration of metal M in component x as measured by ICP-OES, IL,n is the ionic liquid liquor at cycle n, BM is the biomass, r_x is the recovery of component x after pretreatment with respect to the initial biomass weight on an oven-dried basis, ODW_{BM} is the oven-dried weight of the biomass used in pretreatment, m_{IL} is the initial weight of IL solution used for pretreatment and wc_{IL} is the water content of this solution. Extraction of metal M from the biomass is then calculated as 100-$\%M_{pulp}$.

Fermentation

Saccharomyces cerevisiae BY4741 [MATa his3Δ1 leu2Δ0 met15Δ0 ura3Δ0] was used for fermentation studies. Single colonies were used to inoculate 50 mL of YPD medium in 250 mL baffled flasks in triplicate and grown for 16 hours at 30 °C with shaking at 250 rpm. The optical density of these cultures was measured and used to inoculate 7.5 mL of YPD containing varying concentrations of $CuSO_4$ ranging from 128 mM to 100 nM at an initial optical density between 0.05 and 0.15. 7.5 mL medium containing cells was then transferred to individual wells of a 24-well deep well plate (Corning). Plates were sealed with a plastic, non-breathable sealing film (Eppendorf) and cells were cultured anaerobically at 30°C, 100 rpm for 24 hours. The cultures were pelleted by centrifugation and the supernatant was retained for HPLC analysis. The cell pellet was resuspended in 1 mL phosphate buffered saline, transferred to a pre-weighed microcentrifuge tube and pelleted by centrifugation at

3000 rpm. Samples were dried at 100°C for 24 hours and the dry cell weight was determined using an analytical balance (Mettler-Toledo).

Fermentation of hydrolysed wood samples was carried out in small volumes in 1.5 mL microcentrifuge tubes (Eppendorf). Saccharification was carried out so as to obtain final sugar concentrations of around 20 mg/mL: around 330 mg of pretreated samples and 1.6 g of non-pretreated samples were incubated in a medium consisting of 4 mL of 5 M sodium citrate buffer, 4 mL of DI water and 400 µL of CTec2 enzyme mix. Saccharified wood samples were centrifuged to remove the solids and the resulting glucose containing solution was used to make a medium by mixing with 1X yeast nitrogen base with amino acids (Sigma Aldrich). Samples were standardized to the amount of pulp added to the saccharification reaction. Controls containing copper were prepared as follows: a) for samples of pre-treated pine the amount of copper used was equivalent to the total amount of copper in the copper treated wood before extraction as measured by ICP-OES (in this instance 1.118 mM); b) for samples of CCA-treated wood that had undergone extraction, the copper content was adjusted to the original.

For the assay, single colonies were used to inoculate YPD medium as described above. After 16 hours of growth, cultures were diluted to an OD600 of 0.1 in PBS. 1 mL was transferred to each microcentrifuge tube, cells were pelleted by centrifugation, the supernatant was removed and the cell pellet was resuspended in 1 mL of the appropriate wood medium. Cells were grown at 30°C with shaking at 100 rpm in a Vortemp^{TM} 56 shaking incubator (Labnet International) for 48 hours, then fed once with an additional 500 µL of medium and grown for a further 48 hours. The OD600 of cultures was measured against a blank of the same type of medium and then the cells were pelleted by centrifugation and the supernatant retained for HPLC analysis.

The supernatant was pipetted into a HPLC vial and submitted for analysis on a Shimadzu HPLC system with RI and UV/Vis detector and an Aminex HPX-87H column (BioRad, 300 x 7.8 mm) with 0.01 M H_2SO_4 as mobile phase (0.6 mL/min). The column temperature was 55°C and acquisition was run for 60 min. A representative chromatogram can be found in the Appendix. Calibration was carried out using standards with concentrations of 0.01, 0.1, 0.4, 1, 2, 4 and 10 mg/mL of absolute ethanol. Ethanol concentrations in the HPLC sample were calculated using the resulting calibration curves.

Electrochemistry

Cyclic Voltammetry

Cyclic voltammetry (CV) was carried out in a three-electrode cell at room temperature. Platinum foil was used as working and counter electrode, both with an active area of 5.1 cm^2. A AgCl|Ag reference electrode was placed externally to the cell and connected to the main compartment through a Luggin

capillary whose tip was placed as close to the working electrode surface as possible. Potential values are reported with reference to AgCl|/Ag. The electrochemical cell was controlled to an Autolab PGSTAT30 potentiostat/galvanostat. Three consecutive voltammograms with a scan rate of 10 mV s^{-1} were performed from 0.6 to -0.7 V starting at 0.3 V with a negative-going potential sweep.

Cyclic voltammograms of the recycled IL liquors was measured using printed electrodes obtained from DropSens (DRP-110, Spain) with carbon anode and cathode and silver as a quasi-reference. The electrode was connected to the potentiostat (BioLogic SP300, using EC-Lab Software) with a cable connector for screen-printed electrodes (DRP-CAC, DropSens, Spain). A drop of 50 µL was placed on the chip, making sure it covered all three electrodes. The scan rate was 10 mV s^{-1}.

Deposition of Copper

Deposition of copper was carried out by performing a chronopotentiometry experiment in a two-electrode cell at room temperature. Copper foil was used as the dissolving anode and glassy carbon as the cathode, both with an active area of 5.1 cm^2. A current of 0.1 A was applied for 60 min. The electrochemical cell was connected to an Autolab PGSTAT30 potentiostat/galvanostat.

Charge Yield

Charge yield measurements were carried out by performing a chronoamperometry experiment in a two-electrode cell at room temperature. A potential of -0.5 V was applied for 30 s followed by a potential of +0 V for 30 s. The electrochemical cell was connected to an Autolab PGSTAT30 potentiostat/galvanostat.

Reduction of metal content

Reduction of metal content was carried out by performing a chronoamperometry experiment using printed electrodes obtained from DropSens (DRP-110, Spain) with carbon anode and cathode, and silver as a quasi-reference. The electrode was connected to the potentiostat (BioLogic SP300, using EC-Lab Software) with a cable connector for screen-printed electrodes (DRP-CAC, DropSens, Spain). A drop of 50 µL was placed on the chip, making sure it covered all three electrodes. A potential of -0.7 V was applied for a defined amount of time. Most of the drop was collected carefully so as not to remove metal from the electrode surface using an Eppendorf pipette and its weight recorded. It was diluted to 10 mL using 5% HNO_3 and submitted to ICP-OES analysis.

References

1 P. Verdía, A. Brandt, J. P. Hallett, M. J. Ray and T. Welton, *Green Chem.*, 2014, **16**, 1617.

2 M. T. Clough, K. Geyer, P. a Hunt, J. Mertes and T. Welton, *Phys. Chem. Chem. Phys.*, 2013, **15**, 20480–95.

3 F. J. V. Gschwend, A. Brandt, C. L. Chambon, W.-C. Tu, L. Weigand and J. P. Hallett, *J. Vis. Exp.*, 2016.

4 A. Sluiter, B. Hames, R. Ruiz, C. Scarlata, J. Sluiter, D. Templeton and D. Crocker,

Determination of Structural Carbohydrates and Lignin in Biomass, 2012.
5 M. G. Resch, J. O. Baker and S. R. Decker, *Low Solids Enzymatic Saccharification of Lignocellulosic Biomass Laboratory Analytical Procedure (LAP)*, 2015.
6 A. Brandt, L. Chen, B. E. van Dongen, T. Welton and J. P. Hallett, *Green Chem.*, 2015, **17**, 5019–5034.

Part III. Results

Chapter 1: [TEA][HSO_4] Meets *Miscanthus*

The biomass which has been studied in this work is *Miscanthus x giganteus*, a hybrid between *Miscanthus sinensis* and *Miscanthus sacchariflorus*. Originating from tropical areas of Asia, it has been grown widely in Europe and North America as an energy crop[1] and can grow up to 4 m high.[2] Compared to annual crops such as corn, perennial crops (for example, grasses - including *Miscanthus*) have significantly higher yields and much lower maintenance requirements.[3] Additionally, perennial plants have a low establishment cost and a greater resilience to drought, making them attractive bioenergy crops. Furthermore, they have much lower fertilizer requirements than annual biofuel crops and hence lower N_2O emissions.[4] N_2O emissions are an important factor in LCA of biofuels as the 100 year global warming potential of N_2O is 298 times greater than of CO_2.[5] *Miscanthus* yields in the US and Southern Europe reach over 40 t/ha dry matter per year while they are closer to 10-20 t/ha dry matter per year in Northern Europe.[6] *Miscanthus* has therefore been chosen as a promising feedstock for a sustainable biorefinery in the first part of this project.

The exact composition of *Miscanthus* cell walls depends on a variety of factors and several studies have been conducted in order to evaluate environmental and genetic factors to improve cell wall composition for a specific application.[7] A study in Wales showed that *Miscanthus x giganteus* has a higher content of cellulose and lignin and a lower hemicellulose content than the other two *Miscanthus* species mentioned.[1] The growth site has been found to influence cellulose and hemicellulose content, but not lignin content.[1] *Miscanthus* harvested in winter was reported to exhibit higher lignin contents than if harvested in autumn.[7]

The use of *Miscanthus* for the production of fuels and chemicals has been receiving much attention over the past two decades and a comprehensive review has been published looking at pretreatment and thermal technologies for its conversion.[6] Various pretreatment technologies have successfully been used to achieve high sugar yields from *Miscanthus.* Using a solution of NaOH and urea at room temperature for pretreatment, 70% of theoretical glucose yield was achieved after 72 h of hydrolysis.[8] The effect was attributed to a combination of an opening of the fibres and a decrease of the crystallinity of the cellulose, while deposition of lignin droplets was prevented. Ammonia Fibre Expansion (AFEX) pretreatment of *Miscanthus x giganteus* resulted in 96% glucan and 81% xylan conversion after 7 days of hydrolysis.[9] Acid pre-soaking followed by wet explosion, i.e. a combination of wet oxidation, in this case using hydrogen peroxide, and steam explosion, of *Miscanthus* resulted in 64% glucose yield after 96 h of enzymatic hydrolysis.[10] DA pretreatment of *Miscanthus x giganteus* gave 83% glucose yield after 72 h hydrolysis time.[11] As discussed in the introduction, certain ionic

liquids can be used to fully dissolve lignocellulosic biomass. Padmanabhan *et al.* have successfully dissolved up to 5wt% of vacuum dried *Miscanthus* in various ionic liquids including [C_2C_1im][OAc].[2] [C_2C_1im][OAc] was further used to pretreat *Miscanthus* at 160°C for 90 min, yielding a highly digestible pulp which released 90% of sugars after 24 hours of hydrolysis.[12] Delignification was enhanced when the pretreatment was run under a gaseous ammonia or oxygen atmosphere at 9 bar.[13] A mixture of formic acid, acetic acid and water was used to pretreat *Miscanthus* at 107°C for 3 hours, resulting in 86.5% deglignification[14] while the glucose yield from enzymatic saccharification was 76%.[15] While these findings are promising, there is still a lot of progress to be made in order to make second generation bioethanol economically viable. Techno-economic analysis of second generation bioethanol technologies show that solvent cost and recovery are amongst the most sensitive parameters.[16] This chapter focuses on using a low-cost solvent and the potential of process intensification and acceleration by an increased solids to liquid ratio and temperature.

In the first part of this study, virgin *Miscanthus* biomass was pretreated by solutions of 80 wt% of the low-cost ionic liquid [TEA][HSO_4][17] (Figure III-1) with 20 wt% water at a 1:10 solids to solvent ratio at 120°C for various lengths of time. A study comparing various amine based hydrogensulfate salts to [C_2C_1im][OAc] for the pretreatment of switchgrass has found [TEA][HSO_4] to be the best performing amine based ionic liquid of the investigated selection.[18] Indeed this protic ionic liquid was shown to be 75% as effective as [C_2C_1im][OAc] while costing 40 times less. In the second part of this study, the solids to solvent ratio was increased to 1:5 and different temperatures between 150 and 180°C were studied. By increasing the reaction temperature, a shortening of the required reaction time is expected. Combined with an increase in solids loading this is expected to result in a higher space-time yield and thereby reduce the required reactor volume which in turn lowers the reactor capital cost.

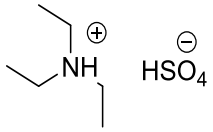

Figure III-1 [TEA][HSO_4].

This chapter conducts a preliminary investigation into factors affecting the pretreatment outcome and in that context also discusses the removal and re-deposition of lignin; however, a more detailed lignin analysis is discussed in Chapter 4.

As explained in the experimental section (or original reference[19]), it should be noted that the reactions were carried out unstirred in small glass pressure tubes which were placed inside a preheated oven at a fixed temperature for a given amount of time. The experiments were therefore conducted under non-isothermal conditions. Indeed, vessels containing the biomass and ionic liquid were at room

temperature at the beginning of each experiment, following a heating period until the pretreatment temperature was reached. When the pre-treatment time was completed, the samples were taken out of the oven and allowed to cool down to room temperature by natural convection.

In order to track the actual temperature profiles of the reaction medium inside the vessels, a thermocouple was placed in a glass pressure tube containing [TEA][HSO_4] with 20wt% water. A typical reaction medium temperature profile is given in Figure III-2 for 180°C. It can be seen that the reaction medium reached 160°C after 15 min heating, and 178°C (99% of the oven temperature) after 30 min heating time. The cooling time from reaction temperature to room temperature was about 30 min. Similar profiles were observed for the other temperatures. This demonstrates that these long heating and cooling times need to be kept in mind when interpreting the results, especially for high temperatures and short pretreatment times (30 min or less). It is important to mention that the temperature profiles were not measured during the actual experiments but were determined separately.

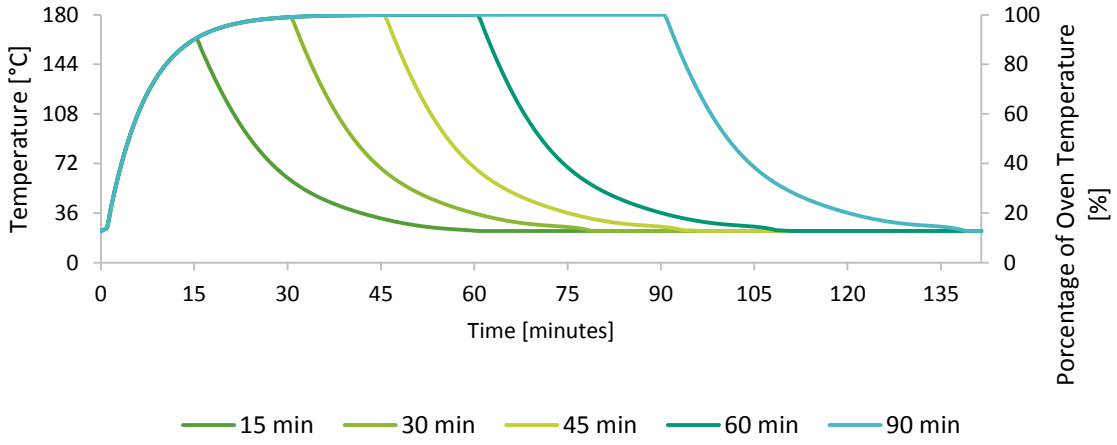

Figure III-2 Reaction medium temperature as a function of time for different pretreatment times at an oven temperature of 180°C. Data obtained from Francisco Malaret.

Pretreatments, saccharification and compositional analysis at 150-180°C were carried out by Dr Somnath Shinde, however all data analysis was performed by the author. The results discussed for the *Miscanthus* time course at 120°C with and without excess acid have been published.[20]

Pretreatment Time Course at 120°C

Cellulose Rich Material (Pulp)

Yield and Compositional Analysis

The cellulose rich pulp is the undissolved material recovered after pretreatment by centrifugation, and is the desired product for isolating cellulose or producing glucose *via* saccharification. Figure III-3 shows the yield of the pulp at different pretreatment times at 120°C and a 1:10 solids loading as well

as its composition (numerical data shown in Table III-1). The data demonstrate that dissolution of material from the virgin biomass mainly occurred during the initial 4 h of the treatment, with little change in pulp composition from 8-24 h.

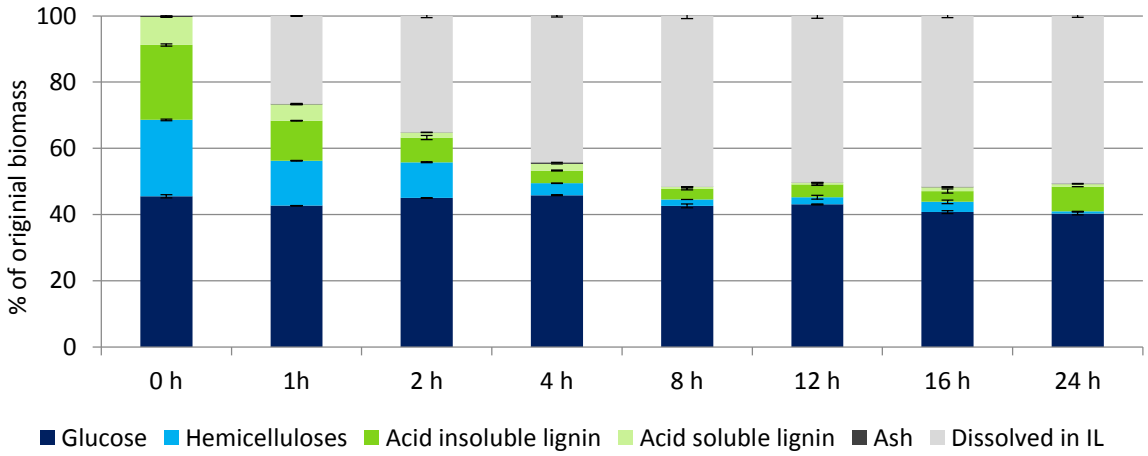

Figure III-3 Compositional analysis of Miscanthus pulp recovered after pretreatment with [TEA][HSO_4] at 120°C with a biomass to solvent ratio of 1:10 g/g and a final water content of 20wt%.

Table III-1 Pulp composition and yields and of lignocellulose components in the *Miscanthus* pulp as determined by compositional analysis as well as lignin precipitate after pretreatment with [TEA][HSO_4] at 120°C with a biomass to solvent ratio of 1:10 g/g and a final water content of 20wt%.

	Pulp Composition							Total pulpLignin	Precipitate
	Glu	Xyl	Ara	AIL	ASL	Ash	Extractives		
Untreated *Miscanthus*	47.3 ±0.8	20.1±0.5	2.2±0.5	22.4±0.1	4.0±0.1	0.6±0.4	2.8±0.1	100	N/A
1 h	42.7±0.1	13.6±0.1	-	12.1±0.1	4.9±0.1	0.2±0.1	N/A	73.5±0.2	7.1±0.1
2 h	45.0±0.0	10.8±0.1	-	7.4±0.7	1.5±0.0	-	N/A	64.8±0.5	10.5±0.0
4 h	45.8±0.2	6.6±0.1	-	3.8±0.2	2.0±0.0	0.5±0.0	N/A	58.8±0.4	15.4±0.1
8 h	42.6±0.6	4.9±0.0	-	3.2±0.3	0.6±0.0	-	N/A	51.3±0.8	19.8±0.7
12 h	43.1±0.2	3.5±0.6	-	3.8±0.2	0.6±0.0	-	N/A	51.0±0.7	20.8±2.9
16 h	40.8±0.5	2.7±0.5	-	3.22±0.7	1.1±0.0	0.2±0.0	N/A	48.0±0.6	21.5±2.0
24 h	42.2±0.4	-	-	3.41±0.0	0.8±0.0	0.1±0.0	N/A	46.4±0.4	19.1±0.2

N/A: not applicable; - not detected; standard deviation calculated for triplicate; Glu: Glucose; Xyl: Xylose; Ara: Arabinose; AIL: acid insoluble lignin; ASL: acid soluble lignin.

Compositional analysis of the pulp material confirmed the extraction of lignin and hemicellulose into the ionic liquid solution as the major reason for the mass loss relative to the initial biomass weight while glucan recovery was near quantitative throughout the time course. Hemicellulose sugars were barely detected after long pretreatment time (24 h), while the measured delignification, i.e. the removal of lignin, fell from ca. 90% at 16 h to below 80% at 24 h. Reasons for the increased lignin content in the pulp at longer pretreatment times are condensation reactions occurring in the lignin

leading to the formation of insoluble, high molecular weight (M_w) polymers (discussed more in detail in Chapter 4) as well as the formation of pseudo-lignin, a substance not exclusively formed by lignin but also by carbohydrate degradation products,[21–23] for which more evidence is discussed later in this chapter. The amount of glucan remaining in the pulp did not change significantly throughout the pretreatment (ca. 90-95% relative to the initial biomass), confirming that cellulose is stable in the ionic liquid under these conditions. I attribute the initial loss of glucan to the hydrolysis of mixed linkage glucans present in the hemicellulose of grasses[24] rather than the cellulose.

Enzymatic Saccharification

Saccharification of the cellulose-rich pulp with cellulolytic enzymes is a key measure of pretreatment effectiveness since enzyme cost and the reactor size of the hydrolysis tank are major cost-barriers.[25] The saccharification yields as a percentage of the respective sugars contained in the untreated biomass are shown in Figure III-4. The unhydrolysed fraction was either dissolved into the ionic liquid solution during pretreatment or is present in the pulp but not accessible to the enzymes within the analysed timeframe. The saccharification yields achieved after fractionation with the [TEA][HSO_4] solution are shown for both xylose and glucose.

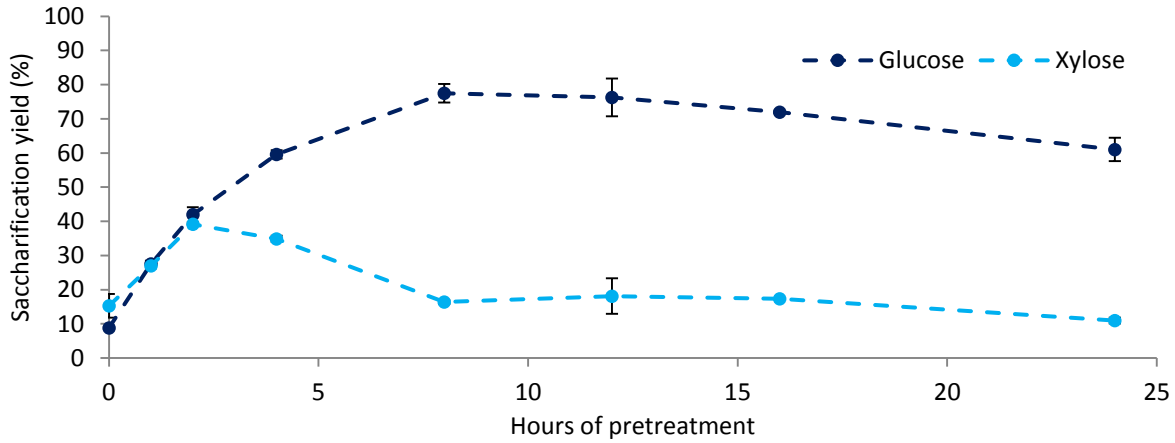

Figure III-4 Glucose and xylose yields after 7 days of enzymatic saccharification of Miscanthus pulp pretreated with [TEA][HSO_4] at 120°C with a biomass to solvent ratio of 1:10 g/g and a final water content of 20wt%. Yields are relative to the glucose and xylose content in the untreated *Miscanthus*. Errors were calculated as standard deviations across triplicates.

The highest glucose yield of 77% was achieved after 8 h of pretreatment; this is 1.7 times the saccharification yield achieved in the previous screening study (45%) using [TEA][HSO_4] for the fractionation of switchgrass,[18] however the authors fail to specify the pretreatment conditions, making it impossible to further explain this significant difference. The glucose yield peaked at around 8 h, something that was not observed in a previous study utilising [C_1C_4im][HSO_4] under otherwise equivalent conditions, where glucose yields remained high after extended treatment (up to 24 h).[26] I speculate that the decline in saccharification yield at longer pretreatment times is caused by re-

deposition of highly condensed lignin and pseudo-lignin onto the exposed cellulose fibrils,[22] and evidence for this was obtained from the results discussed below. The best saccharification yield obtained here is somewhat lower than yields obtained in the past with imidazolium based ionic liquids.[23,26] This is possibly due to a higher residual lignin content (ca. 20%) in the [TEA][HSO_4] pulp, which could include re-deposited lignin and pseudo-lignin, both of which have been reported to inhibit saccharification.[22,27] It was surprising that the glucose yields reached their maximum by 8 h at 120°C for both the triethylammonium and the 1-butyl-3-methylimidazolium based solvents,[23] given that the viscosity[28] and acidity[29] of the solutions are likely to be somewhat different.

The maximum xylose yield was achieved at around 2 h of pretreatment, where it reached 40%. At this time, xylose yields from the pulp became limited by hemicellulose removal, as can be seen by comparison with the pulp xylose content shown in Figure III-3 and the hemicellulose removal shown in Figure III-5. The fact that xylan and glucan yields cannot be optimized simultaneously in the presence of acidic solvents has been reported previously,[26,30] and indicates that the ionoSolv pretreatment is best utilized for producing high purity glucose streams rather than for maximizing pentose yields. Alternatively, hemicellulose pre-extraction using a less acidic medium may be able to afford hemicellulose oligo- or monomers.[31] The fate of hemicellulose sugars dissolved in the ionic liquid is discussed later on (Chapter 4).

Figure III-5 highlights the stability of glucan recovery in the pulp throughout the 24 h pretreatment course, compared to a very pronounced hemicellulose removal. The high glucan recovery may be linked to the moderate acidity of the ionoSolv solution and the fairly mild treatment temperature employed in this study. Figure III-5 also shows that the saccharification yield tracked glucan recovery between 8 h and 16 h, with the saccharification yield being somewhat lower than the glucan recovery.

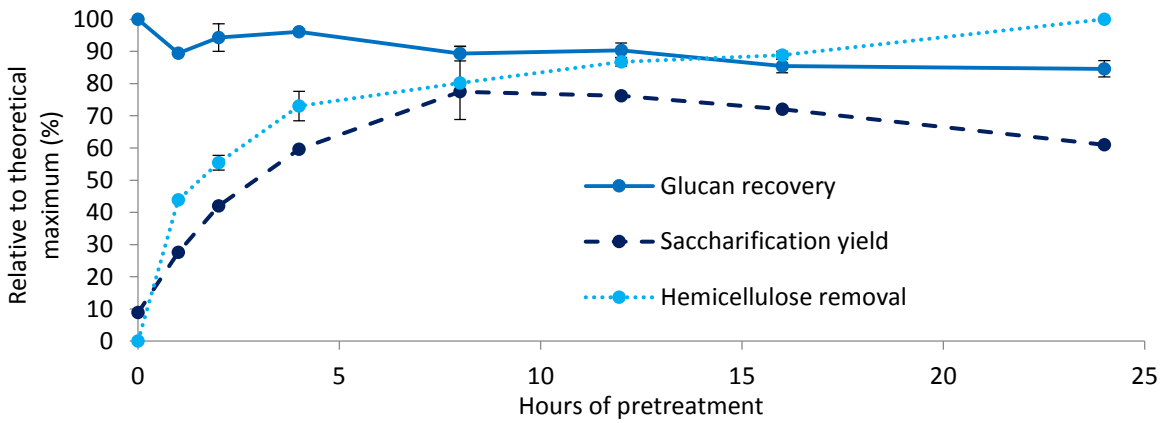

Figure III-5 Trends for carbohydrate recoveries and glucose yield after Miscanthus pretreatment with [TEA][HSO_4] at 120°C with a biomass to solvent ratio of 1:10 g/g and a final water content of 20wt%. Errors were calculated as standard deviations across triplicates.

Lignin

In previous studies using the ionoSolv process it was demonstrated that the lignin dissolved into the IL can be reprecipitated by diluting the black liquor with water.[23,26] After washing and drying the precipitate, the lignin yield can be determined and the precipitate characterized using a number of techniques.[32] Extensive lignin characterisation is discussed in Chapter 4.

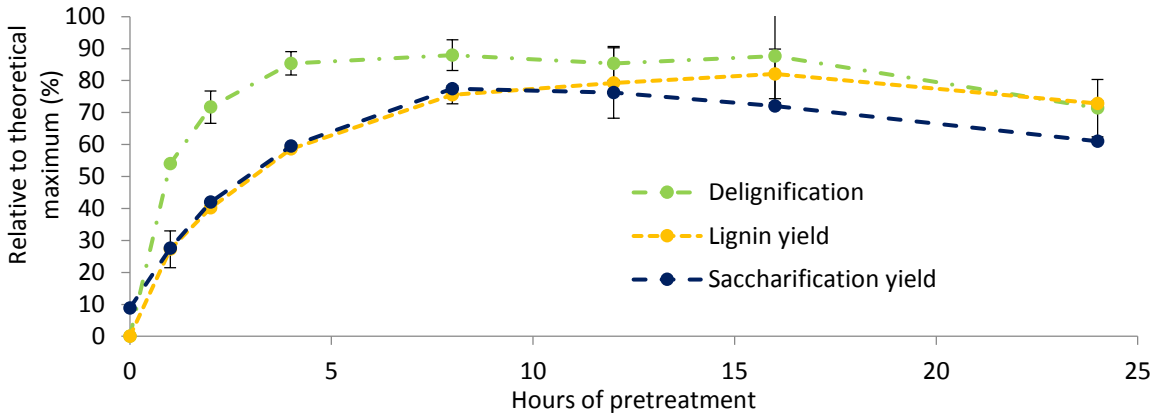

Figure III-6 Trends for lignin removal and lignin yield in relation to saccharification yield after Miscanthus pretreatment with [TEA][HSO_4] at 120°C with a biomass to solvent ratio of 1:10 g/g and a final water content of 20wt%. Errors were calculated as standard deviations across triplicates.

Figure III-6 shows the yield of precipitated lignin obtained for the time course and relates it to the removal of lignin from the biomass, i.e. the delignification (both relative to the original lignin content in the biomass). The saccharification yield is also shown for comparison. The lignin yield increased between 0 and 16 h and then dropped slightly thereafter, while delignification increased rapidly until 4 h, plateaued (4-16 h) and then decreased slightly (16-24 h). The maximum lignin yield was 82% at 16 h, which was only slightly lower than the delignification (88%) at this time. The lignin yield was at the higher end of yields obtained previously with the analogous protic imidazolium IL 1-butylimidazolium hydrogen sulfate (1:1 acid base mixture).[23] The apparent delignification drop at long pretreatment times (24 h), which is equivalent to the lignin content in the pulp increasing, has been attributed to the formation of a lignin-like substance which becomes associated with the pulp during the later stages of [TEA][HSO_4] pretreatment. The compositional analysis employed here fails to distinguish between lignin, and lignin and/or carbohydrate derived substances called pseudo-lignin. The deposition of condensed lignin and/or pseudo-lignin on the pulp surface has been shown to negatively affect enzymatic hydrolysis[22] which could explain the reduction in saccharification yields after 12 h of pretreatment. In summary, Figure III-6 shows that delignification, precipitated lignin yield and saccharification yield loosely track each other. This is distinct from cellulose swelling acetate- or chloride-based IL pretreatment, which rely on the disruption of the hydrogen-bonding network and hence achieve high saccharification yields with only partial lignin removal.[33] Here the lignin yield

reached a later maximum (16 h) than delignification (4 h) or the saccharification yield (8 h). The delayed maximum in lignin yield could be due to the slow coupling of short dissolved lignin fragments which stay in solution upon anti-solvent addition before forming higher molecular weight, less soluble lignin fragments at longer times.[32]

Process Intensification

The use of biomass as a replacement for fossil feedstocks in the production of chemicals and fuels still faces considerable challenges, some of which can be overcome by process intensification.[34,35] One of the major challenges is separating the main biomass components or derivatives at low capital and operating cost with low energy consumption.[35] Therefore, strategies to shorten reaction times, which translate to a lower capital cost as a result of smaller reactor volumes, were investigated. Additionally, a doubling of the solids loading is applied, corresponding to both a lower capital cost through reactor sizing as well as lower energy and chemicals requirements through reduced amounts of ionic liquid solvent used and heated.

Excess Acid

Protic hydrogen sulfate ionic liquids can be created with almost any acid:base ratio desired (and not just a stoichiometric 1:1 complex). Increased acidity was shown to accelerate pretreatment in a previous study using [HC_4im][HSO_4].[23] This would lead to reduced ionic liquid cost, due to using more of the less expensive sulfuric acid component, and to lower reactor cost due to higher throughput. Here, pretreatments were performed at 120°C with [TEA][HSO_4] containing an excess of acid (9 mol% in this case) to investigate if the pretreatment process could be accelerated by applying a more acidic [TEA][HSO_4] solution. The results from saccharification, compositional analysis and lignin precipitate are displayed in Figure III-7.

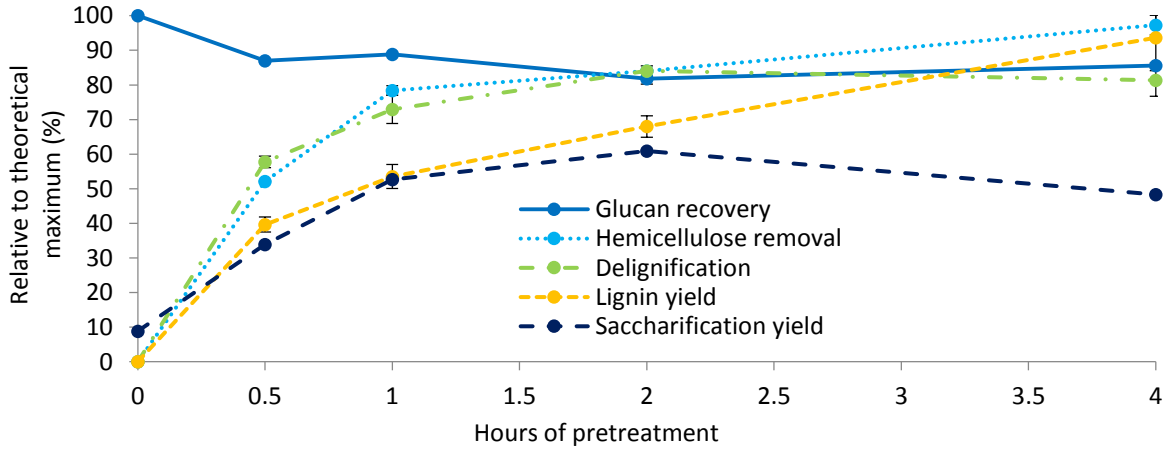

Figure III-7 Time course highlighting trends after Miscanthus pretreatment with [TEA][HSO_4] with a 1.09:1 acid to base ratio at 120°C with a biomass to solvent ratio of 1:10 g/g and a final water content of 20wt%. Errors were calculated as standard deviations across triplicates.

In general, similar pretreatment results were achieved at shorter pretreatment times with additional acid, as reported previously,[23] but also more (unwanted) side reactions (to form pseudo-lignin) were observed. Maximal saccharification yields were achieved earlier than in the case of the standard ionic liquid with a 1:1 ratio of amine and acid. A glucose release of 61% was obtained after 2 hours of pretreatment (Figure III-7), as opposed to 42% without an excess of acid (Figure III-4). However, the maximum glucose yield with an excess of acid was below the maximum glucose yield of 77% found at 8 h for the IL with a 1:1 acid base ratio. Since the glucan recovery was not substantially reduced at 2 h treatment with the excess acid [TEA][HSO_4] solution compared to 8 h treatment with the 1:1 mixture, I suspect that increased re-deposition of condensed material onto the cellulose surface is responsible for the decrease in saccharification yield (which is also likely to be responsible for the reduced saccharification yield for the 1:1 mixture beyond 8 h pretreatment time). Hemicellulose and lignin removal were also accelerated compared to the 1:1 IL solution (Figure III-7). Hemicellulose removal was complete at 4 h compared to 24 h for the 1:1 mixture. Delignification peaked after 2 h, compared to 4 h for the 1:1 ionic liquid solution. The lignin yield continued to rise throughout the time course, with no maximum observed, and exceeded the delignification after 4 h of pretreatment with excess acid (94% vs. 81%). This is further evidence for the formation of water-insoluble pseudo-lignin from carbohydrate components during lignocellulose fractionation with acidic ionic liquid solutions, which then either re-deposits onto the pulp or precipitates with the lignin upon anti-solvent addition.

These findings show that an excess of acid may indeed achieve faster treatment although at the expense of overall lower yields. High yields may be possible to maintain at shortened times by further optimising the process and using a slightly lower excess of acid. Overall improved economics might however be achieved even in the more acidic IL used here, due to higher throughput and lower reactor and energy costs, despite the lower pulp digestibility.

Increased Temperature and Biomass Loading

A study using [C_2C_1im][OAc] for the dissolution and fractionation of sugarcane bagasse and southern yellow pine has shown a shortening of the time to achieve biomass dissolution from 15-16 h at 120°C to 5-15 min at a temperature between 175 and 195°C.[28] Delignification was improved, which was attributed to the fact that the reaction was heated beyond the glass transition temperature of lignin which lies at around 150°C. In addition carbohydrate recovery was improved, however around 15% of the ionic liquid degraded under these conditions. Building on this work, pretreatments were conducted at four different oven temperatures between 150 and 180°C. As above, the recovered pulp was subjected to compositional analysis and enzymatic saccharification in order to obtain glucan recovery, lignin precipitate yield, delignification and hemicellulose removal as well as glucose yields

from hydrolysis. These are shown in Figure III-8 while Table III-2 summarises the composition of the isolated pulps.

Peak saccharification yields were indeed achieved faster than in the previous study at 120°C where maximum glucose release was observed after 8 h of pretreatment. Here, the highest saccharification yields were obtained after 45 min at 150°C (75%), 40 min after at 160°C (70%), 30 min at 170°C (76%) and 15 min at 180°C (76%). This is significantly faster than observed at 120°C and, at the higher end of the temperatures, realistic for an industrial process. Lignin removal was important for a successful enzymatic saccharification, with delignification peaking around the time saccharification yield was highest, as previously observed.

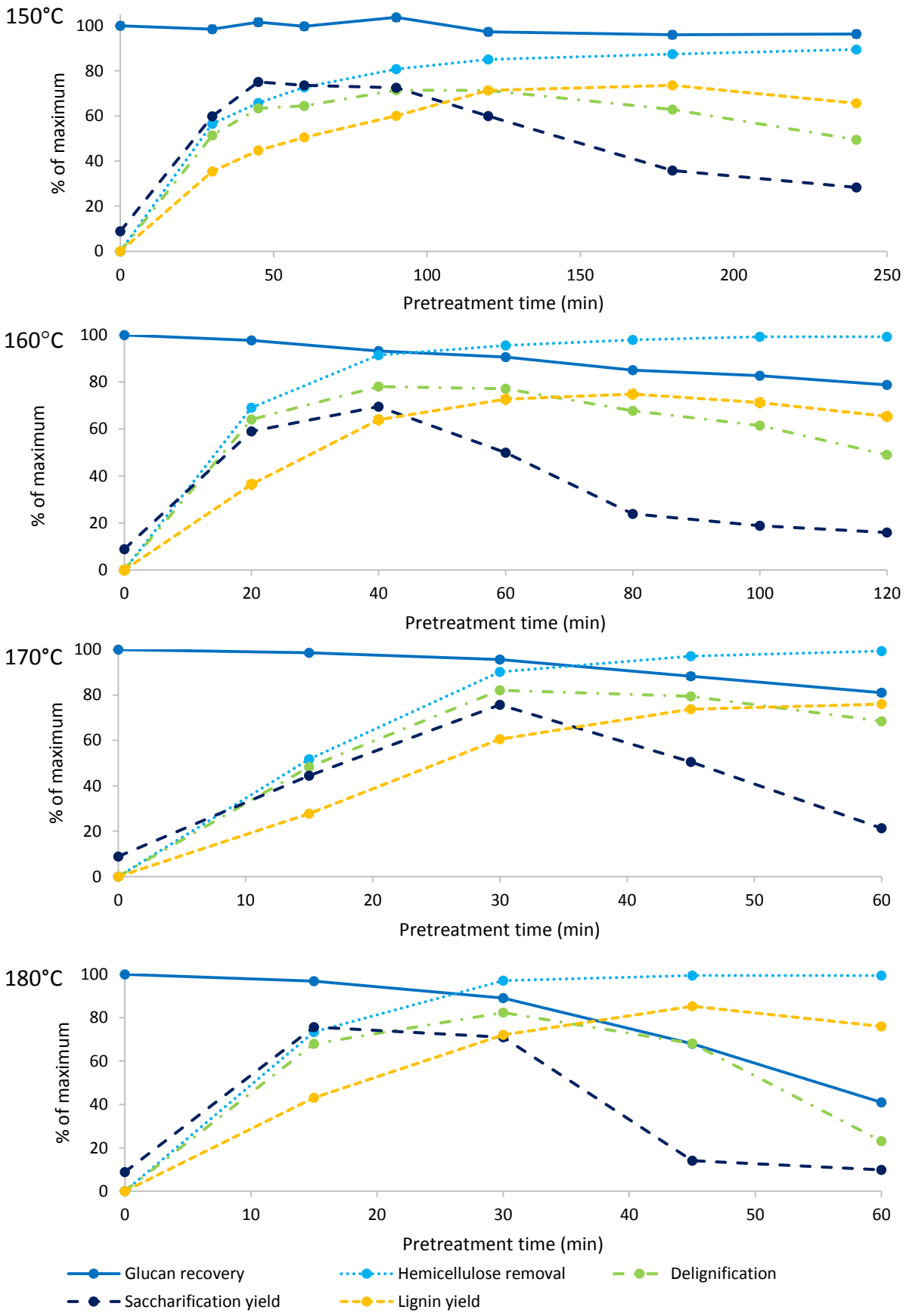

Figure III-8 Time course highlighting trends after Miscanthus pretreatment with [TEA][HSO_4] with a biomass to solvent ratio of 1:5 g/g and a final water content of 20wt%. Errors were calculated as standard deviations across triplicates.

Table III-2 Pulp composition and yields of lignocellulose components, as determined by compositional analysis, as well as lignin precipitate. *Miscanthus* was pretreated with [TEA][HSO_4] with a biomass to solvent ratio of 1:5 g/g and a final water content of 20wt%.

		Pulp Composition				Total pulp	Lignin Precipitate
t (min)	T (°C)	Glucan	Hemicelluloses	Lignin	Ash		
Untreated *Miscanthus*		50.1	22.4	26.8	0.7	100.0	N/A
30	150	49.3	9.7	13.0	0.8	72.9	9.5
45	150	50.9	7.7	9.8	0.2	68.6	12.0
60	150	50.0	6.1	9.5	0.4	66.0	13.5
90	150	51.9	4.3	7.7	0.1	64.0	16.1
120	150	48.7	3.4	7.7	0.1	59.9	19.1
180	150	48.1	2.8	9.9	0.1	61.0	19.7
240	150	48.2	2.4	13.5	0.8	64.9	17.6
20	160	48.9	6.9	9.6	0.2	65.7	9.8
40	160	46.7	1.9	5.9	0.2	54.7	17.1
60	160	45.4	1.0	6.1	0.3	52.8	19.5
80	160	42.6	0.5	8.6	0.5	52.2	20.1
100	160	41.4	0.2	10.3	0.3	52.2	19.1
120	160	39.5	0.2	13.7	0.3	53.6	17.5
15	170	49.4	10.8	13.9	0.4	74.5	7.4
30	170	47.9	2.2	4.8	0.4	55.3	16.2
45	170	44.2	0.7	5.5	0.4	50.8	19.8
60	170	40.6	0.1	8.5	0.4	49.6	20.3
15	180	48.5	5.9	8.6	0.4	63.5	11.5
30	180	44.6	0.7	4.7	0.4	50.4	19.3
45	180	34.0	0.1	8.6	0.4	43.1	22.8
60	180	20.5	0.1	20.6	0.4	41.6	20.4

N/A: not applicable;

Figure III-9 shows the saccharification yields related to the delignification obtained for the experiments discussed up to now. A somewhat stronger relationship between the two observables can be seen for the two time-courses at 120°C than for the time-courses at higher temperatures. A lignin removal of at least 60% was required to achieve saccharification yields exceeding 60%, however lignin removal even above 80% did not guarantee saccharification yields of above 50%. This is suspected to be due to the inability to distinguish between residual lignin and re-precipitated pseudo-lignin and/or high M_w lignin, which impact saccharification yields differently.[22] **Lignin removal is therefore an important part of the pretreatment, but not a guarantee for high saccharification yields**.

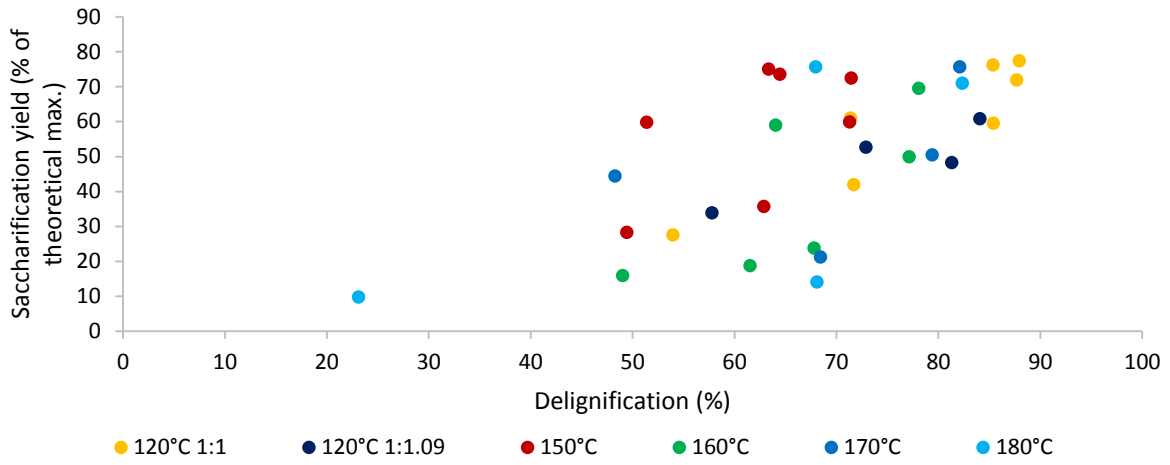

Figure III-9 Saccharification yields vs. delignification of pulps after pretreatment of *Miscanthus* under various conditions.

Figure III-10 shows the enzymatic hydrolysis yields for the selected conditions after 24, 72 and 168 h of incubation. The highest yields were consistently obtained for the 30 min pretreatment at 170°C which were 55.0%, 65.9% and 73.4% after 24, 72 and 168 h of saccharification, respectively. For temperatures where more than one time point gave good results (i.e. saccharification yields above it can be seen that the pretreatment conditions that resulted in the highest 7 day saccharification yield gave comparably lower yields after 24 h of hydrolysis. In the case of the experiments run at an oven temperature of 180°C for example, the 15 min time point gave a lower yield after 24 h of hydrolysis (48.2%) than the 30 min time point (54.5%). After 72 h of hydrolysis they gave very similar yields until, after 7 days of hydrolysis, the 15 min time point outperformed the 30 min time point with 75.7 vs. 71.0% glucose yield from theoretical. The same trend can be observed for the time points at 150°C. With longer pretreatment time faster hydrolysis is therefore achieved at the expense of slightly lower final hydrolysis yields. A possible explanation is that at longer pretreatment times some of the glucan has already been removed, facilitating access to the remaining cellulose and hence improving initial hydrolysis rates, but later limiting the total glucose release that can be achieved. In an industrial setting, where hydrolyses are unlikely to be run for more than 24 hours, these slightly longer pretreatments might therefore be preferred.

Similar to the case with excess acid, at all temperatures studied here, lignin recovery eventually exceeded delignification, again indicating that non-lignin components become incorporated in the lignin precipitate. A lignin-like substance can be seen to deposit onto the pulp surface during pretreatment or cooling, or precipitated during the wash solvent (i.e. ethanol) addition. Evidence for the formation of high molecular weight lignin or pseudo-lignin can further be seen in the increasing pulp lignin content at longer pretreatment times, and was observed at 120°C also. It is important to note that, at higher temperatures, the cellulose became unstable and its recovery also limited

saccharification yields after 40 min, 30 min and 30 min at 160, 170 and 180°C, respectively. Hemicellulose removal proceeded rapidly in all cases and was complete within the first 60 minutes at temperatures of 170°C and above. In the previous study at 120°C, 80% of hemicelluloses were extracted over the first 8 hours of pretreatment.

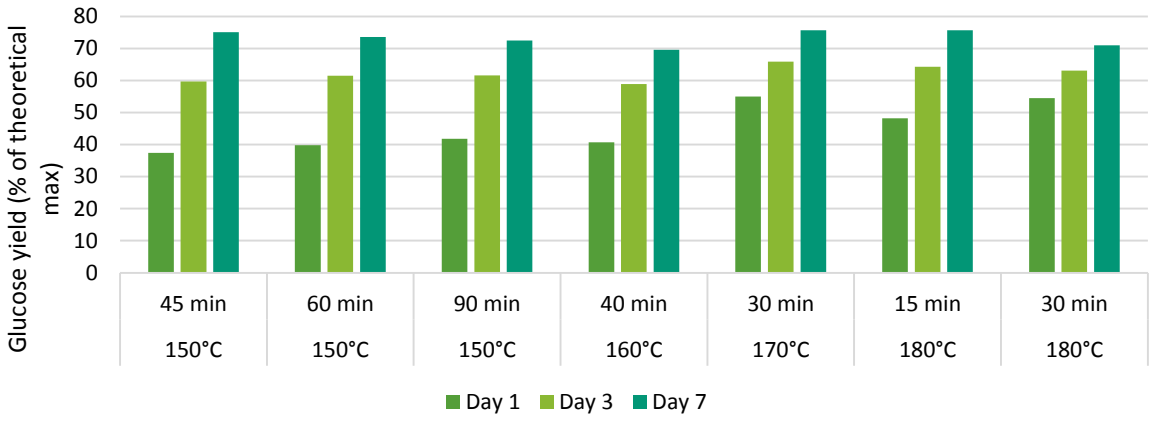

Figure III-10 Enzymatic hydrolysis yields after 1, 3 and 7 days. Miscanthus was pretreated at a 1:5 g/g biomass to solvent ratio with [TEA][HSO_4] with a biomass to solvent ratio of 1:5 g/g and a final water content of 20wt%.

In summary, this shows that increasing the temperature to 150°C – 180°C can shorten pretreatment times by at least 90% compared to pretreatments at 120°C. However, pseudo-lignin formation as well as glucan instability become detrimental soon after peak saccharification is reached and the pretreatment time therefore needs to be chosen very carefully to avoid overtreatment.

Conclusions

Miscanthus pretreatment using the low-cost ionic liquid [TEA][HSO_4] has been successfully demonstrated and high glucose yields were obtained after short residence times when heated above 150°C. Using an excess of acid in the ionic liquid synthesis has shown to further shorten reaction times. These findings are promising for an industrial application of the process. Additional process intensification is expected to be achieved by even further shortening reaction times by improving mass and heat transfer through stirring[34] or by further increasing the biomass to solvent ratio.[36] Most importantly, holistic use of the biomass will be necessary.[35] The effect of stirring is being investigated as part of a different research project. Increased biomass loadings are discussed in the next chapter. The fate of the lignin and hemicellulose is discussed in Chapter 4.

References

1 G. G. Allison, C. Morris, J. Clifton-Brown, S. J. Lister and I. S. Donnison, *Biomass and Bioenergy*, 2011, **35**, 4740–4747.

2 S. Padmanabhan, M. Kim, H. W. Blanch and J. M. Prausnitz, *Fluid Phase Equilib.*, 2011, **309**, 89–96.

3 P. L. Eranki and B. E. Dale, *GCB Bioenergy*, 2011, **3**, 427–438.

4 F. Cherubini, N. D. Bird, A. Cowie, G. Jungmeier, B. Schlamadinger and S. Woess-Gallasch,

Resour. Conserv. Recycl., 2009, **53**, 434–447.
5 D. a Lashof and D. R. Ahuja, *Nature*, 1990, **344**, 529–531.
6 N. Brosse, A. Dufour, X. Meng, Q. Sun and A. Ragauskas, *Biofuels, Bioprod. Biorefining*, 2012, **6**, 580–598.
7 E. M. Hodgson, S. J. Lister, A. V. Bridgwater, J. Clifton-Brown and I. S. Donnison, *Biomass and Bioenergy*, 2010, **34**, 652–660.
8 H. Lou, Q. Hu, X. Qiu, X. Li and X. Lin, *BioEnergy Res.*, 2016, **9**, 335–343.
9 H. Murnen, V. Balan, S. P. Chundawat, L. D. C. Sousa and B. Dale, *Biotechnol. Prog.*, 2007, **23**, 846–850.
10 A. Sørensen, P. J. Teller, T. Hilstrøm and B. K. Ahring, *Bioresour. Technol.*, 2008, **99**, 6602–6607.
11 Z. Ji, X. Zhang, Z. Ling, R.-C. Sun and F. Xu, *Carbohydr. Polym.*, 2016, **154**, 247–256.
12 N. Sathitsuksanoh, K. M. Holtman, D. J. Yelle, T. Morgan, V. Stavila, J. Pelton, H. Blanch, B. a. Simmons and A. George, *Green Chem.*, 2014, **16**, 1236.
13 H. Rodríguez, S. Padmanabhan, G. Poon and J. M. Prausnitz, *Bioresour. Technol.*, 2011, **102**, 7946–7952.
14 C. Vanderghem, A. Richel, N. Jacquet, C. Blecker and M. Paquot, *Polym. Degrad. Stab.*, 2011, **96**, 1761–1770.
15 M.-F. Li, S. Yang and R.-C. Sun, *Bioresour. Technol.*, 2016, **200**, 971–980.
16 N. R. Baral and A. Shah, *Biofuels, Bioprod. Biorefining*, 2016, **10**, 70–88.
17 L. Chen, M. Sharifzadeh, N. Mac Dowell, T. Welton, N. Shah and J. P. Hallett, *Green Chem.*, 2014, **16**, 3098.
18 A. George, A. Brandt, K. Tran, S. M. S. N. S. Zahari, D. Klein-Marcuschamer, N. Sun, N. Sathitsuksanoh, J. Shi, V. Stavila, R. Parthasarathi, S. Singh, B. M. Holmes, T. Welton, B. a. Simmons and J. P. Hallett, *Green Chem.*, 2015, **17**, 1728–1734.
19 F. J. V. Gschwend, A. Brandt, C. L. Chambon, W.-C. Tu, L. Weigand and J. P. Hallett, *J. Vis. Exp.*, 2016.
20 A. Brandt, F. Gschwend, P. Fennell, T. Lammens, B. Tan, J. Weale and J. Hallett, *Green Chem.*, 2017, DOI: 10.1039/C7GC00705A.
21 F. Hu and A. Ragauskas, *RSC Adv.*, 2014, **4**, 4317.
22 F. Hu, S. Jung and A. Ragauskas, *ACS Sustain. Chem. Eng.*, 2013, **1**, 62–65.
23 P. Verdía, A. Brandt, J. P. Hallett, M. J. Ray and T. Welton, *Green Chem.*, 2014, **16**, 1617.
24 M. E. Vega-Sánchez, Y. Verhertbruggen, H. V Scheller and P. C. Ronald, *Plant Signal. Behav.*, 2013, **8**, e23143.
25 L. Mesa, N. López, C. Cara, E. Castro, E. González and S. I. Mussatto, *Renew. Energy*, 2016, **86**, 270–279.
26 A. Brandt, M. J. Ray, T. Q. To, D. J. Leak, R. J. Murphy and T. Welton, *Green Chem.*, 2011, **13**, 2489.
27 L. Kumar, V. Arantes, R. Chandra and J. Saddler, *Bioresour. Technol.*, 2012, **103**, 201–208.
28 W. Li, N. Sun, B. Stoner, X. Jiang, X. Lu and R. D. Rogers, *Green Chem.*, 2011, **13**, 2038.
29 J. Gräsvik, J. P. Hallett, T. Q. To and T. Welton, *Chem. Commun.*, 2014, **50**, 7258–61.
30 D. Diedericks, E. van Rensburg, M. D. P. García-Aparicio and J. F. Görgens, *Biotechnol. Prog.*, 2011, **28**, 76–84.
31 P. Mäki-Arvela, T. Salmi, B. Holmbom, S. Willför and D. Y. Murzin, *Chem. Rev.*, 2011, **111**, 5638–5666.
32 A. Brandt, L. Chen, B. E. van Dongen, T. Welton and J. P. Hallett, *Green Chem.*, 2015, **17**, 5019–5034.
33 G. Cheng, P. Varanasi, R. Arora, V. Stavila, B. a. Simmons, M. S. Kent and S. Singh, *J. Phys. Chem. B*, 2012, **116**, 10049–10054.
34 Z. Qiu, L. Zhao and L. Weatherley, *Chem. Eng. Process. Process Intensif.*, 2010, **49**, 323–330.
35 J. P. M. Sanders, J. H. Clark, G. J. Harmsen, H. J. Heeres, J. J. Heijnen, S. R. A. Kersten, W. P. M.

van Swaaij and J. A. Moulijn, *Chem. Eng. Process. Process Intensif.*, 2012, **51**, 117–136.
36 F. Xu, J. Sun, N. V. S. N. M. Konda, J. Shi, T. Dutta, C. D. Scown, B. A. Simmons and S. Singh, *Energy Environ. Sci.*, 2016, **9**, 1042–1049.

Chapter 2: Feedstock Expansion with Softwood Pine in the Spotlight

Thus far, *Miscanthus* has been the main feedstock investigated for deconstruction and fractionation via the ionoSolv process, while softwoods have received relatively little attention. Softwoods are known to be more recalcitrant than grasses due to a higher lignin content (up to 30%)[1] and a higher content of bi-phenyls, and di-phenyl ethers,[2] therefore presenting a greater challenge to delignify and often requiring a higher enzyme loading for successful saccharification.[3] The carbohydrate composition of softwoods however has the advantage of a high content of hexoses[1] which are readily fermented by conventional yeasts,[4] while many fermentive organisms are not adapted to the conversion of C5 sugars constituting a significant part of grasses and hardwoods.[1]

Pine is a commonly grown softwood with a wide geographical abundance.[5] It is often obtained as a forestry residue and as such has the potential to decrease feedstock costs for bioethanol production which is crucial for its competitiveness.[6] According to a report by the NNFCC Bioeconomy Consultants, there are around 1.3m tonnes of softwood forest waste arising in the UK annually, which can be removed from forests sustainably at a cost of between £18-50/dry tonne vs. around 140kt of *Miscanthus* produced in the UK at a cost of £45-70/tonne (including 16% moisture).[7] Additionally softwoods and specifically pine are widely used in the construction industry and there is therefore a very cheap stream of softwoods available in the form of waste construction and demolition wood.[8] Being able to harness this feedstock therefore represents an incredible advantage over processes using conventional, expensive feedstocks such as grasses and agricultural residues. Hence, effectively fractionating softwoods is a crucial step towards the use of low-cost feedstocks and a cost-effective biorefinery.

Dilute acid pretreatment of scots pine has shown maximal glucose yields of 18 g/100 g of biomass, corresponding to around 43% of theoretical glucose yield.[9] High pressure homogenization, a form of steam explosion where high pressures (around 10 MPa) are released very quickly, has been found to be largely ineffective for the pretreatment of pine.[10] Saturated steam pretreatment of cedar, another softwood, at 35 atm resulted in a glucose yield of 60.4% and pretreatment at 45 atm followed by milling in a glucose yield of 73%.[11] Somewhat more promising results have been obtained with organosolv pretreatment: 70% sugar yield was obtained for Loblolly pine after 1 h at 170°C in 65% ethanol with 1.1% sulphuric acid at a biomass to solvent ratio of 1:7.[12] These conditions however require the use of costly pressure withstanding equipment. Increasing the enzyme loading for the hydrolysis improved the glucose yield from Loblolly pine to 81%.[13] A study focusing on the effect of residual lignin on the enzymatic hydrolysis of steam explosion pretreated Douglas fir found a strong correlation with residual lignin content and hydrolysis yield.[4] In this study, Kumar *et al.* found that softwood lignin binds to cellolytic enzymes, making high enzyme loadings necessary to achieve good

sugar yields. Similar findings were observed in another study looking at the differences between softwood and hardwood lignin. Adding ethanol organosolv softwood lignin to a variety of substrates resulted in a decrease of sugar yields in all cases while ethanol organosolv hardwood lignin improved yields.[3] By measuring the Langmuir constants, they found that cellulases have a higher affinity to lignin than cellulose and a higher affinity to and adsorption capacity on softwood lignin compared to hardwood lignin.

Using the ionoSolv process, previously only around 30% saccharification yield was obtained from pine pretreated for 22 h at 120°C with $[C_4C_1im][HSO_4]$ in the presence of 20wt% water, compared to over 80% from *Miscanthus* pretreated under the same conditions.[2] Li *et al.*[14] reported a slightly higher saccharification yield of 35% after pulverising southern pine for 2 days prior to pretreatment for 5 h at 120°C with $[AC_1im][Cl]$ (1-allyl-3-methylimidazolium chloride) opposed to less than 20% without pulverisation step after a milling process. Pulverisation however is an energy and time consuming process which is not very likely to be incorporated in an industrial process. Good saccharification yields of around 90% were obtained by Torr *et al.*[15] who pretreated pine wood for 3 h at 120°C with $[C_2C_1im][OAc]$. Cox *et al.*[16] found that the initial enzymatic saccharification rate of yellow pine pretreated for 5 h at 130°C with $[C_2C_1im][OAc]$ was faster than with $[HC_1im]Cl$. However, while a maximum of 40% of sugars were released after $[C_2C_1im][OAc]$ pretreatment, higher yields were obtained with the latter ionic liquid and a maximum does not seem to have been achieved yet. Comparing the experimental setup used by Cox and Torr, the main difference seems to be the particle size; while Torr *et al.* used ground wood which they sieved to 850-420 µm (20-40 mesh), Cox *et al.* used wood chips of no specified size and, as demonstrated by Li *et al.*, the particle size has a significant influence on the outcome of a pretreatment. Further, Cox *et al.* conducted the pretreatment in the presence of 2.5wt% water; while the dissolution process using $[C_2C_1im][OAc]$ is negatively affected by the presence of water, pretreatment with $[HC_1im]Cl$ does not result in full dissolution of the wood chips and thus resembles more an ionoSolv process where the presence of water is beneficial.[2] However, both Cox *et al.* and Torr *et al.* used comparably low biomass loadings of 3wt% and 5wt% respectively, which, together with the high production cost of $[C_2C_1im][OAc]$[17] makes the economic scale up of their processes questionable.

A recent study compared and combined different pretreatment technologies for loblolly pine wood particles including ball milling, acetone extraction, disc refining, immersion in sulphuric, phosphoric and acetic acid at various concentrations and for various time periods as well as hydrothermolysis and IL pretreatment ($[C_4C_1im]Cl$).[18] It showed that the highest glucose yield (93%) through enzymatic saccharification is obtained after a multi-step pretreatment sequence consisting of autohydrolysis at

180°C for 40 min followed by disc refining, followed by an acetone wash, filtering and drying in vacuo for 1 h followed by immersion in 85% phosphoric acid for 1 h at 50°C. Using the wet biomass with a moisture content of around 65% directly after autohydrolysis in the phosphoric acid immersion step was shown to compromise the treatment efficacy by the diluting effect of the moisture, resulting in poorer glucose yields. An acetone wash was therefore employed to remove moisture, and vacuum drying at room temperature was carried out rather than oven drying to avoid hornification of the sample through drying at higher temperature. The authors suggest this sequence as an "economical and effective multistep pretreatment sequence", which is somewhat difficult to reconcile with the many steps involved in the process and the capital cost associated, in addition to the somewhat more costly reagents and their potentially poor or challenging recovery.

Another recent study focusing on the alkaline peroxide pretreatment of the softwood Douglas fir reported up to 95% cellulose to glucose conversion after 72 h of hydrolysis.[19] To achieve these yields however, 0.1 g of peroxide and 0.5 g of NaOH per gram of biomass was used for pretreatment at 180°C for 30 min and no strategy for recycling or reusing the reagent was mentioned. The peroxide is potentially used up during the pretreatment which would again imply a relatively high chemical cost. There is therefore still a large scope to improve the production of chemicals and fuels from softwood feedstocks.

This study focuses on the expansion of the ionoSolv process to make it suitable for the fractionation of softwoods, and I here look at pine. Specifically, high glucose yields, short pretreatment times, high biomass to solvent ratios and a low solvent cost are for the chief aims. The solvents investigated here are $[HC_4im][HSO_4]$, which has previously been shown to be very effective for the pretreatment of *Miscanthus*,[20] together with the ultra-low-cost ionic liquid $[TEA][HSO_4]$,[21] investigated in the previous chapter for the pretreatment of *Miscanthus*, as well as its isomer $[DMBA][HSO_4]$. As seen in the previous chapter, an increase in temperature can afford a significant shortening of reaction times. Therefore three different temperatures of 120, 150 and 170°C were investigated. Also as seen in the previous chapter, increasing the biomass to solvent ratio from 1:10 to 1:5 g/g did not result in a loss of performance. In this chapter, this is taken further and biomass to solvent ratios up to 1:2 g/g are tested. Finally, experiments where different feedstocks were mixed are discussed.

Similar to the previous *Miscanthus* chapter, this chapter discusses lignin and pseudo-lignin content in the pulp and its way of affecting saccharification yields. Changes in the lignin structure as analysed by various analytical techniques are discussed in a separate chapter (Chapter 4).

Experiments using pine with [HC_4im][HSO_4] were partly carried out by other members of the group: pretreatment at 150°C and compositional analysis and saccharification of the produced pulps were carried out by Marius Biedka an MRes student (Green Chemistry) I supervised; pretreatment for the initial time course study at 170°C with [HC_4im][HSO_4] at a biomass to solvent ratio of 1:10 g/g was carried out by Clementine Chambon (PhD student).

Pine Pretreatment with 1-Butylimidazolium Hydrogensulfate [HC_4im][HSO_4]

The biomass used here was Scots Pine (*pinus sylvestris)* obtained from Finland. Its composition is represented in Figure III-11 and the numerical data given in Table III-3. Unlike *Miscanthus*, pine has a large amount of mannose (ca. 2/3 of all hemicellulose sugars) and a smaller amount of xylose and arabinose. It also has a relatively higher lignin content of just over 30% of the total biomass weight.

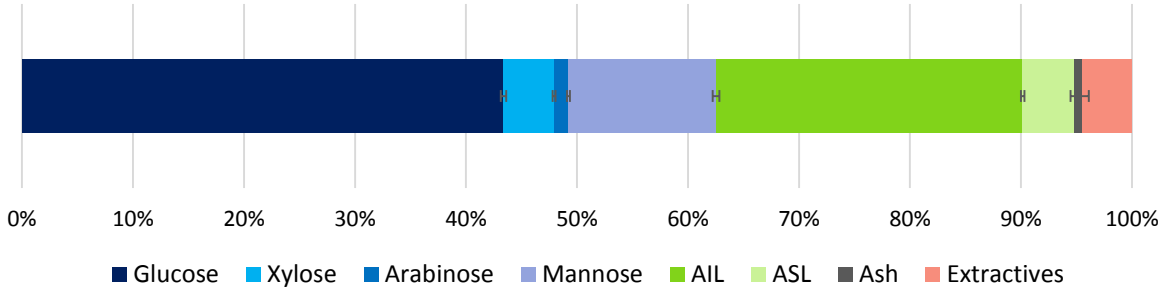

Figure III-11 Composition of the Scots Pine used for pretreatments. AIL: Acid insoluble lignin. ASL: Acid soluble lignin. Standard errors were calculated for triplicate measurements.

Table III-3 Numerical data of the composition of the Scots Pine used for pretreatments. Standard errors were calculated for triplicate measurements.

	Glu	Xyl	Gal	Ara	Man	AIL	ASL	Ash	Extractives
% of total BM	43.4	4.5	0.0	1.3	13.3	27.6	4.6	0.8	4.5
Error	0.2	0.1	0.0	0.1	0.3	0.2	0.3	0.6	0.0

Glu: Glucose; Xyl: Xylose; Gal: Galactose; Ara: Arabinose; Man: Mannose; AIL: Acid insoluble lignin; ASL: Acid soluble lignin.

Effects of Time and Temperature

Pine was first pretreated with [HC_4im][HSO_4], displayed in Figure III-12. Figure III-13 show the saccharification yields of pretreated pulps, pulp recovery and lignin precipitate after pretreatment and the calculated delignification from compositional analysis of pretreated pulps for time courses run at 120, 150 and 170°C respectively using a 1:10 solids to liquids ratio and a 20wt% water content.

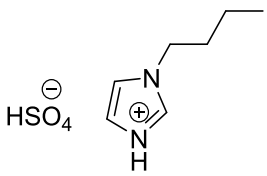

Figure III-12 [HC_4im][HSO_4].

An initial decrease of saccharification yields was observed after short pretreatment times compared to non-pretreated pine. This observation can be attributed to hornification occurring during the air-drying of the pulp after washing;[22] hornification is a phenomenon resulting in the collapsing of pores in the biomass structure upon drying, giving rise to a smaller surface area and hence a reduced accessibility for enzymes. An experiment to validate this hypothesis is discussed below. After the initial decrease, saccharification yields increased in all cases, before decreasing again for temperatures above 120°C. Similarly to *Miscanthus*¸ maximum delignification and saccharification yields for pine coincided and were reached approximately between 1 and 2 h at 150°C and after around 0.5 h at 170°C. At 120°C no saccharification or delignification maximum has been found within the 8 h time course. A strong relationship between lignin removal and saccharification yields has previously been established for *Miscanthus* and is here observed even more strongly (Figure III-9); a linear regression of the data set yields a coefficient of determination of 0.84 in the case of pine vs. 0.39 for *Miscanthus*. The stronger relationship between delignification and saccharification yields in the case of pine is thought to stem from the high affinity of cellolytic enzymes to softwood lignin.[4] After peak saccharification and delignification at 150 and 170°C the measured lignin content remaining in the pulp started to increase again, similar to findings for *Miscanthus.* This has been attributed to both condensation reactions within lignin fragments leading to new high molecular weight structures which are insoluble in the IL, as well as the formation of pseudo-lignin, an insoluble polymer resulting from condensation reactions of carbohydrate degradation products.[23] While the compositional analysis technique fails to distinguish between actual lignin and pseudo-lignin, formation of the latter is strongly suspected under conditions where the lignin precipitate exceeds the measured delignification (e.g. after more than 1 h at 170°C).

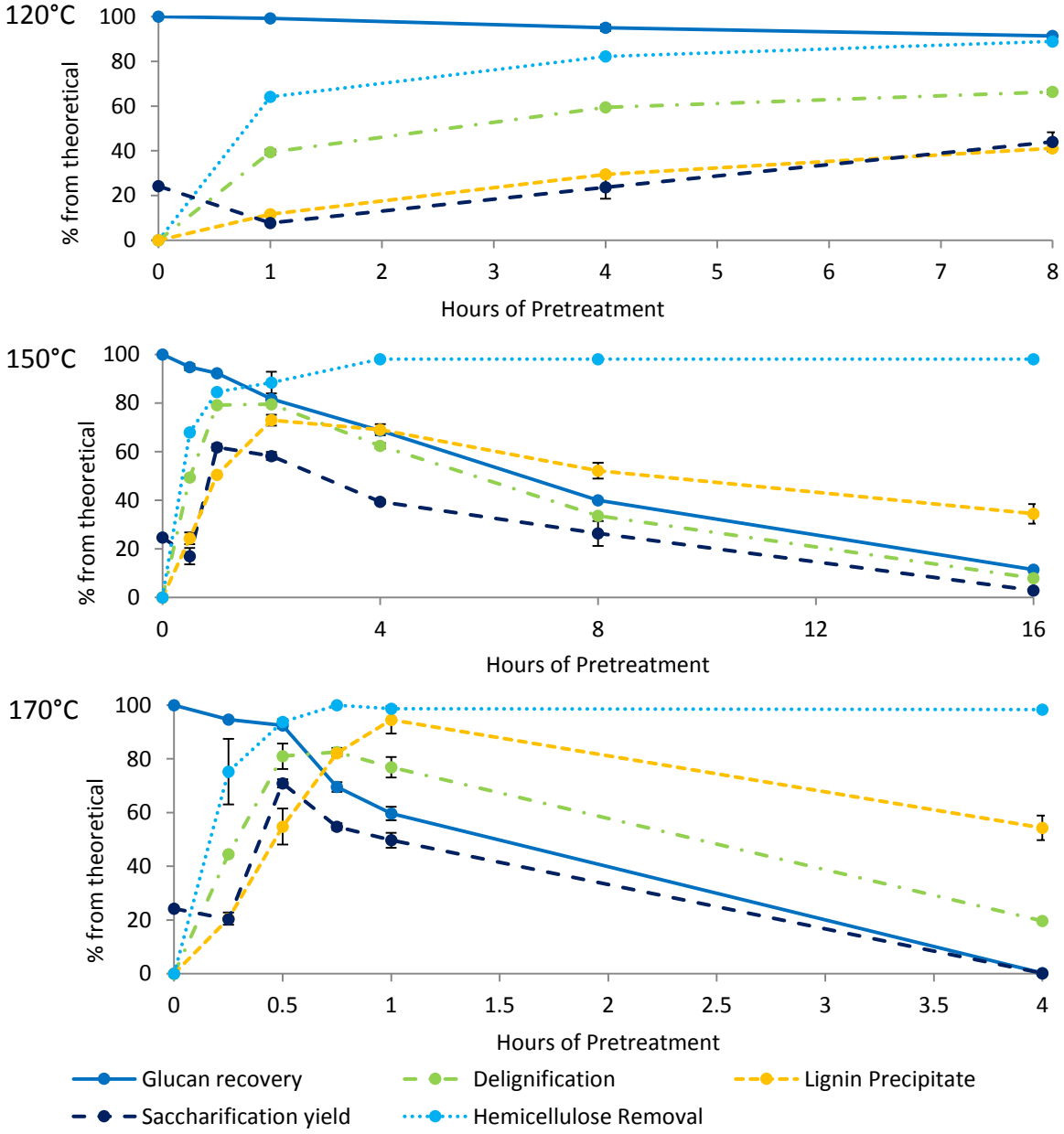

Figure III-13 Saccharification yields, glucan recovery, lignin and hemicellulose removal and lignin precipitate after pretreatment of pine at 120°C (a), 150°C (experiments carried out by Marius Biedka) (b) and 170°C (experiments carried out by Clementine Chambon) (c) with [HC_4im][HSO_4] and a final water content of 20wt% with a biomass to solvent ratio of 1:10 g/g over a time course. Errors were calculated as the standard deviation across triplicates.

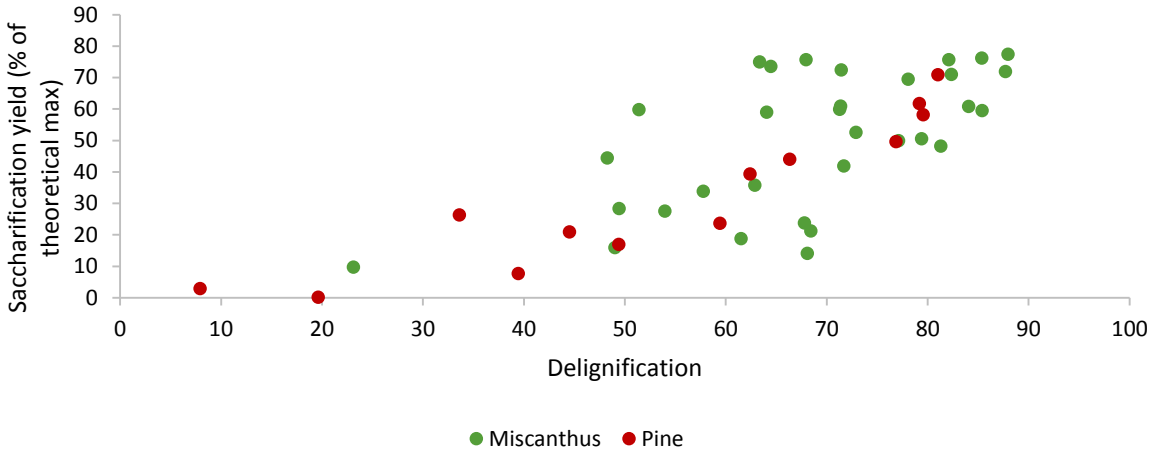

Figure III-14 Saccharification yields vs. delignification of pulps after pretreatment of pine and *Miscanthus* under various conditions.

Evidence for condensation reactions was found when analysing the precipitated lignin, which is discussed in a subsequent chapter (Chapter 4). Both the re-precipitation of lignin onto the cellulose surface and the formation of pseudo-lignin are thought to have a negative effect on saccharification yields and kinetics by making the cellulose substrate less accessible[24] and especially softwood lignin has been shown to have a negative effect on saccharification yields[3] while some of the degradation products are known to deactivate enzymes. Pseudo-lignin was found to have a more detrimental effect on enzymatic hydrolysis than dilute acid-pretreated lignin from poplar, although both were shown to reduce initial hydrolysis rates.[25] Scanning electron microscopy (SEM) pictures of the isolated pulp (Figure III-15) show the presence of a deposited droplet shaped substance that is expected to be composed of lignin or pseudo-lignin, which has been reported by Hu *et al.* also. The reduction of saccharification yield is therefore expected to be partly due to solid precipitating onto the surface.

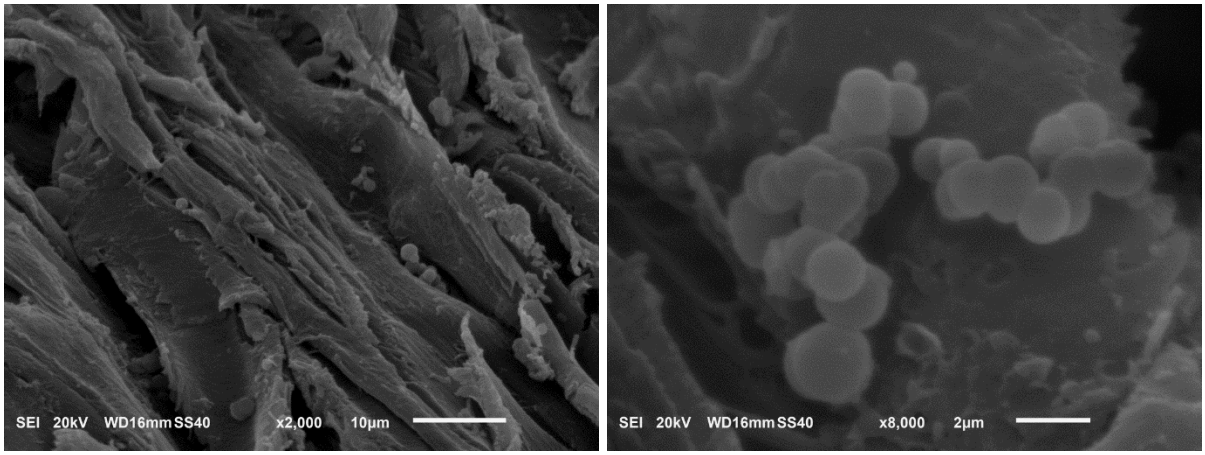

Figure III-15 SEM pictures of pulp isolated after pretreatment of pine for 4 hours at 150°C using $[HC_1im][HSO_4]$ at a final water content of 20wt% with a biomass to solvent ratio of 1:10 g/g.

While glucan recoveries were fairly constant under mild conditions (i.e. up to at least 120°C), hemicelluloses were removed over time, while high temperatures accelerated removal. At

temperatures above 120°C the cellulose was observed to start to degrade as pulp recoveries and saccharification yields dropped after prolonged treatment, similar to findings with *Miscanthus* at elevated temperatures. This was confirmed by compositional analysis of the pulps (numerical data shown in Table S1 in Appendix) showing that at a temperature of 170°C the glucan recovery dropped to virtually 0 after 4 hours of pretreatment. An initial decrease in glucan content of the pulp has been attributed to removal of glucose containing hemicelluloses, such as galactoglucomannans, rather than degradation of cellulose.[26] Galactoglucomannans constitute up to 15% of softwood.[27]

In summary this shows that high glucose yields similar to those achieved for *Miscanthus* can be obtained from the softwood pine. Lignin extraction and the avoidance of redepositing lignin as well as degrading the cellulose have been found to be the most important factors for a successful pretreatment.

Effect of Biomass Loading

In order to improve the economic viability of the process, high solids loadings can afford lower solvent and reactor costs as well as a lower operating cost.[28] While most laboratory scale research is conducted at biomass to solvent ratios of 3:100 to around 1:10 g/g,[29] higher solids loadings are desired. However, mass transfer, especially when working with ILs, can become problematic at higher solids loadings.[28] A study using $[C_2C_1im][OAc]$ for switchgrass pretreatment showed a reduction in delignification capacity when ramping the solid to liquid ratio up from 3 to 50% and an increase in glucose yield from 3 to 10% loading, followed by a decrease to 50% loading.[30] Xu *et al.* employed 10% IL solutions in water for one-pot pretreatment, saccharification and fermentation of corn stover with solids loadings of up to 34.2wt%.[28] In the present study, the pretreatment efficacy at loadings ranging from 5 to 50wt% were investigated, corresponding to a solid to liquid ratio of 1:20 to 1:2 g/g. These experiments were carried out under the optimal conditions found (170°C for 30 min) with $[HC_4im][HSO_4]$ with 20wt% water.

Figure III-16 shows the pulp, lignin and saccharification yields as a function of the biomass loading. Pulp yields showed a steady increase from around 41% to 56% when increasing the loading from 5 to 50wt%. Lignin yields were stable between 5 and 25% loading, giving around 55% of the theoretical lignin yield. Loadings of 35 and 50wt% then resulted in a reduction of the lignin yield down to ca. 30%. The saccharification yield was highest at the lowest loading, giving 75% of the theoretical yield, from where it decreased to under 35% with 50wt% loading. The decrease in lignin yields at higher loading combined with the increased pulp yield is likely due to precipitation of lignin during the dilution of the black liquor with ethanol. Re-precipitation of lignin and therefore the amount of lignin present during saccharification can also be linked to lower saccharification yields. Softwood lignin has in the past been

shown to negatively affect sugar release during enzymatic sacchrification.[3] Evidence for the negative effect of initially dissolved lignin on saccharification yields is given by Berlin *et al.*[31] who compared enzymatic residual lignin and precipitated lignin from organosolv pretreatment of Douglas fir and their effect on the hydrolysis rate. Residual pulp lignin is lignin that, presumably, did not dissolve during organosolv treatment but stayed with the pulp and was isolated after enzymatic hydrolysis while precipitated lignin was dissolved during organosolv treatment and subsequently precipitated upon anti-solvent addition. The enzymatic residual lignin was shown to cause a smaller decrease in hydrolysis rate than the dissolved lignin. Since it is strongly suspected that in the present case, even at higher loadings, lignin initially dissolves but subsequently re-precipitates, avoiding the formation of or removing re-precipitated lignin is critical. The reduction in lignin and saccharification yield as well as the increase in pulp recovery together with higher loading might therefore be improved with an adapted washing protocol that avoids re-precipitation and/or removes re-precipitated lignin from the pulp surface.

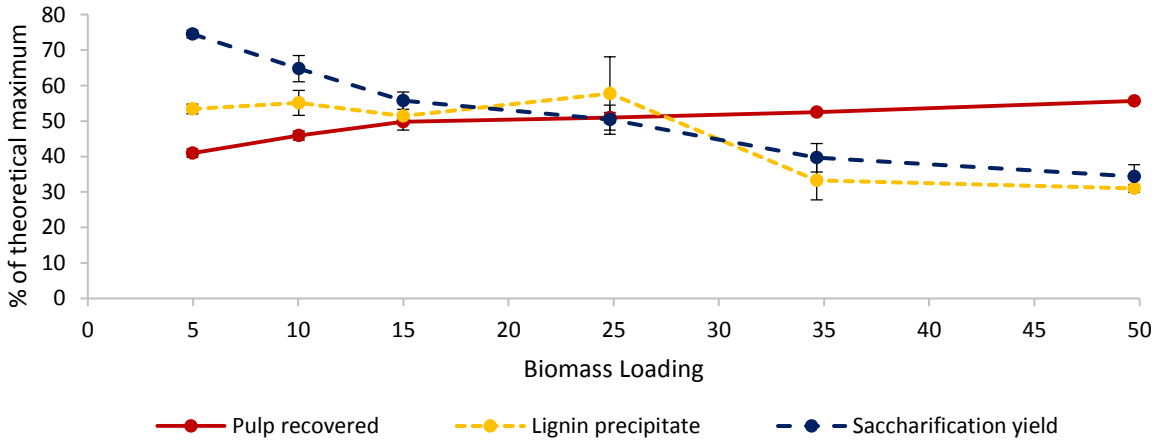

Figure III-16 Pulp, lignin and saccharification yield after pretreatment of pine with $[HC_4im][HSO_4]$ with a final water content of 20wt% for 30 min at 170°C and biomass to solvent ratios ranging from 1:20 to 1:2 g/g, corresponding to loadings from 5 to 50wt%. Errors were calculated as standard deviation across triplicate.

Hornification and its Effect on Saccharification Yields

In an industrial process, the obtained pulp is expected to be subjected to enzymatic hydrolysis directly after washing rather than undergoing an energy consuming air-drying step. Since there is evidence that air-drying leads to hornification of lignocellulosic biomass which negatively affects enzymatic saccharification,[4,22] I investigated if the produced pulps gave higher sugar yields if the air-drying step was omitted. For this, pulp samples were emerged in water after Soxhlet extraction had finished, centrifuged and the supernatant decanted once in order to remove the ethanol and most of the wash water. Moisture contents were determined, immediately followed by weighing out samples of the wet pulps for enzymatic hydrolysis. Moisture contents of pulps obtained with this method were typically

around 90%. This was carried out for pulps obtained with 10 and 50wt% loading (1:10 and 1:2 g/g solid to solvent ratio) after pretreatment for 30 min at 170°C in [HC_4im][HSO_4] containing 20wt% water.

Sugar release was found to increase with this method and quantitative sugar yields were obtained at 10% loading while 50% loading resulted in yields of 75%, representing an increase of 57 and 120% vs. dried pulps for 10 and 50% loading respectively. The results are summarised in Table III-4. In a study using steam explosion pretreated Douglas fir, adding separately isolated lignin to a completely delignified, never dried substrate decreased glucose yields by around 10% while adding the same amount of lignin to the equivalent but oven-dried substrate reduced hydrolysis yields by 48%.[4] The authors concluded that the degree by which lignin affected the hydrolysis depended strongly on the accessibility of the cellulose, which was significantly higher in the case of never dried pulp. This is to some extent in line with the findings here, showing a more pronounced decrease in saccharification yields upon drying at high pulp lignin contents, thought to be originating from the increased reprecipitation of lignin onto the pulp surface at higher biomass loadings of 1:2 vs. the lower lignin content pulp from the 1:10 experiments.

These findings suggest that pulp drying should be strongly discouraged whenever possible. However, if pulp production and utilisation are not in the same location, shipping of additional water may impact the economics by increasing the transport fuel demand. A moisture content of less than 90% might still be able to avoid hornification while not severely impacting the fuel consumption for pulp transport, nevertheless colocation of pretreatment and hydrolysis is likely to be hugely beneficial.

Table III-4 Saccharification yields obtained after 7 days from pulps with and without air drying. Pine was pretreated at 170°C for 30 min with a solid to solvent ratio of 1:10 and 1:2 g/g in [HC_4im][HSO_4] with a final water content of 20wt%. Standard errors were calculated for triplicate measurements.

	Saccharification yield	
Loading	with air drying	without air drying
10%	64.8±3.5%	102.2±1.9%
50%	34.4±3.2%	74.9±2.9%

Selection of Ionic Liquid

In addition to the imidazole based [HC_4im][HSO_4] IL two (lower cost) alkylamine based ILs, triethylammonium and *N,N*-dimethylbutylammonium hydrogensulfate,[17] were tested under the most promising conditions of 30 min at 170°C, 10wt% biomass loading and 20wt% water content. Comparisons of saccharification yields, as well as lignin and pulp recovery are shown in Figure III-17. Once again lignin recovery, which is to some extent linked to delignification, correlated well with saccharification yields: the highest lignin recovery was obtained with [DMBA][HSO_4], reaching 72%,

accompanied by a saccharification yield of 74%, similar to the values of 55 and 70% respectively obtained with [HC_4im][HSO_4]. The lowest saccharification yield and lignin recovery of 36 and 30% respectively were obtained with [TEA][HSO_4]. In the previous chapter, [TEA][HSO_4] has been shown to effectively delignify grassy biomass, resulting in saccharification yields exceeding 80%. It is unclear why in the present case of softwood pretreatment [TEA][HSO_4] is so drastically outperformed by [DMBA][HSO_4] and [HC_4im][HSO_4], giving rise to only 50% of the saccharification yield obtained with [DMBA][HSO_4]. [DMBA] and [TEA][HSO_4] have the same molecular weight and it is therefore unlikely that the difference in performance is linked to an effect of the molar ratio of ionic liquid to water or biomass. [DMBA] and [HC_4im][HSO_4] both contain a butyl chain on the cation which is likely to lower the interaction between the cation and the anion, therefore lowering viscosity, which might have a beneficial effect on delignification. **Due to a lower expected cost of dimethylbutylamine vs. 1-butylimidazole, [DMBA][HSO_4] represents a very promising candidate for the economic fractionation of lignocellulosic biomass including softwoods.**

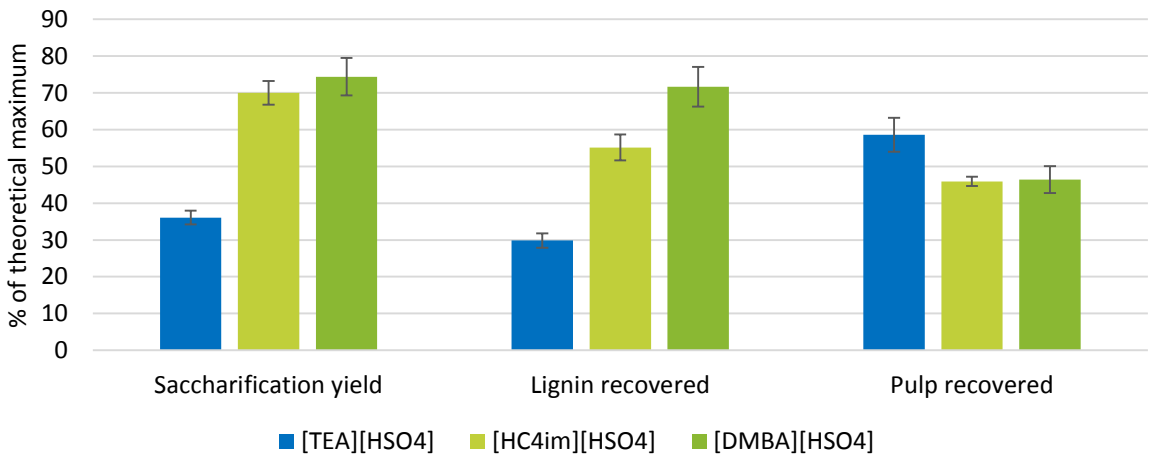

Figure III-17 7 day saccharification yield and lignin and pulp recovery after pretreatment at 170°C for 30 min with three different [HSO_4] ILs with a final water content of 20wt%. Pine was pretreated at a solid to solvent ratio of 1:10 g/g. Standard errors were calculated for triplicate measurements.

Mixed Feedstocks: One Size Fits All

As discussed earlier, there can be substantial differences in biomass composition depending on growth conditions,[32] plant species[27] and plant tissue type,[9] amongst other factors. Feedstock formulation has been proposed as a way of overcoming this variability: different feedstocks are blended together in order to meet a target range of compositional specification so as to overcome seasonal and annual fluctuations.[33] There is however no need for a consistent feedstock input if a robust pretreatment process can deal with these variations without having to be optimised for each batch of feedstock coming in. Shi *et al.* used [C_2C_1im][OAc] to pretreat a combination of switchgrass, pine, corn stover and eucalyptus and were able to release over 90% of sugars after pretreatment for

3 hours at 160°C.[33] The findings from the previous chapter together with the results discussed in this chapter show that, although the two feedstocks *Miscanthus* and pine do not behave identically at lower temperatures (i.e. 120°C), peak saccharification yields at a given higher temperature are obtained roughly after the same time period (e.g. 30 min at 170°C). Even though the two studies were carried out with different ILs it is expected that *Miscanthus* pretreatment will also be successful with [HC_4im][HSO_4] at 170°C as it has been shown at 120°C by Verdia *et al.*[20] Moreover, peak saccharification yield with [HC_4im][HSO_4] was achieved after roughly the same period as using [TEA][HSO_4] at 120°C, and therefore kinetics using different ILs are not expected to change significantly at higher temperatures. This opens up the possibility of using not a single, but various, or a mix of, feedstocks under equal conditions in the ionoSolv process. *Miscanthus*, pine and the hardwood beech and their combinations were therefore pretreated for 30 min at 170°C using [HC_4im][HSO_4]. The results are tabulated in Table III-5.

Table III-5 Pulp and lignin recovered after pretreatment, mass lost to liquor by difference and saccharification yield obtained from beech, pine, Miscanthus and their combinations. All biomass was pretreated at 170°C for 30 min with a solid to solvent ratio of 1:10 g/g in [HC_4im][HSO_4] and a final water content of 20wt%. Numbers in brackets are calculated averages for comparison.

Feedstock	Pulp yield	Lignin yield	Mass lost to liquor	Saccharification yield
Beech	46.7	9.3	44.0	81.5
Pine	53.9	11.5	34.6	59.5
Miscanthus	44.1	14.5	41.4	90.5
Beech-Pine	49.5 (50.3)	12.1 (10.4)	38.4 (39.3)	66.6 (70.5)
Beech-*Misc*	39.8 (45.4)	15.9 (11.9)	44.3 (42.7)	84.8 (86.0)
Pine-*Misc*	45.5 (49.0)	16.6 (13.0)	37.9 (38.0)	78.6 (75.0)
Beech-Pine-*Misc*	42.4 (48.3)	16.2 (11.7)	41.4 (40.0)	81.4 (77.2)

Misc: *Miscanthus.*

As expected, high saccharification yields of 91% were obtained for *Miscanthus.* Slightly lower yields of 82% were obtained for beech while this set of experiments yielded 60% of glucose release for pine. Combining two and all three different biomass types showed no significant deviation from the calculated average: a slight improvement vs. the calculated average was observed for *Miscanthus* mixed with pine and for the mix containing all three feedstocks while the combinations of beech with *Miscanthus* and with pine showed a slight reduction vs. the calculated average. More striking differences can be seen when comparing pulp and lignin yields. In all cases the combining of feedstocks resulted in a lower pulp yield and a higher lignin yield while the total amount of dissolved components after precipitation stayed roughly unchanged. I therefore hypothesise that the reduction in pulp and increase in lignin yield is a result of a lower amount of lignin re-precipitating onto the pulp surface after pretreatment. The lignin chemistry is discussed more in detail in Chapter 4 but as a preliminary

conclusion it can be said that mixing different types of feedstocks does not have a detrimental effect on enzymatic hydrolysis yields and that the here used conditions can indeed be used in a one-size-fits-all process.

Addition of Hardwood Lignin during Saccharification

From the data discussed in this and the previous chapter it can be concluded that the presence of lignin and pseudo-lignin has a strong influence on the saccharification yields obtained. However, contrasting effects of hardwood and softwood lignins on enzymatic hydrolysis have been reported by Lai *et al*.[3] Between 0 and 8 g/L of softwood and hardwood lignin were added during the enzymatic saccharification of organosolv pretreated sorghum and loblolly pine, corresponding to up to 400 mg of lignin per gram of glucan. 8 g/L hardwood organosolv lignin increased the 72 h hydrolysis yield of loblolly pine from 41.2% to 60.8% while the same amount of softwood organosolv lignin decreased the yield to 38.1%. They attributed the positive effect of hardwood lignin to the reduced non-productive binding between cellulases and the bulk lignin.

Here, 20 mg of ionoSolv beech (i.e. hardwood) lignin, isolated via precipitation after pretreatment of beech for 30 min at 170°C using [HC_4im][HSO_4] with 20wt% water, was added during the saccharification of pretreated and untreated pine. Glucose yields were measured after 48 hours and a lignin-only blank was run to ensure no residual sugars present in the lignin are responsible for any possible change in sugar yield. Sugar yields after 48 h from pretreated pine (30 min at 170°C using [HC_4im][HSO_4] with 20wt% water) increased from 43.5 to 57.8% upon addition of beech lignin while the glucose yield from untreated pine increased from 15.2 to 18.2 %, corresponding to an improvement of 33.7 and 20.5% for pretreated and untreated pine respectively. The data are summarised in Table III-6. These findings are in line with what Lai *et al.* reported and ionoSolv hardwood lignin could therefore play a role in industrial applications of enzymes for the utilisation of lignocellulose. If these increased glucose yields by the addition of hardwood lignin can be translated into a saving of enzymes, operating costs of the saccharification step could be decreased by a significant amount. According to a recent study by Mesa *et al.,* enzymatic saccharification represents the largest cost in a second generation bioethanol production facility using sugarcane bagasse.[34] Annual enzyme costs for the 192 t/day two step organosolv plant are estimated at $5.9m. For comparison, the total capital cost is estimated at $4.6m of which around $2.2m, almost half, is for the enzymatic hydrolysis reactor. Reducing enzyme requirements by e.g. 20% would therefore lead to a major cost saving through either a reduction of the enzyme cost (operating costs) or an increased throughput in the enzymatic hydrolysis reactor (capital cost), provided that hardwood lignin can be made available at a comparably much lower cost than enzymes.

Table III-6 Saccharification yields after 48 hours obtained from untreated pine and pine pulps with and without added beech lignin. Pine was pretreated at 170°C for 30 min with a solid to solvent ratio of 1:10 g/g in $[HC_4im][HSO_4]$ with a final water content of 20wt%. Beech lignin was obtained from pretreatment of beech under the same conditions. Standard errors were calculated for triplicate measurements.

	Saccharification yield	
Feedstock	without beech lignin	with beech lignin
Untreated pine	15.2±1.1%	18.2±0.7%
Pretreated pine	43.5±1.6%	57.8±8.6%

Conclusions

In summary, the findings in this chapter show that ionoSolv pretreatment is suitable for the production of highly digestible pulps from a range of feedstocks, including softwoods. A strong relationship between residual pulp lignin and saccharification yields in the case of softwoods was noted. Different types of lignocellulosic biomass can be treated under the same conditions and together, making the ionoSolv process a promising candidate for a wide range of applications. $[DMBA][HSO_4]$ was found to be a valid alternative to the more expensive imidazolium based $[HC_4im][HSO_4]$. Increased saccharification yields were achieved by the addition of hardwood ionoSolv lignin as well as by avoiding the air-drying step, further representing an improvement in the process. The process has also been shown effective at biomass loadings up to 1:2 g/g solid to liquid, however mass and heat transfer as well as the separation of the pulp from the black liquor at such high loadings might be impacted negatively.

References

1 T. E. Timell, *Wood Sci. Technol.*, 1967, **1**, 45–70.
2 A. Brandt, M. J. Ray, T. Q. To, D. J. Leak, R. J. Murphy and T. Welton, *Green Chem.*, 2011, **13**, 2489.
3 C. Lai, M. Tu, Z. Shi, K. Zheng, L. G. Olmos and S. Yu, *Bioresour. Technol.*, 2014, **163**, 320–327.
4 L. Kumar, V. Arantes, R. Chandra and J. Saddler, *Bioresour. Technol.*, 2012, **103**, 201–208.
5 L. Matías and A. S. Jump, *J. Exp. Bot.*, 2014, **65**, 299–310.
6 Y.-H. P. Zhang, *J. Ind. Microbiol. Biotechnol.*, 2008, **35**, 367–75.
7 D. Di Maio, D. Turley and L. Hopwood, *Lignocellulosic feedstock in the UK*, NNFCC, 2014.
8 H. Dick, A. Hennig and P. Scholes, *Comparing the cost of alternative waste treatment options*, WRAP Report, 2016.
9 M. Normark, S. Winestrand, T. a Lestander and L. J. Jönsson, *BMC Biotechnol.*, 2014, **14**, 20.
10 S. Jin, G. Zhang, P. Zhang, S. Fan and F. Li, *Bioresour. Technol.*, 2015, **181**, 270–274.
11 C. Asada, C. Sasaki, T. Hirano and Y. Nakamura, *Bioresour. Technol.*, 2015, **182**, 245–250.
12 P. Sannigrahi, S. J. Miller and A. J. Ragauskas, *Carbohydr. Res.*, 2010, **345**, 965–970.
13 M. Li, M. Tu, D. Cao, P. Bass and S. Adhikari, *J. Agric. Food Chem.*, 2013, **61**, 646–54.
14 B. Li, J. Asikkala, I. Filpponen and D. S. Argyropoulos, *Ind. Eng. Chem. Res.*, 2010, **49**, 2477–2484.
15 K. M. Torr, K. T. Love, Ö. P. Çetinkol, L. a. Donaldson, A. George, B. M. Holmes and B. a. Simmons, *Green Chem.*, 2012, **14**, 778.
16 B. J. Cox and J. G. Ekerdt, *Bioresour. Technol.*, 2013, **134**, 59–65.

17 A. George, A. Brandt, K. Tran, S. M. S. N. S. Zahari, D. Klein-Marcuschamer, N. Sun, N. Sathitsuksanoh, J. Shi, V. Stavila, R. Parthasarathi, S. Singh, B. M. Holmes, T. Welton, B. a. Simmons and J. P. Hallett, *Green Chem.*, 2015, **17**, 1728–1734.
18 X. Du, L. A. Lucia and R. A. Ghiladi, *ACS Sustain. Chem. Eng.*, 2016, **4**, 3669–3678.
19 C. Alvarez-Vasco and X. Zhang, *Biomass and Bioenergy*, 2017, **96**, 96–102.
20 P. Verdía, A. Brandt, J. P. Hallett, M. J. Ray and T. Welton, *Green Chem.*, 2014, **16**, 1617.
21 L. Chen, M. Sharifzadeh, N. Mac Dowell, T. Welton, N. Shah and J. P. Hallett, *Green Chem.*, 2014, **16**, 3098.
22 X. L. Luo, J. Y. Zhu, R. Gleisner and H. Y. Zhan, *Cellulose*, 2011, **18**, 1055–1062.
23 F. Hu and A. Ragauskas, *RSC Adv.*, 2014, **4**, 4317.
24 H. Li, Y. Pu, R. Kumar, A. J. Ragauskas and C. E. Wyman, *Biotechnol. Bioeng.*, 2014, **111**, 485–492.
25 F. Hu, S. Jung and A. Ragauskas, *ACS Sustain. Chem. Eng.*, 2013, **1**, 62–65.
26 P. Mäki-Arvela, T. Salmi, B. Holmbom, S. Willför and D. Y. Murzin, *Chem. Rev.*, 2011, **111**, 5638–5666.
27 R. Pettersen, *The Chemistry of Solid Wood*, American Chemical Society, Washington, DC, 1984, vol. 207.
28 F. Xu, J. Sun, N. V. S. N. M. Konda, J. Shi, T. Dutta, C. D. Scown, B. A. Simmons and S. Singh, *Energy Environ. Sci.*, 2016, **9**, 1042–1049.
29 N. R. Baral and A. Shah, *Biofuels, Bioprod. Biorefining*, 2016, **10**, 70–88.
30 A. G. Cruz, C. Scullin, C. Mu, G. Cheng, V. Stavila, P. Varanasi, D. Xu, J. Mentel, Y.-D. Chuang, B. A. Simmons and S. Singh, *Biotechnol. Biofuels*, 2013, **6**, 52.
31 A. Berlin, M. Balakshin, N. Gilkes, J. Kadla, V. Maximenko, S. Kubo and J. Saddler, *J. Biotechnol.*, 2006, **125**, 198–209.
32 G. G. Allison, C. Morris, J. Clifton-Brown, S. J. Lister and I. S. Donnison, *Biomass and Bioenergy*, 2011, **35**, 4740–4747.
33 J. Shi, V. S. Thompson, N. A. Yancey, V. Stavila, B. A. Simmons and S. Singh, *Biofuels*, 2013, **4**, 63–72.
34 L. Mesa, N. López, C. Cara, E. Castro, E. González and S. I. Mussatto, *Renew. Energy*, 2016, **86**, 270–279.

Chapter 3: From Waste Wood to Ethanol

As discussed in Part I. Background 3. Waste Wood, metal based preservatives are widely used in wood treatment. However, the metals can leach out into the environment. Concerns over migration of these metals into groundwater[1] or even the air, in the case of arsenic,[2] have resulted in bans for the production and use of chromated copper arsenate (CCA) treated wood in new constructions, though existing constructions were unaffected by the ban.[3] This has led to the development of various more benign preservatives such as alkaline copper quaternary (ACQ), copper azole (CA, Tanalith E) and micronized copper quaternary (MCQ) which all contain large amounts of copper (up to 3700 ppm).[4]

After the service life of the wood construction, the wood needs to be disposed of. The amount of CCA treated wood coming out of service in the UK is expected to increase over the next 25 to 50 years.[5] CCA treated wood is considered hazardous waste in many countries[5,6] and different methods for disposal are common in different parts of the world. While there are leaching methods to recover the metals from treated wood, they are costly (estimated $115 per tonne of treated wood) and do not allow for using the wood components for further applications.[7] As a result, more traditional disposal routes are typically used. The US disposes of the treated wood mainly through landfill,[1] while most European countries use specialist incineration.[5] It is needless to say that landfilling is an unsustainable form of waste disposal, but there are environmental issues associated also with incineration of this type of waste. Upon combustion, arsenic volatilises and a gas cleaning system including a particulate filter and liquid scrubber is required in order to avoid the release of harmful vapours into the environment.[8] A synergistic effect of Cr and As leading to an increased carcinogenic risk makes incineration of CCA containing waste particularly problematic.[9] A more pressing issue however is the fact that, despite legislation about the correct disposal of CCA containing waste being in place, a significant proportion remains untraceable, or ends up being incinerated together with benign waste fractions.[5] Indeed, a 9-year study looking at the waste wood sent to combustion facilities in Sweden found that wood coming into the facilities is highly variable in quality and can contain high levels of contaminants.[10] This results in the formation of As and other heavy metal-contaminated slag and fly ashes which prevents their further use, e.g. for spreading in forests.[5] Sorting of wood waste is therefore required, also to enable recycling of the usable waste wood fraction into products of higher value. Sorting is often done visually or augmented by the use of XRF (x-ray fluorescence) and PAN (1-(2-pyridylazo)-2-naphtol) as an indicator stain.[11]

Wood as a building material has excellent strength-to-weight properties, while being renewable.[12] Compared to non-renewable building materials, wood materials require less energy to manufacture and generate less GHG emissions.[13] Since the service life of a durable wood product is longer than the typical natural cycle of an unlogged forest that is only subject to natural disturbances, such as fires

and storms, removing some wood for the production of building materials results in the replacement of the forest population with younger, faster growing trees which are able to sequester additional carbon.[13] With the additional possibility to use post-consumer waste wood as a biomass fuel, wood-intensive houses have been found to be able to act as a net carbon sink and energy producer, especially in temperate climates.[13]

As briefly touched on in Part I. Background 2.3 Technoeconomic and Life Cycle Considerations of Bioenergy Value Chains, factors such as direct and indirect land-use change and the reference energy system can have a significant impact on the outcome of the bioenergy system LCA.[14,15] Indeed, a 2008 study published in Science found that land-use change was the single largest contributing factor to GHG emissions from corn and cellulosic ethanol, causing GHG emissions to increase by 93 and 50% vs. petrol for corn and cellulosic ethanol respectively.[14] Without land-use change however, GHG emissions from cellulosic ethanol are lowered by 70% vs. regular petrol, according to the study, indicating that switching to a post-consumer waste biomass feedstock for biofuel production could afford large CO_2 savings vs. regular petrol and other biofuels. In a similar way the exergy efficiency balance, as carried out by Kang and Tan[16] for the case of bio-ethanol produced from corn, could be drastically improved if the feedstock were switched to a post-consumer waste. The calculation included the total non-renewable energy input needed for the biofuel production, covering seeds, fertilizers and herbicides for cultivation and fuel for transport of the corn, as well as ethanol production and recovery. In the case of a diversion of a waste from landfill, the fossil fuel inputs for cultivation can be argued to be equal to 0 and hence the exergy efficiency would be significantly improved. Additionally diversion of bio-waste from landfills can alleviate some of the environmental concerns, such as methane emissions, associated with landfills.[17] Feedstock cultivation, also in the case of bioenergy crops such as switchgrass and *Miscanthus,* includes sowing, tilling, spreading of fertilizers, harvesting and baling, causing non-negligible cost and associated GHG emissions.[18]

The use of post-consumer waste also represents an economic opportunity. A study comparing six different pretreatment technologies for the production of bio-ethanol from switchgrass and the consequent minimum ethanol selling price (MESP) found that feedstock cost is 45-53% of the MESP across the six investigated pretreatment technologies with switchgrass costing ca. $79/dry tonne.[19] At the same time gate fees for disposal, treatment and recycling reached up to £82/tonne in the UK in 2015/16 for treated but not hazardous wood waste.[20] Landfilling attracts, in addition to the gate fee, a landfill tax which increased the median disposal cost in the UK in 2015/16 to over £100/tonne. This opportunity of a low-cost feedstock and previously shown high effectiveness of IL pretreatment for various feedstocks including softwoods combined with numerous accounts of ILs' ability to leach[21,22]

and extract metals[23–25] and the possibility to recover them via electrodeposition[26,27] therefore makes the ionoSolv process a promising candidate in tackling this waste disposal problem while producing a potentially low-cost and sustainable feedstock for the production of bio-derived chemicals and fuels.

In order to achieve an economically viable process, and especially so when working with relatively costly chemicals and solvents, recovery and reuse of the solvent and/or chemical are crucial.[28] Owing to their low vapour pressure, quantitative recovery of ILs is in theory possible without the need for enclosed systems and/or condensers. This is however only the case if the IL in question is thermally stable under the processing conditions. As discussed earlier, the IL often used for biomass applications [C_2C_1im][OAc] is not thermally stable in the long term.[29] Simmons, who stressed the importance of IL recycling to achieve economic viability of IL based biomass pretreatment, has therefore suggested pervaporation as a highly selective and scalable membrane separation process for IL dehydration.[30] While being energetically more advantageous than standard evaporation techniques, it was shown that this method allowed for >99.9wt% of the IL to be recovered from aqueous solutions and recycled at least 5 times. Alongside, vacuum distillation and electrodialysis were tested also, but gave poorer IL recovery. A much lower IL recovery (maximum 96%) was reported very recently for the IL 1-allyl-3-methylimidazolium chloride [AMim]Cl after microwave assisted pretreatment of *pinus radiata.*[31] Even though the IL structure was found to be unaltered, a gradual decrease in the IL's ability to dissolve the pine was observed, resulting in reductions of the fractionation yields as well as a variation in the composition and crystallinity of the produced fractions. The study did however not investigate the effects on enzymatic hydrolysis and it is therefore impossible to make a statement on the performance of the IL, especially since full dissolution of biomass is not always required in order to achieve good hydrolysis yields.[32] Nevertheless, the authors proposed that a cleaning step might be necessary after a certain number of cycles where an antisolvent would regenerate the IL by removing biomass derived impurities.[31] A study looking at the reuse of [C_2C_1im][OAc] over 8 cycles reported somewhat fluctuating glucose yields from both oak and spruce, ranging from 65.4 % in cycle 7 and 44.7% in cycle 6 for spruce and 63.7% in cycle 6 and 51.1% in cycle 2 for oak.[33] The lignin was not precipitated after the pretreatment but left in the IL to build up. But also outside the IL bubble recycling is being addressed. After alkaline pretreatment of *Miscanthus,* Cha *et al.* recycled the black liquor for two cycles. The fermentable sugar yield after the initial cycle with fresh reagents was 313.6 g/kg biomass which subsequently decreased to 303.0 and 261.1 g/kg biomass, after the first and second recycle respectively, corresponding to a decrease of 17% from the first to the third cycle.[34]

In this chapter, the pretreatment of treated timber with a focus not only on the pulp digestibility, but also the extraction of the metals present in the form of preservatives is discussed. Both copper treated

timber as well as CCA treated wood (pretreatment and saccharification carried out by Leila Carrier-Sippy, a MRes student who worked under my supervision) will be examined. Recycling of the IL solvent will be attempted (pretreatment, saccharificaion and trace element analysis carried out as instructed by the author by Louis Hennequin, a research assistant). Furthermore, pretreatment of real post-consumer waste wood will be discussed (pretreatment, saccharification and trace element analysis carried out by Leila Carrier-Sippy). The recovery of some of the metals via electrodepositon is demonstrated, and last but not least, the obtained glucose is subjected to fermentation for the production of ethanol (carried out by Dr Karen Polizzi).

Copper Treated Timber

Copper is a ubiquitous component in metal based wood preservatives due to its activity as a potent biocide[35] and first benchmarking experiments were therefore carried out using tanalised timber obtained from Travis Perkins (Tanalised timber green, treated with Tanalith E or similar). Copper is an important micronutrient for yeasts in low concentrations.[36] However, above certain concentrations copper is expected to be toxic and inhibit cell growth as well as ethanol production. Copper's inhibitory effect on yeast, an organism typically used in the fermentation of glucose to ethanol, is shown in Figure III-18. As shown, ethanol production is unaffected up to copper concentrations of 8 mM but are strongly reduced at concentrations above 16 mM. Based on the typical copper content of treated timber of 2000 ppm, pulp yields in the order of 50%, glucose yields from the pulp of ca. 80% (if hydrolysis time is limited to 1 or 2 days rather than the here reported 7 days), a typical initial glucose concentration in the fermentation tank of 200 g/L,[37] and the atomic mass of copper, the glucose syrup for fermentation would (without copper removal) be at a Cu concentration of around 16 mM. In order to eventually be able to use waste wood including copper treated timber, the copper concentration in the glucose stream therefore needs to be accordingly reduced.

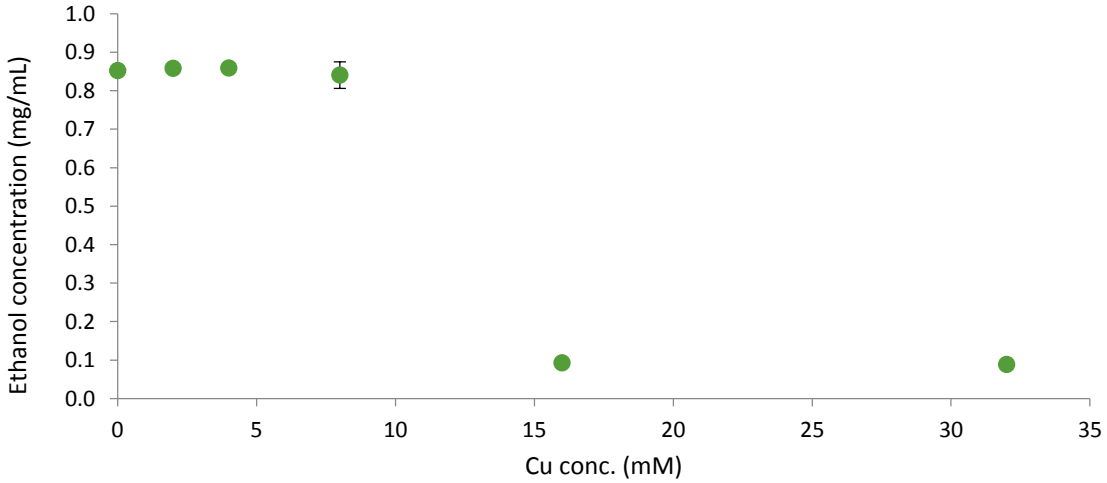

Figure III-18 Ethanol produced through fermentation of YPD medium by *Saccharomyces cerevisiae* as a function of the copper concentration present in the medium.

The initial focus of this study was the extraction of copper and concomitant fractionation of the wood. Throughout the experiments treated timber from Travis Perkins was used (obtained as planks, chopped and sieved by the author). Different batches were used at different stages of the experiments with slightly different compositions and while it is not possible to know the exact tree species from which the wood was obtained from, it can be said with virtual certainty that it was in all cases a softwood. A representative composition is displayed in Figure III-19 and the numeric values given in Table III-7. It should be noted that although strictly speaking the Cu preservative should be counted as ash, the compositional analysis only accounts for acid insoluble ash, which was here found to be below the detection limit.

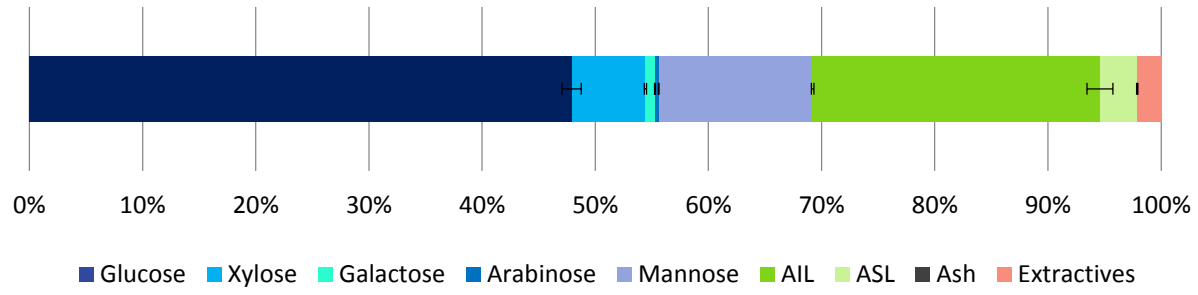

Figure III-19 Representative composition of copper treated wood used in pretreatments. AIL: acid insoluble lignin; ASL: acid soluble lignin.

Table III-7 Representative composition of copper treated wood used in pretreatments.

Glu	Xyl	Gal	Ara	Man	AIL	ASL	Ash	Extr
47.9±0.8	6.5±0.1	0.8±0.0	0.4±0.0	13.6±0.3	25.4±1.1	3.3±0.1	BDL	2.1±0.0

Glu: glucose; Xyl: xylose, Gal: galactose; Ara: arabinose; Man: mannose; AIL: acid insoluble lignin; ASL: acid soluble lignin; Extr: extractives.

The First Attempt: [HC_1im][HSO_4]

Initial tests were carried out with the IL [HC_1im][HSO_4], mainly on the basis that it is fairly cheap[38] and good results were obtained with the slightly more expensive butyl-chain carrying [HC_4im][HSO_4] in a study where *Miscanthus* was fractionated.[39] Conditions of 150°C for 4 hours were initially chosen since preliminary results with softwoods at 120°C for up to 24 hours using the even less expensive [TEA][HSO_4] were rather discouraging. In order to compare the behaviour of treated timber to untreated pine wood, a benchmarking experiment with untreated, i.e. virgin, pine was conducted. In addition to that, a control experiment with virgin pine and added Cu(II) oxide was run as well. 100 mg of the Cu(II) oxide were added to 10 mL of the ionic liquid-water mixture and left at room temperature overnight, which resulted in most of the black Cu(II) oxide dissolving into solution, giving it a blue colour which I attribute to the formation of $CuSO_4$.

Tanalised timber obtained from Travis Perkins (treated with Tanalith E or similar) as well as virgin pine wood from Finland were digested and analysed by ICP-OES for their copper content. While the native pine was found to only contain traces of copper (<1ppm), the tanalised timber tested here contained almost 2100 ppm of copper, which is in accordance with literature values.[4,40] While in all cases saccharification yields were only slightly improved compared to untreated biomass, the copper did not appear to have a negative effect on pretreatment behaviour or saccharification yield (Table III-8). The best results were indeed achieved with the tanalised timber, both for untreated and pretreated biomass. This is likely to stem from a slight difference in the feedstock composition but could also be a result of the pressure treatment.

Table III-8 Results from the pretreatment of virgin pine (VP), virgin pine with CuO (VP+CuO) and Tanalised timber (TT) for 4 hours at 150°C in [HC_1im][HSO_4] (20wt% final water content) and subsequent saccharification for 7 days.

Biomass	Pulp recovered[a]	Lignin precipitated[a]	Saccharification yield	
			Untreated[b]	Pretreated[b]
VP	58.2±0.8	5.7±0.2	7.1±1.3	9.7±0.7
VP+CuO	63.1±0.8	5.6±0.1	7.1±1.3	11.9±0.4
TT	59.8±0.6	4.6±0.4	8.5±3.7	12.5±0.3

[a] % of initial weight of biomass on oven-dried base. [b] % of maximum possible.

After pretreatment, liquor, pulp and lignin were analysed for their copper concentration, and the results compared to the initial copper content of the wood. 82% of the copper were found in the ionic liquid liquor after pretreatment of tanalised timber and 81% of the copper added to virgin pine pretreatment (Table III-9, VP+CuO). Further analysis of the pulp and lignin isolated from tanalised timber pretreatment revealed that the remaining 18% were left in the pulp. The lignin only contained negligible amounts of the total copper as shown in Table III-10.

Table III-9 Copper contents (as measured by ICP-OES) and relative copper recovery in ionic liquid liquors after pretreatment for 4 hours at 150°C Treated timber, virgin pine and virgin pine with 10wt% CuO (with respect to biomass weight) was pretreated for 4 h at 150°C with [HC_1im][HSO_4] and a biomass to solvent ratio of 1:10 g/g.

	Virgin Pine	Tanalised Timber	Virgin Pine+CuO
Cu ppm in feedstock	0.63±0.03	2091±16	3.5±0.6
Cu ppm in IL liquor	3.5±0.6	199±4[a]	8325±587[a]
Cu Recovery	-	82±1%	81±1%[b]

[a]Corrected for background measured of the recycled ionic liquid after the pretreatment of virgin pine. [b]as a percentage of the added CuO (ca. 100 mg)

Table III-10 Copper concentrations (analysed by ICP-OES) and corresponding percentage of total available copper in different streams after pretreatment of treated timber with [HC_1im][HSO_4] for 4 h at 150°C with a biomass to solvent ratio of 1:10 g/g and a final water content of 20wt%.

Liquor		Pulp		Lignin		Mass closure
ppm[a]	%[b]	ppm[a]	%[b]	ppm[a]	%[b]	
199±4	82±1	572±41	18±1	111±3	0	99.97 %

[a]ppm in sample; [b]% of total available Cu.

Next, experiments were carried out to establish whether the remaining 18% of copper found in the pulp was not yet extracted from the wood particles, or if redeposition caused a fraction of the copper to be found on the pulp surface. While the finding that the control experiment with added CuO yielded a very similar copper recovery in the IL of 81% suggests a redeposition, the possibility of a coincidence cannot be excluded. A smaller particle size fraction (<180 µm vs. 180-850 µm) was used to improve penetration of the ionic liquid into the centre of the wood particle in order to see if more copper was extracted this way. To test the redeposition hypothesis, an altered washing protocol was employed, where the isolated pulp was washed again with ionic liquid at room temperature so as to find out whether the copper content in the pulp can be lowered in that way, which would indicate that copper is found predominantly on the surface of the particles after pretreatment. The results are shown in Table III-11.

Table III-11 Copper concentrations (analysed by ICP-OES) and corresponding percentage of total available copper after pretreatment of treated timber with [HC_1im][HSO_4] for 4 h at 150°C with a biomass to solvent ratio of 1:10 g/g and a final water content of 20wt%.

	Control	Repeated IL wash		Smaller particle size
	normal washing protocol	1st IL wash	2nd IL wash	normal washing protocol
Cu ppm in IL	222±8	209±7	45±2	171±4
% from original	81%±3%	79%±2%	17%±1%	65%±1%
% from remaining	n/a	n/a	83%±7%	n/a
overall extracted	81%±3%	96%±2%		65%±1%

When using smaller particle sizes for the pretreatment, the amount of extracted copper was reduced to 65% while washing the pulp with IL at room temperature indeed resulted in an increase of copper removal from the pulp to 96%. Furthermore the second washing step removed approximately the same percentage of the remaining copper content of the pulp as the first wash (around 80%). These findings led to the conclusion that the extraction efficiency under these conditions is not limited by

the accessibility of the copper but that extracted copper is being redeposited onto the pulp surface during the ethanol washing. The separation procedure in an industrial setting is not expected to include dilution with ethanol and therefore a lower degree of redeposition of metals onto the cellulose surface is expected to be achievable.

IL Screening: Copper Extraction and Enzymatic Hydrolysis Yields

While the study using $[HC_1im][HSO_4]$ gave promising results with respect to copper recovery in the ionic liquid, the sugar release from the isolated pulp was disappointing, making it unsuitable for biorefining under the conditions used. It was therefore decided to move on to testing a range of ionic liquids for both their ability to produce a highly digestible pulp, dissolve the copper preservative and keep it in solution during washing. For this the previously very successful conditions of 30 min pretreatment at an oven temperature of 170°C with 20wt% water present in the various ILs was used. A range of different cation and anions were used for the screening in order to also establish whether there are decisive characteristics of the ionic liquids and their constituting ions. The list of ionic liquids screened is given in Table III-12 where [TEA] stands for triethylammonium, [DMBA] for *N,N*-dimethyl-*N*-butylammonium, [DEA] for diethylammonium, [DEtOHA] for diethanolammonium, $[HC_1im]$ for 1-methylimidazolium, $[C_2C_1im]$ for 1-ethyl-3-methylimidazolium, [OAc] for acetate and [OTf] for trifluoromethanesulfonate. The range of ILs includes protic and aprotic ones, cations based on imidazoles, secondary amines, tertiary amines, symmetrically and asymmetrically substituted amines, as well as alcohol functionalised amines and coordinating and non-coordinating anions.

Table III-12 Ionic liquids screened.

Abbreviation	Type of ionic liquid
$[TEA][HSO_4]$	Protic, symmetric, tert. amine based, weakly coordinating anion
$[DMBA][HSO_4]$	Protic, asymmetric, tert. amine based, weakly coordinating anion
$[HC_1im][HSO_4]$	Protic, imidazole based, weakly coordinating anion
$[DEA][HSO_4]$	Protic, symmetric, sec. amine based, weakly coordinating anion
[DEtOHA]Cl	Protic, symmetric, sec. amine based, alcohol side chain, strongly coordinating anion
$[HC_1im]Cl$	Protic, imidazole based, strongly coordinating anion
$[C_2C_1im]Cl$	Aprotic, imidazole based, strongly coordinating anion
$[C_2C_1im][OAc]$	Aprotic, imidazole based, strongly coordinating anion
$[C_2C_1im][OTf]$	Aprotic, imidazole based, mildly coordinating anion

Table III-13 displays the copper extraction, saccharification yield as well as pulp and lignin yields after pretreatment of the copper azole treated softwood with the tested ILs. The data shown here suggest that $[HSO_4]^-$, Cl^- and $[OAc]^-$ ILs are capable of the extraction of over 80% of the present copper from

treated softwood. The only studied IL that extracted a significantly lower amount of copper is $[C_2C_1im][OTf]$ which extracted less than 70% of the copper.

Table III-13 Percentage of copper found in the IL, 7 days saccharification yield and pulp and lignin recovered after pretreatment with various ILs with a final water content of 20wt%. Tanalised timber was pretreated for 30 min at an oven temperature of 170°C with a biomass to solvent ratio of 1:10 g/g. Errors were calculated as standard deviations over triplicates.

Ionic liquid	Copper extraction	Saccharification yield	Pulp yield	Lignin yield
$[TEA][HSO_4]$	87±1 %	55.2±2.6	56.7±0.3	8.7±0.2
$[DMBA][HSO_4]$	**93±0 %**	**72.3±4.1**	42.6±0.3	19.4±1.4
$[HC_1im][HSO_4]$	82±1 %	15.7±2.6	58.9±0.5	7.0±1.7
$[HC_1im]Cl$	**98±2 %**	**75.7±2.5**	43.1±0.8	14.3±0.7
$[DEA][HSO_4]$	85±2 %	0.1±0.1	34.7±1.0	7.3±0.4
[DEtOHA]Cl	81±4 %	11.0±0.3	94.5±0.3	BDL
$[C_2C_1im][OAc]$	86±2 %	43.0±1.9	92.1±1.2	BDL
$[C_2C_1im]Cl$	92±1 %	28.8±2.9	75.9±1.8	1.7±0.2
$[C_2C_1im][OTf]$	68±1 %	9.7±0.3	92.7±0.4	BDL
Untreated	-	9.9±0.2	100	-

A wider range of results was obtained for the saccharification of the recovered cellulose rich pulp; the highest glucose yields were obtained for enzymatic saccharification of $[DMBA][HSO_4]$ and $[HC_1im]Cl$ pretreated biomass (above 70% of theoretical). These results are in line with what was previously reported for untreated softwoods in Chapter 2 in the case of $[DMBA][HSO_4]$ and by Cox *et al.* for $[HC_1im]Cl$.[41] Lower yields but still significant improvements compared to untreated biomass were obtained with $[TEA][HSO_4]$, $[C_2C_1im][OAc]$ and $[C_2C_1im]Cl$. $[C_2C_1im][OAc]$ and $[C_2C_1im]Cl$, reported many times as cellulose dissolving solvents[42] resulting in the decrystallization of cellulose[43] and typically yielding a highly digestible pulp,[44] showed a mediocre performance here, most likely as a result of the presence of water, which hinders cellulose dissolution. However, since the process economics mitigate against excessive water removal and drying, this IL was not tested under its reportedly successful conditions. Pretreatment with $[DEA][HSO_4]$ resulted in the degradation of the biomass, producing a black powder and giving virtually zero glucose yield. However $[DEA][HSO_4]$ was one of several protic ILs screened for pretreatment of switchgrass and was reported to perform only slightly less well than $[TEA][HSO_4]$ under the same conditions.[45] Unfortunately the authors of said study failed to provide comprehensive information on their experimental conditions and it is therefore unclear why such different behaviour was seen here. Only marginally improved glucose yields vs. untreated biomass were obtained with $[C_2C_1im][OTf]$, $[HC_1im][HSO_4]$ and [DEtOHA]Cl. $[C_2C_1im][OTf]$ has been screened for the pretreatment of *Miscanthus* by Brandt *et al.*[32] where, similarly, no significant improvement of pulp digestibility was observed. [DEtOHA]Cl and $[HC_1im][HSO_4]$ have to my

knowledge not been reported for biomass pretreatment and therefore no data are available for comparison. Furthermore, the findings obtained here strongly suggest that using these two PILs for biomass pretreatment should be discouraged.

The presented results suggest that neither cation nor anion are by themselves decisive for the outcome of pretreatment and copper extraction. The two ionic liquids which performed best at producing a highly digestible pulp also resulted in the largest fraction of copper extracted and retained in the IL. From the preliminary study using $[HC_1im][HSO_4]$ I have concluded that copper is redeposited onto the cellulose surface, probably during work up. Lignin has been reported to be a good sorbent for heavy metals[46] which leads to the hypothesis that lignin reprecipitation onto the cellulose surface increases the likelihood of copper redeposition, resulting in a lower proportion found in the ionic liquid when more lignin is redeposited onto the pulp surface. The dilution of the black liquor with ethanol for pulp washing is suspected to cause lignin reprecipitation, which, as discussed above, is expected to be avoided when operating in an industrial setting. Near quantitative copper extraction is therefore expected to be achievable for several ILs.

CCA Treated wood: Metal Extraction and Saccharification

Encouraged by the results from experiments with copper treated timber, we moved on to wood treated with chromated copper arsenate (CCA). Since this type of wood is not sold anymore in the UK or Europe, we had to import it from China. While Cu is a potent biocide, Cr and As are carcinogens[47] and therefore a major health concern in fly ashes and ways of recovering these two metals in a benign or easy to handle form is beneficial.

Compositional analysis of the CCA treated wood suggests that it is a softwood with a slightly lower carbohydrate content compared to the treated timber used in pervious experiments. Its composition is displayed in Figure III-20. CCA treated wood was initially pretreated using the previously successful IL and conditions for pine pretreatment, $[HC_4im][HSO_4]$ with 20wt% water for 1 hour at 150°C. Results from pretreatment, including saccharification yield, metal content and metal extraction can be found in Table III-14. 52.5% of theoretical glucose yield was achieved after 7 days of enzymatic hydrolysis for the pretreated sample vs. 6.8% for the raw biomass. This corresponds to an improvement of a factor of 7.8. Metal extraction under the same conditions were 98, 99 and 99% for Cu, Cr and As respectively, as calculated from the remaining metal content of the pulp measured by ICP-OES.

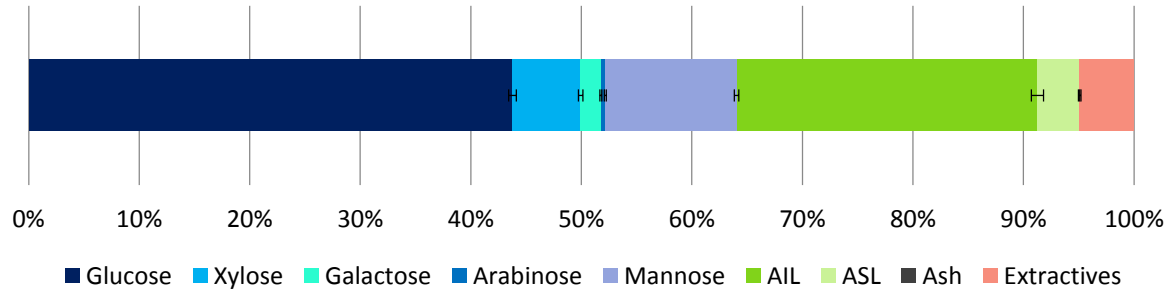

Figure III-20 Compositional analysis of CCA treated wood used in the experiments. AIL: Acid insoluble lignin. ASL: Acid soluble lignin.

Table III-14 Metal Contents as measured by ICP-OES and relative metal extraction in pulp after pretreatment as well as the 7 day saccharification yield of the air-dried pulp and raw biomass. CCA treated wood was pretreated with [HC_4im][HSO_4] for 1 hour at 150°C at a biomass to solvent ratio of 1:10 g/g and a final water content of 20wt%. Standard errors were calculated for triplicate measurements.

	Arsenic	Chromium	Copper	Saccharification yield
Raw CCA wood	4268±605 ppm	4664±745 ppm	2784±365 ppm	6.8±0.3%
Pretreated CCA wood	56.7±8.8 ppm	111.1±15.6 ppm	134.6±30.5 ppm	52.5±2.1%
Improvement[a]	99%	99%	98%	7.8x

[a]Taking pulp yield into account.

These results were, especially with respect to the metal extraction, incredibly encouraging. In order to improve the economic viability we moved on to using [HC_1im]Cl, which is expected to be lower in cost and was shown to have excellent copper removal capabilities in the screening study discussed above. Additionally, we increased the solid to solvent ratio from 1:10 to 1:5 g/g and changed the pretreatment conditions from 1 h at 150°C to 30 min at 170°C in order to increase throughput in a potential industrial process. Furthermore pulps were saccharified without hornification in order to achieve higher sugar yields. The results from metal extraction as well as saccharification yield are displayed in Table III-15. As and Cr extraction were found to decrease to 94 and 88% respectively while Cu extraction from the pulp remained high at almost 100%. Saccharification yields increased to 66% which is mainly attributed to the avoidance of hornification. It is unclear why the Cr and As extraction is lower using the chloride IL. It is possible that the less acidic chloride IL, which is made of the monoprotic acid HCl, fails to keep Cr and As in solution upon dilution with ethanol for the pulp wash, while the more acidic HSO_4 IL, which is made of the diprotic acid H_2SO_4, is capable of keeping the metals in solution even upon dilution.

Table III-15 Metal extraction from the pulp as calculated from the metal content in the pulp as measured by ICP-OES and the pulp yield obtained after pretreatment as well as the 7 day saccharification yield of non-hornified pulps. CCA treated wood was pretreated with [HC_1im]Cl for 30 min at 170°C at a biomass to solvent ratio of 1:5 g/g and a final water content of 20wt%. Standard errors were calculated for triplicate measurements.

Metal Extracted			Saccharification yield
Arsenic	Chromium	Copper	
93.5±0.9%	87.9±0.7%	99.5±0.2%	66.5±3.3%

Recycling

After the encouraging results from single-pass experiments, we moved on to testing if we can recycle the isolated brown liquor and reuse it for repeated pretreatments. This is crucial for any further process development since, despite the ionic liquids used being low-cost, solvent cost has to be kept to a minimum in order to make the produced intermediates suitable for the production of bulk chemicals and fuels. Just as above, CCA treated softwood was used as the feedstock and [HC_1im]Cl as the solvent over 6 cycles of pretreatment. The average brown liquor recovery after each cycle was found to be 99.06±0.72%. Figure III-21 shows metal extraction from the pulp for Cr, Cu and As.

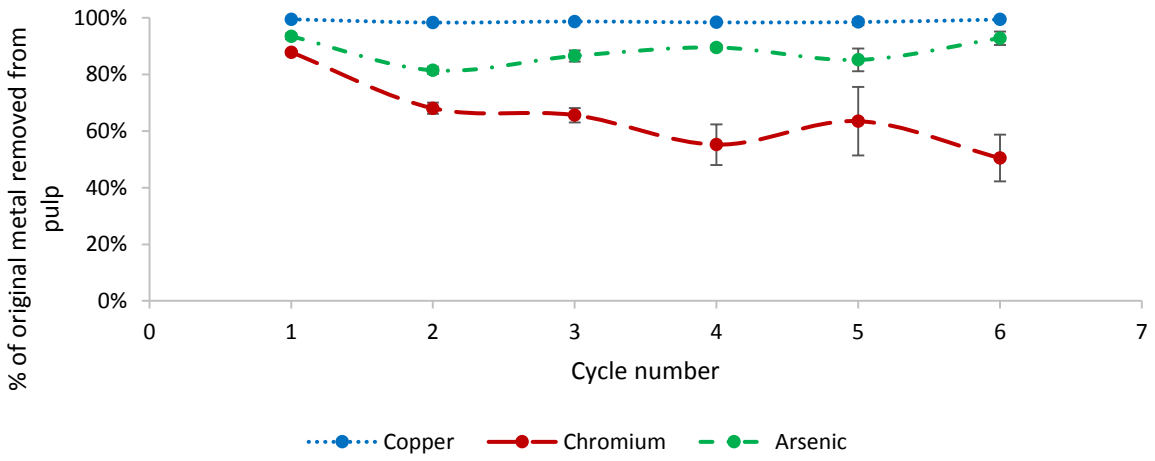

Figure III-21 Metal extractions from the pulp as calculated from the metal content in the pulp as measured by ICP-OES and the pulp yield obtained after pretreatment. CCA treated wood was pretreated with [HC_1im]Cl for 30 min at 170°C at a biomass to solvent ratio of 1:5 g/g and a final water content of 20wt%. Standard errors were calculated for triplicate measurements.

Copper extraction is very high throughout the 6 cycles at no less than 98%. Chromium extraction decreased from an initial 88% to between 68 and 51% for the following cycles. Arsenic extraction was found to fluctuate between 82 and 94% extraction. An altered washing protocol where less wash solvent is used, or where recycled IL is used which contains less lignin, may however be able to yield better metal extractions over many recycles.

In addition to the pulps, also the brown liquor (i.e. the IL after lignin precipitation and water evaporation) was analysed for metal concentration to establish whether the metals accumulate in the IL or leave the system via lignin precipitation. A blank IL without any biomass was subjected to the same ethanol and water additions and removals over the 6 cycles as the working IL in order to account for eventual accumulation of metals from external sources, such as metallic dust found on stirrer bars and chromium leaching from stainless steel spatulas. It was used as a blank in the ICP-measurements and its metal concentrations (below detection limit for As and Cu, <1 ppm for Cr) subtracted from the ones measured for the working ILs. Figure III-22 shows the ppm of Cr, Cu and As found in the brown liquor. As can be seen, Cu and As concentrations steadily increased over the 6 cycles at a relatively stable rate. Despite there being almost twice as much As in the wood than Cu, concentrations in the IL were found to be similar. Cr concentration however only increased slightly over the first 4 cycles and then remained stable at around 1200 ppm. These findings suggest that a large proportion of Cr and smaller amounts of As and Cu precipitate out during the lignin precipitation step. The possibility to maintain high metal concentrations during the process has the advantage of a relatively easier electrodeposition (discussed later) vs. a case where the deposition needs to take place at very low concentrations of metals if the IL cannot keep the metals in solution throughout the different process steps.

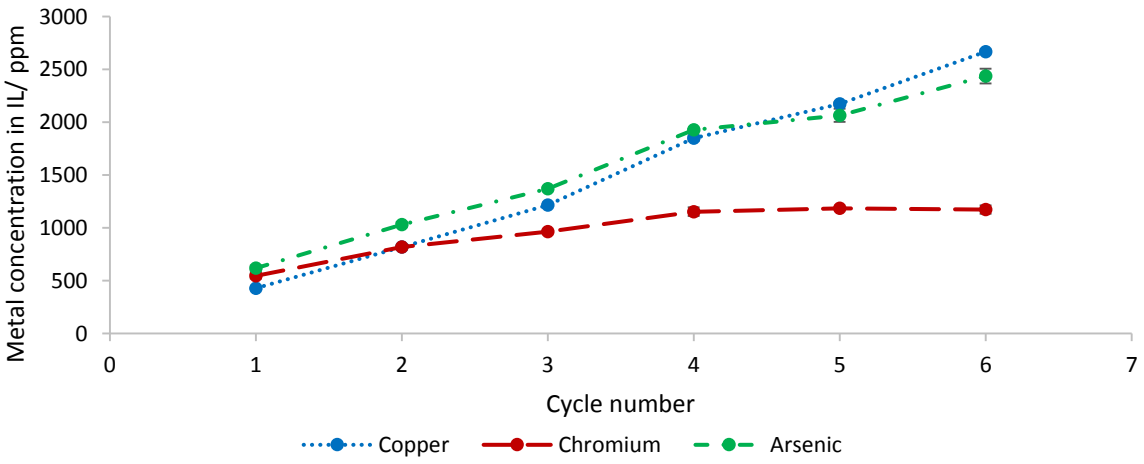

Figure III-22 Metal ppm found in the IL brown liquor after pretreatment for n cycles as analysed by ICP-OES. A 1wt% solution of IL liquor in 5% nitric acid was made and filtered through a 0.22 µm syringe filter. CCA treated wood was pretreated with $[HC_1im]Cl$ for 30 min at 170°C at a biomass to solvent ratio of 1:5 g/g and a final water content of 20wt%. Standard errors were calculated for triplicate measurements.

Figure III-23 shows the percentage of the different metals found in the IL after each stage, taking into account at what concentration the metal was found in the IL at the previous cycle. The exact equations used for the calculations can be found in Part II. Experimental Methods. Cu recovery in the IL started off at just below 90%, before rising to around 95% in cycle 6. Arsenic extraction started off at 81% and subsequently fluctuated at around 75%. Despite the deviation within the triplicate experiments being

fairly small, a spike can be observed at cycle 4 where 102% of Cu appears to have been found in the IL liquor while also the As percentage in the liquor showed an increase. For both metals this was followed by an apparent decrease in percentage of metal found in the IL. It is possible that the Cu and As concentrations in the wood are not homogeneous and that the particles have not been mixed well enough after chopping and sieving, however it is unlikely that the triplicate samples are equally affected by this rather random error. Equally, a contamination from an external source is possible, however there are no known sources of As in the laboratory and again it would be a rather unlikely coincidence that both Cu and As contaminations are introduced during the same cycle. It is more likely that it is due to a measuring error of the ICP. An apparently higher concentration of As and Cu in one cycle would then reflect negatively on the next cycle, where the concentration of the IL in the earlier cycle is the baseline for the consecutive cycle. Cr appears to be unaffected by this outlier, quite possibly due to the system having reached a saturation limit as we saw in Figure III-22 where Cr concentration in the IL stagnated after cycle 4. This is reflected in Cr recovery in the IL fluctuating around 60% after an initial 69% was found in the IL after the first cycle.

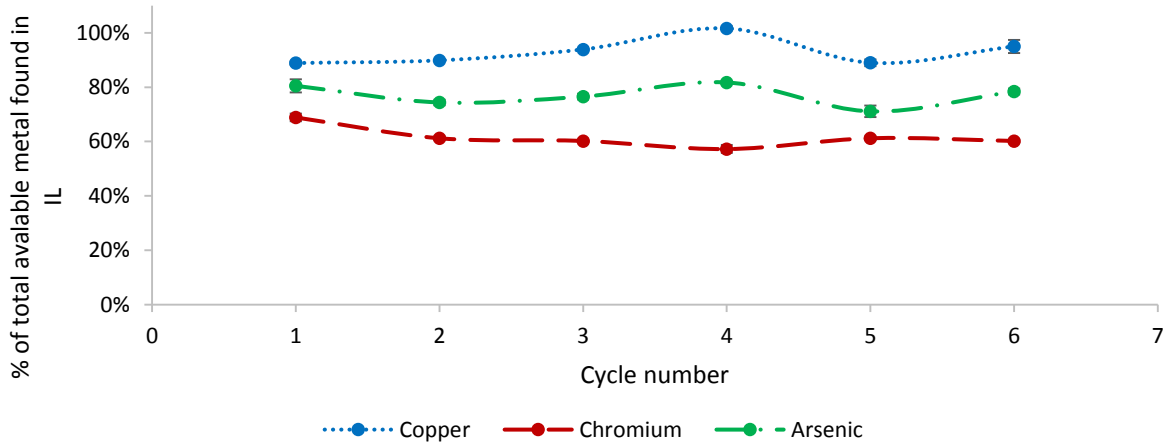

Figure III-23 Percentage of Cu, Cr as As found in the IL brown liquor after n cycles based on the metal concentration prior to the cycle and the amount of new metal entering the system. CCA treated wood was pretreated with [HC_1im]Cl for 30 min at 170°C at a biomass to solvent ratio of 1:5 g/g and a final water content of 20wt%. Standard errors were calculated for triplicate measurements.

For completeness, the lignin was analysed for its metal content and the metals' mass closure calculated (Table III-16). For As and Cu the mass closures were in the vicinity of 100% for the various cycles. In the case of Cu, numbers fluctuated around 100% while they are consistently below 100% for As. Volatilisation of As compounds is a possible explanation for this observation, however it is unclear whether this would have happened during one of the biomass processing steps or during the sample preparation for ICP analysis. Also it should be noted that the errors associated with the various measurements resulted in a relatively large overall error. In the case of Cr often more than 100% of the theoretical maximum was found and large variations were observed across the triplicate

experiments. While all numbers are corrected for a blank IL which went through the same process steps of ethanol and water addition and evaporation, it cannot be excluded that Cr contamination was introduced to one or more of the samples. There are multiple sources of Cr found in all laboratories, stainless steel being a major one.

Table III-16 Mass closures from ICP-OES analysis of pulp, lignin and brown liquor isolated after each cycle of pretreatment of CCA treated timber. CCA treated wood was pretreated with $[HC_1im]Cl$ for 30 min at 170°C at a biomass to solvent ratio of 1:5 g/g and a final water content of 20wt%. Standard errors were calculated for triplicate measurements.

	Cu	Cr	As
Cycle 1	94.7±4.3%	95.1±4.3%	92.3±3.0%
Cycle 2	93.8±0.7%	111.4±2.9%	98.1±0.8%
Cycle 3	99.0±2.4%	125.9±0.2%	97.6±1.8%
Cycle 4	105.4±2.9%	133.1±26.4%	99.6±6.7%
Cycle 5	98.9±7.2%	109.7±19.6%	92.9±6.3%
Cycle 6	105.4±2.3%	128.9±4.2%	97.8±0.9%

As discussed above, metal extraction is not the only measure of success for the pretreatment of hazardous wood. The pulps were also subjected to enzymatic hydrolysis and these results, together with lignin and pulp yields, are displayed in Figure III-24. Saccharification yields, starting at 67% after the first cycle, gradually decreased over the subsequent 3 cycles to 55% in cycle 4 and then increased again to 75% in the 6th cycle. Lignin yields, calculated from the initial amount of lignin in the biomass, were lowest in cycle 1 at 39% and monotonously, with the exception of cycle 5 which had a slightly lower lignin yield than cycle 4, increased to 69% in cycle 6. Pulp yields somewhat oscillated between 62 and 54% with no apparent trend. Lignin yields were relatively low compared to previous experiments, especially after the first two cycles. At the same time the pulp yields were relatively high throughout the series. Again the reprecipitation of lignin onto the pulp surface upon dilution of the black liquor may be the underlying cause. It is however unclear if the differences between this set of experiments and the previously reported pretreatment of pine with $[HC_4im][HSO_4]$ are due to a difference in feedstock or the properties of the ionic liquid.

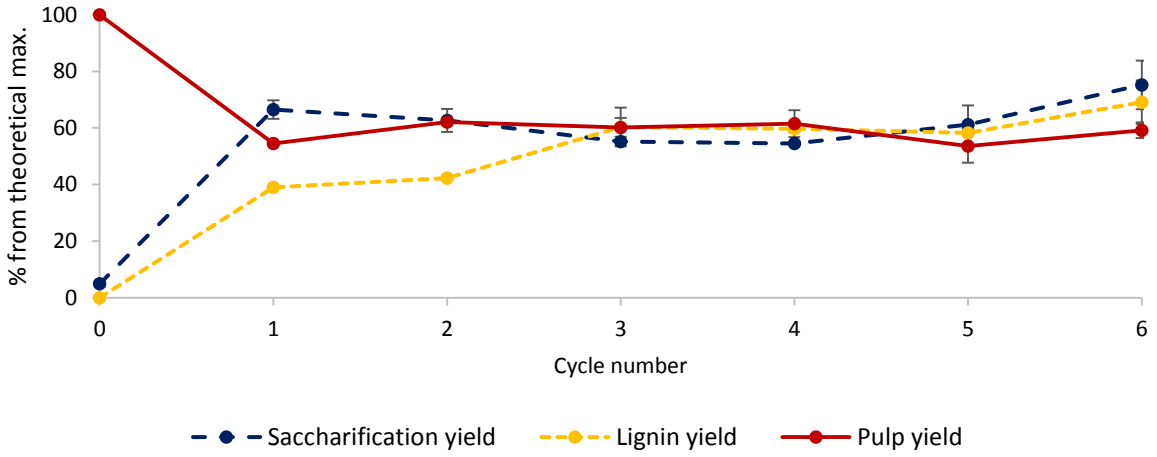

Figure III-24 Lignin, pulp and 7 day saccharification yield of untreated and pretreated CCA treated wood over 6 cycles. CCA treated wood was pretreated with [HC_1im]Cl for 30 min at 170°C at a biomass to solvent ratio of 1:5 g/g and a final water content of 20wt%. Standard errors were calculated for triplicate measurements.

Overall these results are very promising. Performance of the IL for pretreatment of CCA treated wood over at least 6 cycles was shown to be maintained with respect to both producing a digestible pulp as well as removing the main metals present, and especially Cu, which is the main biocide in the formulation.

The Real Stuff: Infeed and Processed Waste Wood

In addition to the clean CA and CCA treated wood, which are at best representative of pre-consumer construction waste, real post-consumer waste wood obtained from SUEZ Environment was tested under some of the most promising conditions, i.e. 30 min at 170°C. The ionic liquid chosen for this study was [HC_1im]Cl as a result of the very promising results in the screening study discussed above. Two different types of waste wood were tested: so-called infeed wood, which is wood as received, and processed wood, which has gone through a simple separation step where most ferrous metals were removed. The waste wood is expected to contain various metals at different concentrations. A study from Sweden suggests that waste wood coming into incineration plants comes at varying degrees of quality and contamination.[10] Since ICP-OES analysis only renders results for the metals specifically analysed for, and since there is a limited number of metals that can be analysed in a given sample size, only a selection of metals was analysed for. Compositional analysis of the two types of wood can be seen in Figure III-25 and the results from pretreatment and metal content and extractions in Table III-17 and Table III-18. As we can see from Figure III-25, infeed and processed wood have very similar compositions. Judging from the relatively high xylose content alongside the mannose, it appears that the wood is composed of a mixture of soft- and hardwoods. Pretreatment of soft- and hardwoods together has been successfully demonstrated in Chapter 2.

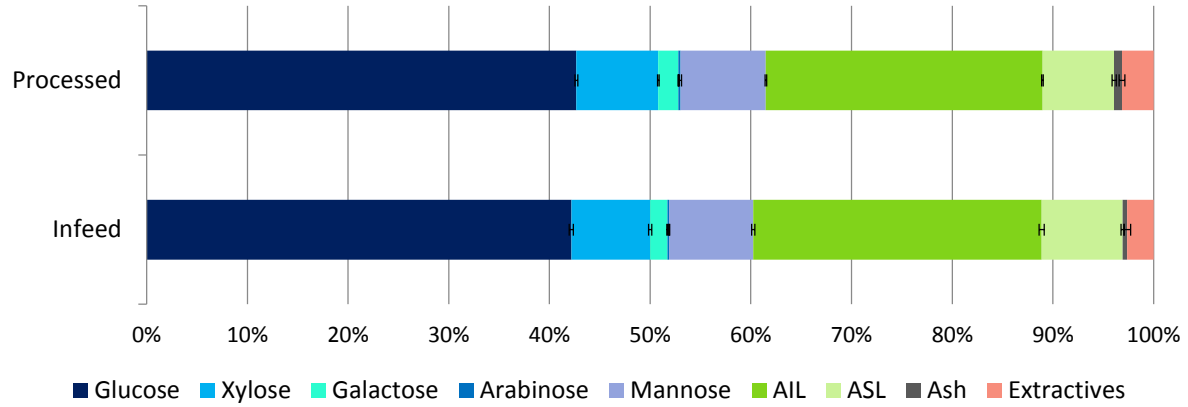

Figure III-25 Compositional analysis of the infeed and processed wood obtained from Suez. AIL: Acid insoluble lignin. ASL: Acid soluble lignin. Standard errors were calculated for triplicate measurements.

The initial contents of Zn, Pb, Fe, Cr and Cu are displayed in Table III-17 and Table III-18 for unprocessed infeed and processed wood respectively. Arsenic content was determined also but was found to be below the detection limit in both cases and is therefore not discussed below. Cu content was selected for analysis due to its inhibitory effect on yeast growth, as shown above. Zn was chosen because it is the most abundant naturally occurring metal in plant matter. The incineration of municipal solid waste in Switzerland and the subsequent disposal of the fly ash results in a loss of 2200 tons of Zn every year, according to Schlumberger.[48] A relatively complex acid washing of the fly ash makes it possible to recover the Zn, but the potential to recover Zn integrated in the pretreatment process would represent an economic opportunity. Pb and Cr contents were determined due to the health concern associated with these metals.[47,49] Fe, being ubiquitous in civilisation, was expected to be present in significant amounts and therefore Fe content was also determined.

In the case of infeed wood Fe was indeed found to have the highest concentration of the analysed metals with over 500 ppm. Cr and Cu concentration were found to be below 50 ppm, indicating that only a small amount of the wood was treated with Cr or Cu containing preservatives. Pb was found at around 170 ppm and Zn at around 140 ppm. All metals, with the exception of Fe (65%), were at least 80% extracted, reducing their final concentrations in the pulp to under 30 ppm.

Table III-17 Metal Contents as measured by ICP-OES and relative metal extraction from the pulp after pretreatment of the unprocessed mixed wood (i.e. infeed wood). Unprocessed mixed wood was pretreated with [HC_1im]Cl for 30 min at 170°C and a water content of 20wt%. Standard errors were calculated for triplicate measurements.

	Zinc	**Lead**	**Iron**	**Chromium**	**Copper**
Metal Content /ppm	138±0	173±8	567±12	9.1±1.2	37±7
Metal Extracted	86±3%	85±1%	65±5%	80±3%	90±1%

For processed wood, the initial Fe concentration was lower than for infeed wood at around 330 ppm. The concentrations of the other metals was higher than for infeed wood, with the exception of Zn. Extraction of the metals was found to be close to or above 90% except for Fe (56%). The increased extraction of the heavy metals when the initial Fe content is lower could be indicative of a competition for ligand ions. It is however difficult to be certain since the two types of wood are likely to differ in other ways, such as the presence of glue and other metals (e.g. Ti and Al from paint), which are likely to affect the system as well.

Table III-18 Metal Contents as measured by ICP-OES and relative metal extraction from the pulp after pretreatment of the processed mixed wood. Processed mixed wood was pretreated with [HC_1im]Cl for 30 min at 170°C and a water content of 20wt%. Standard errors were calculated for triplicate measurements.

	Zinc	Lead	Iron	Chromium	Copper
Metal Content /ppm	114±0	367±19	331±32	55±2	82±5
Metal Extracted	89±0%	96±2%	56±9%	93±1%	97±0%

The isolated pulps were also subjected to enzymatic saccharification. The results are displayed in Table III-19. In both cases the untreated biomass gave saccharification yields of around 14% which is significantly higher than for the copper and CCA treated wood analysed previously. It is possible that being exposed to weather and fungi has resulted in a mild pretreatment already.[50] The pretreated pulps showed saccharification yields around 4 times higher. The processed wood gave slightly higher yields than the infeed wood, though again it is unclear whether this has to do with the removal of ferrous metals or if the difference in composition and presence of other contaminants is responsible.

Table III-19 7 day saccharification yield of air-dried untreated and pretreated infeed and processed wood. Infeed and processed mixed wood were pretreated with [HC_1im]Cl for 30 min at 170°C and a water content of 20wt%. Standard errors were calculated for triplicate measurements.

	Untreated biomass	Pretreated biomass	Improvement
Unprocessed	13.5±0.1	52.8±2.9	3.9x
Processed	14.8±0.5	59.6±5.8	4.0x

These findings demonstrate that the ionoSolv process is potentially a valid alternative to current waste wood disposal routes. The potential to use mixed wastes or waste woods of different grades further allows to omit a thorough separation step which could further afford a reduction in disposal cost.

Metal Recovery

While the above findings suggest that copper extraction from CCA treated wood is maintained over at least 6 cycles, the Cu concentration in the IL cannot keep rising indefinitely. One way of reducing the content of Cu and other metals in a solution is via electrodeposition.[51] Electrodeposition is potentially easily integrated in a large scale plant by inserting two electrodes at a suitable point in the process line, hence resulting in minimal additional complexity. Electrodeposition of Cu and Cr in various ILs,[52] including PILs,[53] has been reported in the past. Arsenic deposition has to the knowledge of the author not been studied in PILs.

It should be pointed out that the content of copper in the IL does not need to be reduced completely, but in a steady state process should be reduced each time by the amount that has entered the system since the last deposition step. It is also clear that certain more reactive metals, such as Ti and Al, will not be deposited since that would require strongly negative potentials which lie outside the electrochemical window of the water containing PIL.[52]

Copper doped ILs

The deposition of copper out of an ionic liquid liquor was demonstrated for [HC_1im][HSO4] as well as for the lower cost IL [TEA][HSO_4] by means of cyclic voltammetry (CV) and chronoamperometry (CA). In cyclic voltammetry, current is measured in response to a time-dependent applied electrode potential, swept cyclically at a defined rate between two potential limits. Chronoamperometry also involves current measurement, but as a function of time at a constant potential. By arbitrary convention, a negative current corresponds to a reduction occurring, while a positive current corresponds to an oxidation. For both experiments, liquor from biomass pretreatment was saturated with copper ions by dissolution of CuO and filtering off undissolved solid. This was done in order to obtain a measurable current. The concentrations from single pass pretreatment experiments of metal treated timber are expected to be too low to detect with the available potentiostat. The liquors tested contained 20wt% water in order to mimic the conditions of pretreatment.

Preliminary results of solubility tests of CuO in the two protic ionic liquids showed a higher solubility in the imidazolium salt than in the alkylammonium salt (just over 2000 ppm for the [TEA] salt vs. close to 5000 ppm for the [HC_1im] salt, both containing 20wt% water).[54] Therefore, the focus of further tests was on the imidazolium salt. Cyclic voltammetry was used to determine the electrode potentials required to effect oxidation and reduction in the system. In order to establish the effect of biomass degradation products present in the liquor on the deposition behaviour of copper, CV (Figure III-26) scan of copper-saturated fresh ionic liquid and copper saturated recycled ionic liquid were compared. The oxidation peak in the CV scan of the recycled liquor was shifted slightly towards higher potentials

compared to that in the fresh ionic liquid and exhibited a small side peak before the main peak. However, onset potentials of the oxidation and reduction were virtually identical.

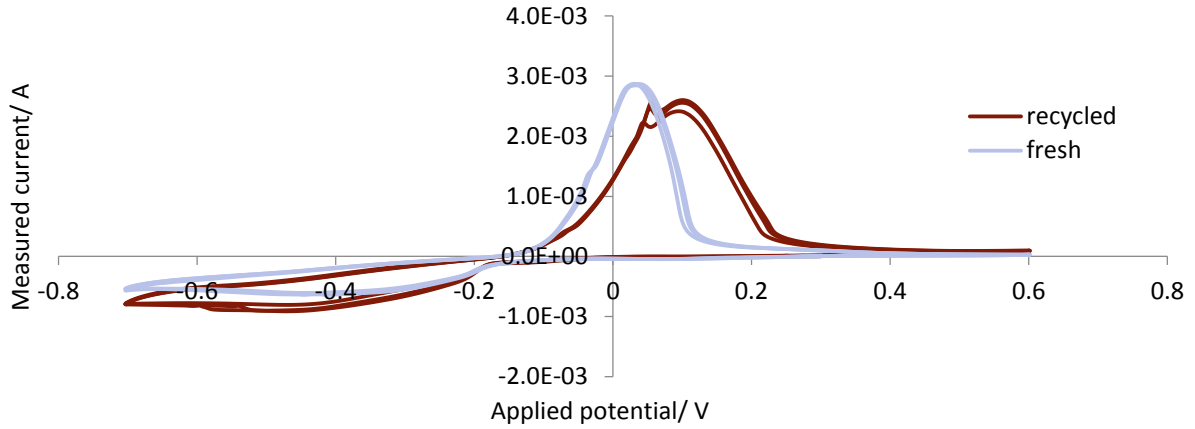

Figure III-26 Cyclic voltammograms of carbon electrode in recycled and fresh [HC_1im][HSO_4] containing 20wt% water and doped with CuO to saturation; potential sweep rate 10 mV s^{-1}. Recycled [HC_1im][HSO_4] was obtained from pretreatment of copper treated timber for 4 hours at 150°C at a biomass to solvent ratio of 1:10 g g^{-1}.

Next it was shown that copper can indeed be deposited from the chosen IL by applying a constant current as evidenced by the characteristic colour of the deposit on the glassy carbon (GC) electrode in the photograph shown in Figure III-27 obtained using a copper sheet as a dissolving cathode. In a chronoamperometry experiment, it was further confirmed that the charge yield of the copper deposition, i.e. the amount of charge resulting in the desired reaction (reduction of copper ions to metallic copper) as a percentage of the total amount of charge used, was not affected measurably by biomass degradation products. The charge yield, calculated by first applying a reductive potential of -0.5 V for 30 s followed by an oxidative potential of +0 V for 30 s and integrating the area under both peaks. This further confirmed that the charge efficiency of the copper deposition is not measurably affected by biomass degradation products. Under the tested conditions, 94% charge yield was obtained for both the fresh and the recycled [HC_1im][HSO_4] containing approximately 5000 ppm of Cu. The chronoamperograms are shown in Figure III-28.

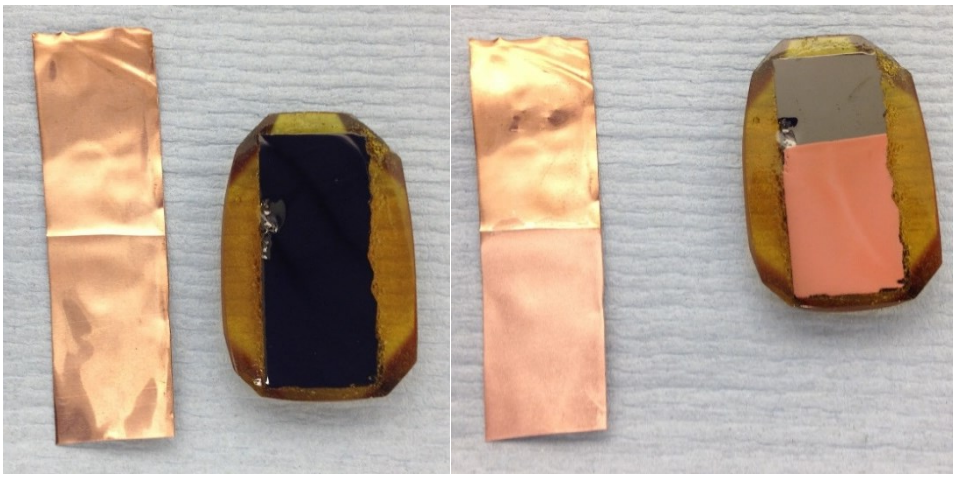

Figure III-27 Copper sheet used as a dissolving cathode and a GC electrode used as anode before chronopotentiometry (left) and after (right). The deposit on the GC electrode has a characteristic copper colour. Deposition was performed by applying a current of 0.1 A for 1 hour without reference electrode.

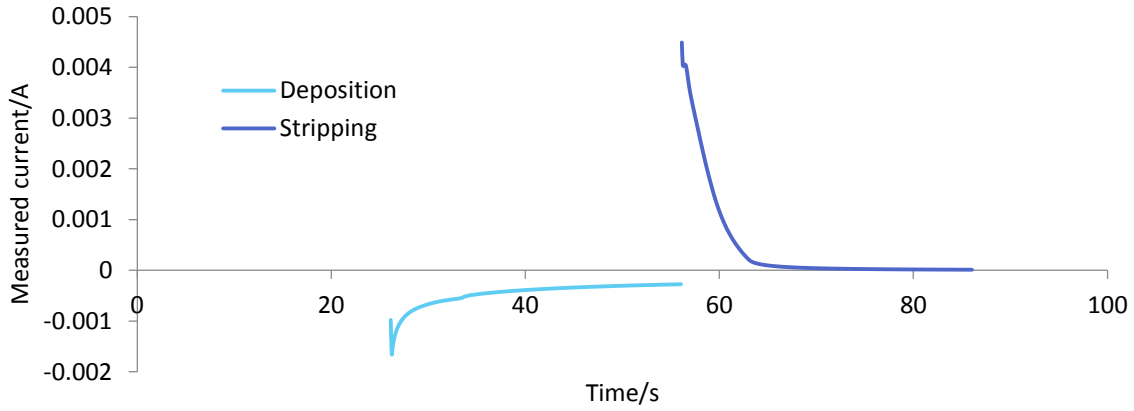

Figure III-28 Chronoamperometry of $[HC_1im][HSO_4]$ containing approx. 5000 ppm Cu. A potential of -0.5V was applied for the deposition (i.e. reduction) and 0 V for the stripping (i.e. oxidation). A stripping potential of 0.1 V was applied prior to deposition in order to make sure that all copper was found in state +2 and no copper was already deposited on the electrode surface.

Recycled IL

After establishing that copper deposition out of an IL containing 20wt% water and various biomass derived products is possible, the IL obtained after 2 and 6 cycles of pretreatment of CCA treated wood was tested next. Unfortunately, pretreatment with $[HC_1im][HSO_4]$ yielded very poor pulp digestibility, and the IL was therefore changed to $[HC_1im]Cl$ for subsequent experiments. The CVs of the blank $[HC_1im]Cl$ and the 6 times recycled $[HC_1im]Cl$ are displayed in Figure III-29. The scan window was chosen to be from -1 V to +1 V in order to avoid excessive hydrogen production at the former potential, as well as the oxidation of water and chloride at the latter potential.[55] While the blank shows only a strong cathodic current at potentials < -0.5 V, which was assumed to be hydrogen evolution, several reduction and oxidation peaks are evident in the voltammogram of the recycled IL. It is extremely difficult to establish which peak corresponds to which reaction, especially since literature data on the deposition of chromium and arsenic from PILs are scarce and factors like electrode material and acidity

of the medium all have an influence. Abbott *et al*. reported the deposition of copper out of a deep eutectic solvent based on choline chloride.[56] They observed two distinct reduction processes corresponding to Cu(II)/Cu(I) at +0.43 V and Cu(I)/Cu(0) -0.45 V vs. a silver wire quasi-reference electrode, resembling the here observed peaks at +0.4 V and -0.55 V, also vs. a silver quasi-reference electrode. The two step reduction is something that is enabled by the presence of chloride ions which are able to stabilise Cu(I), unlike HSO_4^- and SO_4^{2-} ions.[51] An electrochemical study of arsenic in dilute sulfuric acid showed that elemental arsenic, As(III), As(V) and As(-III) in the form of arsine (AsH_3) are stable forms.[57] They observed, amongst others, a reduction peak at around -0.25 V and an oxidation peak at around +0.25 V vs. a saturated calomel electrode which they attributed to the As(III)/As(0) couple. Chromium deposition from aprotic imidazolium based ILs has been shown to require more strongly negative potentials of around -1 to -2 V vs. Fc^+/Fc.[58] In a study using $[C_4C_1im][HSO_4]$ as the solvent with Cr(III) in solution showed a first deposition peak at -1.25 V vs. saturated calomel electrode which the authors attributed to the reduction to Cr(II), followed by a second cathodic peak at around -1.96 V which corresponds to the reduction to metallic Cr.[26]

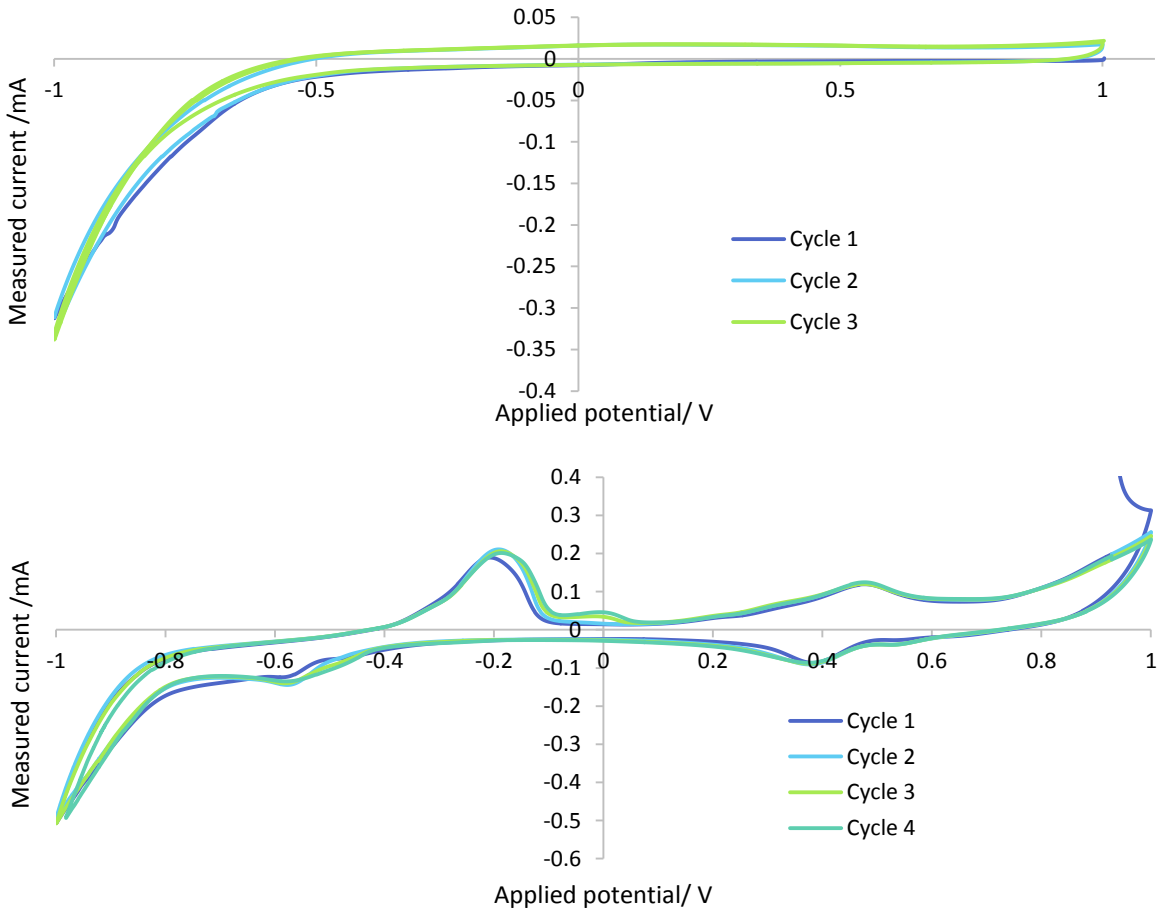

Figure III-29 Cyclic voltammograms of a printed carbon electrode in: (a) blank $[HC_1im]Cl$ containing 5.6 wt% water and (b) 6 times recycled $[HC_1im]Cl$ containing 17.7 wt% water ; silver quasi reference electrode and potential sweep

rate 10 mV s^{-1}. Recycled [HC_1im]Cl was obtained from 6 cycles of pretreatment of CCA treated timber for 30 min at 170°C at a biomass to solvent ratio of 1:5 g g^{-1} and a final water content of 20 wt%

In the voltammograms shown in Figure III-29, there is a small oxidative peak at around 0 V, followed by an increasing anodic current from +0.1 V onwards. Similarly, there is a small reduction peak at -0.45 V preceding the larger peak at -0.55 V, and a small peak at +0.55 V preceding the larger one at +0.4 V, both better to be seen in the zoomed in version of the CV scan in Figure III-30.

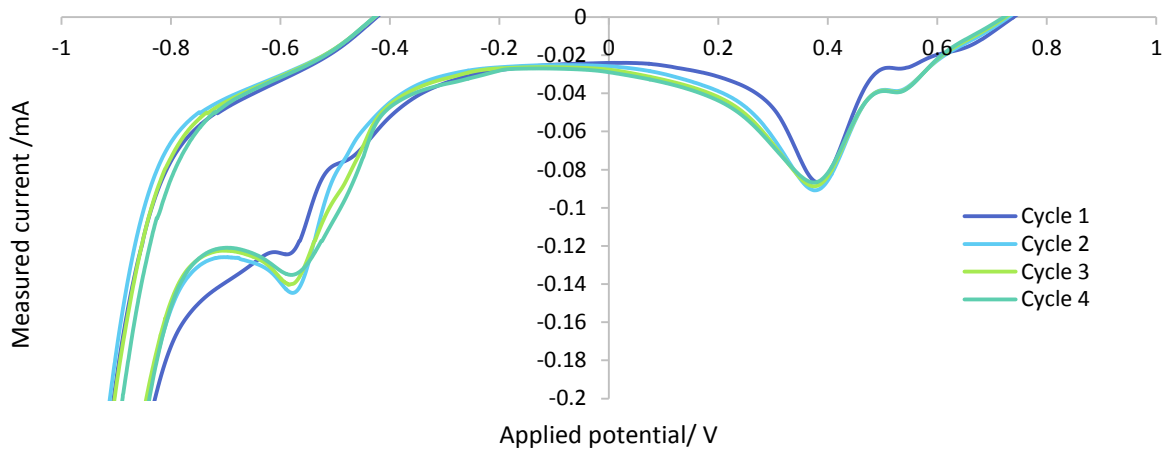

Figure III-30 Zoom of CV of 5 times recycled [HC_1im]Cl containing 17.7wt% water on a printed carbon electrode with a silver quasi reference. Recycled [HC_1im]Cl was obtained from 6 cycles of pretreatment of CCA treated timber for 30 min at 170°C at a biomass to solvent ratio of 1:5 g/g and a final water content of 20wt%.

In order to confirm that the reduction peak at +0.4 V is indeed coupled to the oxidation peak at +0.5 V and also to separate the two peaks between -0.4 and -0.6 V, CV scans over a smaller range were measured. Figure III-31 shows the CV scans from +0.2 to +0.7 V (top) as well as -0.7 V to -0.1 V (bottom), covering the potential ranges that are thought to be where the Cu(II)/Cu(I) and Cu(I)/Cu(0) reductions and oxidations occur. Figure III-31 (top) shows that the reduction peak at +0.5 V is indeed linked to the oxidation peak at +0.54 V. Figure III-31 (bottom) further confirms that the reduction peak originally occurring at -0.5 to -0.6 V is coupled to the oxidation peak at -0.2 V. No shoulder before the reduction peak was observed in this scan, further confirming that the small oxidation peak at around +0 V was coupled to that shoulder. Here, where the scan only reaches -0.1 V, the species responsible for the shoulder does not become oxidised and hence cannot undergo reduction when the potential is lowered again. We can also observe that the reduction peak shifts towards -0.45 V in the second and third scan, possibly as a result of the absence of any other oxidised species which could be reduced before the Cu.

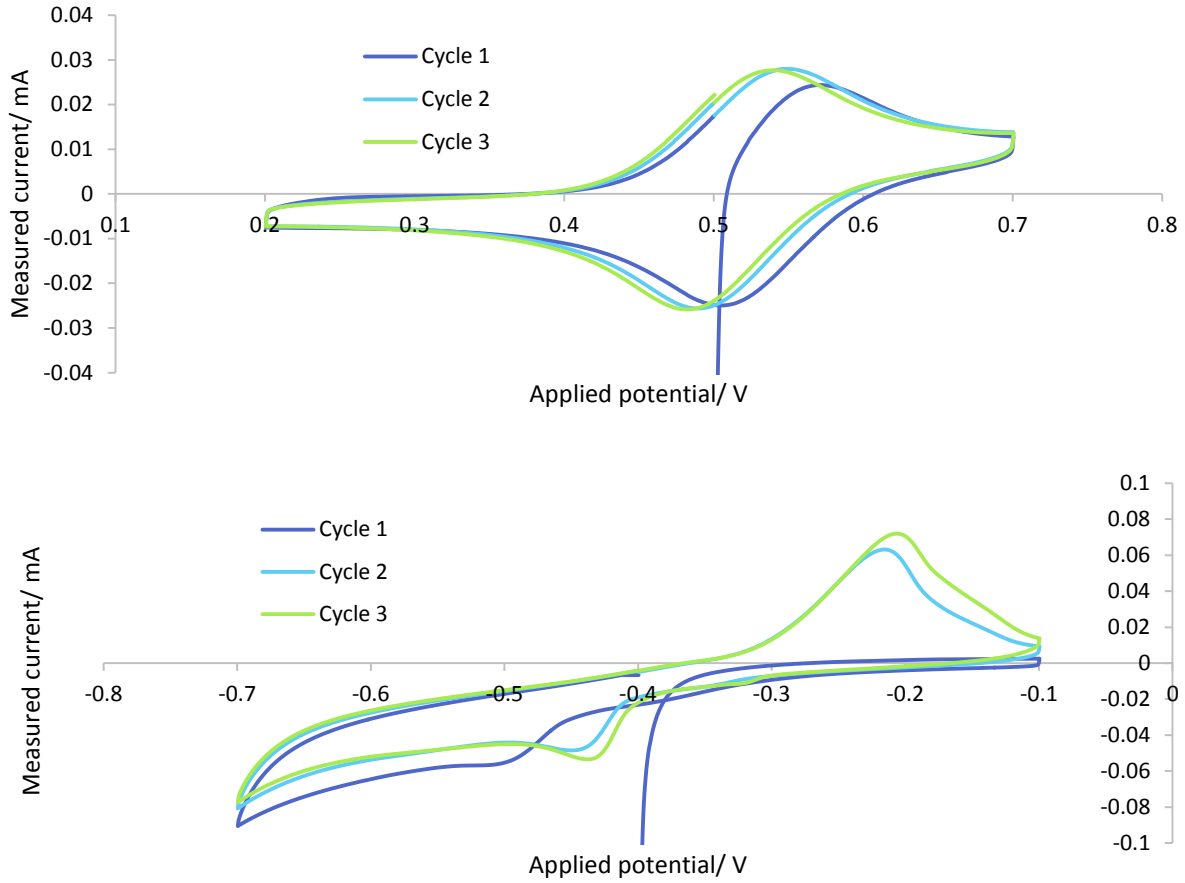

Figure III-31 Cyclic voltammograms of a printed carbon electrode in recycled [HC_1im]Cl containing 20wt% water; silver quasi reference. Recycled [HC_1im]Cl was obtained from 2 cycles of pretreatment of CCA treated timber for 30 min at 170°C at a biomass to solvent ratio of 1:5 g g^{-1} and a final water content of 20wt%.

Figure III-32 shows the CV scans obtained for a potential range of -0.45 to +0.05 V. These scans were carried out in order to further confirm that the shoulder peak at around -0.4 V does indeed belong to the same species as the oxidation peak at around +0 V. A cathodic current is observed between -0.3 and -0.45 V, but very little anodic current is observed at -0.2 V, where in the above discussed CV the counter peak to the deposition peak at -0.5 V was observed. The anodic current then picks up slightly towards the upper vertex potential. This confirms that there are two different species present in solution with very similar oxidation and reduction potentials. It appears that these can be separated and deposited selectively by choosing a stepwise deposition if the potentials are chosen carefully. Whether these peaks belong to Cr or As oxidation and reduction is however unclear. Considering that the peak area is small compared to the peaks attributed to Cu suggests that the associated species is present in a lower concentration, which would lead to the conclusion that those small peaks belong to Cr, presumably Cr(III) to Cr(II). Alternatively the reduction peak at +0.55 could correspond to that first one-electron reduction and this second peak to the two-electron reduction to elemental chromium.

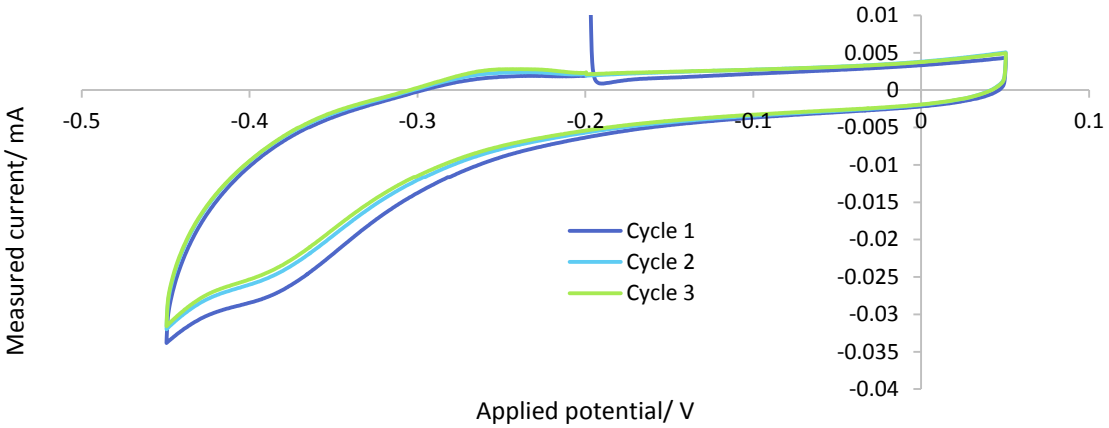

Figure III-32 CV scans of recycled [HC_1im]Cl containing 20wt% water on a printed carbon electrode with a silver quasi reference. Recycled [HC_1im]Cl was obtained from 2 cycles of pretreatment of CCA treated timber for 30 min at 170°C at a biomass to solvent ratio of 1:5 g/g and a final water content of 20wt%.

Reduction in metal content

The difficulty of determining which species are reduced under which conditions by CV has been highlighted. We therefore moved on to attempting the deposition of some of the metals out of the brown liquor by applying a potential of -0.7 V for varying lengths of times. For these experiments, screen printed carbon electrodes were used and a 50 µL drop of the recycled IL spread over it. After the potential was applied, as much of the IL as possible was removed again using a pipette. The metal content was subsequently tested by ICP-OES and compared to the metal content before the deposition. The ppm found before and after 2, 5 and 10 min of deposition can be seen in Figure III-33. Table III-20 summarises the relative amount remaining in solution after deposition. As can be seen, the content of all three analysed metals decreased over the first 2 min of deposition. Thereafter, the Cu and Cr content continued to decrease slightly while the As content remained more or less stable. It should however be noted that the error bars at this point are almost equal to the change observed. The final metal contents correspond to between 85 and 92% of the original metal content, translating to a deposition of between 8 and 15% of the present metals. This result is encouraging as it shows that all three metals can be deposited out of solution together. The reason that the metal concentration did not decrease past this initial reduction is likely due to the very limited mass transfer within the drop sitting on the electrode as well as the very small electrode areas.

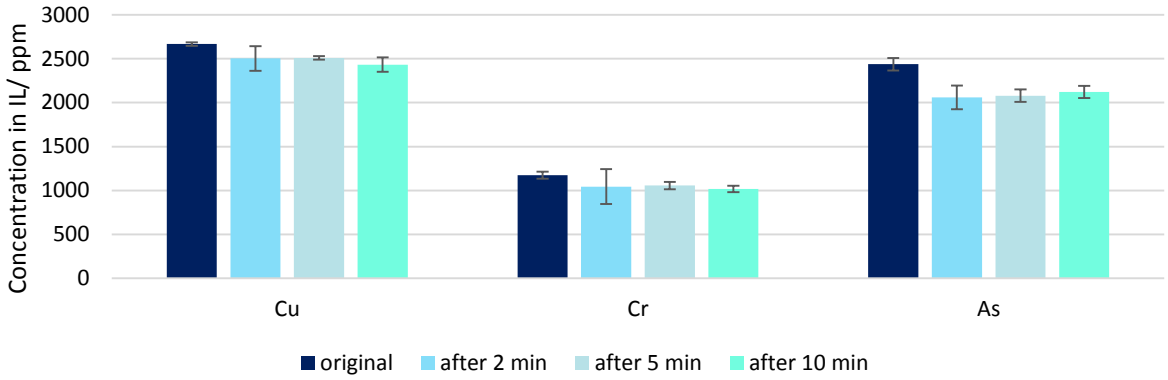

Figure III-33 Metal concentrations found in the brown liquor before and after applying a potential of -0.7 V on a screen printed electrode. Recycled [HC_1im]Cl was obtained from 6 cycles of pretreatment of CCA treated timber for 30 min at 170°C at a biomass to solvent ratio of 1:5 g/g and a final water content of 20wt%. Standard errors were calculated for triplicate measurements.

Table III-20 Metal contents relative to the initial metal content found in the brown liquor after applying a potential of -0.7 V on a screen printed electrode. Recycled [HC_1im]Cl was obtained from 6 cycles of pretreatment of CCA treated timber for 30 min at 170°C at a biomass to solvent ratio of 1:5 g/g and a final water content of 20wt%. Standard errors were calculated for triplicate measurements.

	after 2 min	after 5 min	after 10 min
Cu	93.8±4.8%	93.6±0.7%	91.6±3.6%
Cr	89.0±4.6%	89.0±0.9%	88.9±2.9%
As	84.6±5.2%	86.4±1.7%	85.3±2.5%

Fermentation

The final part of this project looked at producing ethanol from the obtained sugars. It was attempted to grow yeast cells on media obtained from the enzymatic hydrolysis of non-pretreated virgin pine (VP), pretreated VP and pretreated treated timber (TT) with an initial copper concentration of around 2000 ppm. Yeast cells were able to grow in all media except for that made from non-pretreated VP, presumably due to low sugar concentrations obtained from this feedstock (demonstrating a need for pretreatment). Additionally, yeast cells were successfully grown in media from pretreated VP and pretreated TT where copper was added in order to mimic the original copper content of TT. Figure III-34 shows the final ethanol concentration in the samples, normalised for the initial amount of pulp that was used for the experiment. Pretreated TT is seen to give higher ethanol yields than pretreated VP. Furthermore, the yeast showed a surprising tolerance towards copper, although experiments with added copper resulted in rather large errors. Copper is an important micronutrient for yeasts[36] and it is suspected that the here used concentrations of Cu may have resulted in an improved growth of cells in the case of the VP medium. Statistical tests will however be required to distinguish between an actual improvement and a random variation. Furthermore, in an industrial fermentation, solids loading are expected to be higher, resulting in copper concentrations which are likely to exceed the tolerance of most common yeast strains unless the copper is at least partially extracted from the biomass. The experiments conducted here used *Saccharomyces cerevisiae* BY4741, which is not

engineered for high ethanol productivity; thus the ethanol yields from industrial strains would be expected to be higher. In any case, the results clearly show that **bioethanol production from waste wood is technically feasible.**

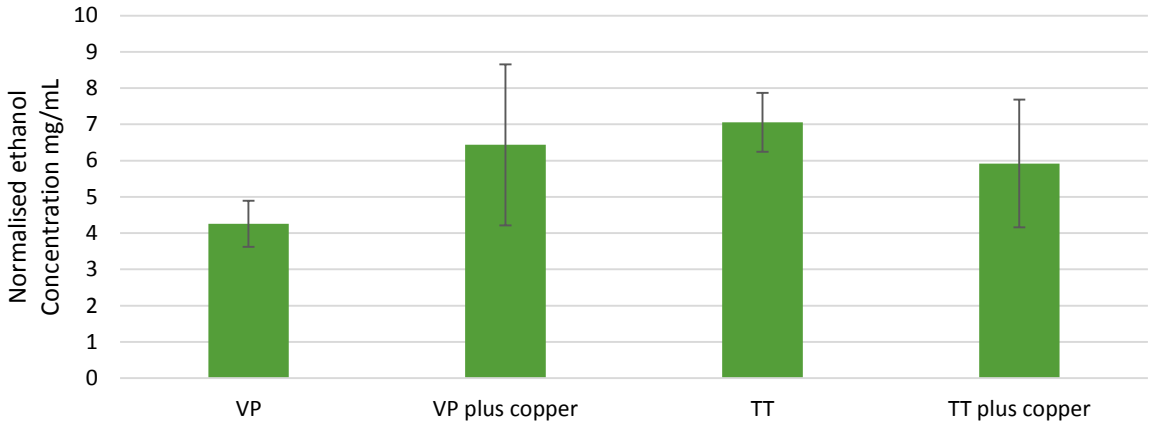

Figure III-34 Ethanol yields obtained by fermentation of sugar solutions obtained from the enzymatic hydrolysis of pretreated virgin pine (VP) and treated timber (TP) with and without the addition of copper equivalent to a copper concentration of 2000 ppm in the biomass. VP was pretreated using [HC_4im][HSO_4] with a biomass to solvent ratio of 1:10 g/g for 30 min at 170°C and a final water content of 20wt%. TT was pretreated using [DMBA][HSO_4] with a biomass to solvent ratio of 1:5 g/g for 30 min at 170°C and a final water content of 20wt%.

Conclusions

It has been demonstrated that certain ILs are capable of extracting Cu from timber while producing highly digestible pulps. In addition, Cr and As were also successfully extracted and it was shown that close to quantitative Cu extraction, As extraction exceeding 90% and Cr extraction of 50% could be maintained over 6 cycles of pretreatment while producing highly digestible cellulose pulps. Concomitant deposition of the three metals out of the brown liquor was also demonstrated. Finally, ethanol could be produced from the sugars obtained after enzymatic hydrolysis of copper treated timber pulp. Overall, these findings are promising and show that the route from waste wood to bio-derived products such as ethanol is technically feasible. This could open up the possibility of economical bioethanol production from waste wood. Further process development looking at the separation steps needs to be conducted since the current washing protocol includes an uneconomical amount of wash solvents.

References

1 J. K. Saxe, E. J. Wannamaker, S. W. Conklin, T. F. Shupe and B. D. Beck, *Chemosphere*, 2007, **66**, 496–504.
2 T. G. Mercer and L. E. Frostick, *J. Hazard. Mater.*, 2014, **276**, 10–18.
3 T. G. Mercer and L. E. Frostick, *Sci. Total Environ.*, 2012, **427–428**, 165–174.
4 L. Coudert, J. Blais and G. Mercier, *J. Environ. Eng.*, 2013, **139**, 576–587.
5 A. Augustsson, L. Sörme, A. Karlsson and J. Amneklev, *J. Ind. Ecol.*, 2016, **0**, 1–11.
6 DEFRA, *Wood waste : A short review of recent research*, 2012.
7 A. Janin, J.-F. Blais, G. Mercier and P. Drogui, *J. Hazard. Mater.*, 2009, **169**, 136–45.
8 J. Kramb, J. Konttinen, R. Backman, K. Salo and M. Roberts, *Fuel*, 2016, **181**, 319–324.

9 N. Ohgami, O. Yamanoshita, N. D. Thang, I. Yajima, C. Nakano, W. Wenting, S. Ohnuma and M. Kato, *Environ. Pollut.*, 2015, **206**, 456–460.
10 M. Edo, E. Björn, P. E. Persson and S. Jansson, *Waste Manag.*, 2016, **49**, 311–319.
11 G. Jacobi, H. Solo-Gabriele, T. Townsend and B. Dubey, *Waste Manag.*, 2007, **27**, 1617–1625.
12 J. A. Hingston, C. D. Collins, R. J. Murphy and J. N. Lester, *Environ. Pollut.*, 2001, **111**, 53–66.
13 J. Salazar and J. Meil, *J. Clean. Prod.*, 2009, **17**, 1563–1571.
14 T. Searchinger, R. Heimlich, R. A. Houghton, F. Dong, A. Elobeid, J. Fabiosa, S. Tokgoz, D. Hayes and T.-H. Yu, *Science (80-.).*, 2008, **319**, 1238–1240.
15 R. Melamu and H. Von Blottnitz, *J. Clean. Prod.*, 2011, **19**, 138–144.
16 Q. Kang and T. Tan, *Sustainability*, 2016, **8**, 76.
17 F. Cherubini, N. D. Bird, A. Cowie, G. Jungmeier, B. Schlamadinger and S. Woess-Gallasch, *Resour. Conserv. Recycl.*, 2009, **53**, 434–447.
18 F. Cherubini and G. Jungmeier, *Int. J. Life Cycle Assess.*, 2010, **15**, 53–66.
19 L. Tao, A. Aden, R. T. Elander, V. R. Pallapolu, Y. Y. Lee, R. J. Garlock, V. Balan, B. E. Dale, Y. Kim, N. S. Mosier, M. R. Ladisch, M. Falls, M. T. Holtzapple, R. Sierra, J. Shi, M. a. Ebrik, T. Redmond, B. Yang, C. E. Wyman, B. Hames, S. Thomas and R. E. Warner, *Bioresour. Technol.*, 2011, **102**, 11105–11114.
20 H. Dick, A. Hennig and P. Scholes, *Comparing the cost of alternative waste treatment options*, 2016.
21 J. a. Whitehead, J. Zhang, N. Pereira, a. McCluskey and G. a. Lawrance, *Hydrometallurgy*, 2007, **88**, 109–120.
22 J. a. Whitehead, G. a. Lawrance and A. McCluskey, *Green Chem.*, 2004, **6**, 313–315.
23 C. H. C. Janssen, N. A. Macías-Ruvalcaba, M. Aguilar-Martínez and M. N. Kobrak, *Sep. Purif. Technol.*, 2016, **168**, 275–283.
24 M. Abai, M. P. Atkins, A. Hassan, J. D. Holbrey, Y. Kuah, P. Nockemann, A. a. Oliferenko, N. V. Plechkova, S. Rafeen, A. a. Rahman, R. Ramli, S. M. Shariff, K. R. Seddon, G. Srinivasan and Y. Zou, *Dalt. Trans.*, 2015, **44**, 8617–8624.
25 S. Rabieh, M. Bagheri and B. Planer-Friedrich, *Microchim. Acta*, 2013, **180**, 415–421.
26 X. He, Q. Zhu, B. Hou, C. Li, Y. Jiang, C. Zhang and L. Wu, *Surf. Coatings Technol.*, 2015, **262**, 148–153.
27 A. P. Abbott and K. J. McKenzie, *Phys. Chem. Chem. Phys.*, 2006, **8**, 4265–79.
28 N. R. Baral and A. Shah, *Biofuels, Bioprod. Biorefining*, 2016, **10**, 70–88.
29 M. T. Clough, K. Geyer, P. a Hunt, J. Mertes and T. Welton, *Phys. Chem. Chem. Phys.*, 2013, **15**, 20480–95.
30 B. Simmons, *Enhanced Mixed Feedstock Processing Using Ionic Liquids*, CRADA Final Report, 2016.
31 V. Rigual, T. M. Santos, J. C. Domínguez, M. V. Alonso, M. Oliet and F. Rodriguez, *ACS Sustain. Chem. Eng.*, 2017, acssuschemeng.6b02723.
32 A. Brandt, M. J. Ray, T. Q. To, D. J. Leak, R. J. Murphy and T. Welton, *Green Chem.*, 2011, **13**, 2489.
33 T. Auxenfans, S. Buchoux, D. Larcher, G. Husson, E. Husson and C. Sarazin, *Energy Convers. Manag.*, 2014, **88**, 1094–1103.
34 Y. L. Cha, J. Yang, S. Il Seo, G. H. An, Y. H. Moon, G. D. You, J. E. Lee, J. W. Ahn and K. B. Lee, *Fuel*, 2016, **164**, 322–328.
35 J. S. Valentine and E. B. Gralla, *Science (80-.).*, 1997, **278**, 817 LP-818.
36 S. Labbe, Z. Zhu and D. J. Thiele, *J Biol Chem*, 1997, **272**, 15951–15958.
37 Y. Lin and S. Tanaka, *Appl. Microbiol. Biotechnol.*, 2006, **69**, 627–642.
38 L. Chen, M. Sharifzadeh, N. Mac Dowell, T. Welton, N. Shah and J. P. Hallett, *Green Chem.*, 2014, **16**, 3098.
39 P. Verdía, A. Brandt, J. P. Hallett, M. J. Ray and T. Welton, *Green Chem.*, 2014, **16**, 1617.
40 K.-E. Saarela, L. Harju, J. Rajander, J.-O. Lill, S.-J. Heselius, a Lindroos and K. Mattsson, *Sci.*

Total Environ., 2005, **343**, 231–41.
41 B. J. Cox and J. G. Ekerdt, *Bioresour. Technol.*, 2013, **134**, 59–65.
42 P. Mäki-Arvela, I. Anugwom, P. Virtanen, R. Sjöholm and J. P. Mikkola, *Ind. Crops Prod.*, 2010, **32**, 175–201.
43 G. Cheng, P. Varanasi, R. Arora, V. Stavila, B. a. Simmons, M. S. Kent and S. Singh, *J. Phys. Chem. B*, 2012, **116**, 10049–10054.
44 A. G. Cruz, C. Scullin, C. Mu, G. Cheng, V. Stavila, P. Varanasi, D. Xu, J. Mentel, Y.-D. Chuang, B. A. Simmons and S. Singh, *Biotechnol. Biofuels*, 2013, **6**, 52.
45 A. George, A. Brandt, K. Tran, S. M. S. N. S. Zahari, D. Klein-Marcuschamer, N. Sun, N. Sathitsuksanoh, J. Shi, V. Stavila, R. Parthasarathi, S. Singh, B. M. Holmes, T. Welton, B. A. Simmons and J. P. Hallett, *Green Chem.*, 2015, **17**, 1728–1734.
46 F. Xu, T.-T. Zhu, Q.-Q. Rao, S.-W. Shui, W.-W. Li, H.-B. He and R.-S. Yao, *J. Environ. Sci.*, 2016, 1–9.
47 A. Arita and M. Costa, *Metallomics*, 2009, **1**, 222–228.
48 G. Meylan and A. Spoerri, *Waste Manag.*, 2014, **34**, 93–100.
49 S. Zhou, T. V. Morozova, Y. N. Hussain, S. E. Luoma, L. McCoy, A. Yamamoto, T. F. C. MacKay and R. R. H. Anholt, *Environ. Health Perspect.*, 2016, **124**, 1062–1070.
50 A. J. Ragauskas, G. T. Beckham, M. J. Biddy, R. Chandra, F. Chen, M. F. Davis, B. H. Davison, R. a Dixon, P. Gilna, M. Keller, P. Langan, A. K. Naskar, J. N. Saddler, T. J. Tschaplinski, G. a Tuskan and C. E. Wyman, *Science*, 2014, **344**, 1246843.
51 D. Grujicic and B. Pesic, *Electrochim. Acta*, 2002, **47**, 2901–2912.
52 F. Endres, D. MacFarlane and A. Abbott, *Electrodeposition from Ionic Liquids*, Wiley-VCH Verlag GmbH & Co. KGaA, Weinheim, Germany, 2008.
53 C. Zhao, G. Burrell, A. a J. Torriero, F. Separovic, N. F. Dunlop, D. R. MacFarlane and A. M. Bond, *J. Phys. Chem. B*, 2008, **112**, 6923–6936.
54 L. Carrier-Sippy, MRes Thesis, Imperial College London, 2015.
55 L. Yu, H. Sun, J. He, D. Wang, X. Jin, X. Hu and G. Z. Chen, *Electrochem. commun.*, 2007, **9**, 1374–1381.
56 A. P. Abbott, K. El Ttaib, G. Frisch, K. J. McKenzie and K. S. Ryder, *Phys. Chem. Chem. Phys.*, 2009, **11**, 4269.
57 F. Brusciotti and P. Duby, *Electrochim. Acta*, 2007, **52**, 6644–6649.
58 L. Sun and J. F. Brennecke, *Ind. Eng. Chem. Res.*, 2015, **54**, 4879–4890.

Chapter 4: The Secret Lives of Lignin and Hemicellulose

While the previous chapters have been focused around obtaining a highly digestible cellulose pulp, and factors affecting digestibility, this chapter focuses on the two other fractions, lignin and hemicellulose. As discussed earlier, holistic utilisation of biomass and the production of low-volume, high-value products can significantly improve the economic viability of a biorefinery.[1] Various applications for lignin and the fact that, depending on the nature of this application, different characteristics are required, while others may be detrimental, have also been discussed. Additionally the previous results chapters have shown that residual lignin[2] and/or the presence of hemicellulose derived pseudo-lignin[3] can strongly reduce saccharification yields. A fuller understanding of the lignin and hemicellulose chemistry occurring during pretreatment is therefore essential for simultaneous optimization of the process for pulp digestibility and co-product valorisation.

The difficulty of lignin analysis has been described in the background section, showing that a multitude of analytical methods are required in order to obtain a good picture of the lignin properties at hand. In this chapter, isolated lignins of both *Miscanthus* and pine are characterised using ^{31}P and 2D HSQC NMR to quantify functional groups and degree of condensation, as well as gel permeation chromatography (GPC) for information on molecular weight and elemental analysis (EA) to analyse for ionic liquid incorporation and changes in elemental composition. General time course trends, as well as the possibility to tune lignin characteristics while maintaining high saccharification yields are discussed. *Miscanthus*, pine and beech lignin and lignins obtained from pretreatments with mixed feedstocks are analysed by HSQC NMR in order to gain insight into the interaction between the lignins of the different plant species. Finally, the effects of recycling on lignin structure as well as alternative lignin isolation methods are discussed.

Lignin forms during plant growth through a series of radical polymerisation reactions between mainly three phenyl-propanoids, so called monolignols, namely *p*-coumaryl (H), coniferyl (G) and sinapyl (S) alcohol.[4] Since coupling is favoured in the β position, the most common interunit linkages are β-*O*-4', β-β' and β-5', but also spirodienone and β-1' linkages. Coupling on the aromatic ring on the other hand yields 4-*O*-5' and 5-5' linkages. 5-5' linkages can further undergo subsequent coupling to form dibenzodioxocine units (5-5'-*O*-4). Dibenzodioxocine and 4-*O*-5' are resulting in branching in lignin.[5] All structures depicted in Figure I-9 and the most important ones are shown again here in Figure III-35.

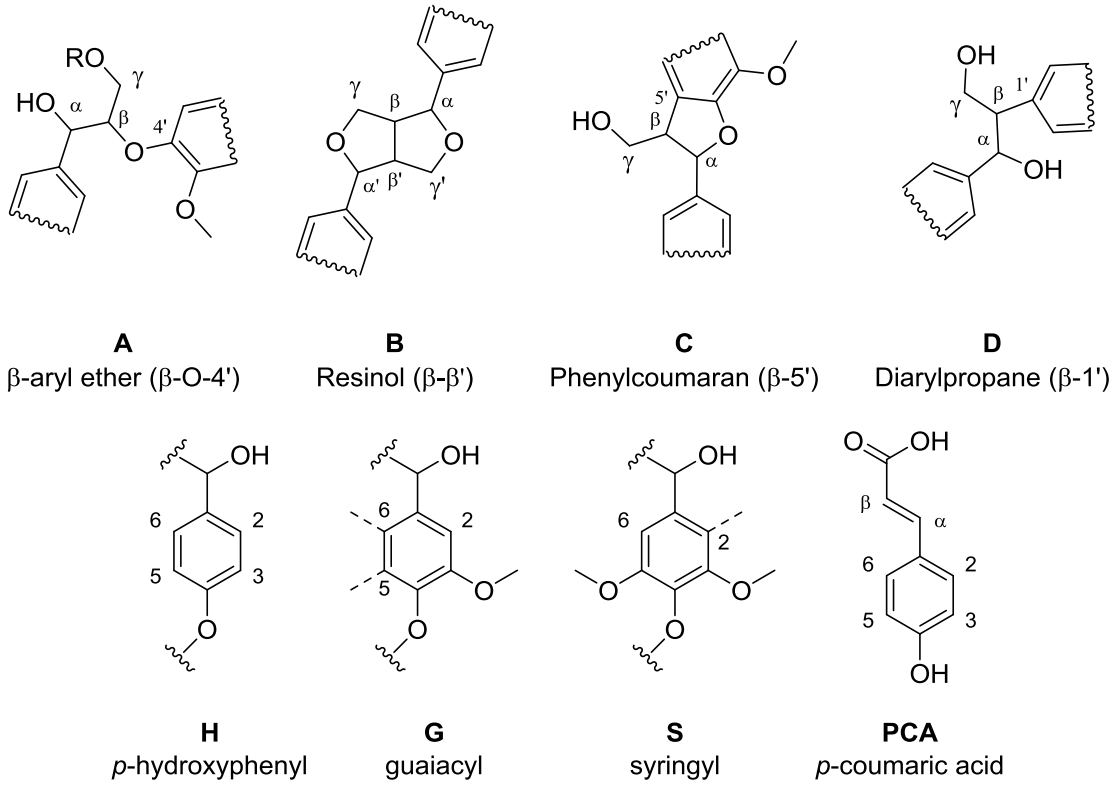

Figure III-35 The most prominent ether bonds and lignin subunits.

Miscanthus giganteus lignin has previously been characterized as a G/S/H type lignin, containing around 52% guaiacyl (G), 44% syringyl (S) and 4% *p*-hydroxyphenyl (H) units, approximately 40 β-*O*-4' linkages and *ca.* 10 *p*-coumarate ester units (PCA) per 100 aromatic rings.[6] Hardwood lignin, such as beech lignin, is a S/G type lignin with an S/G ratio of around 1.67 and an overwhelming 60 β-*O*-4' linkages per 100 aromatic rings.[4] As a result of the high content of syringyl units, which are substituted in both the 3 and 5 position, only very few β-5' and dibenzodioxocine linkages can be found, while the β-β' and β-1' linkages are more abundant.[7] Pine lignin (and more generally softwood lignin) consists predominantly of guaiacyl (G) units (95%) as well as traces of *p*-hydroxyphenyl (H) units and around 45-50 β-*O*-4' linkages per 100 aromatic rings.[8] The second most abundant linkage in softwood lignin is the β-5' linkage with around 10-13 linkages per 100 aromatic units. In addition, softwood lignin also contains around 5-7 dibenzodioxocine linkages per 100 aromatic units,[4] which together with 4-*O*-5' linkages are responsible for branching. Despite this, the degree of branching of milled softwood lignin has been found to be relatively low.[5]

In the second part of this chapter carbohydrate derived solutes present in the ionic liquid liquor are analysed and discussed. Just as is the case for lignin, the hemicellulose composition differs for the three types of biomass. Softwoods are typically rich in galactoglucomannan, arabinoglucuronoxylan and arabinogalactan,[9] resulting in mainly the C6 sugars mannose (10-12wt% of total biomass) and galactose (3-5wt%) to be present in the hemicelluloses with a smaller amount of the C5 sugars xylose

(ca. 6wt%) and arabinose (ca. 2wt%).[10] Hardwoods on the other hand contain predominantly glucuronoxylan and smaller amounts of galactan, arabinan and glucomannan[9] resulting in a high abundance of C5 sugars (up to over 20wt% xylose of total biomass weight) and a much smaller amount of C6 sugars (ca. 3wt% combined mannose and galactose) in the hemicellulose fraction.[11] Herbaceous biomass, similar to hardwoods, has a pentose dominated hemicellulose with over 20wt% C5 sugars[12] consisting of mainly arabinoxylans.[13]

The results discussed for the *Miscanthus* time course at 120°C (lignin with and without excess acid as well as liquor analysis) have been published.[14]

Changes in Lignin Structure

Effect of Time and Temperature

Linkages and Subunit Composition

^{1}H-^{13}C heteronuclear quantum coherence (HSQC) NMR spectroscopy can be used to estimate the subunit composition, the degree of condensation as well as the cleavage of ether bonds in isolated lignins by comparing peak intensities (i.e. volume integrals) of selected peaks over a time or temperature course. While the volume of correlation peaks depend to a large extent on the relaxation rates of the nuclei which are rather long for the ^{13}C nucleus and therefore make fully quantitative analysis extremely time consuming, the observed peak volume is linear with respect to the concentration of the analyte.[4] It is therefore possible to obtain semi-quantitative data from shortened experiments by comparing the peak volume of a certain correlation with respect to another correlation that is considered constant over a range of experiments. Literature reports that the volume of the G_2 signal can be used as such a reference in the case of softwoods since softwood lignin consists of predominantly G units and condensation in the 2 position is highly uncommon.[4] The G_2 signal in softwoods can therefore be used to represent the total number of phenolic units which the other signals can be normalised and compared to over e.g. a temperature or time course. It should be noted that this refers to the sum of the G_2 and $G_{2,cond.}$ signal, since both refer to the 2 position of the G unit, the signal shifting if another position of the aromatic ring reacts to from a new C-C bond. Hardwoods, having a majority of S and some G units, are best analysed by taking the sum of G_2, $G_{2,cond.}$, $S_{cond.}$ and $S_{2,6}/2$ for the total number of aromatic units. The $S_{2,6}$ signal is divided by two since one non-condensed S unit gives a twice as strong signal due to the symmetry in the substructure. Grass lignin, such as from *Miscanthus*, on the other hand contains all three units, G, S and H, as well as some PCA and FA, resulting in some signal overlap which, in theory, makes it impossible to have a reliable representation of the total number of phenolic units.

In the experiments presented here, using a pulse sequence that only gives semi-quantitative information, changes in abundance of different sub-units and linkages are reported by using volume integration versus the G_2+$G_{2,cond.}$ integral for both pine and *Miscanthus*. By taking *Miscanthus* lignin from an early (1h) time point and a late (24 h) time point and adding a known amount of *para*-xylene as internal standard, it was shown that, despite the presence of other phenolic moieties, the G_2+$G_{2,cond.}$ integral is very stable over the 23 h time period (a change of 6.6% in volume integral was recorded, data in Table S2 in the Appendix) and is therefore suitable to gain some insight into the change in lignin subunits.

Figure III-36 depicts the key parts of the HSQC spectra for *Miscanthus* lignin isolated with the [TEA][HSO_4] water mixture at an early stage (1 h), a mid-stage (4 h) and a late stage (72 h) of pretreatment at 120°C. Both the aromatic and side chain regions are highlighted. The side chain region shows, amongst others, the three most common linkages, β-*O*-4' ether (A), β-β' (resinol, B) and β-5' (phenylcoumaran, C), while the aromatic region shows the most common unsaturated subunit structures, syringyl ($S_{2,6}$, $S_{cond.}$), guaiacyl (G_2, G_5, G_6, $G_{cond.}$), *p*-coumaric acid ($PCA_{2,6}$, PCA_{β}) and *p*-hydroxyphenyl ($H_{2,6}$). Peaks were also observed at 7.7/128, 7.7/131 ppm and 4.1/67 ppm, which I assign to the plasticizer bis(2-ethylhexyl) phthalate (DEHP) based on the HSQC NMR and also a complementary HMBC NMR spectra (see Figure S61 in the Appendix). It is presumed that the plasticizer was leached from the seals of the pressure tubes used for heating the biomass with the ionic liquid and subsequently precipitated with the lignin fraction during antisolvent addition. Figure III-37 shows an analogous spectrum of pine lignin obtained after 30 min pretreatment with the [HC_4im][HSO_4] water mixture at 170°C and a 10% biomass loading.

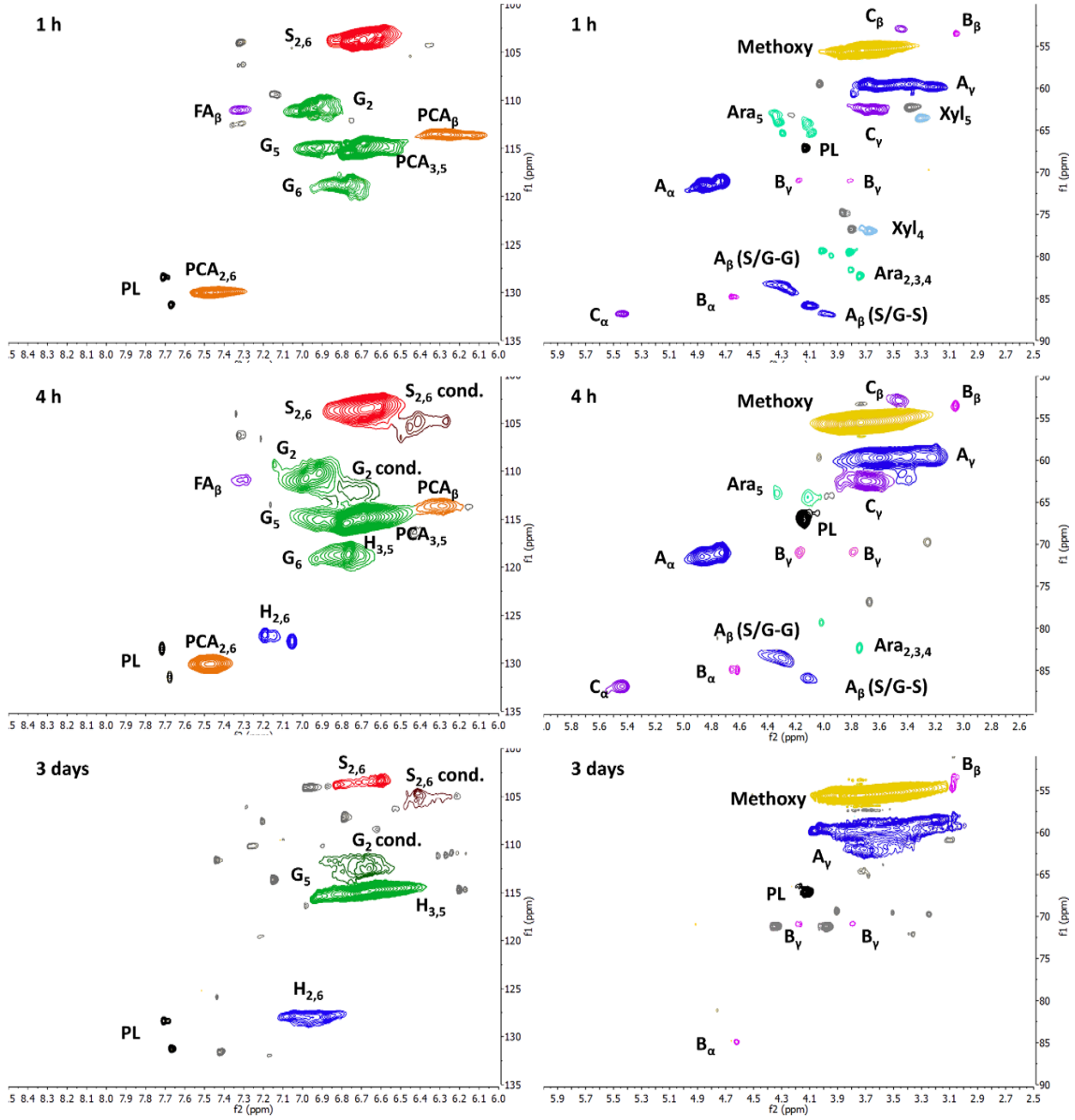

Figure III-36 HSQC NMR spectra of *Miscanthus* lignin isolated after extraction with [TEA][HSO_4] with a biomass to solvent ratio 1:10 g/g and a final water content of 20wt%, aromatic region (left side) and side chain region (right side).

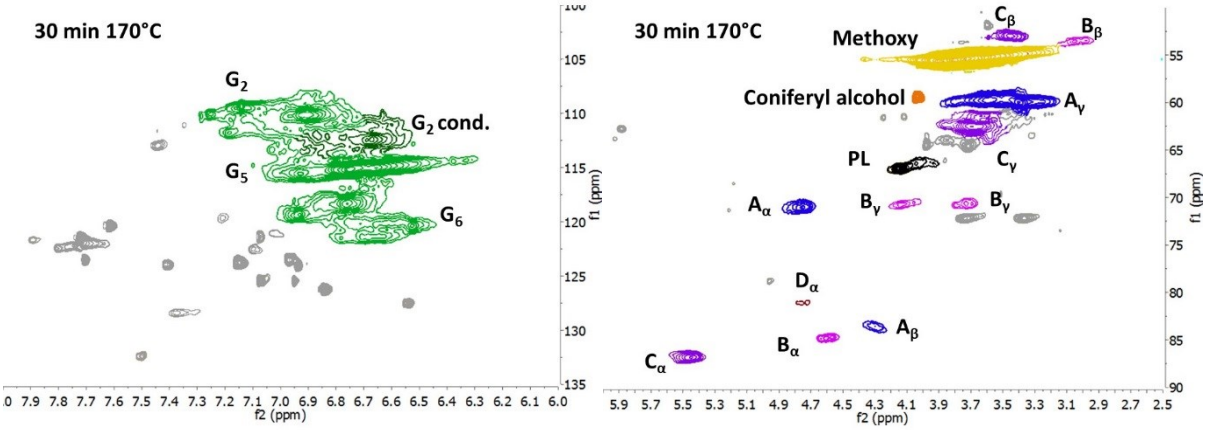

Figure III-37 HSQC NMR spectra of pine lignin isolated after extraction with [HC_4im][HSO_4] with a biomass to solvent ratio 1:10 g/g and a final water content of 20wt%, aromatic region (left side) and side chain region (right side).

I first want to draw attention to the side chain region. Figure III-38 (top) shows the abundance of the linkages obtained after peak volume integration for the *Miscanthus* time course at 120°C. The β-*O*-4' ether linkage, the most abundant linkage in lignin,[4] is shown to disappear very rapidly while the less abundant β-β' and β-5' ethers disappear at a somewhat lower rate. It can be seen that 80% of the β-*O*-4' linkages, present in the earliest lignin precipitate (arguably the closest to a native lignin structure) were broken or modified after 24 h. The decreased intensities of signals assigned to β-β' and β-5' linkages indicate that their ether linkages were cleaved, but as they contain C-C bonds, it is unlikely that the linkages are truly broken and more likely that they are chemically altered. Evidence exists that the five-membered tetrahydrofuran rings contained in both structures can be hydrolysed and substituted.[6] The side chain region further contained signals from residual carbohydrates, which disappeared over time, resulting in a carbohydrate-free lignin after 4 h. Figure III-38 (bottom) shows the relative integral of the three different main ether linkages of lignin obtained after pretreatment of pine in [HC_4im][HSO_4] for 1 hour at 120, 150 and 170°C. Similar to prolonged treatment, an increase in temperature resulted in a strong decrease in signal intensity of the β-*O*-4' ether linkage and to a lesser extent of the β-β' and β-5' linkages.

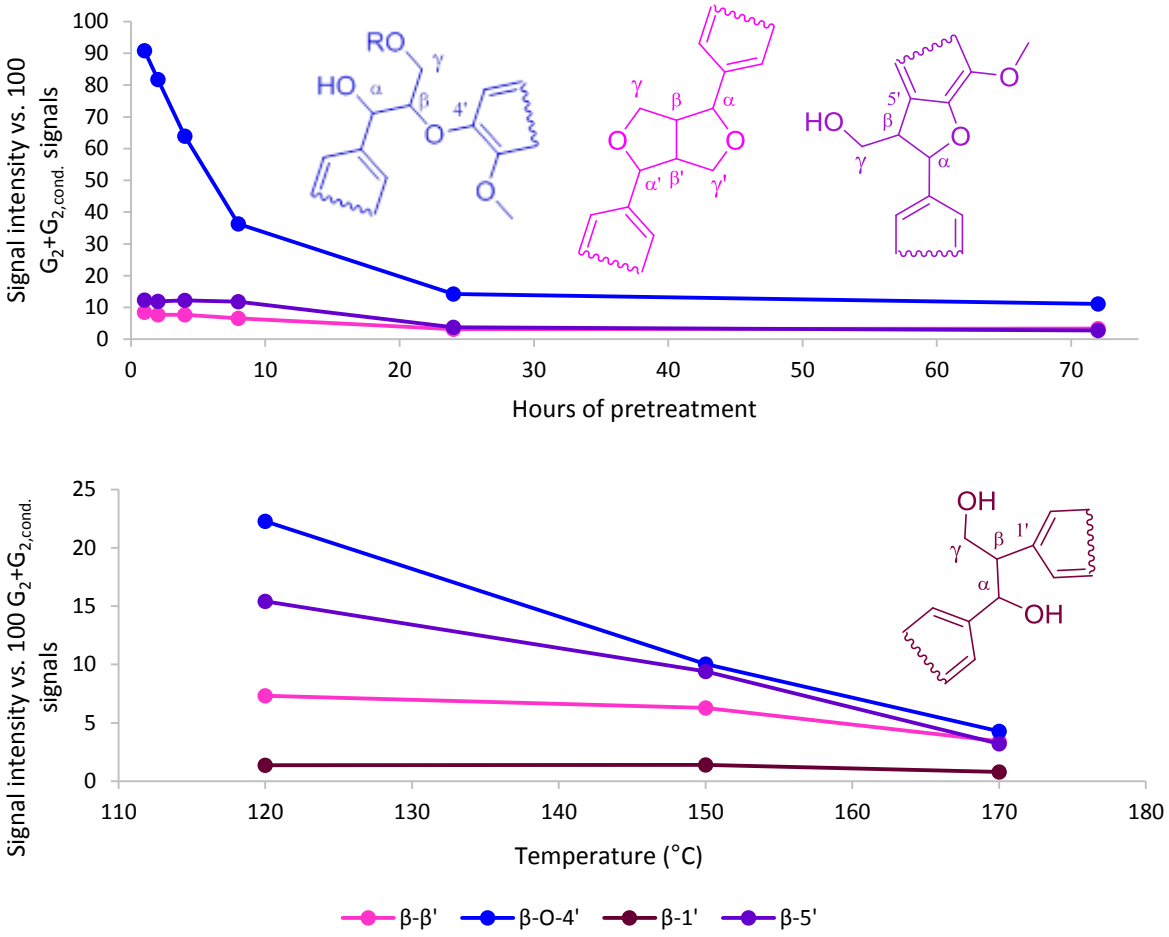

Figure III-38 Relative signal intensity of major lignin linkages in the precipitated lignin relative to the combined $G_2/G_{2,cond}$ volume integral as evidenced by HSQC NMR spectroscopy (top) throughout the time course of *Miscanthus* pretreated with [TEA][HSO_4] at 120°C with a biomass to solvent ratio 1:10 g/g and a final water content of 20wt% and (bottom) throughout a temperature course of pine pretreated with [HC_4im][HSO_4] for 1 h with a biomass to solvent ratio 1:10 g/g and a final water content of 20wt%.

The analysis is slightly more complex in the aromatic region. Figure III-39 (top) shows how the relative abundance of $S_{2,6}$, $H_{2,6}$, $PCA_{2,6}$, G_2, G_6, S_{cond} and $G_{2,cond}$ C-H units changed with pretreatment time for *Miscanthus* lignin and Table III-21 summarises the trends. Since the $H_{3,5}$ and $PCA_{3,5}$ signals overlap with G_5, volume integrals for those units are not reported for *Miscanthus* lignin. Since softwoods, unlike grassy biomass, do not have significant amounts of H or PCA units, whose signals overlap with the G_5 unit in the HSQC spectrum, all the different positions of the guaiacyl unit found in the precipitated pine lignin after pretreatment were also analysed and are depicted in Figure III-39 (bottom). Signal intensities and spectra of further pine lignins isolated by pretreatment of 10wt% pine with [HC_4im][HSO_4] at a water content of 20wt% at temperatures from 120 to 170°C for between 30 min and 4 hours can be found in the Appendix (Figures S62-64).

Similar to findings reported by Brandt *et al.* for [HC_4im][HSO_4] lignin from *Miscanthus*,[15] the H content of the precipitated lignin increased over time while the PCA content decreased in a complementary

fashion, suggesting that PCA is converted to H during pretreatment in these acidic ionic liquids (through decarboxylation and subsequent polymerisation). For both *Miscanthus* and pine lignin, a decrease in the G_6 signal as well as G_2 and an increase in $G_{2,cond}$ was observed. In addition, in the case of *Miscanthus* the $S_{2,6}$ signal decreased while the $S_{cond.}$ signal increased. As mentioned in earlier chapters, hydrolysis of the lignin polymer is thought to compete with lignin condensation under certain conditions. The previous study by Brandt *et al.* concluded that the decrease of G_6 signal intensity relative to G_2 is an indication of lignin condensation taking place in acidic ionic liquid solutions.[15] The same can be observed now for both *Miscanthus* as well as pine lignin. Condensation between aromatic rings was observed to a larger extent at higher temperatures and/or prolonged treatment times. In the case of pine, the G_5 signal was found to slightly increase with higher pretreatment temperatures. An increase in G_5 signal could, in theory, relate to cleavage of β-5' and 4-*O*-5' bonds if the bond between the G_5 carbon and the attached carbon/oxygen breaks to form a new C-H bond, which in practice is highly unlikely since these types of structures do not typically break in this position and this has not been reported or even suggested in the literature. An alternative explanation is that the amount of H units in pine is significant and, just as in the case of *Miscanthus*, there is signal overlap, with an increasing relative amount of H units present in the lignin. However, since pine does not contain PCA which can be transformed into H units as is the case for grass lignin, there is no reason to expect the apparent H content of the isolated lignin to increase with an increase in severity of the pretreatment. Yet, it is not to be excluded that some other newly formed structure results in the same signal overlap and an apparent increase in G_5 C-H units, e.g. structures derived from hemicellulose degradation products such as humins. Unpublished data by another member of the research group do indeed suggest that cooking of both xylose and glucose in ionic liquid results in the formation of a precipitate which has signal intensity in the HSQC spectrum that coincides with the G_2 (mainly in the condensed part) and the G_5 peak. An increase in the G_5 signal intensity could therefore be explained by the incorporation of hemicellulose derived moieties into the lignin. Furthermore condensation on the G unit might be overestimated. Finding a suitable "humin peak" to quantify the degree of humins incorporated into the lignin structure could improve estimating condensation in G and is part of ongoing research.

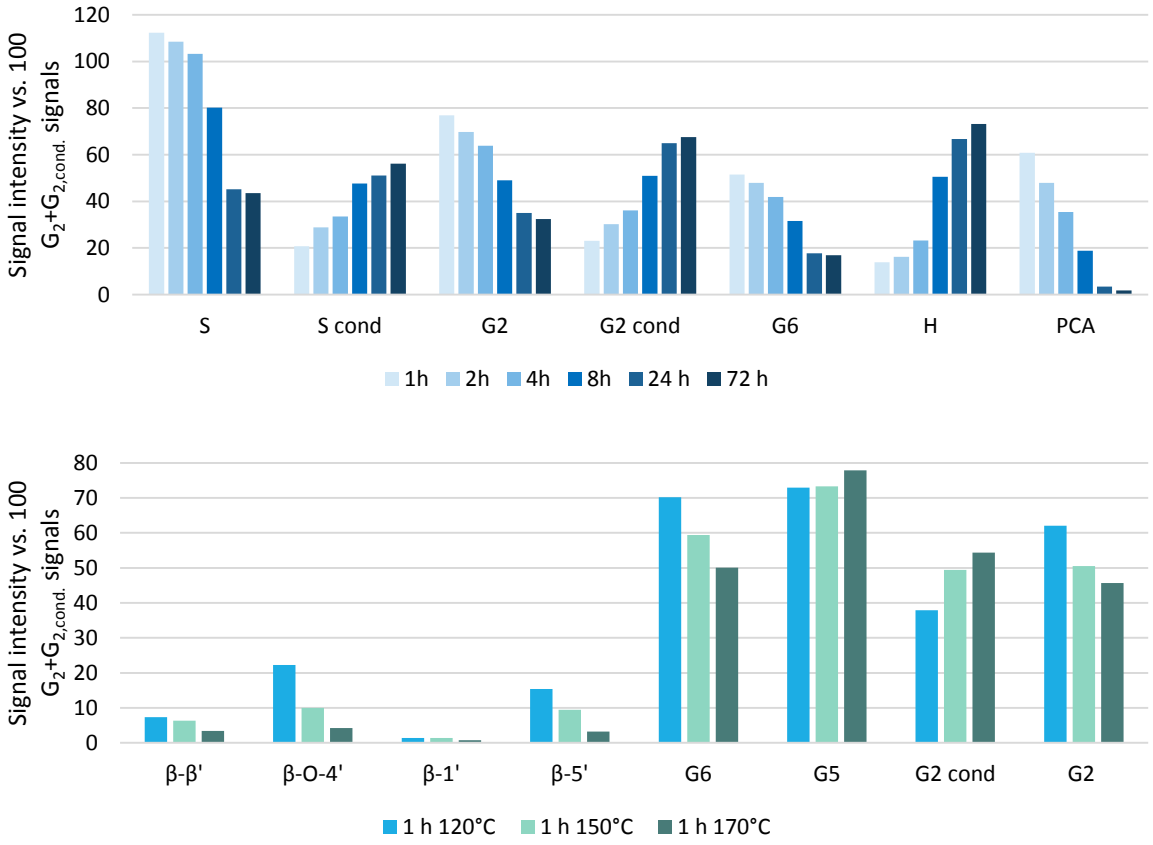

Figure III-39 Relative signal intensity of major lignin subunits and linkages in the precipitated lignin relative to the combined $G_2/G_{2,cond.}$ volume integral as evidenced by HSQC NMR spectroscopy. *Miscanthus* was pretreated at 120°C with [TEA][HSO_4] with a biomass to solvent ratio 1:10 g/g and a final water content of 20wt% (top). Pine was pretreated for 1 h at various temperatures with [HC_4im][HSO_4] with a biomass to solvent ratio 1:10 g/g and a final water content of 20wt% (bottom).

Table III-21 Changes in signal intensity observed for the different subunit positions as a result of increased severity.

	Miscanthus	Pine	Potential overlap with humins
$S_{2,6}$	↘	N/A (none)	
$S_{cond.}$	↗	N/A (none)	
G_2	↘	↘	
$G_{2,cond.}$	↗	↗	✓
G_5	N/A (overlap)	→ or ↗	✓
G_6	↘	↘	
$H_{2,6}$	↗	N/A (low)	
$H_{3,5}$	N/A (overlap)	N/A (low)	
$PCA_{2,6}$	↘	N/A	
$PCA_{3,5}$	N/A (overlap)	N/A	

N/A: not analysed.

There are a number of unidentified peaks in the HSQC spectrum (grey) which could be caused by pseudo-lignin and other condensed lignin adducts. Elucidating the nature of structures causing this is the subject of further investigations. I further notice that at long pretreatment times or under harsh conditions two new peaks arise next to the γ-signal of the β-β' linkage. They are however differently shifted for pine and *Miscanthus* and I speculate that incorporation of furfural derived from C5 sugars in the case of *Miscanthus* and HMF derived from C6 sugars in the case of pine is responsible for this shift. This is currently subject to further investigation as part of the PhD project of a fellow member of the Hallett research group which tries to elucidate the formation of pseudo-lignin in acidic ionic liquids.

Post-Hydrolysis Solid

HSQC NMR analysis on the solid remaining after saccharification of *Miscanthus* pulp, the 'post-hydrolysis solid', was performed to characterise the lignin present in the pulp which has either not been removed from or reprecipitated onto the pulp (Figure III-40). The post-hydrolysis solids obtained at an early time point (2 h of pretreatment at 120°C) and at a late time point (24 h of pretreatment at 120°C) were compared.

For the 2 h post-hydrolysis lignin, the HSQC spectrum contained signals typical for early stage lignin (no noticeable $G_{2,cond.}$, $S_{cond.}$ or H peaks, significant PCA signal) and carbohydrates. The spectrum of the 24 h post-hydrolysis lignin showed signal intensity in the area of the $G_5/H_{3,5}/PCA_{3,5}$ peak and the methoxy signal but barely any signals that could be assigned to linkages or other lignin subunits. I attribute this to the presence of pseudo-lignin and highly condensed lignins in the 24 h pulp, which contain few aromatic or oxygenated C-H units. In general, the 24 h spectrum was of poor quality, either due to a low amount of C-H_n signals in the non-dissolved 'lignin' or due to its high molecular weight, which is likely to reduce solubility in the NMR solvent. Post-hydrolysis lignin after [C_2C_1im][OAc] treatment of *Miscanthus* has in the past been found to be similar in structure to native lignin.[16] In the present study this might be true for the 2 h post-hydrolysis lignin, the 24 h post-hydrolysis lignin however is suspected to have reprecipitated onto the pulp surface after it was strongly chemically altered in the ionic liquid solution.

There are again a number of unidentified peaks, especially in the aromatic region of the 24 h residue spectrum. These peaks are not the same as the unidentified peaks in the HSQC NMR spectrum of the precipitate and it is unclear what the reason for this difference is.

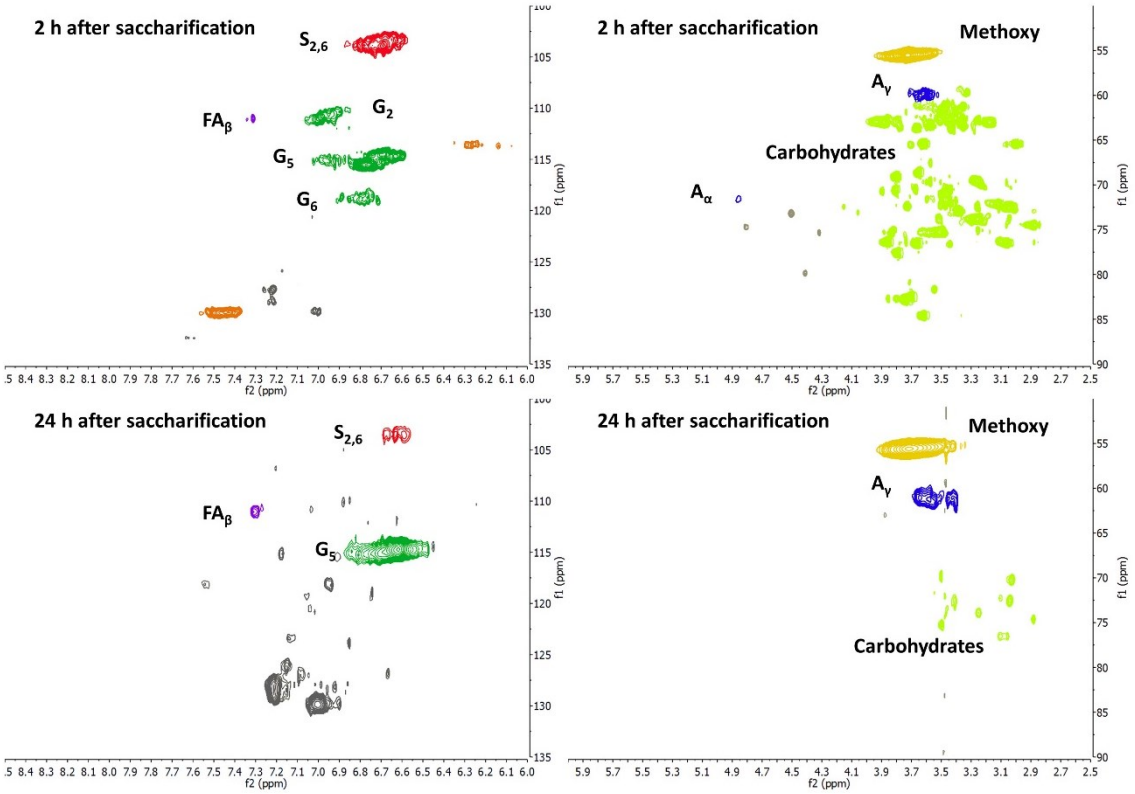

Figure III-40 HSQC NMR spectra of *Miscanthus* lignin remaining in the pulp after 2 h and 24 h of pretreatment. The aromatic region is shown on the left and the side chain region on the right. *Miscanthus* was pretreated at 120°C with [TEA][HSO_4] with a biomass to solvent ratio 1:10 g/g and a final water content of 20wt%.

Hydroxyl group content

Isolated lignins can be modified with a phosphitylating agent and subjected to ^{31}P NMR analysis, which provides information on the abundance of different OH-groups in the lignin structure. Abundance of phenolic –OH groups has been shown to be important for various applications of lignin, for example as a replacement of phenol in phenol formaldehyde resins.[17] Table III-22 shows the abundance (in mmol/g of lignin) of different hydroxyl group types found in isolated *Miscanthus* lignins from pretreatments at temperatures between 150 and 180°C. Similar to previous findings,[15] this sample set shows an initial decrease in aliphatic OH groups followed by an increase, while the abundance of all other OH groups continuously increases over time, namely the phenolic S, G and H hydroxyl groups, as well as the carboxylic acid groups. In the case of the lignins isolated from pretreatment at 170°C and to a lesser extent at 150°C, the aliphatic OH-groups started to increase again from 30 to 45 min and 60 to 90 min respectively. While this has been reported in a previous study by Brandt *et al.* for *Miscanthus* using [HC_4im][HSO_4] at 120°C,[15] no explanation was given. In addition, the 150°C time course showed a slight decrease in *p*-hydroxyphenyl OH group content initially before beginning to increase after 60 min of pretreatment. This initial decrease was also observed by Brandt *et al.* where it was attributed to the release of PCA into the IL solution.[15]

Table III-22 ^{31}P NMR integrals of phosphitylated lignins converted to mmol of OH per gram of lignin. *Miscanthus* was pretreated in [TEA][HSO_4] with a biomass to solvent ratio 1:5 g/g and a final water content of 20wt%.

t (min)	T (°C)	aliphatic	aromatic			acid
			S	G	H	
45	150	1.77	1.01	1.09	0.65	0.02
60	150	1.27	1.02	1.14	0.59	0.02
90	150	1.30	1.38	1.51	0.75	0.16
40	160	1.33	1.78	1.80	0.94	0.16
15	170	3.04	0.66	0.98	0.80	0.09
30	170	1.66	2.13	2.17	1.11	0.12
45	170	2.04	4.38	4.37	2.17	0.74
15	180	2.54	1.22	1.33	0.85	0.01
30	180	0.92	1.89	1.89	0.95	0.19

S: syringyl, G: guaiacyl, H: p-hydroxyphenyl

An increase in both aliphatic and aromatic hydroxyl groups is thought to be a result of cleavage of ether bonds. Cleavage of the β-5'/α-*O*-4' ether bond for example is expected to give rise to a new aliphatic and a new aromatic OH group while cleavage of the β-β' ethers should result in 4 new aliphatic OH groups and cleavage of the β-*O*-4' bond in an aromatic OH group and the loss of an aliphatic OH group (Figure III-41).[6] The initial strong decrease in aliphatic OH groups followed by a relatively smaller increase could therefore be a result of the abundant β-*O*-4' bonds breaking relatively fast, resulting in a loss of aliphatic OH groups, while the less abundant β-5' and β-β' ethers break at a slower rate, resulting initially in a net loss of aliphatic OH followed by an increase once β-*O*-4' ether cleavage has ceased. A reduction of aliphatic hydroxyl content during dilute acid pretreatment has further been attributed to the loss of carbohydrate residues.[6] An increase in carboxylic acid groups has been associated with the cleavage of ester bonds from LCC.[6] Ester bonds however are not very stable under acidic conditions and expected to break rapidly. However, a rapid increase in carboxylic acid groups was here only observed after prolonged treatment, the reasons for which remain unclear.

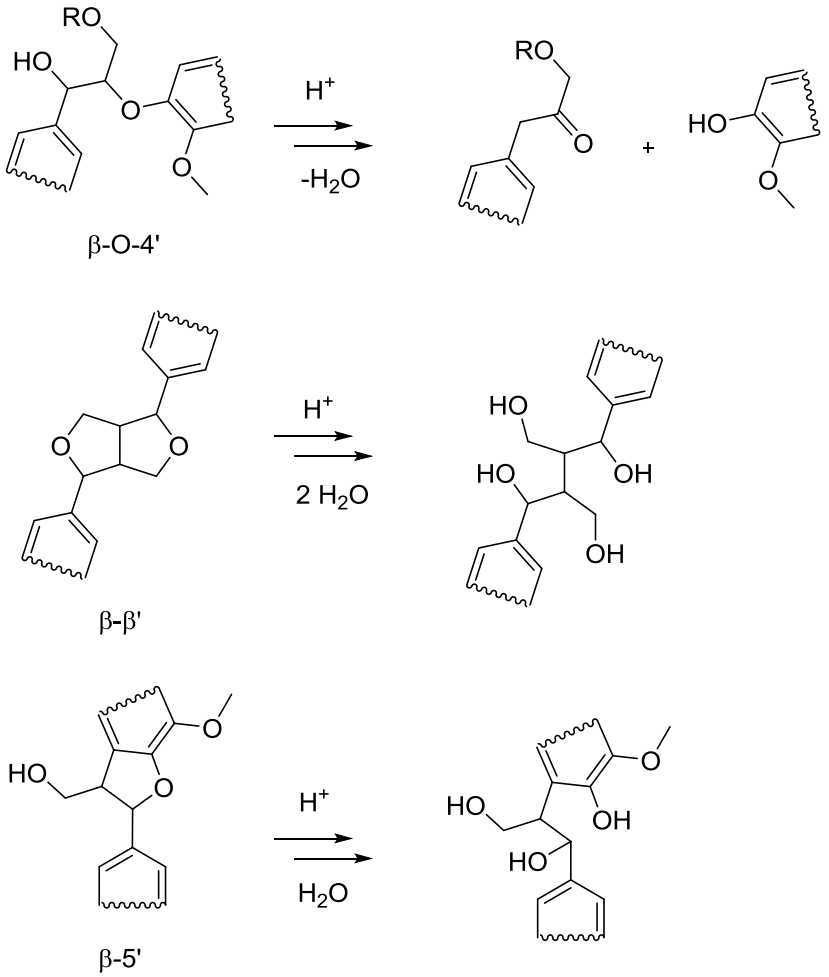

Figure III-41 Cleavage of ether bonds in lignin under acidic conditions.[6]

Molecular Weight

While HSQC and ^{31}P NMR give structural information about lignin, they only contain information on the average lignin fragment. GPC on the other hand allows to assess the relative size of the macromolecules and the size distribution. Brandt *et al.* reported an initial decrease in both M_w and M_n of ionoSolv lignin before they increased again.[15] As can be seen from Figure III-42, the molecular weight of the *Miscanthus* lignin isolated at 120°C (both number average molecular weight, M_n, and weight average molecular weight, M_w) decreased in the first 4 h of pretreatment. The M_n decreased from 1600 to 1000 Da, while the M_w decreased from 4600 to 3800 Da. Ball-milled *Miscanthus* lignin has previously reported to have an M_w of 13,700 Da and an M_n of 8300 Da.[18] This finding and the reduction of ether linkage signals observed by HSQC NMR indicate that the lignin polymers were progressively shortened by hydrolysis of ether bonds and appear to be shorter than native lignin already after only one hour of pretreatment.

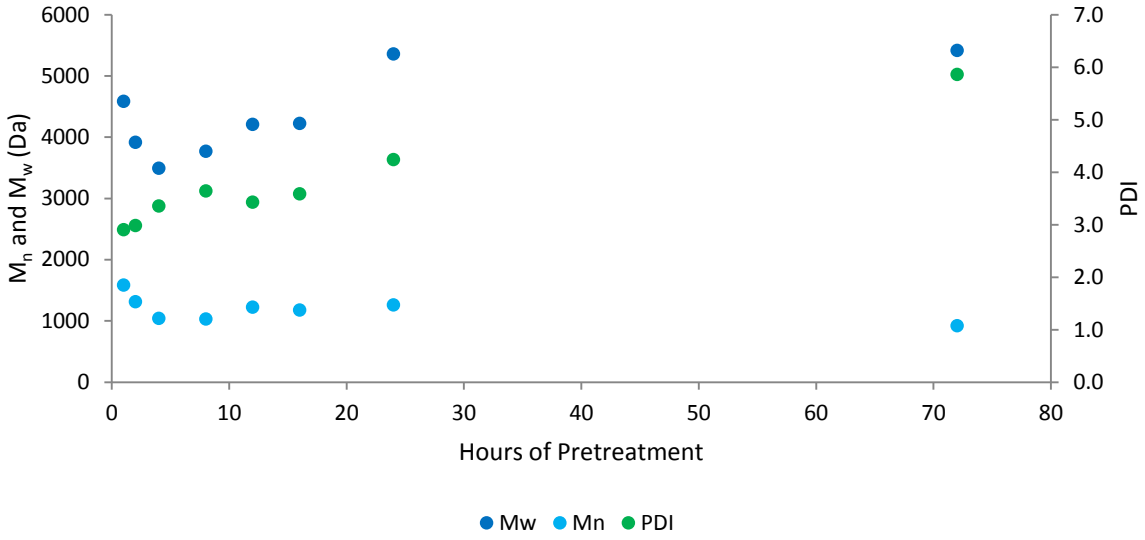

Figure III-42 Molecular weight markers of isolated *Miscanthus* lignins. *Miscanthus* was pretreated in [TEA][HSO_4] at 120°C with a biomass to solvent ratio 1:10 g/g and a final water content of 20wt%. M_w: Average molecular weight; M_n: number average weight; PDI: Polydispersity index.

The decrease in M_w was followed by an increase to around 5400 Da beyond 4 h pretreatment time. The M_n changed to a lesser extent at longer pretreatment times, remaining at around 1200 Da. The different trends for M_n and M_w, highlighted by an increasing polydispersity index (PDI), indicate that there was a small fraction of higher molecular weight polymers in the isolated lignin whose size continued to increase to around 5400 Da but not beyond. Since it is not expected that condensation ceases at 5400 Da, this supports the hypothesis that **high molecular weight lignin may become insoluble in the ionic liquid solution or the ethanol-diluted IL after pretreatment and redeposits onto the cellulose surface.** Evidence for this was discussed in Chapter 1 where compositional analysis of the pulp revealed that the delignification dropped from 88% after 16 h to 73% after 24 h of pretreatment. Further evidence for this can be found when comparing the molecular weight profiles obtained for different lignins (Figure III-43). Lignin obtained after 1 h of pretreatment appears to have a shoulder of high M_w in the GP chromatogram which disappears within the next 3 h, reflected in the overall decrease in M_w. After 4 h the shoulder reappears until, after 24 hours of pretreatment, the high M_w shoulder is almost the same size as the low M_w peak. Lignin isolated after 72 h of pretreatment however does not exhibit this shoulder anymore, which is likely due to the high M_w (condensed) fragments becoming too large to be solubilized in the IL or ethanol-diluted IL, hence precipitating onto the pulp surface rather than staying in solution until the lignin precipitation step.

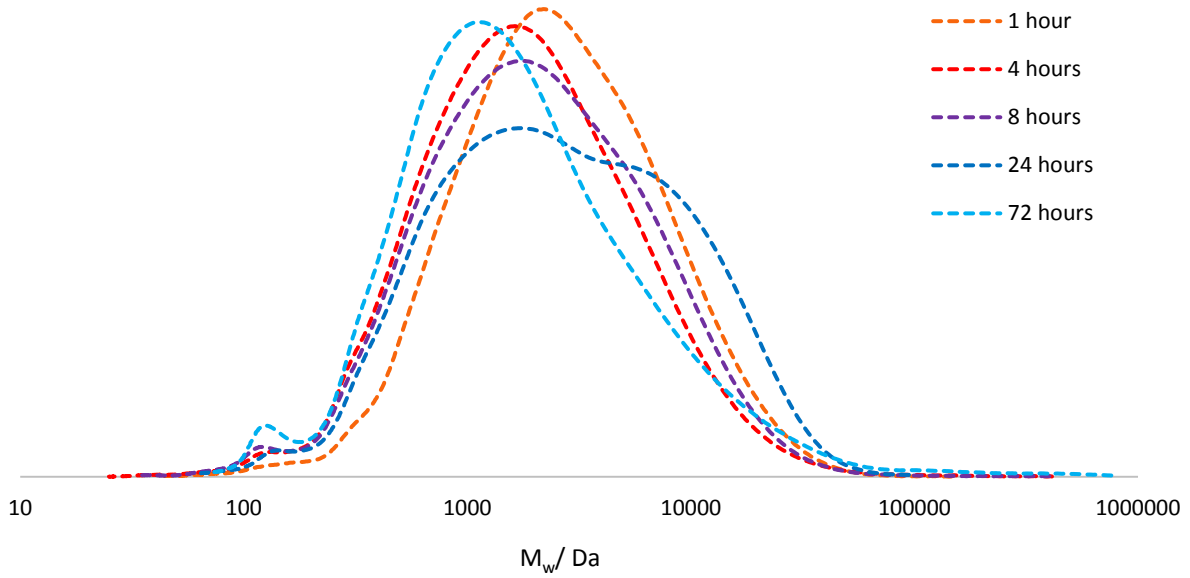

Figure III-43 Area normalised GPC Traces for lignins obtained after pretreatment of *Miscanthus* in [TEA][HSO_4] at 120°C with a biomass to solvent ratio 1:10 g/g and a final water content of 20wt%.

The *Miscanthus* lignins obtained at higher temperatures, shown in Table III-23, only show the initial stages of these trends, hence the M_w and M_n decreased over time in all cases where more than one time point was studied. At 150°C, the PDI was surprisingly found to increase between 30 and 60 min and decrease again between 60 and 90 min. The same trend was observed in a less pronounced way between 15 and 30 and 30 and 45 min at 170°C and even the 120°C time course shows a dip in PDI between 8 and 12 hours. The PDI decreased from 15 to 30 min at 180°C. An initial increase in PDI was observed by Sun *et al.* who subjected enzymatic hydrolysis lignin from poplar and switch grass to dilute acid pretreatment.[6] They attributed this observation to "the behaviour of M_n and M_w", which, considering the PDI is defined as M_w/M_n, is true, but fails to explain the underlying reason.

Table III-23 Molecular weight of isolated lignins measured with GPC. *Miscanthus* was pretreated in [TEA][HSO_4] with a biomass to solvent ratio 1:5 g/g and a final water content of 20wt%.

t (min)	T (°C)	M_n	M_w	PDI
30	150	1216	3570	2.9
45	150	1081	3414	3.2
60	150	950	3569	3.8
90	150	925	2938	3.2
40	160	928	3508	3.8
15	170	1454	4946	3.4
30	170	948	3395	3.6
45	170	937	3312	3.5
15	180	1207	4391	3.6
30	180	923	3230	3.5

M_n: Number average molecular weight (Da); M_w: Weight average weight (Da); PDI: Polydispersity index.

We are hypothesizing that lignin extraction, depolymerisation and condensation goes through four stages. In a 1st stage, large lignin fragments are extracted from the biomass into the IL, resulting in a recovered lignin with high M_w, high M_n and low PDI, most similar to native lignin although presumably already slightly shortened. In a 2nd stage, extraction of large lignin fragments from the biomass continues while early extracted lignin chains have begun to break up into shorter chains, mirrored in a lignin precipitate with a lower M_n while the M_w is largely unchanged, resulting in a higher PDI. In a 3rd stage, lignin extraction from the biomass has ceased and most large lignin fragments will have broken down to somewhat smaller fragments, as evidenced by a decrease in both M_n and M_w and as a result also a lower PDI. At longer pretreatment times is a 4th stage, where condensation of lignin fragments to form new larger chains co-existing with small fragments then contributes to an again increasing M_w while the M_n continues to decrease or level off, resulting in an increase of the PDI. Here this 4th stage is only observed for the prolonged study at 120°C.

There is a remarkable decrease in M_w between 15 and 30 min at 170°C, 15 and 30 min at 180°C and to a lesser extent 60 and 90 min at 150°C, which are therefore likely a result of the lignin extraction to have finished just before or within this window of observation. Further evidence for this can be obtained when comparing the M_w to the residual lignin content in the pulp as discussed in Chapter 2. It appears that the sharp decrease in M_w coincides with the minimum lignin content in the pulp as depicted in Figure III-44 (top). In the case of the 120°C time course, the most pronounced decrease in M_w was found early on, between 1 and 4 h of pretreatment although minimum lignin content was only reached at around 8 h of pretreatment (Figure III-44 (bottom)). It is speculated that the lower temperature impacted the lignin extraction more strongly than the depolymerisation and condensation, something that will be discussed more in detail later on. As a consequence, condensation started to manifest while extraction was still ongoing, resulting in an overall increase in M_w before extraction was finished and the minimum lignin content was reached. It is also very much surprising to see how closely the M_w of the lignin precipitate is reflected in the residual lignin content. This suggests that the lignin solubility in the IL or ethanol diluted IL is a direct function of the M_w.

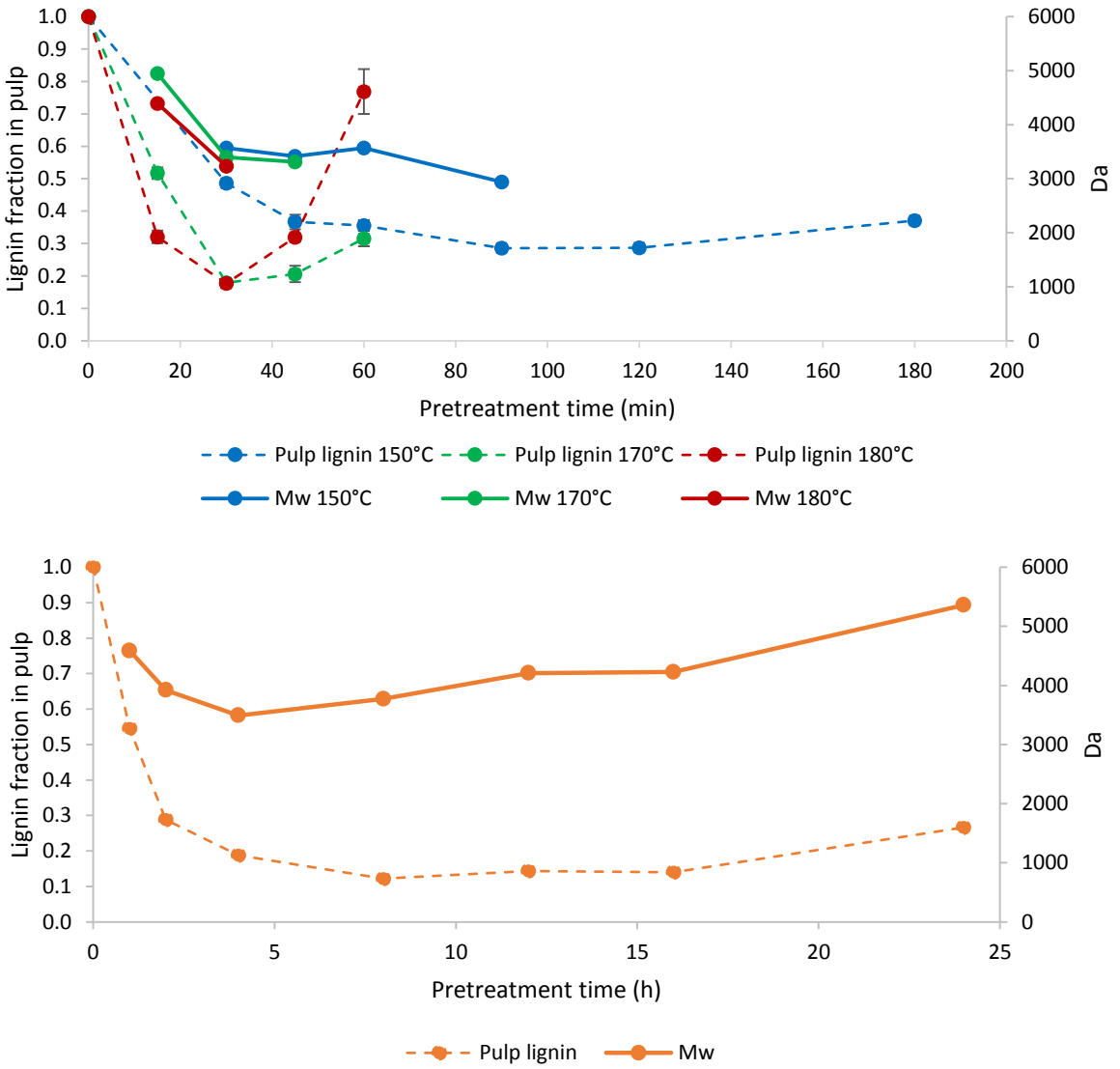

Figure III-44 Weight average molecular weight, M_w, as measured by GPC, and residual lignin content in the pulp, as measured by compositional analysis, as a fraction of the initial lignin content of the biomass. *Miscanthus* was pretreated in [TEA][HSO_4] with a biomass to solvent ratio 1:5 g/g and a final water content of 20wt% (top). *Miscanthus* was pretreated in [TEA][HSO_4] at 120°C with a biomass to solvent ratio 1:10 g/g and a final water content of 20wt% (bottom).

Elemental Analysis

A previous study conducted by Brandt *et al.* at 120°C found both N and S present in the lignin isolated after pretreatment of *Miscanthus* with the ionic liquid 1-butylimidazolium hydrogensulfate [HC_4im][HSO_4], which was attributed to residual ionic liquid in the lignin, confirmed by NMR and Py-GC-MS analysis.[15] In the present study, no significant amounts of IL were detected by NMR. It is however possible that ionic liquid cations and/or anions react with and get incorporated in the lignin. Elemental analysis of the obtained lignins was therefore conducted in order to assess ionic liquid incorporation into the lignin structure, and whether elevated temperature led to increased reactivity between biomass components and the ionic liquid. The results are summarised in Table III-24. In all cases, the sulfur detected, a measure of anion incorporation and/or precipitation (in the form of

$[M]_x[SO_4]$ where [M] is likely to be an alkali or earth alkaline metal present in native biomass), was close to or below detection limit (in all cases below 1%). Where more than one data point was measured for a given temperature, the sulfur content stayed similar or decreased slightly over time, indicating that the lignin does not become enriched in the anion over time and a maximum of 2.3wt% of anion was incorporated in the lignin (30 min at 150°C). In all cases, the nitrogen content was below the detection limit, from which it was concluded that no ammonium cation was incorporated into the lignin. Other changes that occurred were an increase in carbon content, and a decrease in hydrogen content and "other", where "other" was assumed to be composed of mainly oxygen. This is well in line with the findings from other analytical techniques discussed earlier, which indicate the dehydration of alkyl chains and formation of new C-C bonds, resulting in a slight reduction in the lignin's oxygen content.

Table III-24 Elemental analysis of lignins from various conditions. *Miscanthus* was pretreated in $[TEA][HSO_4]$ with a biomass to solvent ratio 1:5 g/g and a final water content of 20wt%.

t (min)	T (°C)	C%	H%	N%	S%	O%[a]
45	150	61.5	6.1	BDL	0.8	31.7
60	150	62.5	5.9	BDL	0.5	31.1
90	150	63.3	5.7	BDL	0.4	30.5
40	160	62.9	5.8	BDL	0.5	30.9
15	170	60.0	6.1	BDL	0.4	33.5
30	170	62.8	5.8	BDL	0.5	31.0
45	170	64.3	5.6	BDL	0.4	29.8
15	180	60.7	6.0	BDL	0.5	32.8
30	180	63.7	5.6	BDL	0.5	30.2

C: carbon, H: hydrogen, N: nitrogen, S: sulfur, O: oxygen content, [a] by difference, BDL: Below detection limit.

The Whole Picture

By combining the information from two or more techniques discussed above, further insight can be gained. Comparing the two data points collected for 180°C pretreatment with respect to the information gained from both HSQC NMR and GPC shows that, despite the fact that the later time point contains more condensed signals in the HSQC NMR spectrum, the average molecular weights M_w and M_n and the PDI were lower than in the case of the early time point. Furthermore, lignin extraction from the pulp and the lignin precipitate yield were both higher for the second time point. Therefore the changes in lignin structure, such as cleavage of ether bonds and condensation as evidenced by HSQC, up to 30 min at 180°C mainly resulted in a shortening of the chains rather than the formation of high M_w condensed lignin. The breakage of around 75% of ether bonds therefore

outweighs the increase in the ratio of condensed vs. non-condensed G units from 0.6 to 1.3 with respect to the molecular weight of the precipitated lignins.

Table III-25 Summary of several lignin characteristics. *Miscanthus* was pretreated in [TEA][HSO_4] with a biomass to solvent ratio 1:5 g/g and a final water content of 20wt%.

t (min)	T (°C)	M_n	M_w	Residual pulp lignin	Lignin yield	Sum of ether bond signals[a]	Cond./non-cond.[b]
15	180	1207	4391	52%	43%	76	0.6
30	180	923	3230	18%	72%	20	1.3

M_w: Weight average weight (Da); [a] β-*O*-4', β-β' and β-5' α-signals were used; [b] Ratio of $G_{2,cond.}$ and G_2

By comparing data obtained from ^{31}P NMR and HSQC NMR we can further obtain information about the mechanisms of ether cleavage. As an example, we can compare the number of OH groups, as evidenced by ^{31}P NMR, and the number of ether bonds, as evidenced by HSQC NMR, for the lignins isolated from *Miscanthus* after pretreatment at 150 and 170°C. From the graphs displayed in Figure III-45 we can see that the number of ether bonds decreases while the concentration of phenolic and carboxylic acid OH increases. In the case of the 150°C time course, the changes from 45 to 60 min with respect to ether bond cleavage are less pronounced than from 60 to 90 min. Similarly, the changes in S, G, H and carboxylic acid signals are not strongly pronounced in this first interval, but more so in the second. The aliphatic OH content however decreases along with a decreasing number of ether signals over the first interval. This might be a result of predominantly the β-*O*-4' bond being cleaved initially, resulting in the loss of aliphatic OH groups as a result of the elimination of formaldehyde after hydrolysis.[15] Especially at 170°C the strongest change observed between 15 and 30 min of pretreatment is the loss of β-*O*-4' bonds. Between 30 and 45 min however, the change in signal intensity for the three ether linkages is more similar and the formation of new aliphatic OH groups from the cleavage of β-5' and especially β-β' is likely to outweigh the loss of aliphatic OH groups associated with cleavage of β-*O*-4' bonds. It has further been suggested that a decrease in aliphatic OH is linked to the degradation of carbohydrate residues and the transformation of the α- and γ-OH groups to ketones, aldehydes and alkene structures.[6]

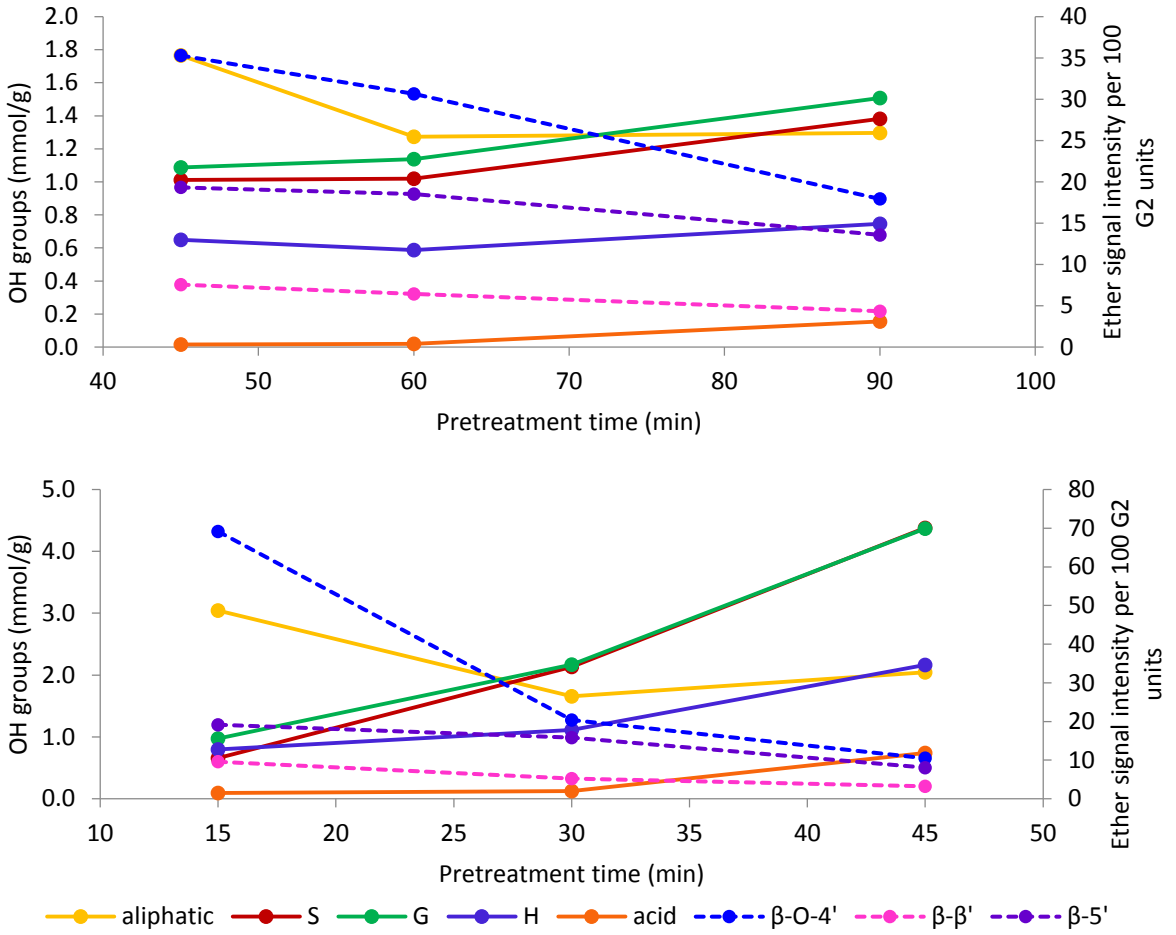

Figure III-45 Concentration of various OH groups (solid lines) as evidenced by ^{31}P-NMR and abundance of ether bonds (dotted lines) as evidenced by HSQC NMR for *Miscanthus* lignins obtained from pretreatment at 150°C (top) and 170°C (bottom) with [TEA][HSO_4] with a biomass to solvent ratio of 1:5 g/g and a final water content of 20wt%.

Effect of Excess Acid

To understand whether changes in the structure of the recovered lignin were affected by the presence of excess acid, HSQC NMR spectroscopy was applied again to quantify the relative abundance of different lignin functionalities. The relative size of the volume integrals are displayed in Figure III-46, while the spectra can be found in the Appendix. The trends in Figure III-46 show that the more acidic environment led to an acceleration of ether bond cleavage. After 2 h of pretreatment with ionic liquid containing 9% excess acid, the recovered lignin contains fewer ether bonds than after 8 h without an excess of acid under otherwise equivalent conditions. Similar trends were observed for the aromatic signals: extraction with the more acidic ionic liquid led to an accelerated change in the signal intensities in the uncondensed and condensed $S_{2,6}$ and G_2 cross-signals.

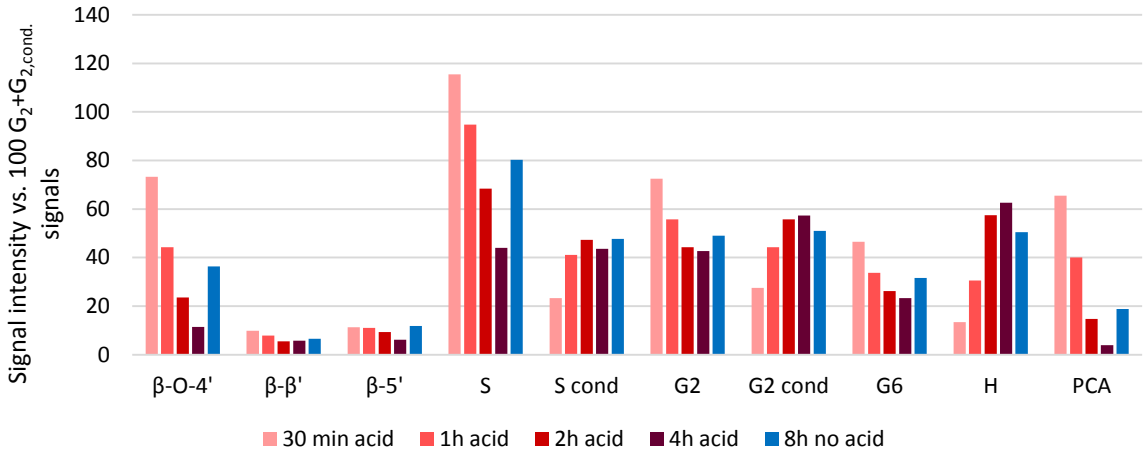

Figure III-46 Relative signal intensity of major lignin subunits and linkages in the precipitated lignin relative to the combined $G_2/G_{2,cond.}$ volume integral as evidenced HSQC NMR spectroscopy. *Miscanthus* was pretreated in [TEA][HSO_4] with an acid to base ratio of 1.09:1, a 1:10 g/g biomass to solvent ratio and a final water content of 20wt% water.

GPC analysis (Figure III-47) shows that the M_n decreased throughout the time course and was only slightly higher than for the lignin isolated with the 1:1 IL solution, while M_w and PDI had a minimum at around 2 h (3800 Da and 3.1). The M_w of the lignin of the earliest time point (30 min) with excess acid is found to be much higher (ca. 7800 Da) than for any other early *Miscanthus* lignin analysed (4600 Da for 1 h at 120°C, 4900 Da for 15 min at 170°C). As a consequence of the high M_w, the PDI found here for the 30 min time point however was significantly higher than for the 1:1 IL at almost 4.4. Ball milled *Miscanthus* lignin has been reported to have an M_w of around 13,700 Da and a relatively low polydispersity of 1.65.[18] The M_w of the 30 min pretreatment, being roughly half of what is reported for native *Miscanthus* lignin, therefore suggests that some of **the extracted lignin might have been fragmented into as few as two chains.**

In the previously studied lignins obtained with a 1:1 IL solution, the highest M_w of the isolated lignin was around 5400 Da, which was obtained after 24 hours of pretreatment and beyond, where the M_w had started to level off. The absence of a further increase in M_w beyond 5400 Da was attributed to these higher molecular weight fragments becoming insoluble in the IL or the ethanol-diluted IL, hence precipitating onto the cellulose surface. The data obtained here however suggest that lignin of an M_w close to 7800 Da and therefore exceeding this value of 5400 Da can be isolated with the employed separation protocol. The lignin with an M_w of 7800 Da however was isolated after the very initial period of pretreatment and chemically different than the highly condensed lignins after 24 and 72 h in the 1:1 IL, as evidenced by the HSQC data, showing significantly more ether bonds and fewer condensed moieties in the 30 min time point with excess acid. It is therefore suspected that higher M_w lignin can be solubilised in the IL and the ethanol-diluted black liquor as long as the lignin contains sufficient polar moieties.

Unlike for the previously discussed *Miscanthus* lignins, the PDI of the analysed lignins does not show an initial increase. However, since the PDI of ball milled *Miscanthus* has been reported to lie at around 1.65,[18] the here found PDI of 4.4 after the shortest pretreatment period does represent a significant increase with respect to the PDI of native lignin. There is currently no strong hypothesis as to why the initial M_w is this high in the presence of 9% excess acid. A tentative speculation is that the increased acidity results in a very rapid cleavage of the LCC, releasing very large lignin fragments with a higher M_w than for the 1:1 IL where the LCC is expected to break at a slower rate where lignin depolymerisation might have started by the time the lignin is fully solubilised in the IL, and hence no such big lignin fragments are observed. These very large lignin fragments are then cleaved rapidly, resulting in an M_n similar to the one seen for the 1:1 IL solution at short pretreatment times, which, together with the very high M_w, results in a PDI higher than for any other lignin obtained at short pretreatment times.

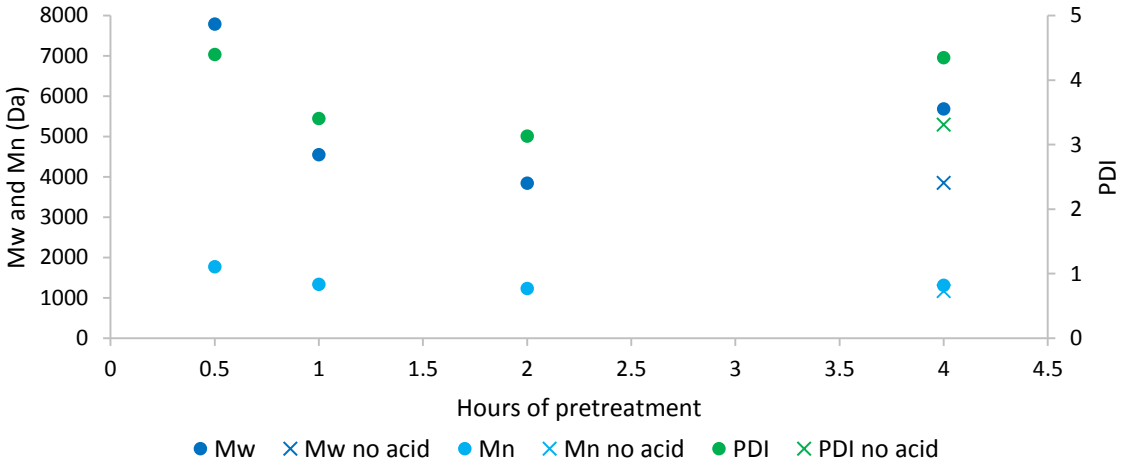

Figure III-47 M_w, M_n and PDI obtained by GPC from isolated lignins. *Miscanthus* was pretreated at a 1:10 g/g biomass to solvent ratio in [TEA][HSO_4] with an acid to base ratio of 1.09:120% and a final water content of 20wt%.

After the initial 30 min, the M_w and PDI both decrease rapidly before starting to increase again. The minimum for M_w and PDI was at 2 h for the excess acid pretreatment, which also resulted in the best saccharification yields. The earlier minimum for M_w together with the trends observed with HSQC NMR analysis indicate that both cleavage and re-condensation reactions proceed faster in the presence of excess acid.

These results suggest that the lignin extraction, depolymerisation and recovery can be accelerated by additional acid, but the concomitant acceleration of pseudo-lignin formation and condensation reactions requires careful control of reaction conditions.

Effect of Biomass Loading

The importance of running pretreatments at high solids to liquid ratios has been mentioned previously (Chapter 2). Saccharification yields were somewhat impacted by the increased loading and an increase in pulp yield was observed, most likely as a result of a higher pulp lignin content. The suspicion of lignin reprecipitation as a result of the limited lignin solubility in the ethanol-diluted IL was mentioned. Here it is investigated whether properties of the isolated lignin can give any further confirmation of this hypothesis. Lignin chemistry at higher loading is possibly altered towards favouring intermolecular reactions while lower loadings are favouring intramolecular reactions as a result of the difference in lignin concentration in solution.

Figure III-48 shows the HSQC NMR signal intensities as well as GPC data of the isolated lignins after pretreatment of pine at different biomass loadings. HSQC NMR analysis of the recovered lignin shows only modest differences between high loading and low loading experiments. There appears to be a slight trend towards more ether bond cleavage at higher loadings in the isolated lignin. The signal intensity of the G_5 and $G_{2,cond.}$ signal increases while they decrease for G_6 and G_2 when the loading is increased. Increasing loading therefore has a similar effect on ether cleavage and condensation as an increase in temperature or prolonging pretreatment time (see Table III-21) where the increase in G_5 signal intensity is once more thought to stem from the incorporation of carbohydrate derived compounds. Interestingly, and somewhat in contrast to the higher degree of condensation observed, the GPC data show a general decrease in M_n and M_w with higher loading, although there are some inconsistencies and large errors between 15 and 25wt% loading. Further, the PDI of the isolated lignin was found to be lower at higher loadings.

These observations from GPC are in line with the hypothesis of lignin precipitating during pulp wash; the isolated lignin was dissolved in the ionic liquid and stayed solubilised during ethanol addition. While some protic ionic liquids can dissolve up to 70wt% lignin[19] and it is therefore not expected that our ILs are saturated with lignin even at the highest loadings, the ethanol can precipitate larger fragments out of solution during the dilution. At higher loadings and therefore higher lignin concentrations the cut-off for larger fragments in ethanol is expected to lie at slightly lower molecular weight than for lower loadings, resulting in a lower M_w and M_n in the isolated lignin. Especially the decrease of the PDI is thought to stem from the narrower window of molecular weights isolated after the pulp washing step at higher loadings. It should also be noted that the here observed M_w of almost 8000 Da with a 5wt% biomass loading is the highest observed M_w in this work and is slightly higher than the M_w of around 7800 Da obtained from lignin after pretreatment of *Miscanthus* for 30 min at 120°C using [TEA][HSO_4] with an excess of acid. It is suspected that the low loading and the resulting low concentration of lignin allowed for such large fragments to remain in solution upon dilution with

ethanol. Southern Pine milled wood lignin has been reported to have an M_w of 14,900 Da and an M_n of 4700 Da, resulting in a PDI of 3.2.[18] The M_w of the lignin recovered from 5wt% loading show similar trends to the *Miscanthus* lignin, with an M_w of 7800 Da being roughly half of what is reported for native pine lignin. **This further suggests that pine lignin is also extracted from the biomass after minimal depolymerisation.**

The differences observed in the HSQC NMR are somewhat harder to explain. It is hypothesised that at higher loadings, an increased lignin concentration leads to an increased chance of new C-C bonds forming as a result of the higher concentration of potential reactants. This in turn is thought to result in accelerated intermolecular condensation reactions. The observation of a lower number of ether bonds but higher degree of condensation in lignin with a lower M_w and M_n obtained with high loadings is therefore thought to stem from the isolation method: the lignin fragments that condensed while having intact ether bonds end up having a molecular weight that is too high to allow solubilisation during the ethanol dilution of the black liquor. This means only the condensed lignin fragments with cleaved ether bonds are carried through to the water precipitation. In the case of low biomass loadings, a lower degree of condensation allows for a higher number of ether bonds to be intact and still guarantee solubilisation during the ethanol wash.

More similar lignin properties from different solids loadings are however expected if the black liquor does not get diluted with ethanol prior to separation as it will avoid this first “lignin fractionation” we observe where some lignin precipitates onto the pulp surface, and more so at higher loadings. It will however be difficult to separate the black liquor from the pulp at very high solids loadings as most of the IL is within the biomass pores at this point. A filtration at elevated temperature might be able to separate some of the liquid from the pulp.

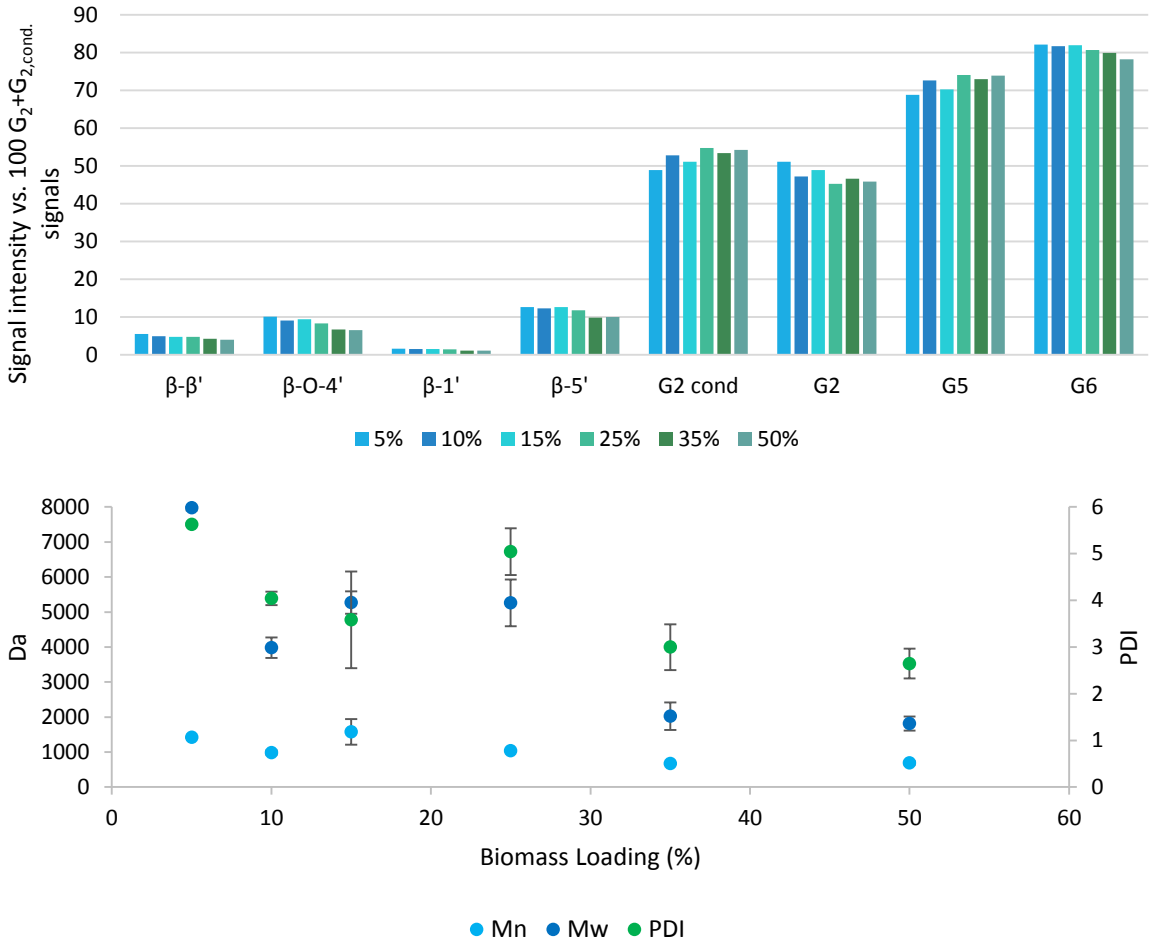

Figure III-48 Analysis of lignin obtained from pretreatment of pine in $[HC_4im][HSO_4]$ with a final water content of 20wt% for 30 min at 170°C with various biomass loadings. Relative signal intensity of major lignin subunits and linkages in the precipitated lignin relative to the combined $G_2/G_{2,cond.}$ volume integral as evidenced by HSQC NMR spectroscopy (top). M_w, M_n and PDI obtained by GPC (bottom).

Effect of Ionic Liquid

Since the pretreatment outcome has been shown to be significantly altered by the identity of the ionic liquid, as seen in the case of pine but also treated timber discussed in two previous chapters (Chapters 2 and 3), and has to some extent been linked to lignin precipitate yield, the isolated lignin of pine pretreated with [DMBA], $[HC_4im]$ and $[TEA][HSO_4]$ for 30 min at 170°C was analysed.

HSQC NMR of the isolated lignins showed a decrease in intact ether bonds in the lignin in the order [TEA]>$[HC_4im]$>[DMBA] with volume integrals for the β-*O*-4' bond of 13.6 vs. 10.4 vs. 6.9 respectively, while condensation, as evidenced by the G_2 and $G_{2,cond.}$ signals, increased in the same fashion (Figure III-49). The [DMBA] lignin can therefore be regarded as the most modified or least native lignin of the three, which indicates that either lignin removal is faster (giving rise to longer lignin residence times in solution) or the lignin reactivity is higher in $[DMBA][HSO_4]$ than in the other two ILs. This is further confirmed by GPC (Table III-26). Pretreatment with $[DMBA][HSO_4]$ led to a lower M_n and a higher M_w than the other two ILs. As a result, a high PDI of 5.1 was found for this IL vs. PDIs of 3.7 and 3.9 for

[TEA] and [HC_4im][HSO_4] respectively. A high PDI is typically not beneficial for lignin applications, however an industrial process would probably only use a small amount of anti-solvent (vs. the three equivalents of water used here), hence selectively precipitating high M_w lignin with a lower PDI. This is the topic of an ongoing research project.

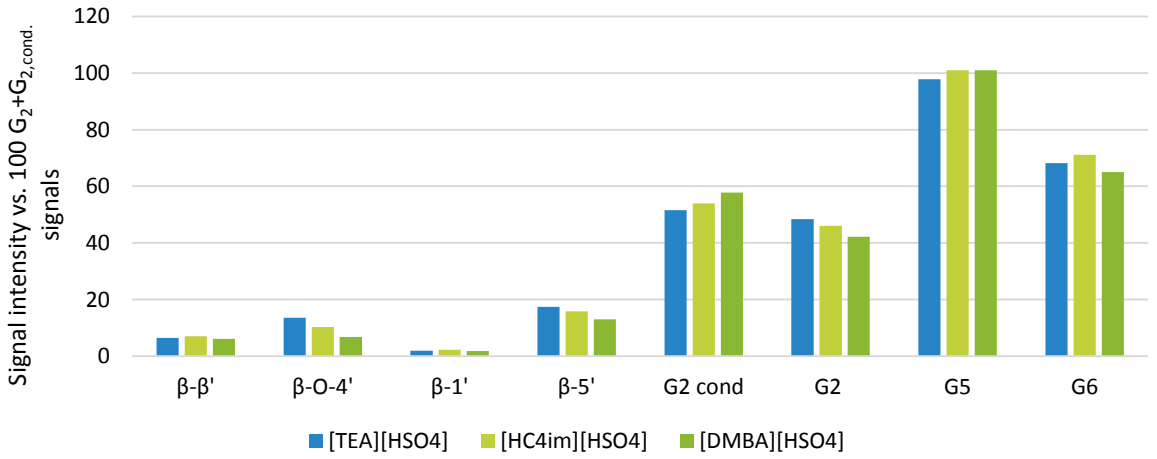

Figure III-49 HSQC NMR results of lignin recovered after pretreatment at 170°C for 30 min with three different [HSO_4] ILs. Pine was pretreated at a solid to solvent ratio of 1:10 g/g and a final water content of 20wt%.

Table III-26 Results from GPC analysis of lignin recovered after pretreatment at 170°C for 30 min with three different [HSO_4] ILs. Pine was pretreated at a solid to solvent ratio of 1:10 g/g.

IL	M_n	M_w	PDI
[TEA][HSO_4]	922	3452	3.7
[HC_4im][HSO_4]	967	3810	3.9
[DMBA][HSO_4]	775	3949	5.1

M_n: Number average molecular weight (Da), M_w: Weight average molecular weight (Da), PDI: Polydispersity index.

Lignin Properties vs. Saccharification Yield: Independent Characteristics?

While these general findings about lignin reactivity are unsurprising, it raises the question of whether certain lignin properties are closely linked to and indicative of high saccharification yields or if there is room for tuning lignin properties while maintaining high glucose yields. Condensation reactions within the lignin structure which result in high M_w lignin have been shown to severely impact sugar yields from pretreated biomass.[20] Therefore, in order to establish whether there is a link, not only between high saccharification yields and the removal of lignin, but also with the specific lignin structure, ^{31}P NMR as well as 2D HSQC NMR was carried out in order to characterise the functional groups present in the isolated *Miscanthus* lignins that were accompanied by saccharification yields exceeding 75% together with selected other lignins for comparison. Gel Permeation Chromatography (GPC) was further used to determine molecular weights of these isolated lignins. In addition, pine lignins obtained under different conditions will be discussed briefly.

Linkages and Subunit Composition

Lignin obtained from two successful (i.e. high glucose yields) and two less successful pretreatments of *Miscanthus* were compared by HSQC NMR. First the two lignins which gave high saccharification yields are compared. Figure III-50 shows the aromatic region, containing the peaks of the G, S, H, PCA and FA aromatic C-H units, and the oxygenated region, containing the ether peaks, of the lignin HSQC spectra of the two successful pretreatments (15 and 30 min pretreatments at 180°C using [TEA][HSO_4] and a final water content of 20wt%). The coloured in HSQC spectra for 15 min and 45 min at 170°C are shown in Figure S65 in the Appendix. Even though both pretreatments had similarly high glucose yields from the isolated pulp, it is obvious from visual inspection of the two spectra that the two lignins differ much with regards to their chemical composition. While after 15 min a high number of ether signals remain, as well as some sugar signals, many ether signals and virtually all of the carbohydrate signals have disappeared after 30 min. In the aromatic region, an increase in the S and G condensed signals and a dramatic decrease in non-condensed G_2 and G_6 can be observed.

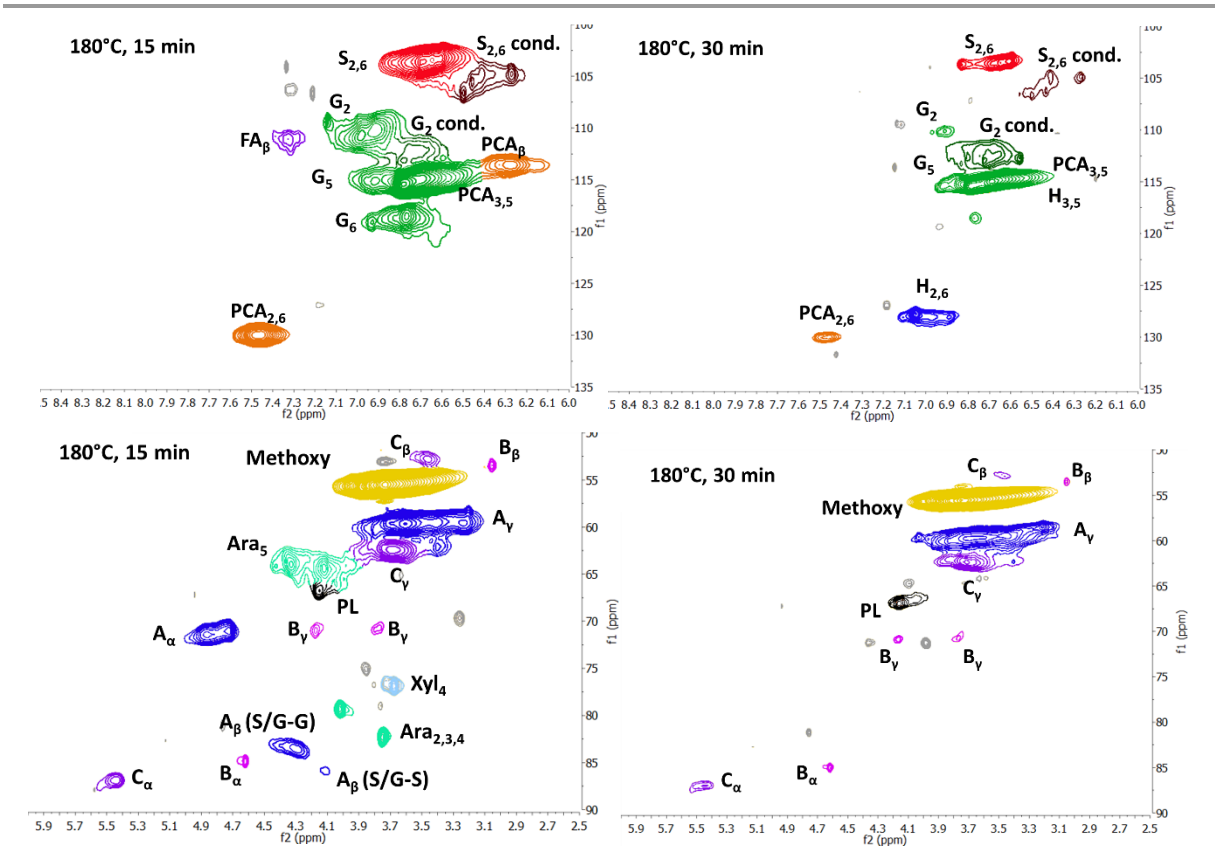

Figure III-50 HSQC NMR spectra of *Miscanthus* lignin isolated after extraction with [TEA][HSO_4] with a biomass to solvent ratio 1:5 g/g and a final water content of 20wt%, aromatic region (left side) and side chain region (right side).

Then, those two lignins are compared to two lignins obtained from less successful conditions. Figure III-51 (top) shows the saccharification yields as well as the signal intensities of the analysed lignin sub-units and ether bonds for the four selected *Miscanthus* lignins obtained after pretreatment with [TEA][HSO_4]: two early lignins (15 min at 170 and 180°C, solid fill in the graph) and two late lignins (45

min at 170°C and 30 min at 180°C, diagonal fill in the graph), one of each isolated after a pretreatment with high (>70%) glucose yields (15 and 30 min at 180°C) while the other two were derived from pretreatments with low (<55%) saccharification yields (15 and 45 min at 170°C). There were indicators for incomplete pretreatment, such as very strong signals for ether bonds, as can be seen in the case of 15 min at 170°C, accompanied by a low saccharification yield of 45%. However, the differences in subunits and ether bonds signals in the HSQC between this lignin (15 min at 170°C) and the lignin after 15 min at 180°C (accompanied by a high saccharification yield of 76%) were less pronounced than the differences between the two lignins accompanied by high saccharification yields. The same was found when comparing more reacted lignins. The most cleaved (and most condensed) lignins in the analysed selection were the lignin isolated after the 30 min pretreatment at 180°C, which yielded around 71% of glucose, and the lignin isolated after the 45 min pretreatment at 170°C, which yielded only 51% of glucose, showing only slight differences in the HSQC spectra, but rather large differences in terms of glucose yields. In other words, two pretreatment conditions might result in similar looking lignins but may have very different glucose release from the cellulose pulp and vice-versa. **Lignin quality is therefore not directly linked to glucose release.**

Furthermore the lignins from pretreatments with high glucose yields such as lignin after 15 min at 180°C had more than twice as strong β-*O*-4' linkage signals compared to lignin isolated after 30 min at 170°C, while the β-5', β-β', $S_{2,6}$, G_6, G_2 and $PCA_{2,6}$ signals were also stronger and $S_{cond.}$, $G_{2,cond.}$ and $H_{2,6}$ were weaker in comparison. Both pretreatment conditions, however, gave high saccharification yields exceeding 70%. This indicates that there is a possibility to adapt pretreatment conditions in a way to obtain high saccharification yields while tuning the degree of ether cleavage and condensation of the lignin, within certain limits.

Time course pretreatments of pine using $[HC_4im][HSO_4]$ at different temperatures showed similar behaviour. Figure III-51 (bottom) shows ether linkage signals and guaiacyl signals for lignin isolated after 30 min at 170°C, 1h at 150°C and 4h at 120°C as well as the lignin precipitate as a percentage of the initial lignin content of the biomass and the saccharification yield. Although the isolated lignins resemble each other in terms of degree of condensation, as evidenced by the abundance of G_5 and G_6 signals, and the number of ether linkages surviving the treatment, lignin and saccharification yields are not mirrored in this. A possible explanation for this observation is that the cleavage of ether linkages and the condensation within the aromatic core are reactions that occur once the lignin is dissolved in the ionic liquid but are not primarily involved in the extraction process of the lignin from the solid into the liquid phase. While the effect of temperature on the rate of ether cleavage and condensation appears to be virtually identical, the rate of lignin extraction appears to be affected

more strongly. Dissolution of biomass, including lignin, in [C_2C_1im][OAc] was observed to be accelerated above the glass-transition temperature of lignin (ca. 150°C), compared to below the glass-transition temperature, by Li *et al.* They reported that complete dissolution of bagasse was achieved in 5-15 min at 175-195°C vs. 15-16 hours at 110°C.[21] It might therefore be possible to extract more lignin and lignin that is less reacted (i.e. more native) by further increasing the temperature.

In conclusion, the findings suggest that lignin may be extracted from the biomass and precipitated out again before it can fully depolymerise and/or condense if a high temperature can be achieved fast enough.

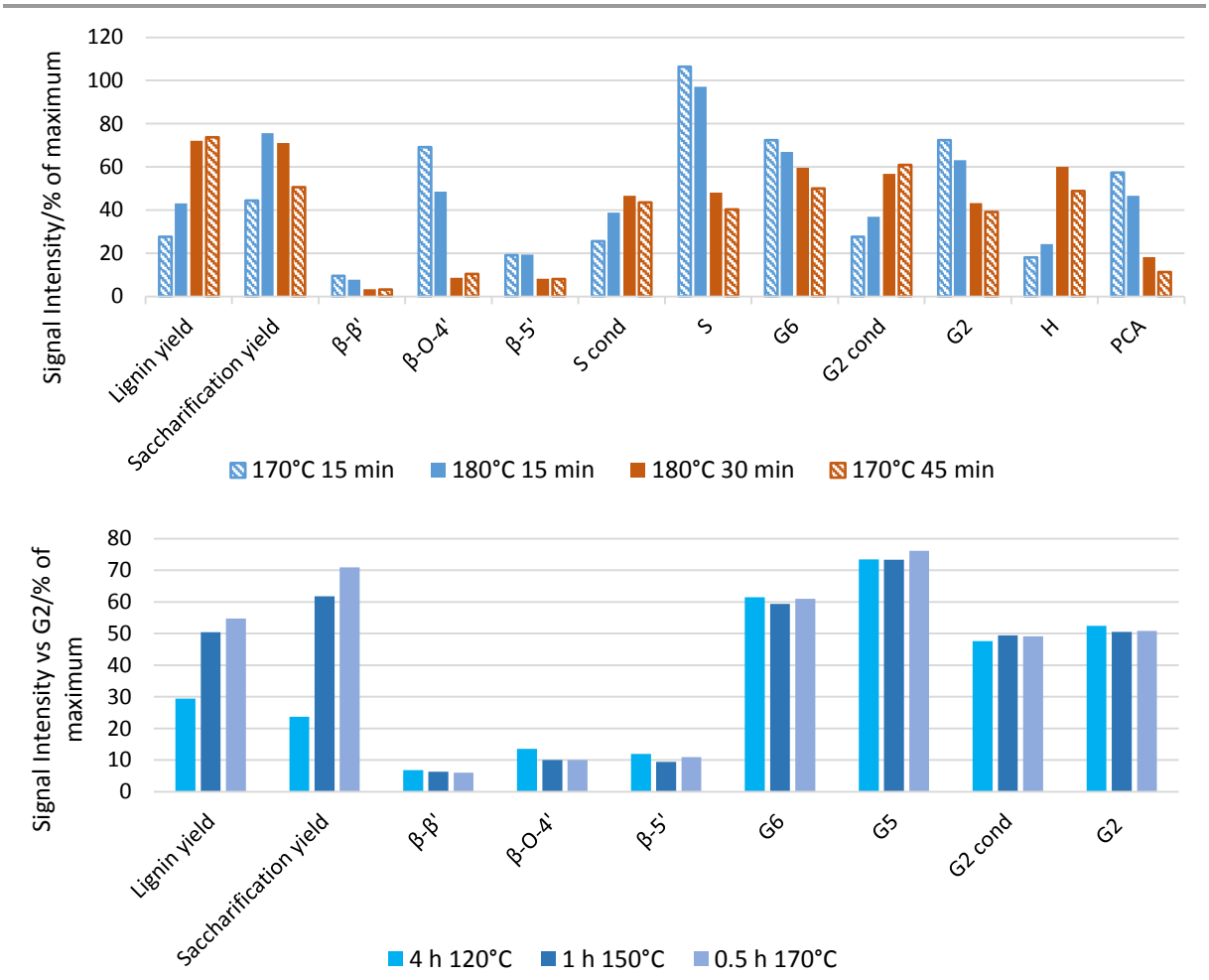

Figure III-51 Relative signal intensity of major lignin subunits and linkages in the precipitated lignin relative to the combined $G_2/G_{2,cond.}$ volume integral as evidenced by HSQC NMR spectroscopy. *Miscanthus* was pretreated with a 1:5 g/g biomass to solvent ratio in [TEA][HSO_4] with a final water content of 20wt% (top). Pine was pretreated with a 1:10 g/g biomass to solvent ratio in [HC_4im][HSO_4] with a final water content of 20wt% (bottom).

Hydroxyl Group Content

Similar to the results obtained with HSQC NMR, there is no clearly observable trend in the number of hydroxyl groups that is indicative for a high saccharification yield. Using ^{31}P NMR to compare the same four selected lignins (15 and 45 min at 170°C and 15 and 30 min at 180°C, displayed in Figure III-52)

that were analysed in detail by HSQC NMR, however, shows that we can see larger differences between the strongly treated lignins (170°C 45 min and 180°C 30 min) than between the less treated lignins (15 min at 170 and 180°C), which are now similar to the differences between the two lignins from successful pretreatment, i.e. the time points at 180°C. The hydroxyl group content might therefore contain strong indicators for over-treatment (high G, S and H hydroxyl group content). Interestingly, comparing the two 30 min time points from the 170 and 180°C pretreatments (also displayed in Figure III-52), it appears that the lignin from the lower temperature has more hydrolysed ether bonds than the one from the higher temperature, since S, G and H hydroxyl groups are more abundant. While it is unclear what the cause of this unexpected observation is, the high content of phenolic –OH groups accompanied by high saccharification yields makes pretreatment for 30 min at an oven temperature of 170°C a promising condition for both lignin and cellulose applications.

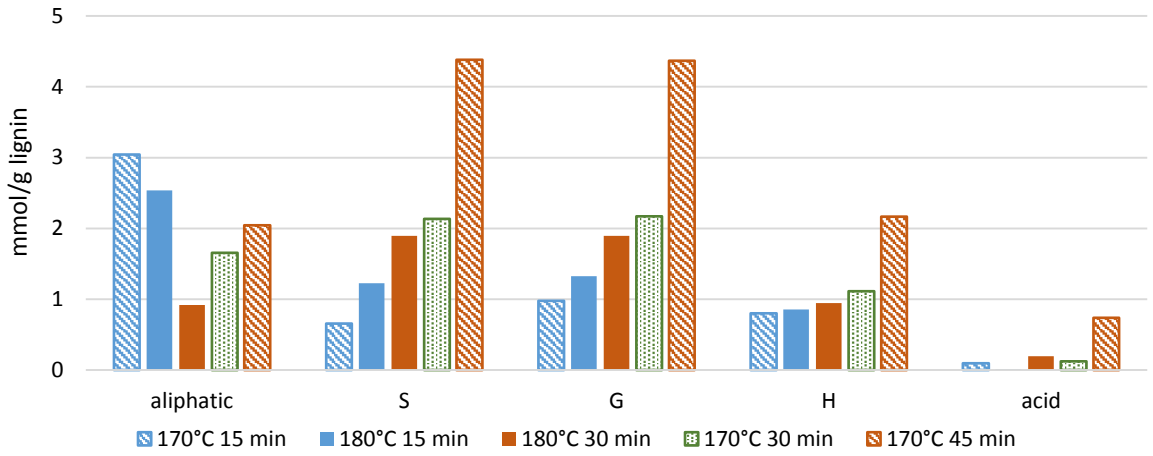

Figure III-52 ^{31}P NMR integrals of phosphitylated lignins converted to mmol of OH per gram of lignin. *Miscanthus* was pretreated in [TEA][HSO_4] with a biomass to solvent ratio of 1:5 g/g and a final water content of 20wt%.

Molecular Weight

In line with the findings from HSQC and ^{31}P NMR analysis, there is no obvious characteristic in the GPC analysis that indicates high saccharification yields, and two lignins with similar characteristics may not necessarily stem from pretreatments leading to similar glucose yields. First, in the focus are two *Miscanthus* lignins which appear almost identical in the GPC analysis, obtained after 30 and 45 min pretreatment at 170°C (Table III-27). GPC analysis revealed an M_n of 948 Da and 937 Da, an M_w of 3395 Da and 3312 Da and a PDI of 3.6 and 3.5 for 30 and 45 min of pretreatment at 170°C respectively, while saccharification yields were 76 and 51% respectively. While it was previously established that M_w is a good marker for residual pulp lignin, it fails to establish whether the residual lignin is native lignin or high M_w condensed lignin, the latter of which has been shown to have a detrimental effect on pulp digestibility and GPC analysis of lignin is therefore largely insufficient to predict pulp digestibility.

Table III-27 Results from GPC analysis of lignin recovered after pretreatment at 170°C [TEA][HSO_4] ILs. *Miscanthus* was pretreated at a solid to solvent ratio of 1:5 g/g.

t (min)	T (°C)	M_n	M_w	PDI	Saccharification yield
30	170	948	3395	3.6	75.7%
45	170	937	3312	3.5	50.5%

M_n: Number average molecular weight (Da); M_w: Weight average weight (Da); PDI: Polydispersity index.

Mixed Feedstocks and Direct Comparison Between Lignins of Different Feedstocks

Pine, *Miscanthus* and beech lignin were isolated under identical conditions and characterised by HSQC NMR alongside lignins obtained from pretreatment of two and all three feedstocks mixed together. Figure III-53 shows the different signal intensities relative to the sum of G_2 signal (sum of condensed and non-condensed) and half the $S_{2,6}$ signal (divided by two to account for two C-H units present in S vs. one in G) for lignin from beech, *Miscanthus* and pine. As one would expect from a hardwood, the beech lignin showed the highest S and $S_{cond.}$ signal intensity of the three tested feedstocks as well as the lowest intensities in all G signals as well as H. Virtually no PCA was detected. As typical for softwoods, the pine lignin had strong signals in all G regions as well as very small signals in both S and H. Similarly to beech, no PCA was detected. *Miscanthus* lignin showed fairly similar signals in S and G_6. Somewhat smaller signals were seen in $S_{cond.}$ and G_2 and $G_{2,cond.}$ The signal in the G_5 area was very strong, presumably due to the overlap with $H_{3,5}$. Both PCA and $H_{2,6}$ were detected. Further, the three types of lignin differed in the abundance of the various ether linkages. The strongest ether signal was in all three cases the β-*O*-4' with the pine lignin giving the strongest signal and *Miscanthus* the weakest. The β-5' linkage was most abundant in the isolated pine lignin and weakest in the beech lignin which is expected from the relative abundance of the different subunits: G rich lignin with a free 5 position is able to form β-5' linkages while S rich lignin, where the 5 position is substituted, forms fewer of these linkages. Beech lignin however showed a relatively large number of β-β' linkages. Lastly, the signal for coniferyl alcohol end-groups was most intense in the case of pine which is in line with the high abundance of G units from which this end-group derives.[22] Table III-28 shows the signal intensities in the S and G_2 condensed areas as a percentage of the total signal as well as the sum of the ether signal intensity for the three different feedstocks (and their combination). While pine lignin has the highest combined intensity of the three ether signals, *Miscanthus* has the highest degree of apparent condensation and the lowest combined intensity of ether signals. Whether the *Miscanthus* lignin is therefore the most reacted of the three is however difficult to tell, since that would require a comparison to their respective native forms.

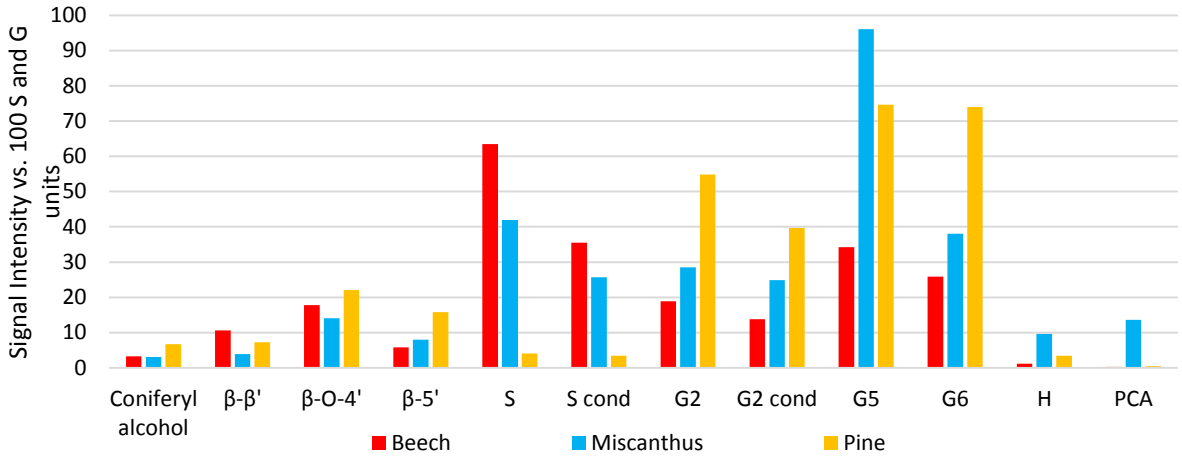

Figure III-53 HSQC NMR results of lignin recovered after pretreatment of different feedstocks at 170°C for 30 min with $[HC_4im][HSO_4]$ with a biomass to solvent ratio of 1:10 g/g and a final water content of 20wt%.

The lignins from mixed feedstock pretreatments were analysed in the same manner and compared to the lignins of the two individual species as well as to the calculated average. The data are displayed in Figure III-54 and Table III-28. Pine-beech lignin matches more or less the calculated average of pine and beech with respect to ether bonds and condensation, but has a slightly higher S signal and lower G signals. The same is true for pine-*Miscanthus* lignin. The beech-*Miscanthus* lignin on the other hand appears to be more reacted than the calculated average with a higher signal intensity in $S_{cond.}$, $G_{2,cond.}$ and H and a lower signal intensity for all the ether bonds as well as well as for PCA, G_2 and S.

Since the three feedstocks differ significantly in their S content and therefore the signal intensity of $S_{2,6}$, this peak was used as an estimate for the relative shares of the different feedstocks in the precipitated lignins from mixed feedstocks. As discussed in Chapter 2, the lignin precipitate yield was in all cases higher than the yields of the separate feedstocks or their average. The relative shares of the different lignins were therefore used to estimate to what extent lignin recovery was improved for which lignin type. Lignin precipitate from only beech was relatively low at 8.9% of initial biomass weight while pine lignin gave around 11.5% and pine-beech lignin gave 12.1%. From the S signal of the three lignins pine, beech and pine-beech we can estimate that the pine-beech lignin is around 57% beech and 43% pine. From this we can calculate an improvement of 56% for the recovery of beech lignin while pine lignin recovery went down by 9%. Pine-*Miscanthus* lignin similarly contained around 56% of *Miscanthus* and 44% pine lignin. Here, pine lignin recovery improved by 28% and *Miscanthus* lignin recovery by 32%. Beech-*Miscanthus* lignin consisted of 55% *Miscanthus* and 45% beech lignin and lignin recoveries were improved by 62 and 21% for beech and *Miscanthus* respectively. In order to estimate the share of the different lignins in the lignin isolated from all three feedstocks mixed together, also the H signal was taken into consideration. Solving the linear equations using the S and

H volume integrals we obtain a composition of 26% beech, 36% *Miscanthus* and 38% pine where the lignin recoveries were improved by 83, 12 and 42% respectively.

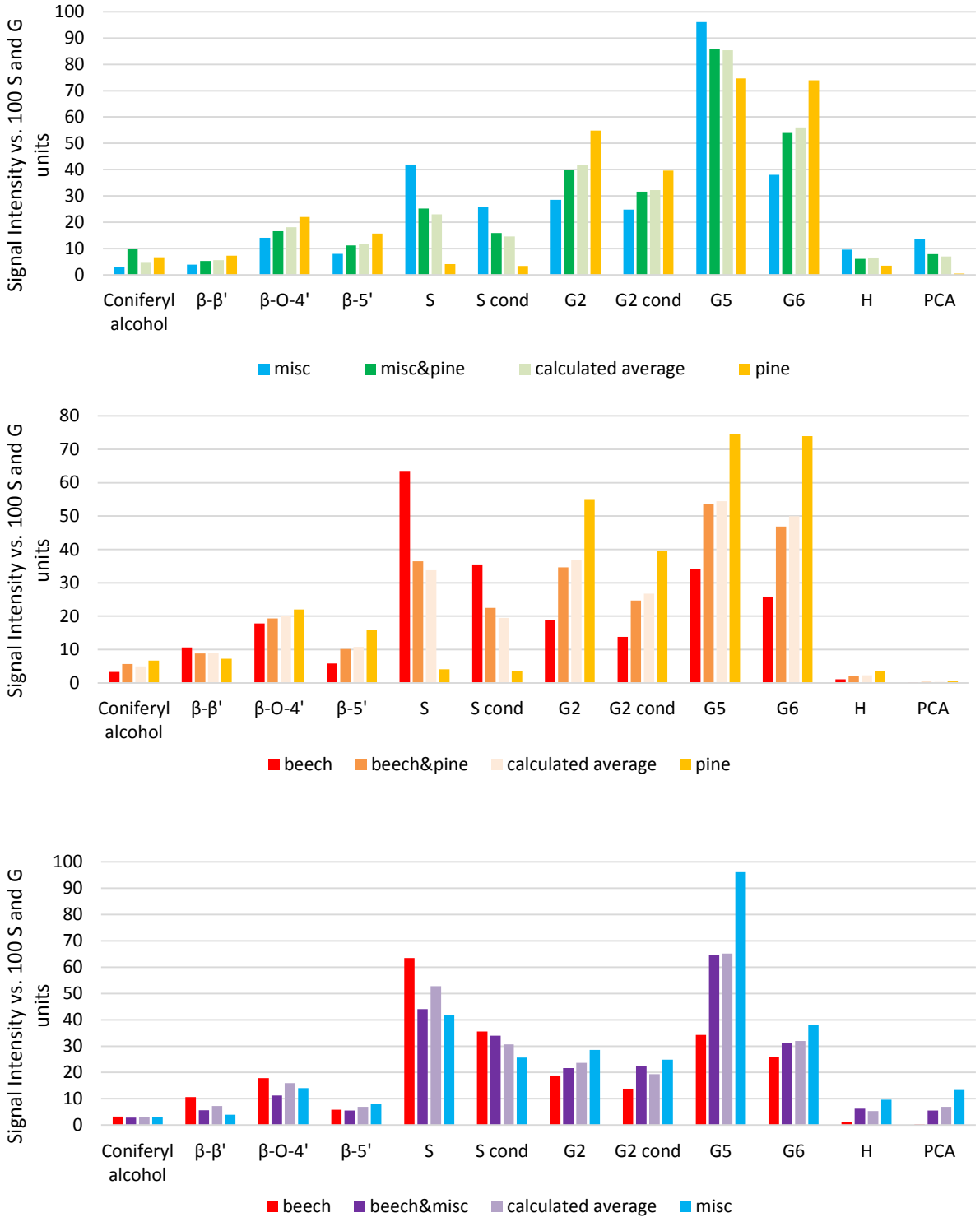

Figure III-54 HSQC NMR results of lignin recovered after pretreatment of *Miscanthus,* pine and their mix (top), beech, pine and their mix (middle) and beech, *Miscanthus* and their mix (bottom). All pretreatments were carried out at 170°C for 30 min with $[HC_4im][HSO_4]$ with a biomass to solvent ratio of 1:10 g/g and a final water content of 20wt%.

Most remarkably in this data set is the improved lignin recovery for beech in the presence of other lignins. Hardwood lignin, being rich in S, typically results in only very little crosslinking, quite possibly resulting in a large fraction of small lignin fragments which stay dissolved upon anti-solvent addition (44% of initial biomass weight was lost to the liquor during beech pretreatment vs. 41% for *Miscanthus* and 35% for pine). It is hypothesised that beech lignin might therefore get incorporated more readily into higher molecular weight fragments if fragments with a higher G content are present since they crosslink more easily than S rich fragments. The reason why pine lignin recovery decreased in the presence of beech lignin however is unclear. A lower chance of producing relatively large, condensed lignins and a higher chance of producing water soluble small fragments as a result of some radical scavenger ability of S-rich beech lignin might be a possible explanation. Similarly, the higher lignin yields were in all cases also accompanied by lower pulp yields, indicating that less lignin reprecitiated onto the pulp surface which, again, might stem from less high molecular weight lignin being formed if a combination of S rich and G rich lignin is present.

Table III-28 HSQC NMR results of lignin recovered after pretreatment of *Miscanthus,* pine, beech and their mix. All pretreatments were carried out at 170°C for 30 min with $[HC_4im][HSO_4]$ with a biomass to solvent ratio of 1:10 g/g and a final water content of 20wt%. Expected average in brackets.

	S_{cond}/total S	$G_{2,cond}$/total G_2	Sum of ether bonds[a]
Beech	36%	42%	34
Miscanthus	38%	47%	26
Pine	N/A	42%	45
Beech & *misc.*	44% (37%)	51% (45%)	22 (30)
Beech & pine	38% (37%)	42% (42%)	38 (40)
Misc. & pine	39% (39%)	44% (44%)	33 (36)
Beech, *misc.* & pine	41% (37%)	46% (43%)	28 (35)

Misc: Miscanthus; S: syringyl; G: guaiacyl; [a]Sum of β-*O*-4', β-5' and β-β' α signals.

While this shows that combining feedstocks results in interesting lignin chemistry it should be noted that the shares of the different lignin types are likely to be different upon recycling of the ionic liquid. Therefore, no conclusions should be drawn from this about the lignin properties which can be expected from a mixed feedstock system under steady state.

Lignin during Recycling

While all the above results give insight into the lignin chemistry occurring during pretreatment, they do not necessarily translate to the lignin obtained from a steady state process. Since the lignin recovery through precipitation after pretreatment with fresh IL generally lies below the measured

delignification under favourable conditions (i.e. conditions which give high glucose yields), there are some lignin fragments still in solution which will be present at the beginning of the next cycle. HSQC NMR was therefore used to analyse the lignin obtained after 6 cycles of pretreatment of CCA treated softwood with the same [HC_1im]Cl solution and compared it to the lignins obtained after the first cycle (i.e. fresh IL) and second cycle (i.e. first recycle). The results are displayed in Figure III-55. The data indicate that recycling of the IL has a similar effect on lignin properties as we have seen for prolonging of the pretreatment. Indeed, part of the lignin precipitating from the liquor at the second cycle will have been in the IL for two cycles, but was in the form of water soluble fragments after the first cycle. Precipitating after the second cycle, those fragments are likely to have had their ether bonds broken and a significant amount of condensation between aromatic units, resulting in a decreased signal intensity in the ether and G_2 areas, and an increase in signal in $G_{2,cond.}$ The same, but in a more pronounced way, can be observed for lignin precipitated after cycle 6. Especially the signal intensity for β-*O*-4' and G_6 have changed significantly between cycles 2 and 6, potentially an indication that lignin fragments can spend several cycles in the IL before precipitating. The G_5 signal remained relatively stable, quite likely again indicating that the incorporation of carbohydrate degradation products increases signal intensity in this area while the condensation occurring in G_5 decreases it in a complementary fashion.

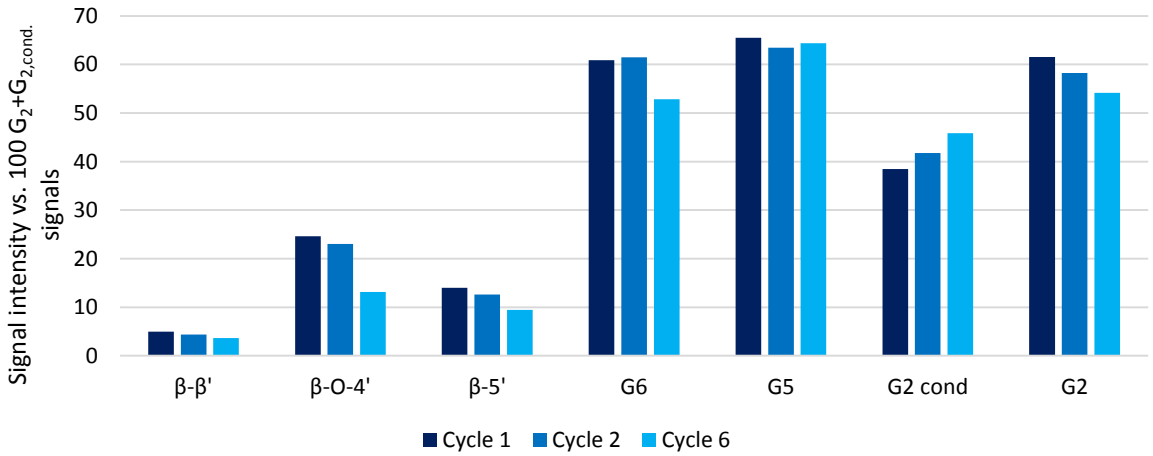

Figure III-55 HSQC NMR results of lignin recovered after pretreatment of CCA treated softwood at 170°C for 30 min with fresh, recycled and 5 times recycled [HC_1im]Cl with a biomass to solvent ratio of 1:5 g/g and a final water content of 20wt%.

Formation of Ethanol Insoluble Lignin

In order to keep energy costs during the eventual process low, ethanol was investigated as a potential alternative to water for the lignin precipitation since it has a lower boiling point and a lower latent heat of vaporisation. Ethanol is used as the wash solvent for the pulp in the regular protocol, without resulting in precipitation of much lignin. However, we have seen evidence that some lignin is

precipitated during this ethanol dilution step. In a larger scale process, separation of pulp and black liquor would ideally be carried out without the need for dilution of the liquor, and lignin precipitation at this stage should therefore be minimal. Furthermore, additional cooking of the black liquor, after the pulp has been removed, could result in a higher amount of lignin fragments which are insoluble in ethanol. This was tested after pretreatment of tanalised timber with [DMBA][HSO_4] for 30 min at 170°C. Figure III-56 shows the ethanol insoluble lignin (EIL) obtained after one, two and three cooks of the black liquor for 1 hour at 170°C. For comparison, the water insoluble lignin (WIL) after just the regular pretreatment using the normal lignin precipitation protocol is also shown. As can be seen, there is indeed lignin precipitating out by adding ethanol. It should be noted that a "zero-th" EIL is included in the pulp yield. EIL yields decreased from 5.6, to 3.9 to 1.7% with respect to initial biomass weight, giving a total of 11.2% EIL from the initial biomass after three cycles of 1 hour at 170°C. For comparison, WIL after just the pretreatment was 18.6%. This suggests that ethanol may be a suitable anti-solvent for lignin precipitation but would require extensive heating of the black liquor in order to achieve similar yields to water. Additionally, the lignin properties will be strongly affected. Also, there might be other antisolvents with a low heat of vaporisation but also lower lignin solvation power.

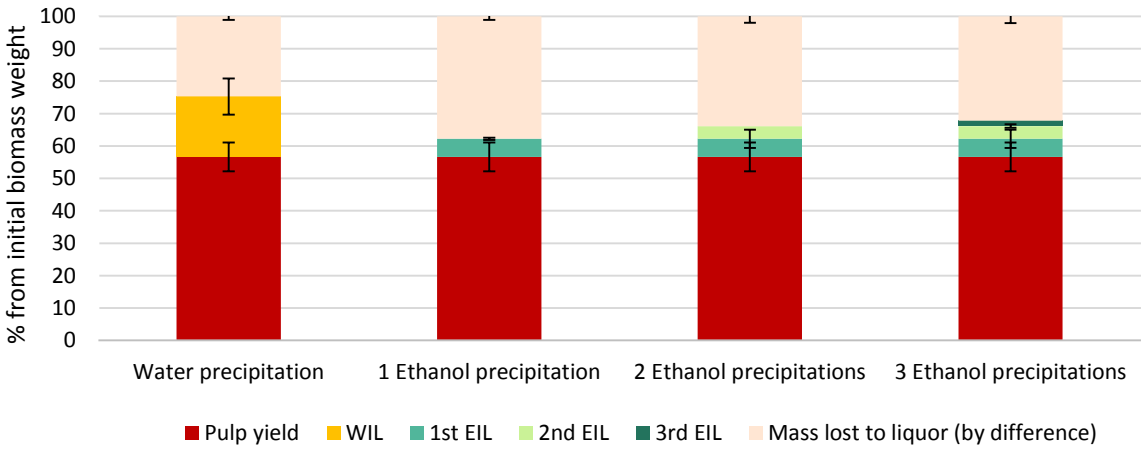

Figure III-56 Solid fractions recovered after pretreatment. Tanalised timber was pretreated for 30 min with [DMBA][HSO_4] at 170°C with a biomass to solvent ratio of 1:5 g/g and a final water content of 20wt%. The black liquor was collected and split evenly. To half of it, 3 eq. (vol.) water were added to precipitate water insoluble lignin (WIL). The other half was heated again to 170°C and ethanol added to precipitate ethanol insoluble lignin (EIL). The ethanol was removed and this step repeated twice more. Standard errors were calculated for triplicate measurements.

Solutes in the Ionic Liquid Solutions

Compositional analysis of the pulp, as discussed in Chapters 1 and 2, shows that the hemicelluloses are extracted from the biomass and dissolve into the ionic liquid over time during pretreatment. At early stages of pretreatment some carbohydrate signals can also be detected in the lignin precipitate when subjected to HSQC NMR while at later times carbohydrate degradation products are suspected to be the cause of the apparent increase in signal intensity of the lignin G_5 signal. Xylose and arabinose are capable of dehydrating to furfural under acidic conditions (Figure I-7), and glucose and galactose

to 5-hydroxymethylfurfural (HMF) (Figure I-6). Furfural is an interesting biorefinery product that has a high value today, albeit in a limited and mature market. It can be converted into a number of other products such as fuels, solvents and fine chemicals,[23] which will become especially attractive if the furfural can be produced at lower cost than is possible with current processes.

I hence analysed the ionic liquid solutions by HPLC for glucose, arabinose and other hemicellulose monomers (xylose, galactose and mannose unfortunately elute together in this HPLC method), acetic and formic acid, the pentose and hexose dehydration products furfural and HMF, and the HMF hydrolysis product levulinic acid (Figure III-57).

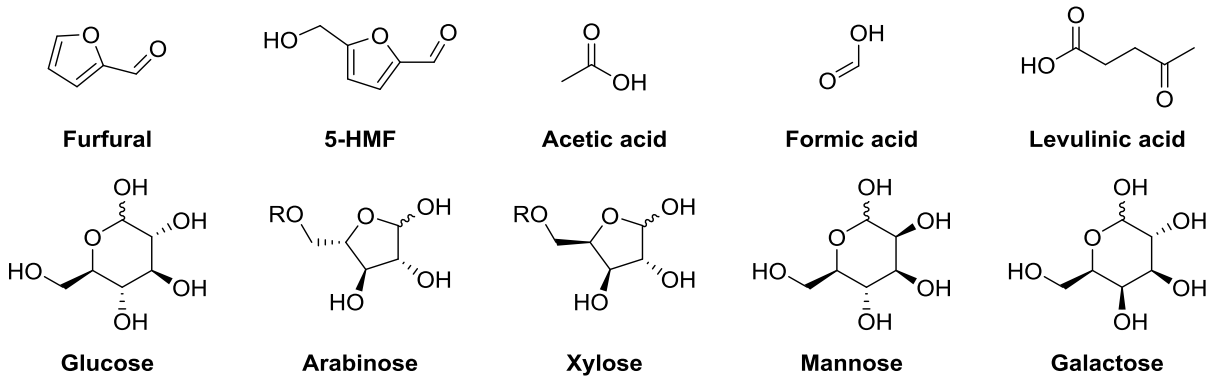

Figure III-57 Solutes in the IL analysed by HPLC.

Miscanthus Time Course 120°C

As mentioned earlier, *Miscanthus* hemicelluloses are composed predominantly of arabinoxylans. The eluent peak of xylose/mannose/galactose was therefore attributed exclusively to xylose. Figure III-58 shows the amount of solutes detected in the black liquor (i.e. the ionic liquid solution directly after pretreatment) as treatment of *Miscanthus* with [TEA][HSO_4] progressed at 120°C. Until 4 h, an increasing proportion of the hemicellulose was detected in the liquid phase, in the form of arabinose and xylose. The amount of xylose detected in the liquor at 4 h was around 10% of the total biomass and *ca.* 50% of the xylan in untreated *Miscanthus*. This maximum coincided with xylan content in the pulp becoming limited for enzymatic release of xylose. The decreasing xylose concentrations in the IL solution after 4 h was due to more xylose being consumed in dehydration and other side reactions than xylan dissolving into the ionic liquid solution and hydrolysing.

The furfural content increased until 12 h and then stabilized, indicating that furfural is reacting further, potentially to polymeric products,[24] and that production of furfural and transformation of furfural into other products were balanced during the second half of the time course. Incorporation of hemicellulose derived products into the lignin has been suggested above to explain an increase in signal intensity in the HSQC spectra of harshly treated lignins in the G_5 area which has been found to

overlap with hemicellulose derived pseudo-lignin. Figure III-58 further shows that another major solute in the ionic liquid solutions was acetic acid. The acetic acid concentration increased in the first 4 h and subsequently remained stable over time. Once the concentration stabilised, roughly 4.5% of the initial biomass weight was detected as acetic acid. This tallies well with the acetic acid content in the untreated *Miscanthus* as determined by compositional analysis (which was 4.4%, analysis carried out by Dr Agi Brandt) suggesting that essentially all of the acetic acid ends up dissolved in the [TEA][HSO_4] solution.

It is noteworthy that only small quantities of glucose, traces of HMF and no levulinic acid were detected in the ionic liquid solution after *Miscanthus* pretreatment. The small amounts of glucose in the liquor compared to xylose agree with the high retention of glucan in the cellulose-rich pulp. As there was some loss of glucose from the pulp over time, the stable glucose content in the ionic liquid solution suggests that glucose reacts to form HMF and other products. HMF formation from C6 sugars via isomerisation to fructose and subsequent dehydration in [HSO_4] ionic liquids has been reported by Eminov *et al.*[25] In the liquors from the present study the amount of HMF increased slightly with pretreatment time; nevertheless the stable HMF concentration indicates that the rate of HMF formation was approximately equal to the rate of its conversion into further degradation products. Since levulinic acid was not detected, the major pathway of HMF reactivity in the IL solution appears to be humin formation with certain biomass components, consistent with the absence of levulinic acid formation from HMF in hydrogen sulfate ionic liquids previously reported by Eminov *et al.*[26]

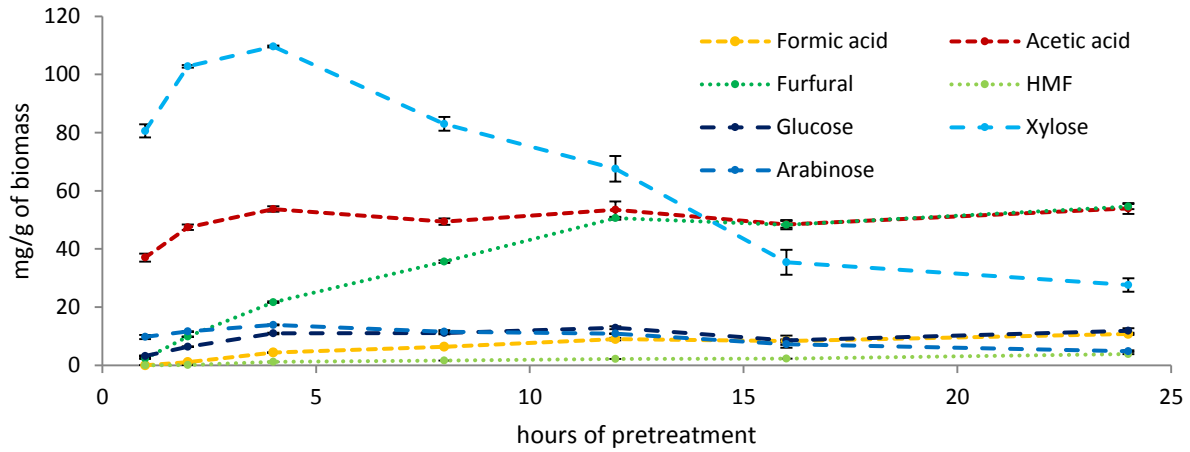

Figure III-58 Time course of solutes found in the black liquor as analysed by HPLC. *Miscanthus* was pretreated with [TEA][HSO_4] at 120°C with a biomass to solvent ratio of 1:10 g/g and a final water content of 20wt%. Standard errors were calculated for triplicate measurements.

HPLC analysis of the ionic liquid solution after lignin precipitation and drying of the ionic liquid (brown liquor) was also carried out (Figure S66 shown in the Appendix). The analysis revealed that the furfural and acetic acid were removed completely during work-up. It is speculated that the removal of the volatile fraction from the ionic liquid happens during concentration of the ethanol ionic liquid washes

and during removal of water after lignin precipitation. The amount of sugar monomers found in the reconstituted solution, in particular xylose, was very similar to the fraction of sugar monomers found directly after pretreatment, suggesting that the lignin isolation and the subsequent drying do not dehydrate or otherwise alter the dissolved sugar monomers. It should however be noted that the lab-scale protocol uses vacuum and only mild heating to no more than 40°C to remove wash ethanol and water. In an industrial setting on the other hand it is expected that no vacuum and higher temperatures would be used in order to remove the water used for lignin precipitation which is likely to result in some reactions between the remaining solutes.

Softwoods

As seen earlier, softwood hemicelluloses are composed of a large fraction of galactoglucomannans giving rise to C6 sugars when hydrolysed. Unfortunately, since the HPLC method used in our lab does not separate galactose, mannose and xylose, these three sugars have to be considered together. As discussed for the case of *Miscanthus*, C6 sugars dehydrate to HMF, which can, but has not been observed to, further react to levulinic and formic acid.[26] Data obtained from virgin pine as well as metal preservatives containing timber is discussed in the following paragraphs.

Trace metals and ILs

Different heavy metals have been reported to catalyse the dehydration reactions of sugars to HMF and other compounds. Therefore, the effect of heavy metals on the liquor composition was investigated and the liquor of four different pretreatments were analysed: $[HC_4im][HSO_4]$ liquors after pretreatment of CCA treated wood and virgin pine and liquors of $[HC_1im]Cl$ and $[DMBA][HSO_4]$ after pretreatment of copper azole (CA) treated timber (all 30 min at 170°C with 10% biomass loading). Yields in mmol/g of biomass are displayed in Figure III-59. Taking the compositional analysis of the different biomass feedstocks into account, also the percentage yield relative to the content of the originating species in the initial biomass was calculated and is displayed in Table III-29. It should be noted that the here analysed liquors were isolated after lignin isolation and water removal (brown liquor), therefore no furfural or acetic or formic acid was detected.

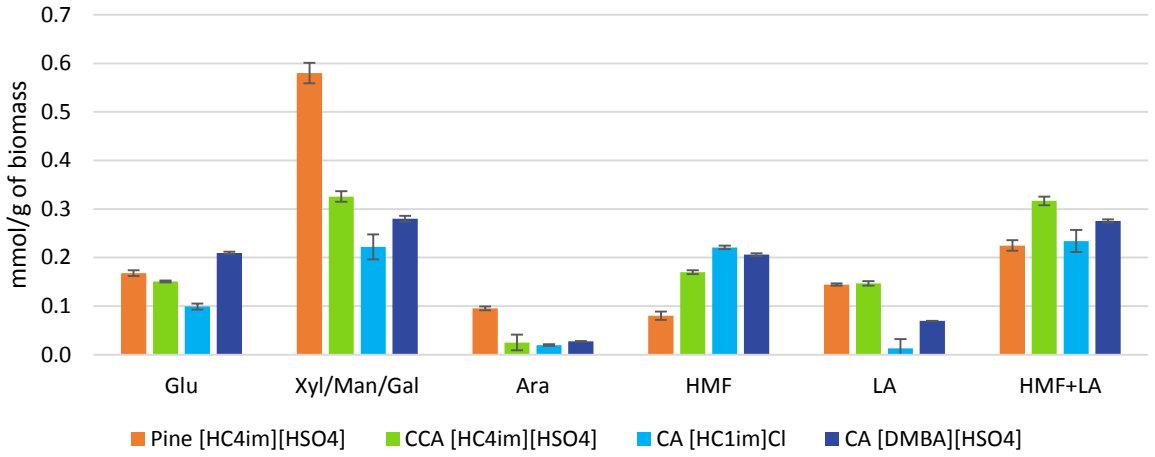

Figure III-59 Solutes found in the brown liquor as analysed by HPLC. Softwood feedstocks were pretreated at a 1:10 g/g biomass to solvent ratio in IL with a final water content of 20% for 30 min at 170°C. Glu: glucose; Xyl/Man/Gal: xylose/mannose/galactose; Ara: arabinose; LA: levulinic acid. Standard errors were calculated for triplicate measurements.

In all cases, some glucose (0.10-0.21 mmol/g of biomass) as well as xylose/galactose/mannose (0.25-0.66 mmol/g of biomass) and HMF were observed. The amount of arabinose detected, although present in only small amounts, corresponded to 74-100% of arabinose present in the initial biomass. More HMF (0.17-0.21 mmol/g of biomass) was observed after pretreatment of the metal containing feedstocks CCA and CA treated softwood compared to virgin pine (0.08 mmol/g of biomass). Unlike for the case of *Miscanthus*, LA was also detected (up to 0.15 mmol/g of biomass), possibly as a result of the higher HMF concentration, which is likely to stem from the higher amount of C6 hemicelluloses present in softwoods.[11,27] The highest HMF yields of 0.22 and 0.21 mmol/g of biomass were obtained from CA treated wood, pretreated with $[HC_1im]Cl$ and $[DMBA][HSO_4]$ respectively. Zhao and co-workers have in the past shown improved HMF yields from fructose and glucose in $[C_2C_1im]Cl$ in the presence of various metal salts, including $CuCl_2$,[28] so it is conceivable that the copper preservative present in the biomass catalysed the conversion of dissolved C6 sugars to HMF, albeit being present in a much lower concentration than the metal salt catalysts studied. LA yields from CA treated wood were very low in $[HC_1im]Cl$ compared to $[DMBA][HSO_4]$. Zhao *et al.* have also shown that HMF stability was increased by the addition of metal salts or mineral acids.[28] Whether the improved stability of HMF in $[HC_1im]Cl$ observed here is a result of the chloride anion interacting with the copper from the wood preservative or an effect of the cation (e.g. π-π stacking) is however unclear.

While Eminov and co-workers did not detect HMF from cellulose in $[C_4C_1im][HSO_4]$ without metal salt catalyst,[29] here 0.08 and 0.14 mmol/g of biomass of HMF and LA respectively were detected after pretreatment of virgin pine with the more acidic $[HC_4im][HSO_4]$. LA yields were very similar for both virgin pine (0.14) and CCA treated wood (0.15) in $[HC_4im][HSO_4]$. Comparisons made between these experiments should however be considered carefully since differences in yields might be due to

variation in the feedstock rather than an effect of the presence or absence of metal salts. Nevertheless it shows that HMF and LA formation is possible in the absence of both relatively high amounts of metal salts as well as chloride anions. Furthermore, taking the original composition of the two feedstocks into consideration around 2.3 and 4.7% of C6 sugars (glucan, mannan, galactan combined) are found as HMF in the case of virgin pine and CCA treated wood respectively and 4.1% as LA in both cases.

Despite the differences in HMF to LA conversion, the sum of LA and HMF was relatively constant across the analysed samples and was between 0.22 and 0.32 mmol/g of biomass, accounting for 6.0 to 8.8% of the initial C6 content. Much larger differences can be observed in the amount of hemicellulosic sugars present, with the most hemicelluloses found as dissolved monomers in the case of virgin pine (almost 100% of arabinose and 50% of xylose/mannose/galactose). It is unclear whether this stems from differences in the hemicellulose composition or if hemicellulosic sugars are less stable in the presence of trace metals and more readily form humins. It should also be noted that no significant differences can be seen in the lignin NMR which therefore have not been discussed in detail.

Table III-29 Solutes analysed in the brown liquor expressed as percentage of their originating biomass component as analysed by compositional analysis. Xylose, mannose and arabinose were assumed to be represented in the same relative amounts as in the original biomass. Softwood feedstocks were pretreated at a 1:10 g/g biomass to solvent ratio in IL with a final water content of 20% for 30 min at 170°C.

Feedstock	IL	Glu	Xyl/Man/Gal	Ara	HMF	LA	HMF+LA
CCA	$[HC_4im][HSO_4]$	5.6%	24.8%	83.5%	4.7%	4.1%	8.8%
Pine	$[HC_4im][HSO_4]$	6.3%	49.4%	98.4%	2.3%	4.1%	6.3%
CA	$[HC_1im]Cl$	3.4%	16.2%	73.5%	5.7%	0.3%	6.0%
CA	$[DMBA][HSO_4]$	7.2%	20.4%	101.5%	5.3%	1.8%	7.1%

Glu: glucose; Xyl/Man/Gal: xylose/mannose/galactos; Ara: arabinose

Recycling

While the *Miscanthus* time course data give a good picture about which solutes are present at which stage of the pretreatment if starting from fresh IL, only limited information can be drawn from it that would apply to a process where the IL is recycled. For this exercise, the brown liquor was first analysed after a pretreatment of tanalised timber with fresh ionic liquid. Half of the resulting brown liquor was taken and cooked again for 1 hour at 170°C, additional lignin was precipitated, and the liquor analysed again thereafter. Then both, the original brown liquor and the recooked brown liquor, were recycled for a second round of pretreatment. The resulting brown liquors were analysed as well. The data are displayed in Figure III-60. The numbers are displayed in mg per g of IL for the ease of comparing recycled ILs to fresh ILs and in order to identify the potential build-up of one or several solutes. We can see that the contents of all sugars decreased drastically by recooking the brown liquor. The HMF concentration remained stable and LA concentration increased, however not by enough to account

for all the sugar that was consumed, suggesting that there are alternative sugar degradation pathways, likely including humin formation. Furthermore the LA content did not increase further after a second round of pretreatment. This indicates that we are not expecting LA to accumulate in the IL over several cycles but that it further reacts. HMF content after the second cycle was lower if the IL was cooked in between cycles, likely due to the intermediate cook consuming most of the dissolved sugars present. Interestingly, the sugar content in the IL was lower after the second cycle with an intermediate cook than after the first cycle. Possible explanations are that the recycled and recooked IL is less effective at extracting and/or hydrolysing hemicelluloses than the fresh or normally recycled IL, or that the intermediate cook results in the formation of species that readily react with monomeric sugars to from compounds that are not detected here and may include humins/pseudo-lignin. In conclusion**, no single analysed solute appears to accumulate over these initial cycles**. This indicates that no deterioration is expected after more cycles, potentially making ionoSolv pretreatment a self-cleaning and sturdy process.

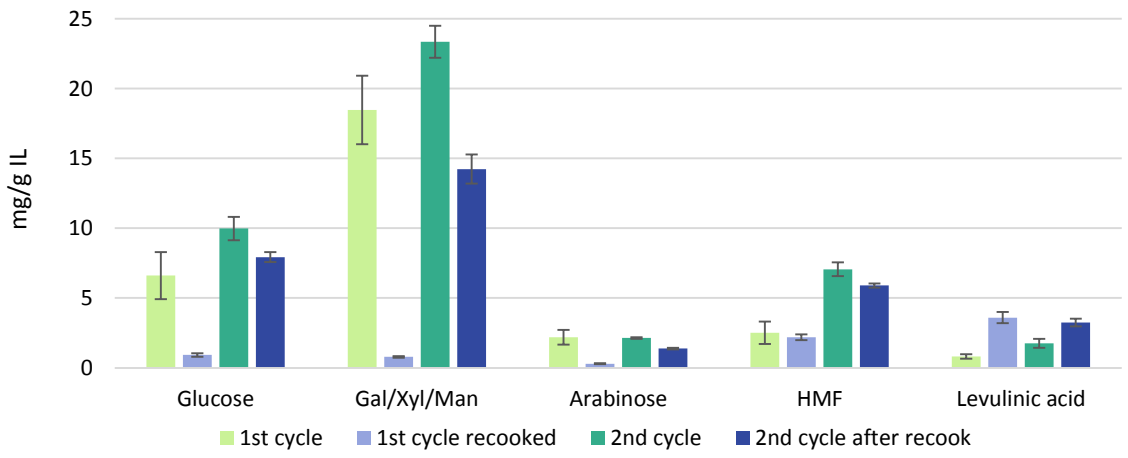

Figure III-60 Solutes found in the brown liquor as evidenced by HPLC analysis. Tanalised timber was pretreated for 30 min with [DMBA][HSO_4] at 170°C with a biomass to solvent ratio of 1:5 g/g and a final water content of 20wt%. Where the liquor was recooked, that was carried out at the brown liquor stage for 1 h at 170°C, followed by lignin precipitation.

Conclusions

New insights into lignin chemistry occurring during ionoSolv process have been gained through this project. General trends were identified or further confirmed. Information gained from GPC analysis has been found to be the best indicator for lignin extraction, yet no lignin characteristic has been found to be indicative of the digestibility of the pulp isolated alongside. Additionally, the importance of temperature to decouple lignin extraction and lignin modification was highlighted. This makes it possible to potentially tune the pretreatment conditions to obtain lignin for a certain application while maintaining high pulp quality.

Lignins of different feedstocks were studied and a synergistic effect was found for lignin recovery. This makes ionoSolv pretreatment especially interesting for applications where various feedstocks are processed together. Lastly, the dissolved hemicelluloses and their degradation products were studied. The findings suggest that furfural from C5 sugars and acetic acid could be valuable by-products obtained from the process. HMF and levulinic acid derived from C6 sugars were found after pretreatment of softwoods, especially in the presence of trace heavy metals. However, none of the studied molecules appear to accumulate in the IL over several cycles, indicating that ionoSolv pretreatment is a potentially robust process not requiring solvent reconditioning. While the isolation of HMF from the IL will be very challenging and is most likely not going to be viable as part of the pretreatment process, this opens up the possibility to use a modified version of this protocol for the specific production of HMF and its further conversion to a product that is more easily isolated, e.g. furan dicarboxylic acid.

References

1 J. P. M. Sanders, J. H. Clark, G. J. Harmsen, H. J. Heeres, J. J. Heijnen, S. R. A. Kersten, W. P. M. van Swaaij and J. A. Moulijn, *Chem. Eng. Process. Process Intensif.*, 2012, **51**, 117–136.

2 H. Yang, Y. Xie, X. Zheng, Y. Pu, F. Huang, X. Meng, W. Wu, A. Ragauskas and L. Yao, *Bioresour. Technol.*, 2016, **207**, 361–369.

3 F. Hu, S. Jung and A. Ragauskas, *ACS Sustain. Chem. Eng.*, 2013, **1**, 62–65.

4 M. Sette, R. Wechselberger and C. Crestini, *Chemistry*, 2011, **17**, 9529–35.

5 C. Crestini, F. Melone, M. Sette and R. Saladino, *Biomacromolecules*, 2011, **12**, 3928–3935.

6 Q. Sun, Y. Pu, X. Meng, T. Wells and A. J. Ragauskas, *ACS Sustain. Chem. Eng.*, 2015, **3**, 2203–2210.

7 J. Ralph and L. Landucci, in *Lignin and Lignans*, CRC Press, 2010, pp. 137–243.

8 K. A. Y. Koivu, H. Sadeghifar, P. A. Nousiainen, D. S. Argyropoulos and J. Sipilä, *ACS Sustain. Chem. Eng.*, 2016, **4**, 5238–5247.

9 R. Pettersen, *The Chemistry of Solid Wood*, American Chemical Society, Washington, DC, 1984, vol. 207.

10 M. Normark, S. Winestrand, T. a Lestander and L. J. Jönsson, *BMC Biotechnol.*, 2014, **14**, 20.

11 T. E. Timell, *Wood Sci. Technol.*, 1967, **1**, 45–70.

12 M. Yoshida, Y. Liu, S. Uchida, K. Kawarada, Y. Ukagami, H. Ichinose, S. Kaneko and K. Fukuda, *Biosci. Biotechnol. Biochem.*, 2008, **72**, 805–810.

13 N. Brosse, A. Dufour, X. Meng, Q. Sun and A. Ragauskas, *Biofuels, Bioprod. Biorefining*, 2012, **6**, 580–598.

14 A. Brandt, F. Gschwend, P. Fennell, T. Lammens, B. Tan, J. Weale and J. Hallett, *Green Chem.*, 2017, DOI: 10.1039/C7GC00705A.

15 A. Brandt, L. Chen, B. E. van Dongen, T. Welton and J. P. Hallett, *Green Chem.*, 2015, **17**, 5019–5034.

16 N. Sathitsuksanoh, K. M. Holtman, D. J. Yelle, T. Morgan, V. Stavila, J. Pelton, H. Blanch, B. a. Simmons and A. George, *Green Chem.*, 2014, **16**, 1236.

17 N. Tachon, B. Benjelloun-mlayah and M. Delmas, *BioResources*, 2016, **11**, 5797–5815.

18 A. Tolbert, H. Akinosho, R. Khunsupat, A. K. Naskar and A. J. Ragauskas, *Biofuels, Bioprod. Biorefining*, 2014, **8**, 836–856.

19 T. Rashid, C. F. Kait, I. Regupathi and T. Murugesan, *Ind. Crops Prod.*, 2016, **84**, 284–293.

20 T. Pielhop, G. O. Larrazábal and P. Rudolf von Rohr, *Green Chem.*, 2016, **18**, 5239–5247.

21 W. Li, N. Sun, B. Stoner, X. Jiang, X. Lu and R. D. Rogers, *Green Chem.*, 2011, **13**, 2038.

22 B. B. Hallac, Y. Pu and A. J. Ragauskas, *Energy & Fuels*, 2010, **24**, 2723–2732.
23 R. Mariscal, P. Maireles-Torres, M. Ojeda, I. Sádaba and M. López Granados, *Energy Environ. Sci.*, 2016, **9**, 1144–1189.
24 L. Yan, A. a. Greenwood, A. Hossain and B. Yang, *RSC Adv.*, 2014, **4**, 23492.
25 S. Eminov, A. Brandt, J. D. E. T. Wilton-Ely and J. P. Hallett, *PLoS One*, 2016, **11**, e0163835.
26 S. Eminov, J. D. E. T. Wilton-Ely and J. P. Hallett, *ACS Sustain. Chem. Eng.*, 2014, **2**, 978–981.
27 J. B. Binder, A. V. Cefali, J. J. Blank and R. T. Raines, *Energy Environ. Sci.*, 2010, **3**, 765.
28 H. Zhao, J. E. Holladay, H. Brown and Z. C. Zhang, *Science*, 2007, **316**, 1597–1600.
29 S. Eminov, P. Filippousi, A. Brandt, J. Wilton-Ely and J. Hallett, *Inorganics*, 2016, **4**, 32.

Part IV. Conclusions

The work undertaken in this project has furthered the process from four years ago to improve sugar yields from a wider variety of feedstocks with a more diverse and intense process and a cheaper solvent. Additionally, a waste management problem has been solved. A deeper scientific understanding of the chemistry occurring during pretreatment has been gained, which will allow for a more educated optimisation of process parameters. The effect of temperature on the delignification has been established, which allows to decouple the lignin properties from the digestibility of the pulp and therefore potentially the valorisation of both biomass components. Some other highlights include quantitative sugar release from the recalcitrant softwood pine, the successful concomitant pretreatment of a combination of grasses, softwoods and hardwoods and the successful extraction and recovery of various heavy metals from different types of construction and waste woods. Last but not least, it was demonstrated that ethanol can be produced from heavy metal containing construction wood.

In summary, the here presented work demonstrates the ionoSolv pretreatment has the potential to be used for the production of various bio-derived products from a variety of feedstocks while valorising an unwanted waste. The process further appears to be robust, maintaining its performance over at least 6 cycles without accumulating any inhibitors. There remains however still considerable amount of work required in order to make this process an industrial reality.

Remaining Gaps and Proposed Future Work

While this work's outcome is encouraging, there is still an incredibly long path ahead until a first ionoSolv plant will produce its first tonne of pulp. While pretreatment is now well understood, the main challenges remaining lie in the way, the pulp and lignin are currently washed and the amount of resulting wash solvent that needs to be evaporated before the IL can be recycled. Alternative washing protocols for the pulp wash have been suggested already. In the first instance, the black liquor should be separated from the pulp without dilution. Somewhat drastic changes are expected as a result, mainly due to less lignin precipitation onto the pulp surface which is currently triggered by the dilution of the black liquor. This will then impact the lignin characteristics and yields. However, there is currently no data available on this since suitable equipment for such separations is not commonly available at the scales on which we have been operating. Separation may well be facilitated if carried out at elevated temperature where IL viscosity is comparatively low, something that will be difficult to test if manual handling is required. The resulting IL soaked pulp will still require washing, and using the regenerated brown liquor has been suggested as a wash solvent: rather than going directly back in for the next round of pretreatment, the brown liquor would be used once to wash the remaining

lignin-rich black liquor out of the pulp first. The pulp, at this point containing mainly brown liquor, could then be washed with water. This wash water could then be used for subsequent lignin precipitation.

The amount of water used for lignin precipitation will affect not only the energy requirements for evaporation, but also the proportion of lignin coming out of solution and its properties. Adding a smaller amount of water will likely result in smaller lignin fragments remaining in solution. Whether and how they will affect pretreatment and lignin properties in subsequent cycles remains to be tested and analysed. Additionally, the water removal step might well happen under atmospheric pressure, therefore requiring high temperatures which are likely going to cause further reactions in the brown liquor. Associated with the gap in understanding washing requirements is the separation efficiency which is to be expected for the different separation steps. These will likely depend on the type of equipment used, which will then have an effect again on capital costs. The major driver in this separation is likely to be viscosity, and a more comprehensive data set of physical properties of the ionic liquids at various water contents and temperatures is urgently needed.

All pretreatments in this thesis were run with a water content of 20wt% since it was found that this water content gave the best sugar yields in a previous study. It is however possible that, while possibly compromising sugar yields, a slightly higher water content could afford a more economical process due to lower viscosity and better separations further down-stream. This would also mean that less water needs to be added to precipitate the lignin, and therefore less water needs to be removed again.

Apart from water contents and separations, a major obstacle in furthering the process is the material compatibility. As we have seen, ILs are very good at extracting metals and there are numerous publications on the use of ILs for the extraction of metals from ores. Unfortunately this metal extraction ability is not limited to places one wants to extract metals from. Preliminary results from corrosion and leaching experiments from Jason Hallett's research group suggest that any reactor built for pretreatment will likely have to be glass lined or otherwise resistant towards corrosion by the IL. This also has impacts for the separation equipment, although less so, since most separations will be conducted at lower temperatures or with a higher water content, where the IL is less corrosive. However, also more data on this are required.

Comparison of the ionoSolv Process to Other Technologies

Table IV-1 summarises various pretreatment technologies with respect to the feedstocks their applicable to, their way of working as well as some of the associated cost. The list is not exhaustive since we have seen in several instances now that combinations of different pretreatments are

proposed which are very unlikely to become a commercial reality. I have therefore limited the presented information to the most common and established technologies.

Table IV-1 Comparison of different pretreatment technologies.

	Ball-milling	Aq.	SE	AFEX	Alkaline	DA	oSolv	IL dis	iSolv
Agri. and grasses	yes	yes	yes	yes	yes	yes	yes	yes	yes
Hardwoods	-	-	yes	a bit	-	-	yes	yes	yes
Softwoods	-	-	-	-	-	-	a bit	yes	yes
Hemicellulose removal	-	H	H	-	L	H	H	M	H
Lignin removal	-	L	L	-	M	L	H	M	H
Cellulose decrystallization	M	-	-	L	-	-	-	H	-
Inhibitors	L	M to H	H	L	L	H	L	L	L
Reactor cost	L	L	H	M	L	H	M	M	H
Chemical and recovery cost	-	-	-	H	H	L	M	H	L to M
Energy requirement	H	M to H	M	L	L	L	L	H	L to H

L: low; M: medium; H: high; -: no; Agri.: agricultural residues; Aq.: aqueous; SE: steam explosion; AFEX: ammonia fibre expansion; DA: dilute acid; oSolv: Organosolv; IL dis: IL dissolutions; iSolv: ionoSolv.

All of the considered technologies are effective on agricultural residues and grasses, fewer on hardwoods and only the ionic liquid based technologies on softwoods. Hemicellulose and lignin removal during pretreatment are beneficial as it reduces the required reactor size for hydrolysis. Additionally it means that cellulose pulp can be obtained as a product by itself in case hydrolysis to sugars is not wanted and therefore offers a wider product portfolio that is accessible. Hemicellulose removal is fairly common across the technologies, however effective lignin removal is limited to organosolv and ionoSolv pretreatments. Cellulose decrystallization, historically thought to be one of the main goals of pretreatment, is only achieved by cellulose dissolving technologies, such as the IL dissolution process, and to a lower extent by ball-milling and AFEX. The formation of inhibitors is a major problem in the aqueous pretreatments, including steam explosion and dilute acid. A more difficult comparison is done across the technologies with respect to their costs: reactor cost is influenced by required resistances towards high pressures, temperatures and acidity. It is thought that

ionoSolv pretreatment would require glass lined reactors to avoid corrosion. Similarly, DA pretreatment requires corrosion resistant equipment while steam explosion requires equipment that can handle high pressures and a fast pressure release. On the side of the chemicals cost and the cost of their recovery, the aqueous pretreatments, as well as ball-milling, have a strong advantage. Alkaline pretreatment and AFEX on the other hand have relatively high initial chemical cost and/or require complex chemical recovery systems. Finally, the energy requirement of the processes spans a large range. Drying is one of the main energy consumers in the IL dissolution process, but also in the ionoSolv process if the amount of wash solvent and water for lignin precipitation is not adjusted. Overall, the ionoSolv process does appear to outperform most of its competitors, however many of the made assumptions with regard to its performance on a large scale remain to be tested.

A Brighter Future?

IonoSolv pretreatment does, in my eyes, hold the potential to overcome many of the barriers that exist for bio-based products to enter the market and slowly help replace our petrochemical industry while reducing waste. If we really want to keep oil, coal and gas in the ground, and I do, then we need to replace everything that is currently made from it. Wind, solar and other forms of renewable energy, combined with some suitable energy storage technology, hold great potential for decarbonising electricity, but will never be able to produce all the materials and chemicals we use in our daily lives. I do not envisage a future where ionoSolv ethanol is poured in the tanks of all our cars, in my view battery electric vehicles are a much better and easier way of decarbonising road transport, although there might be some need for bio- fuels in aviation and for HGV. The real importance of bio-refining however lies in the production of everything else.

In addition to the petrochemical industry, our society has been relying on another extractive industry, mining for metals. We do not actually use metals up, rather we mix them, dilute them, dump them. Also this practice needs to be stopped if we want to stop destroying forests, polluting water, endangering wildlife and humans, and again, I do. We have seen that one of the great advantages, of ionic liquids is their ability to extract metals. As shown in this project, we can successfully extract various metals from biomass. Lastly, ionic liquids can potentially also be used for the recovery of metals from various other sources, such as waste electronics, or remove them from places where they are unwanted, for example sewage sludge, which contains valuable phosphorus but often contains too high levels of heavy metals to be spread on land. I therefore hope that ionic liquids will make it well past the field of bio-refining to general waste refining, closing loops, reversing damage we have already caused and enabling us to live in comfort without compromising the livelihood of future generations (which incidentally is the definition of sustainability).

Appendix

Figures and Tables

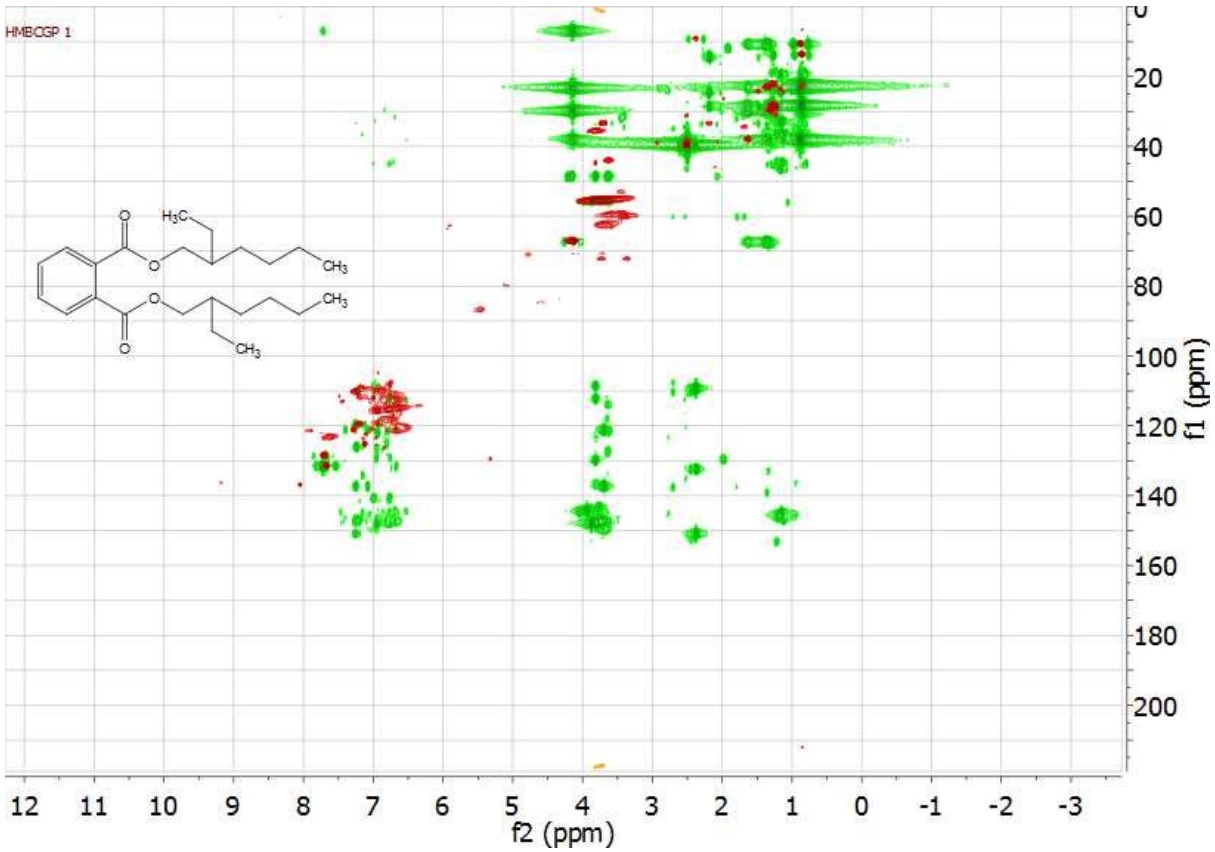

Figure S0-1 HSQC (red) and HMBC (green) NMR spectra of copper treated softwood lignin isolated after extraction with [HC_1im]Cl at 170°C for 30 min with a biomass to solvent ratio 1:10 g/g and a final water content of 20wt%. The peaks at 7.66/131 ppm and 7.71/128 ppm and others are thought to stem from the plasticizer bis(2-ethylhexyl) phthalate (DEHP).

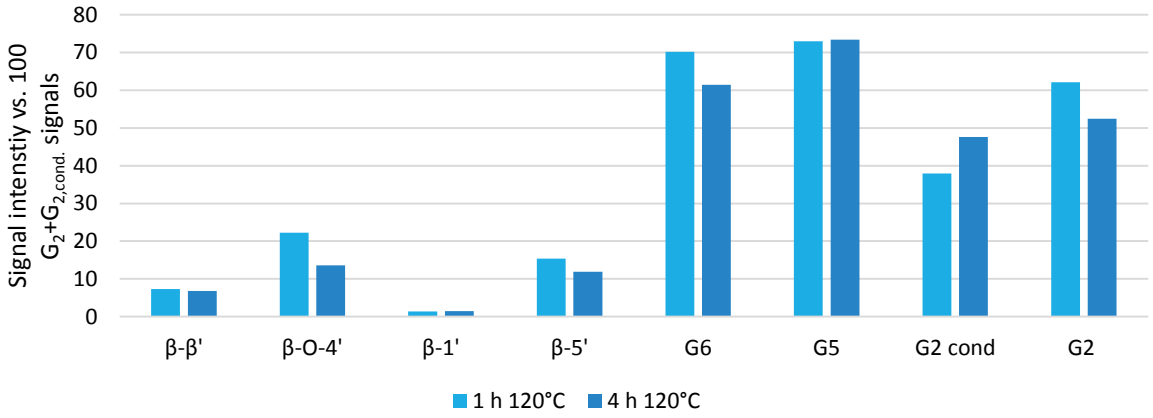

Figure S0-2 Relative signal intensity of major lignin subunits and linkages in the precipitated lignin relative to the combined $G_2/G_{2,cond.}$ volume integral as evidenced HSQC NMR spectroscopy. Pine was pretreated at 120°C [HC_4im][HSO_4] with a biomass to solvent ratio 1:10 g/g and a final water content of 20wt%.

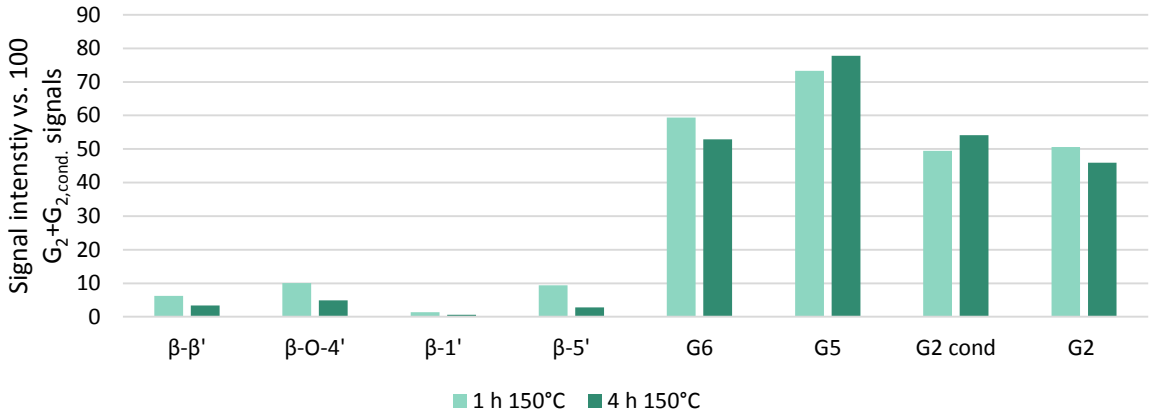

Figure S0-3 Relative signal intensity of major lignin subunits and linkages in the precipitated lignin relative to the combined $G_2/G_{2,cond.}$ volume integral as evidenced HSQC NMR spectroscopy. Pine was pretreated at 150°C $[HC_4im][HSO_4]$ with a biomass to solvent ratio 1:10 g/g and a final water content of 20wt%.

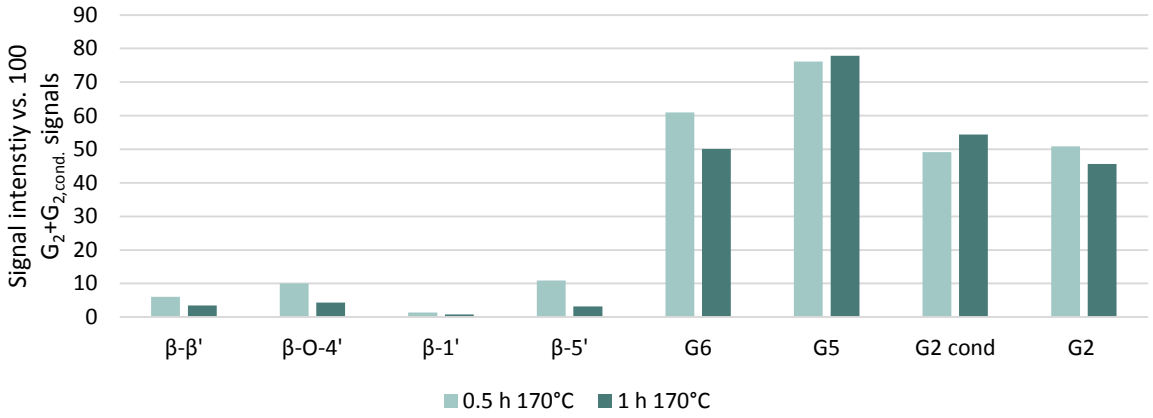

Figure S0-4 Relative signal intensity of major lignin subunits and linkages in the precipitated lignin relative to the combined $G_2/G_{2,cond.}$ volume integral as evidenced HSQC NMR spectroscopy. Pine was pretreated at 170°C $[HC_4im][HSO_4]$ with a biomass to solvent ratio 1:10 g/g and a final water content of 20wt%.

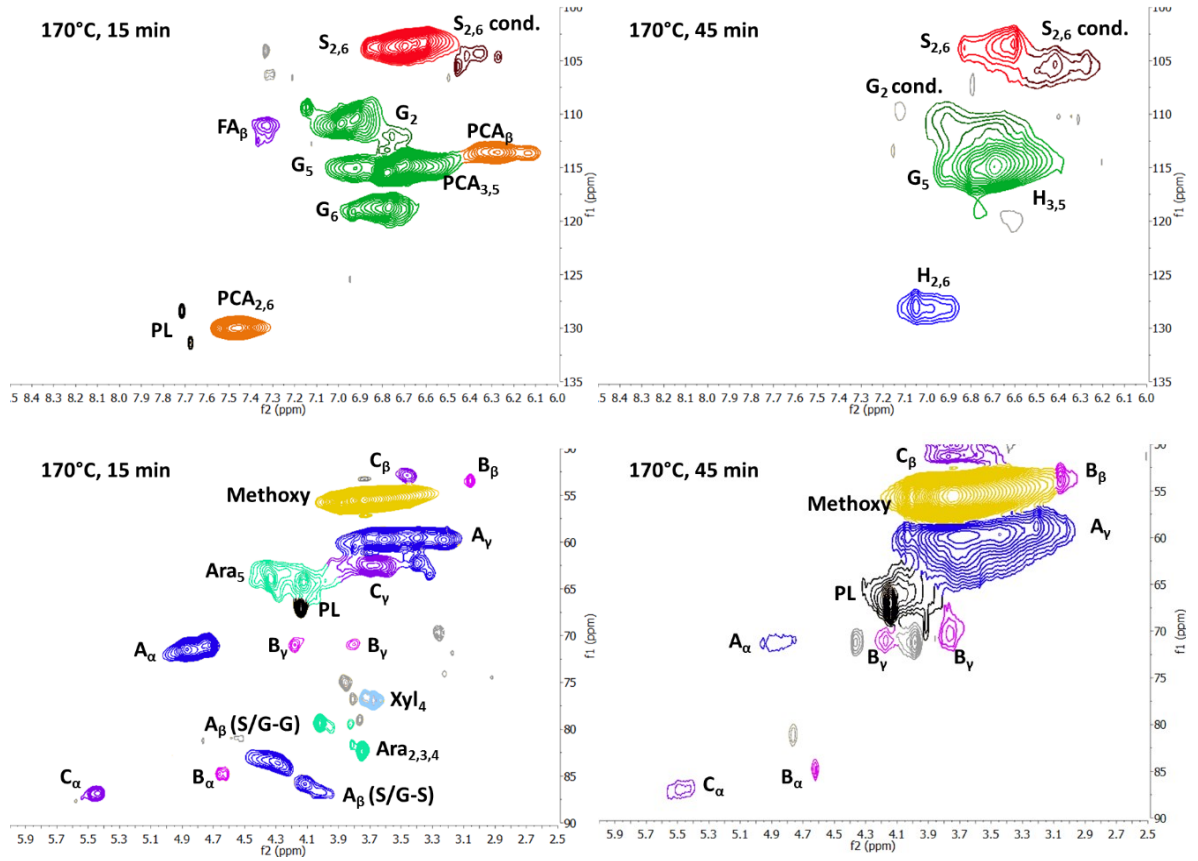

Figure S0-5 HSQC NMR spectra of *Miscanthus* lignin isolated after extraction with [TEA][HSO_4] with a biomass to solvent ratio 1:5 g/g and a final water content of 20wt%, aromatic region (left side) and side chain region (right side).

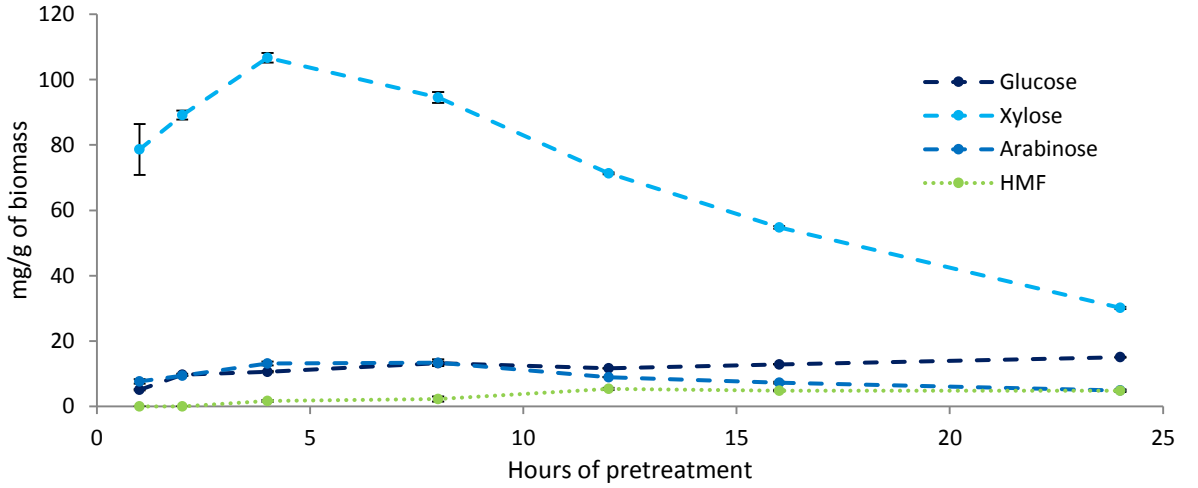

Figure S0-6 Time course of solutes found in the recycled IL (i.e. after drying) as analysed by HPLC. *Miscanthus* was pretreated with [TEA][HSO_4] at 120°C with a biomass to solvent ratio of 1:10 g/g and a final water content of 20wt%. Standard errors were calculated for triplicate measurements.

Table S2 Pulp composition and yields and of lignocellulose components in the pine pulp as determined by compositional analysis as well as lignin precipitate after pretreatment with [HC_4im][HSO_4] with a biomass to solvent ratio of 1:10 g/g and a final water content of 20wt%.

T	t	Glucan	Hemicelluloses[a]	Lignin[b]	Ash	Extractives	Mass loss[c]
Untreated pine		43.4	19.1	32.2	0.8	4.46	0.0
120°C	1 h	40.3	9.3	22.2	0.0	N/A	28.2
120°C	4 h	38.6	4.6	14.9	0.1	N/A	41.8
120°C	8 h	37.1	2.9	12.5	0.0	N/A	47.5
150°C	30 min	40.3	8.3	15.8	0.0	N/A	35.6
150°C	1 h	39.2	4.0	6.5	0.0	N/A	50.3
150°C	2 h	34.7	3.0	6.4	0.0	N/A	55.9
150°C	4 h	28.1	0.5	11.0	0.0	N/A	60.4
150°C	8 h	17.0	0.5	20.8	0.0	N/A	61.7
150°C	16 h	4.9	0.5	28.8	0.0	N/A	65.8
170°C	15 min	38.8	6.2	20.2	0.0	N/A	27.9
170°C	30 min	37.5	1.6	7.3	0.0	N/A	53.6
170°C	45 min	28.2	0.0	6.5	0.1	N/A	65.1
170°C	1 h	24.2	0.3	9.1	0.0	N/A	66.4
170°C	4 h	0.1	0.4	27.0	0.0	N/A	72.5

[a]Sum of mannose, xylose, arabinose and galactose; [b]Sum of acid soluble and acid insoluble lignin; [c]Mass dissolved in IL during pretreatment.

Table S3 Signal intensities of selected peaks in the 1 h and 24 h lignins with respect to the CH_3 signal of xylene, corrected for lignin weight. *Miscanthus* was pretreated in [TEA][HSO_4] at 120°C with a biomass to solvent ratio of 1:10 g/g and a final water content of 20wt%.

	G_2[a]	G_5	G_6	S[a]	β-O-4'
1 h signal intensity	5.6	11.9	3.5	9.1	5.6
24 h signal intensity	5.2	10.3	1.3	7.3	0.9
Percentage change	7%	16%	161%	25%	489%

[a]Sum of condensed and non-condensed.

Spectra

Ionic Liquid Synthesis NMRs

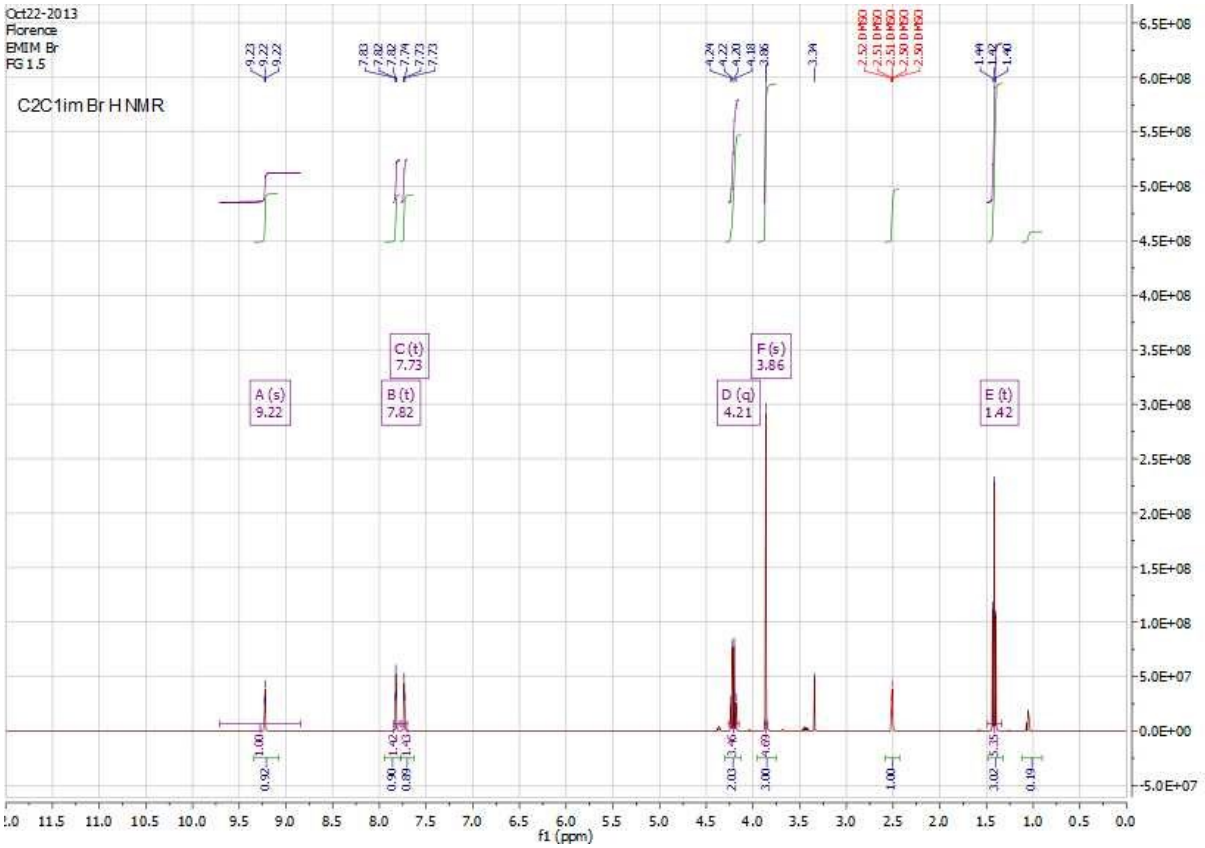

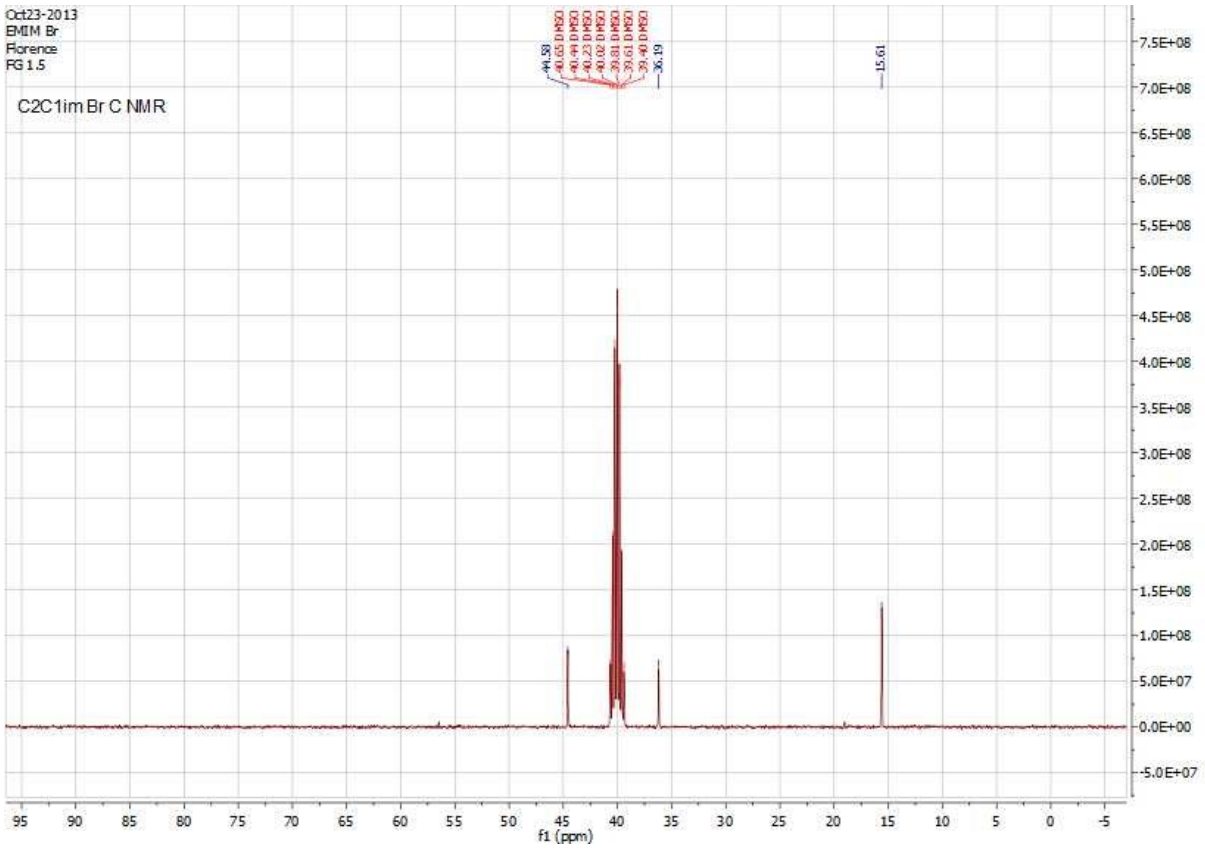

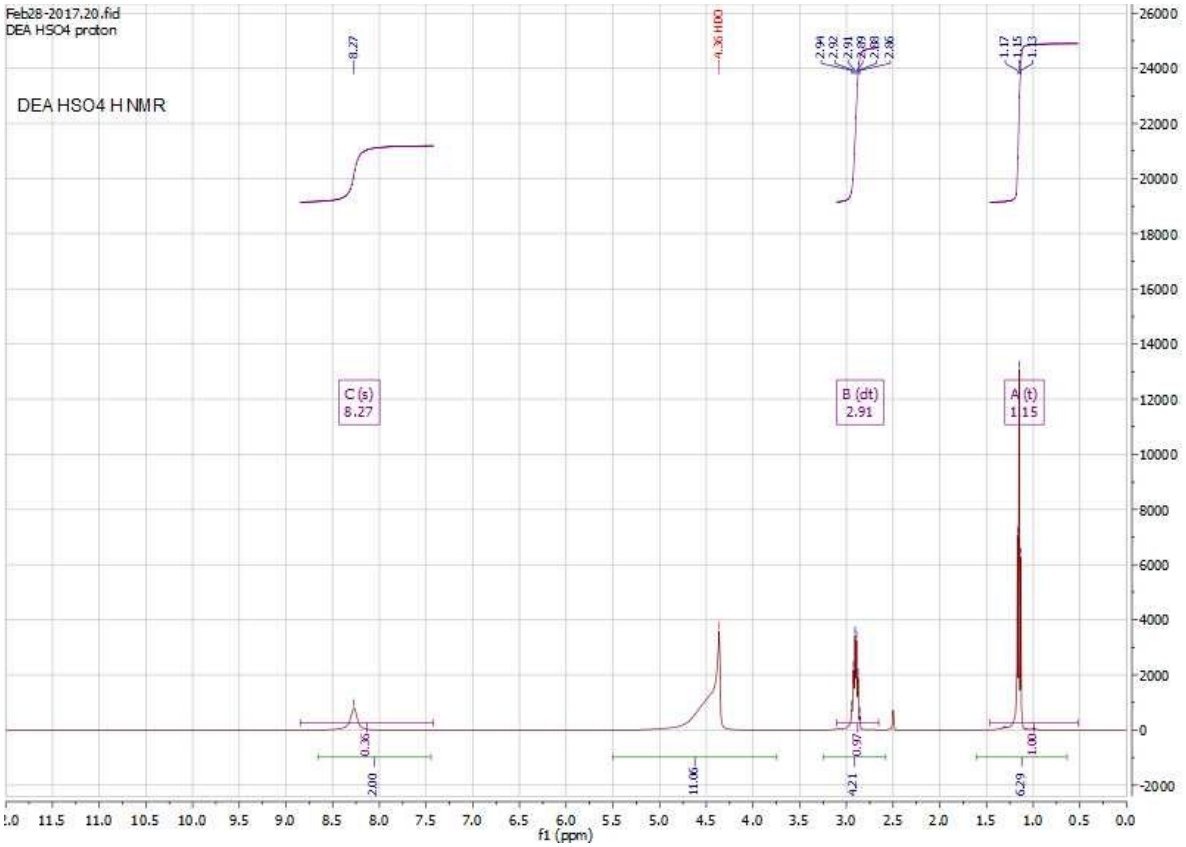
Feb28-2017.20.fid
DEA HSO4 proton
DEA HSO4 H NMR
8.27
4.36 HDO
2.91
2.92
2.91
2.89
2.88
2.86
1.17
1.15
1.13
C (s)
8.27
B (dt)
2.91
A (t)
1.15
0.36
2.00
11.06
0.97
4.21
1.00
6.29
f1 (ppm)

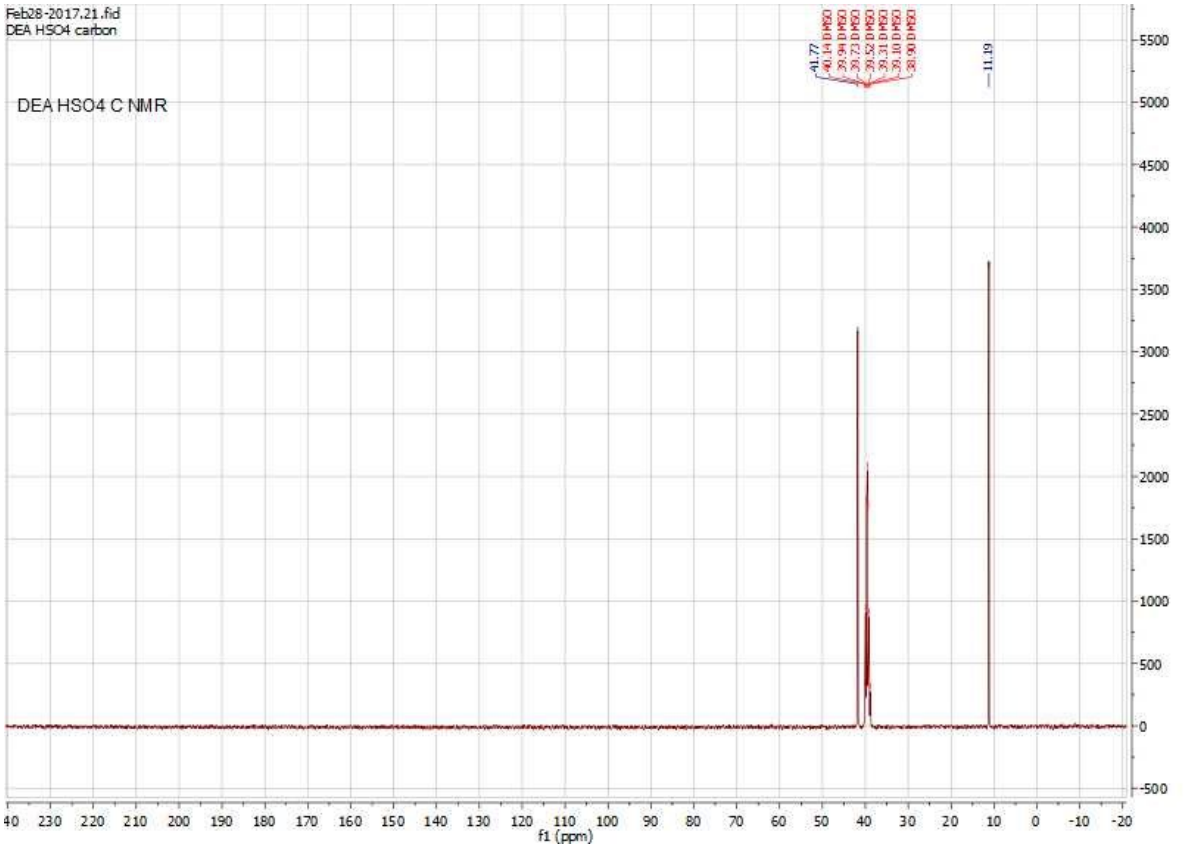
Feb28-2017.21.fid
DEA HSO4 carbon
DEA HSO4 C NMR
41.77
40.14 DMSO
39.94 DMSO
39.73 DMSO
39.52 DMSO
39.31 DMSO
39.10 DMSO
38.90 DMSO
11.19
f1 (ppm)

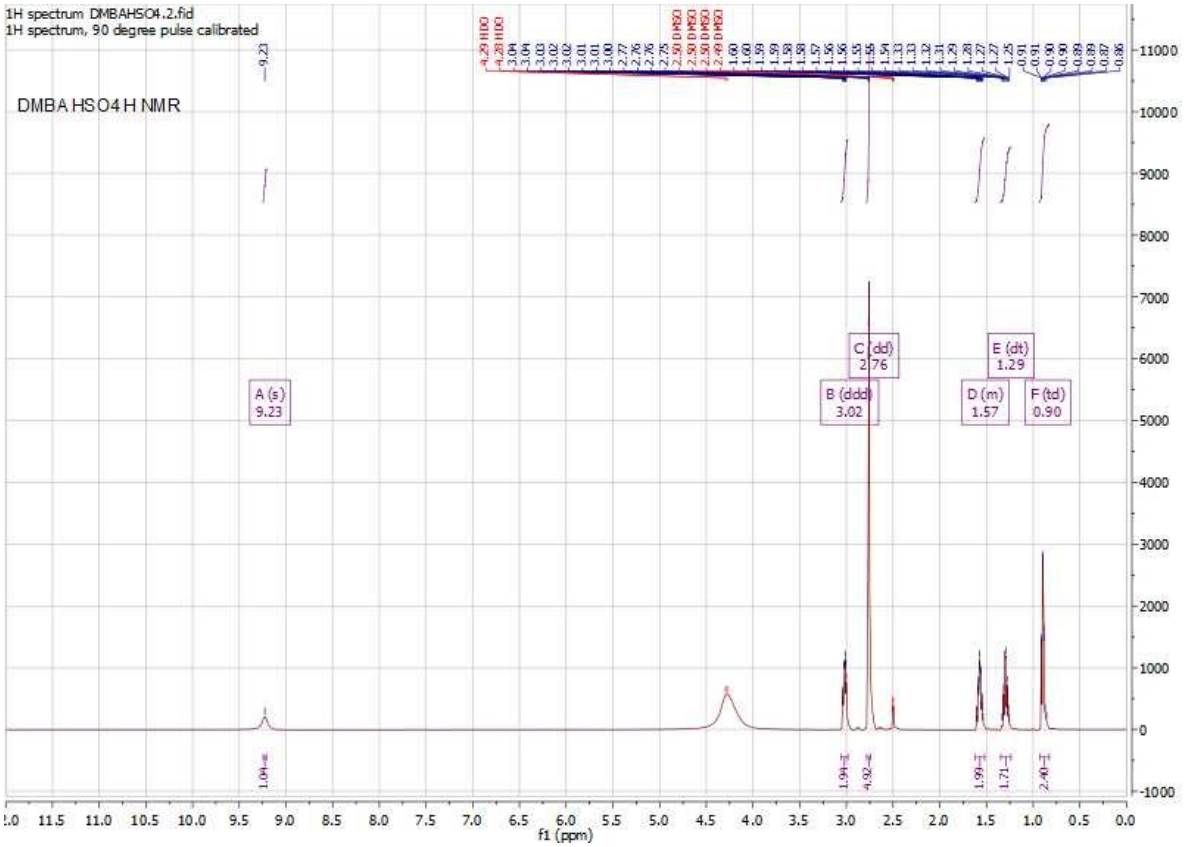
1H spectrum DMBAHSO4.2.fid
1H spectrum, 90 degree pulse calibrated
DMBA HSO4 H NMR
A (s)
9.23
B (ddd)
3.02
C (dd)
2.76
D (m)
1.57
E (dt)
1.29
F (td)
0.90
f1 (ppm)

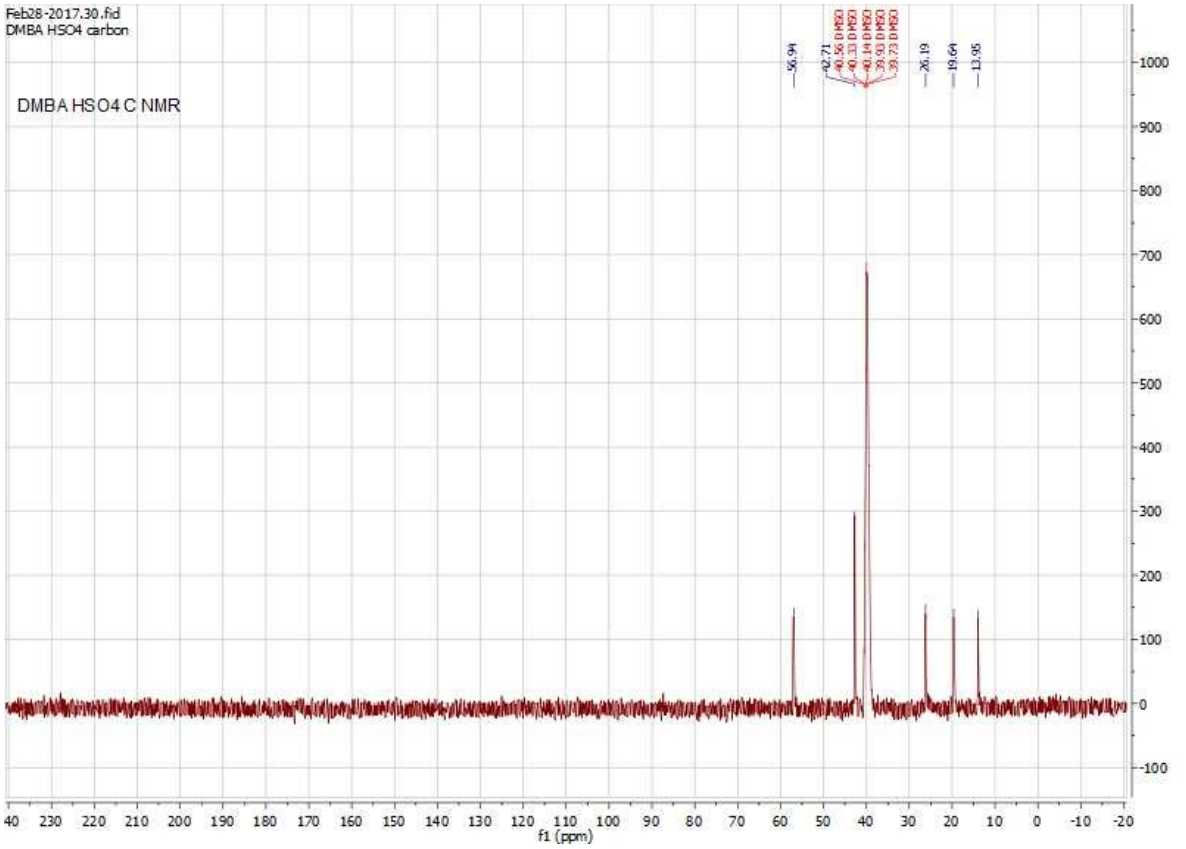
Feb28-2017.30.fid
DMBA HSO4 carbon
DMBA HSO4 C NMR
56.94
42.71
26.19
19.64
13.96
f1 (ppm)

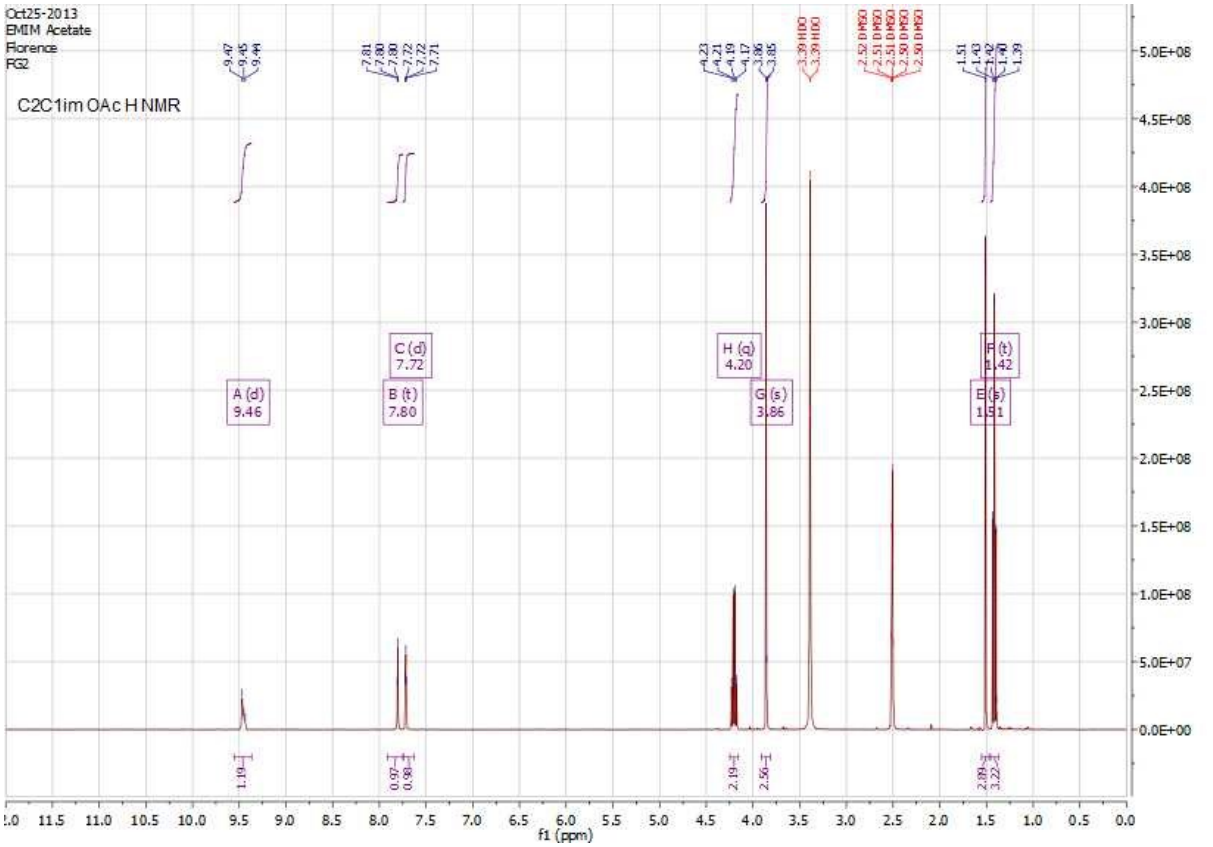
Oct25-2013
EMIM Acetate
Florence
FG2
C2C1im OAc H NMR
A (d) 9.46
B (t) 7.80
C (d) 7.72
H (q) 4.20
G (s) 3.86
F (t) 1.42
E (s) 1.91
f1 (ppm)

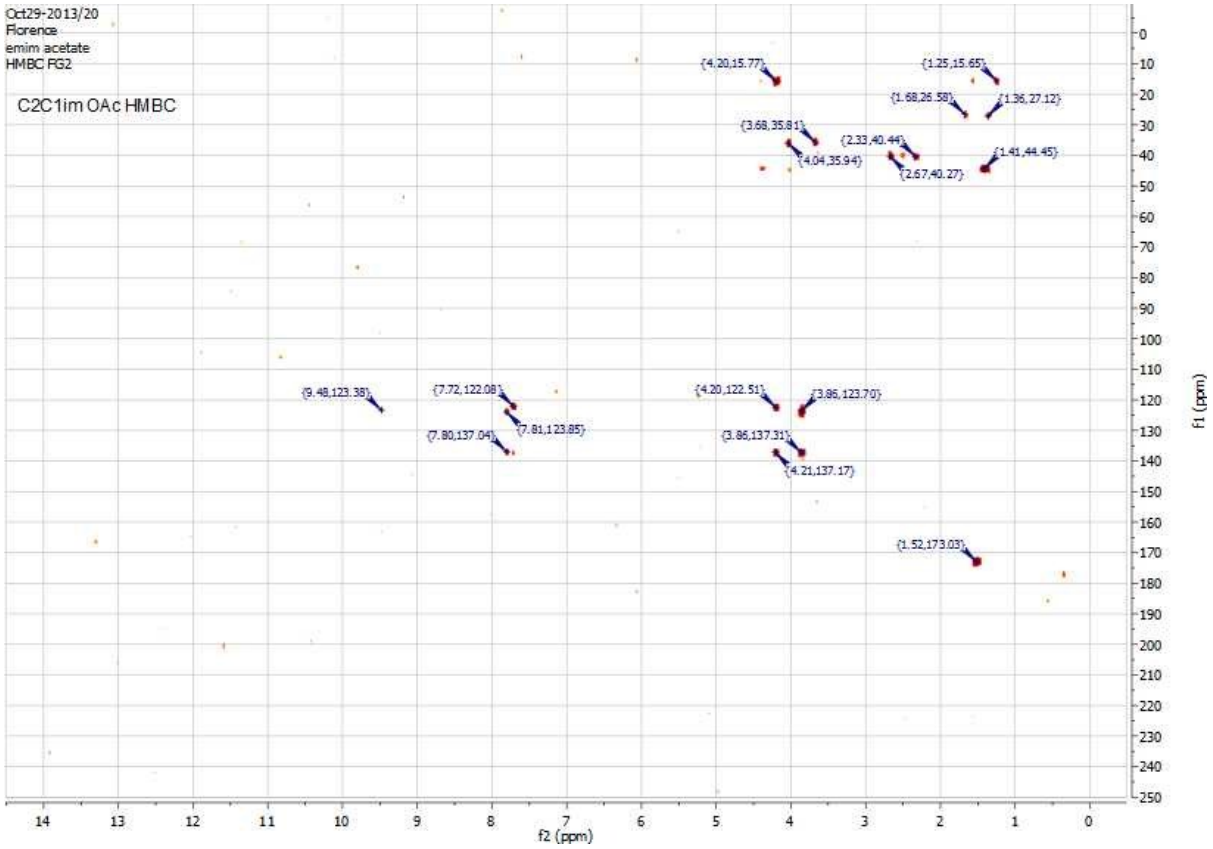
Oct29-2013/20
Florence
emim acetate
HMBC FG2
C2C1im OAc HMBC
{4.20,15.77}
{1.25,15.65}
{1.68,26.58}
{1.36,27.12}
{3.68,35.81}
{2.33,40.44}
{4.04,35.94}
{1.41,44.45}
{2.67,40.27}
{9.48,123.38}
{7.72,122.08}
{7.81,123.85}
{7.80,137.04}
{4.20,122.51}
{3.86,123.70}
{3.86,137.31}
{4.21,137.17}
{1.52,173.03}
f2 (ppm)
f1 (ppm)

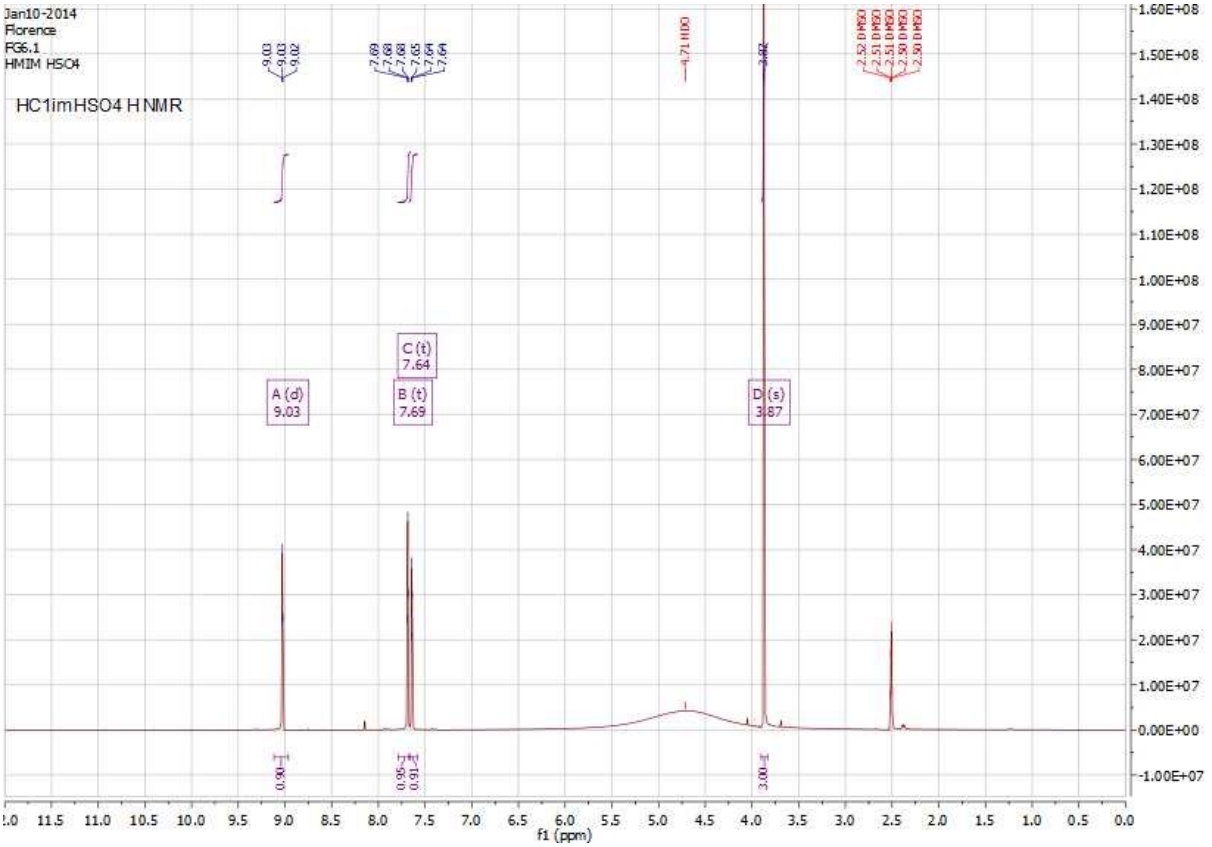
Jan10-2014
Florence
FG6.1
HMIM HSO4
HC1imHSO4 HNMR
A (d)
9.03
B (t)
7.69
C (t)
7.64
D (s)
3.87
f1 (ppm)

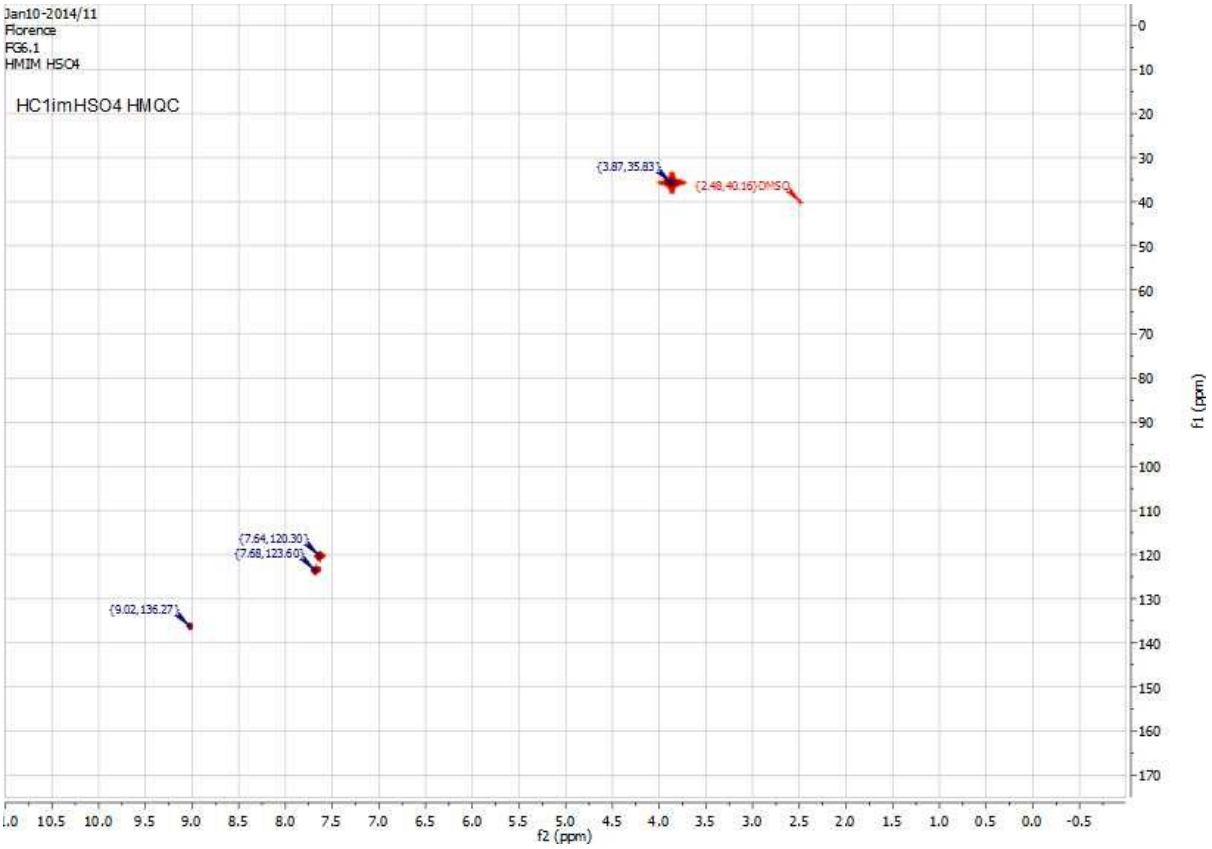
Jan10-2014/11
Florence
FG6.1
HMIM HSO4
HC1imHSO4 HMQC
{3.87,35.83}
{2.48,40.16}DMSO
{7.64,120.30}
{7.68,123.60}
{9.02,136.27}
f2 (ppm)
f1 (ppm)

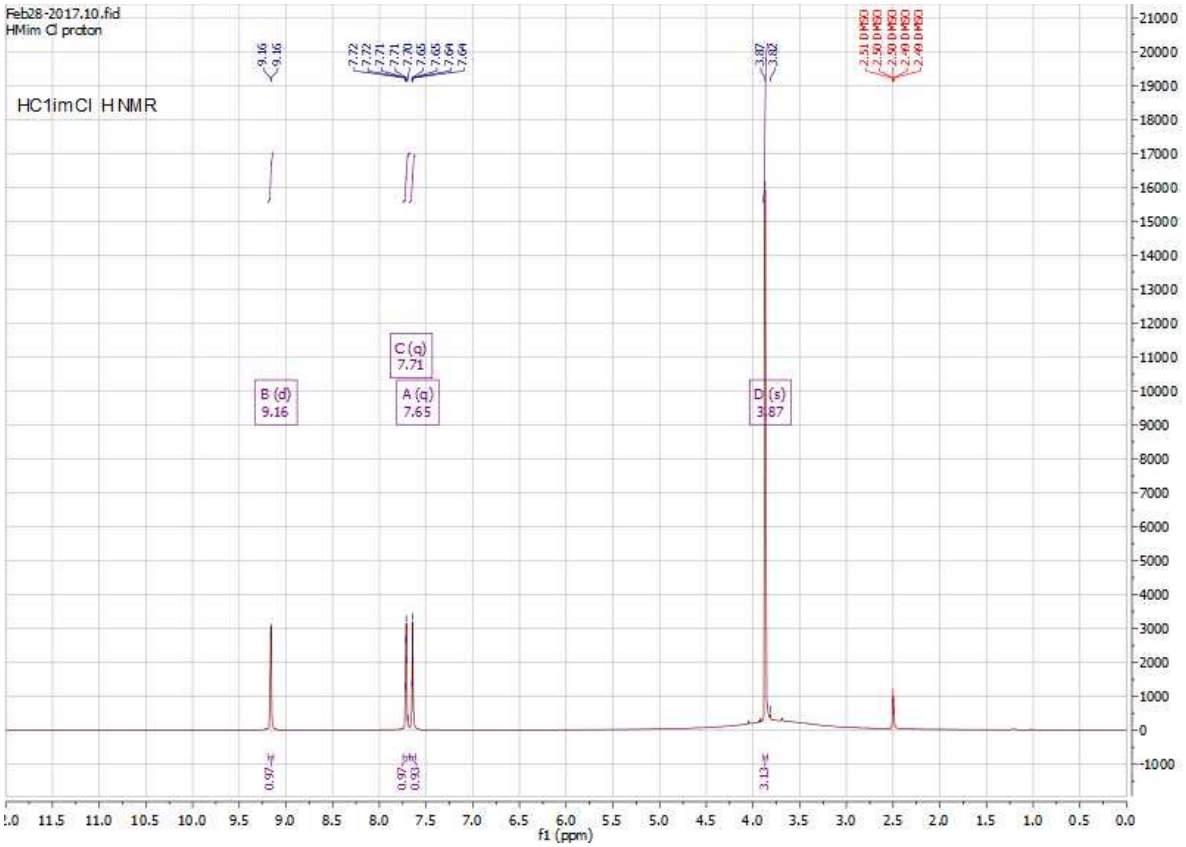
Feb28-2017.10.fid
HMim Cl proton
HC1imCl H NMR
C (q)
7.71
B (d)
9.16
A (q)
7.65
D (s)
3.87
f1 (ppm)

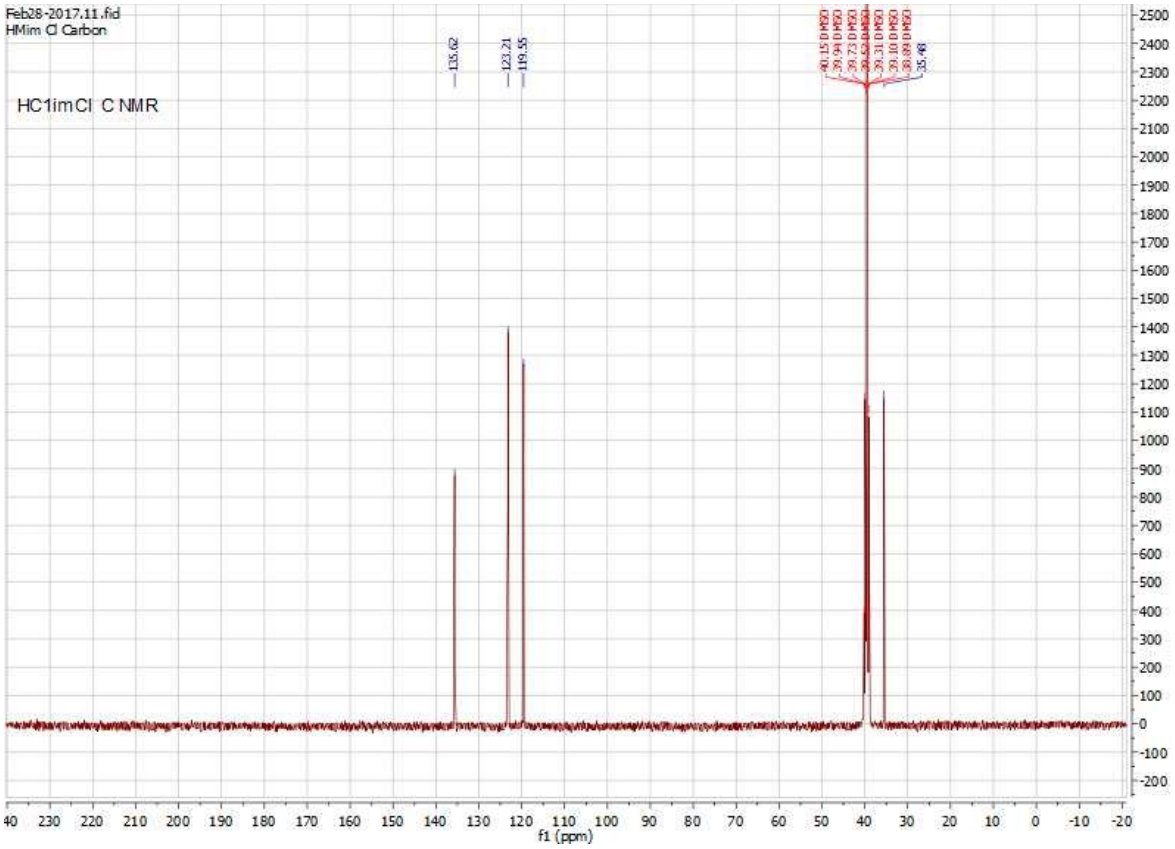
Feb28-2017.11.fid
HMim Cl Carbon
HC1imCl C NMR
135.62
123.21
119.55
f1 (ppm)

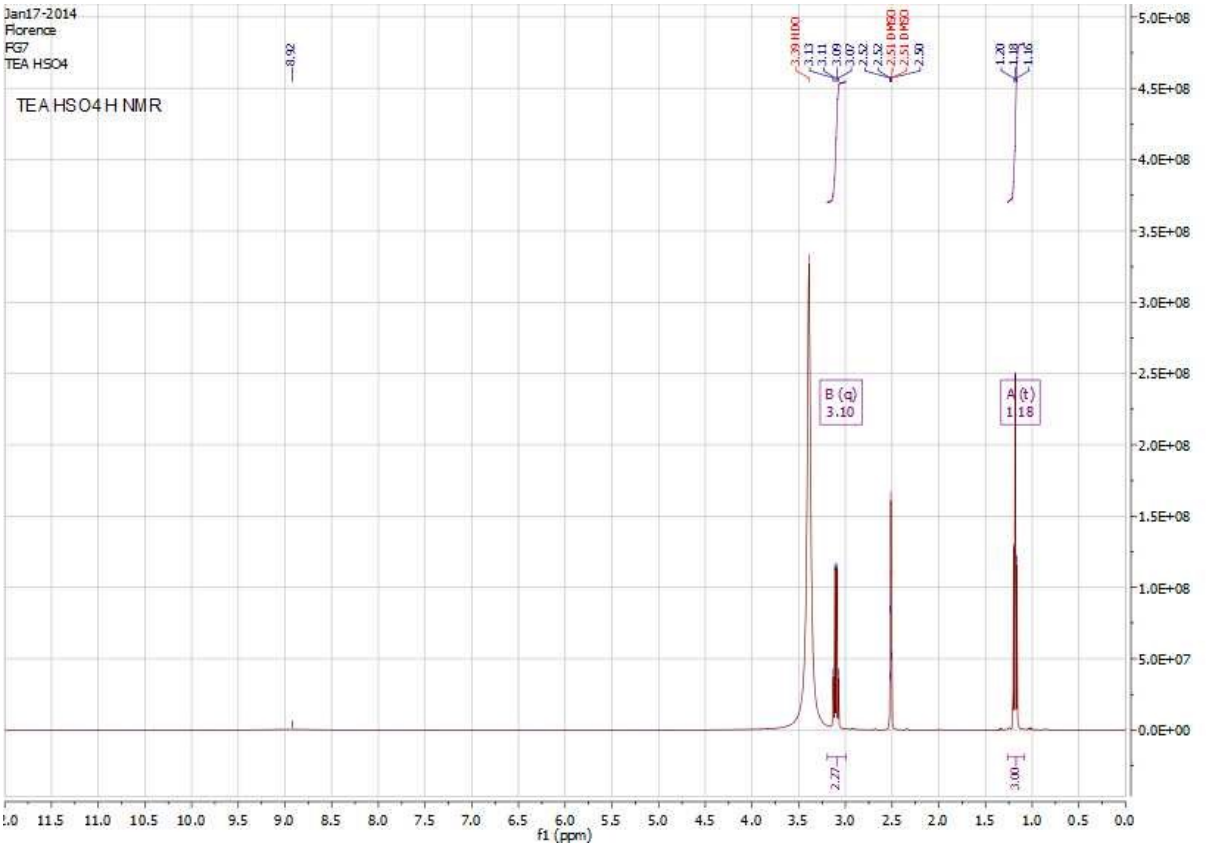
Jan17-2014
Florence
FG7
TEA HSO4
TEA HSO4 H NMR
8.92
3.39 H2O
3.13
3.11
3.09
3.07
2.52
2.52
2.51 DMSO
2.51 DMSO
2.50
1.20
1.18
1.16
B (q)
3.10
A (t)
1.18
2.27
3.00
f1 (ppm)

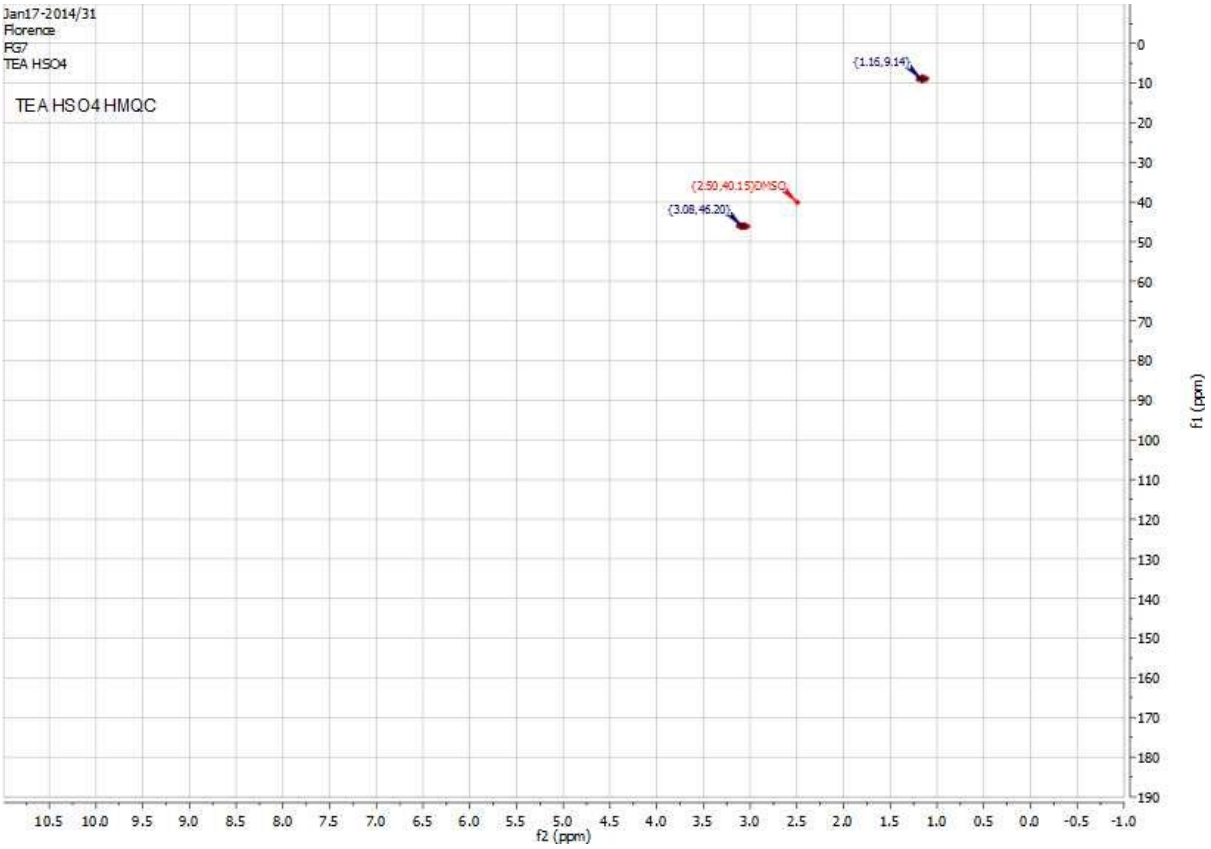
Jan17-2014/31
Florence
FG7
TEA HSO4
TEA HSO4 HMQC
(1.16,9.14)
(2.50,40.15)DMSO
(3.08,46.20)
f2 (ppm)
f1 (ppm)

Lignin HSQCs

Miscanthus [TEA][HSO_4] 120°C

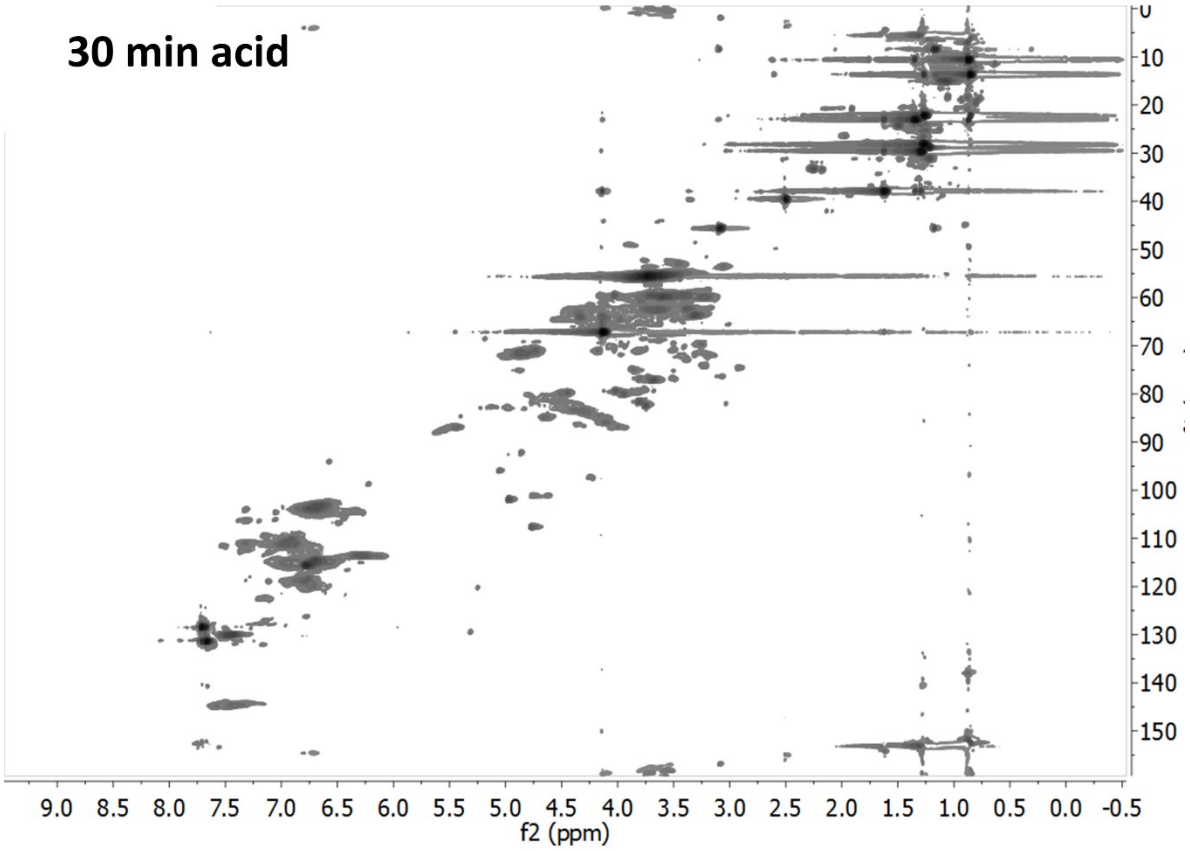

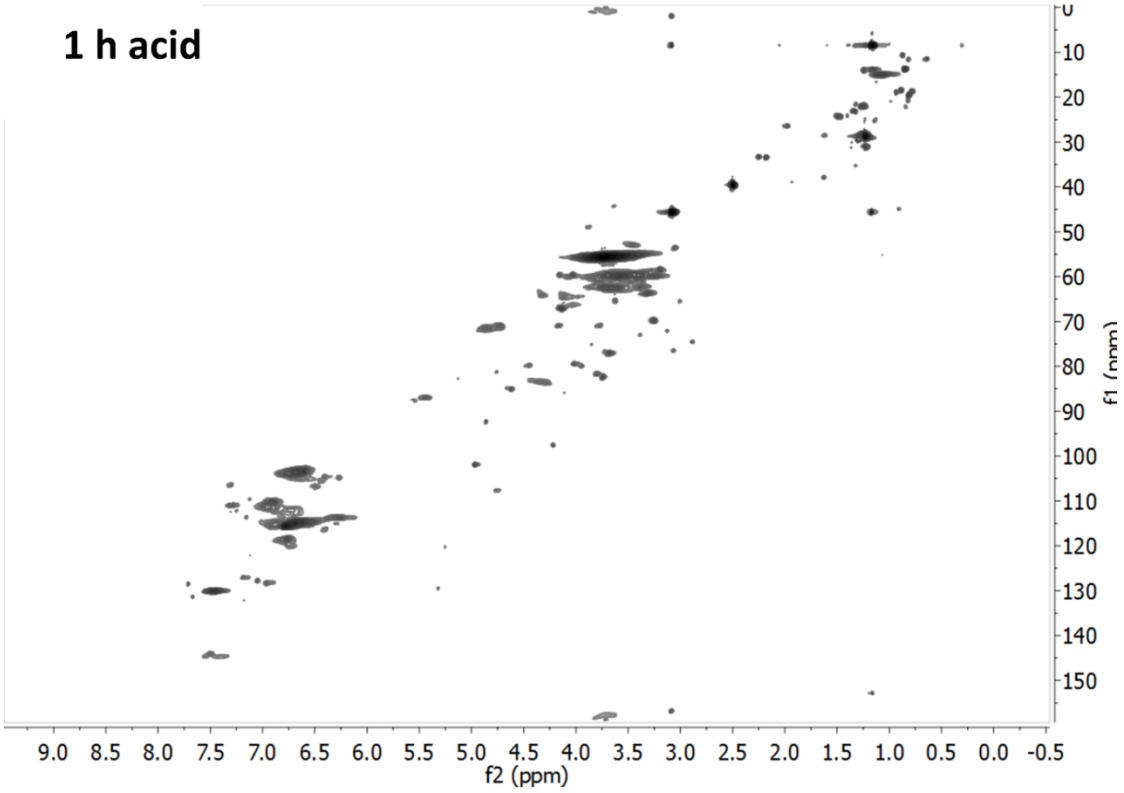

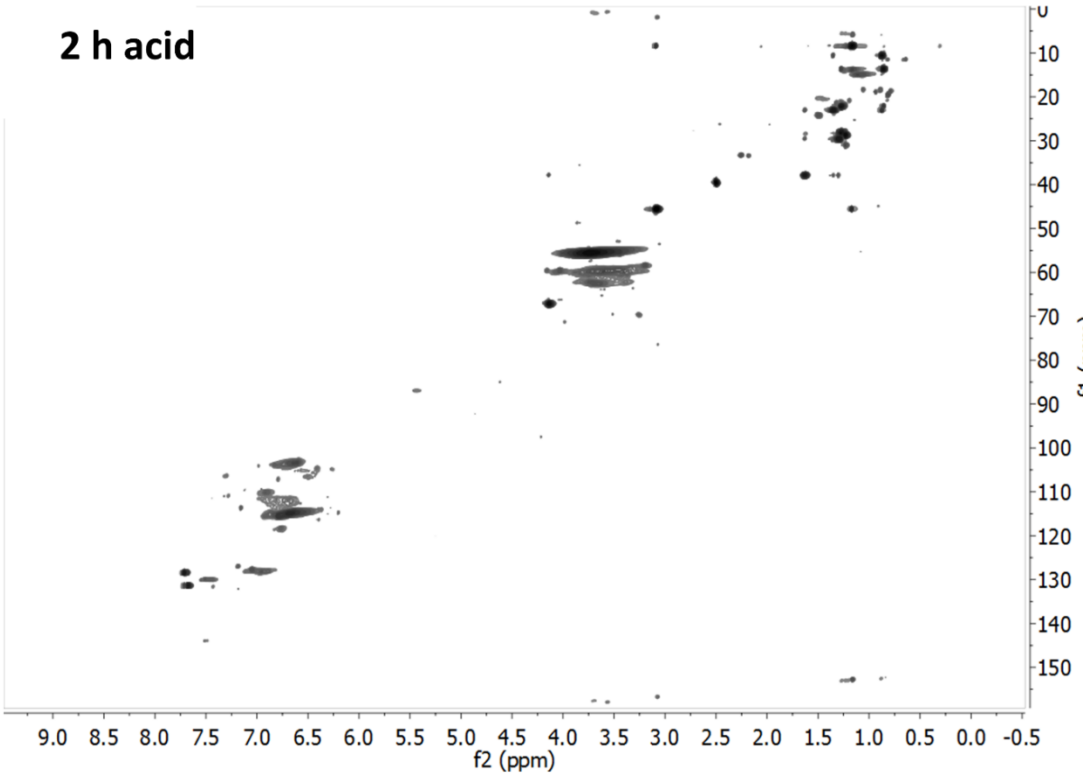
2 h acid
0
10
20
30
40
50
60
70
80
90
100
110
120
130
140
150
9.0 8.5 8.0 7.5 7.0 6.5 6.0 5.5 5.0 4.5 4.0 3.5 3.0 2.5 2.0 1.5 1.0 0.5 0.0 -0.5
f2 (ppm)

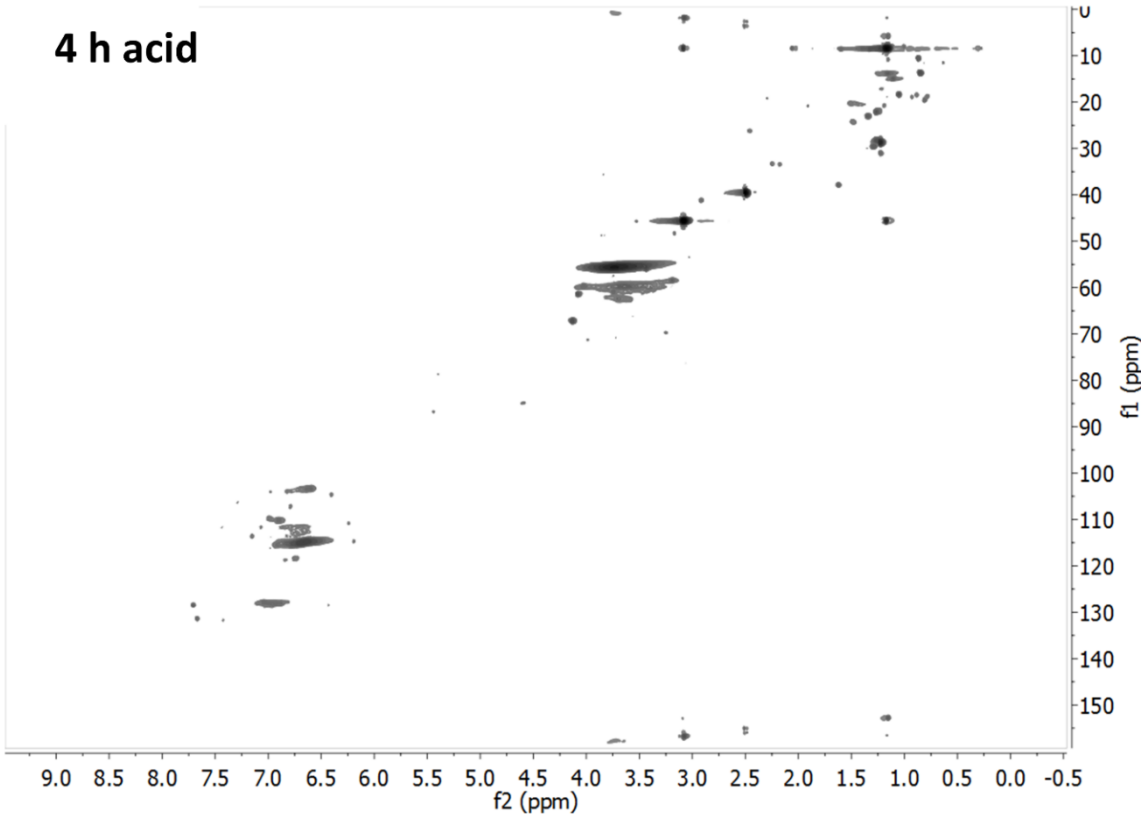
4 h acid
0
10
20
30
40
50
60
70
80
90
100
110
120
130
140
150
f1 (ppm)
9.0 8.5 8.0 7.5 7.0 6.5 6.0 5.5 5.0 4.5 4.0 3.5 3.0 2.5 2.0 1.5 1.0 0.5 0.0 -0.5
f2 (ppm)

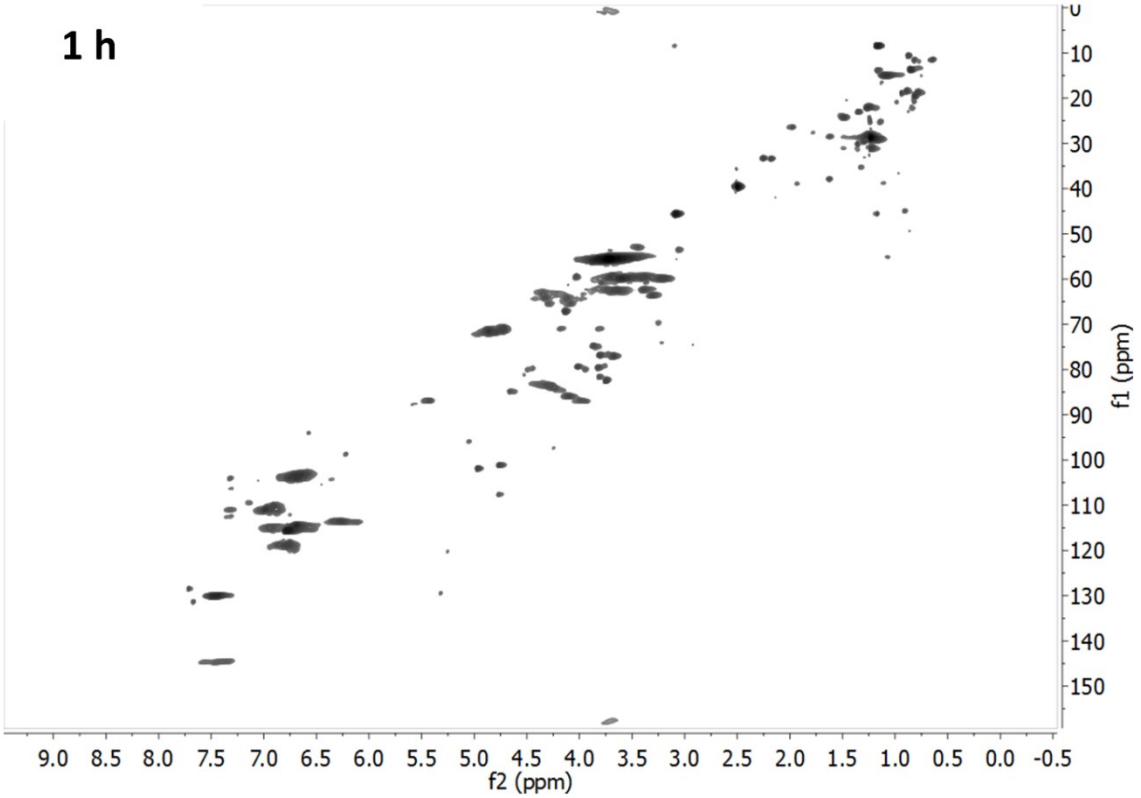
1 h
f1 (ppm)
f2 (ppm)

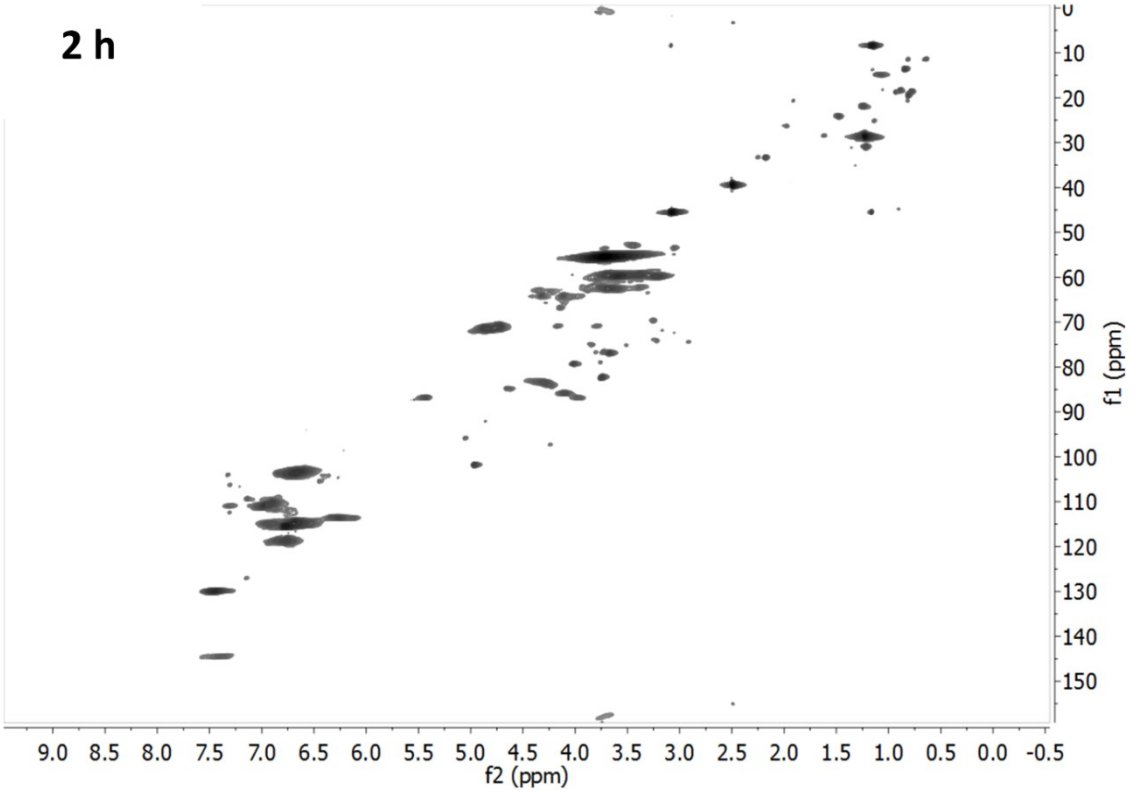
2 h
f1 (ppm)
f2 (ppm)

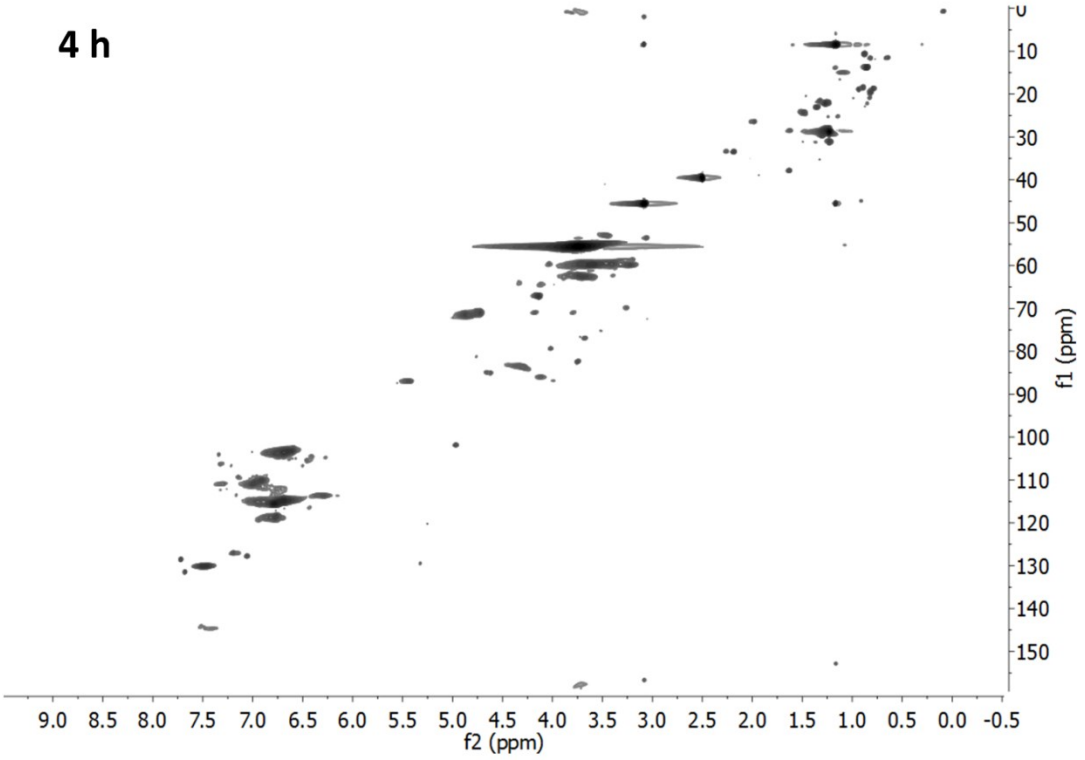
4 h
f1 (ppm)
f2 (ppm)

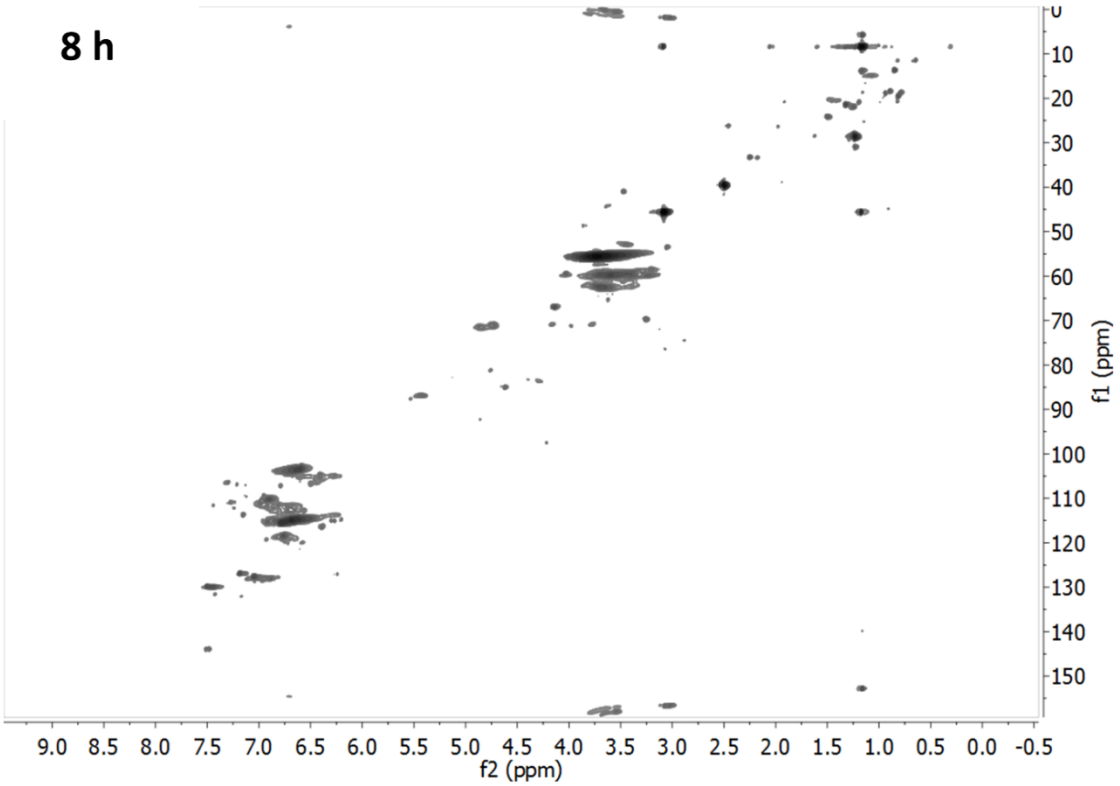
8 h
f1 (ppm)
f2 (ppm)

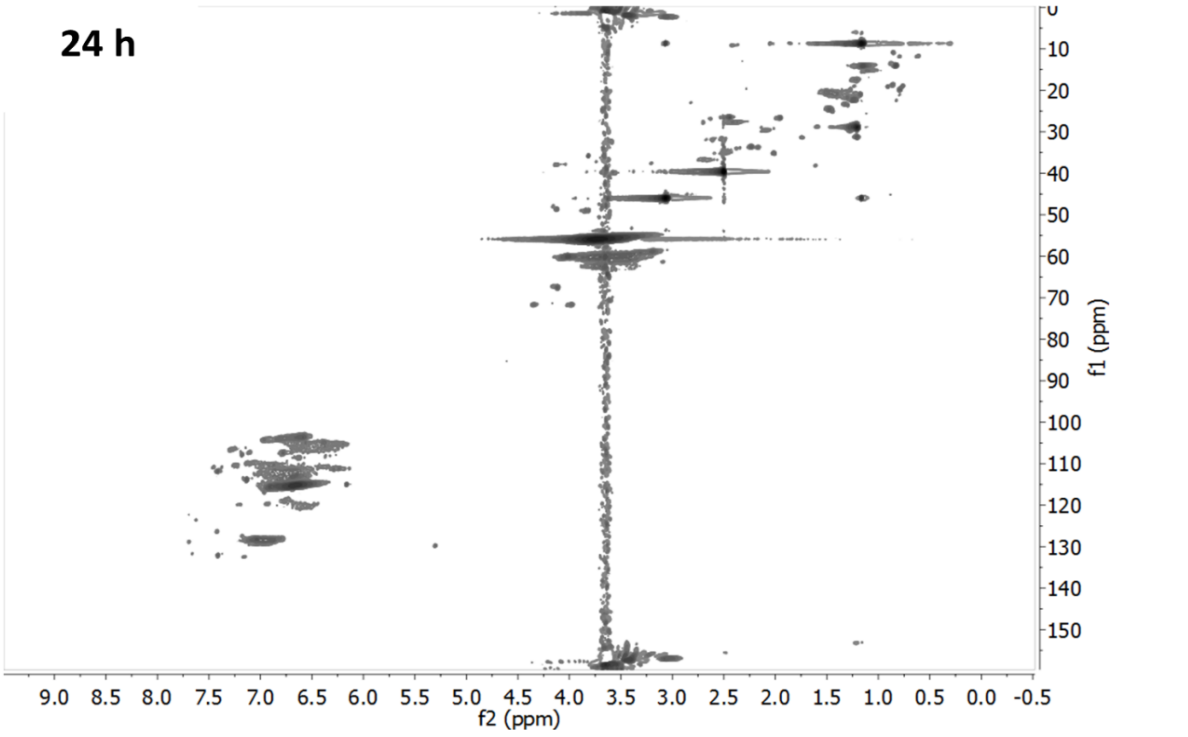
24 h
f1 (ppm)
f2 (ppm)

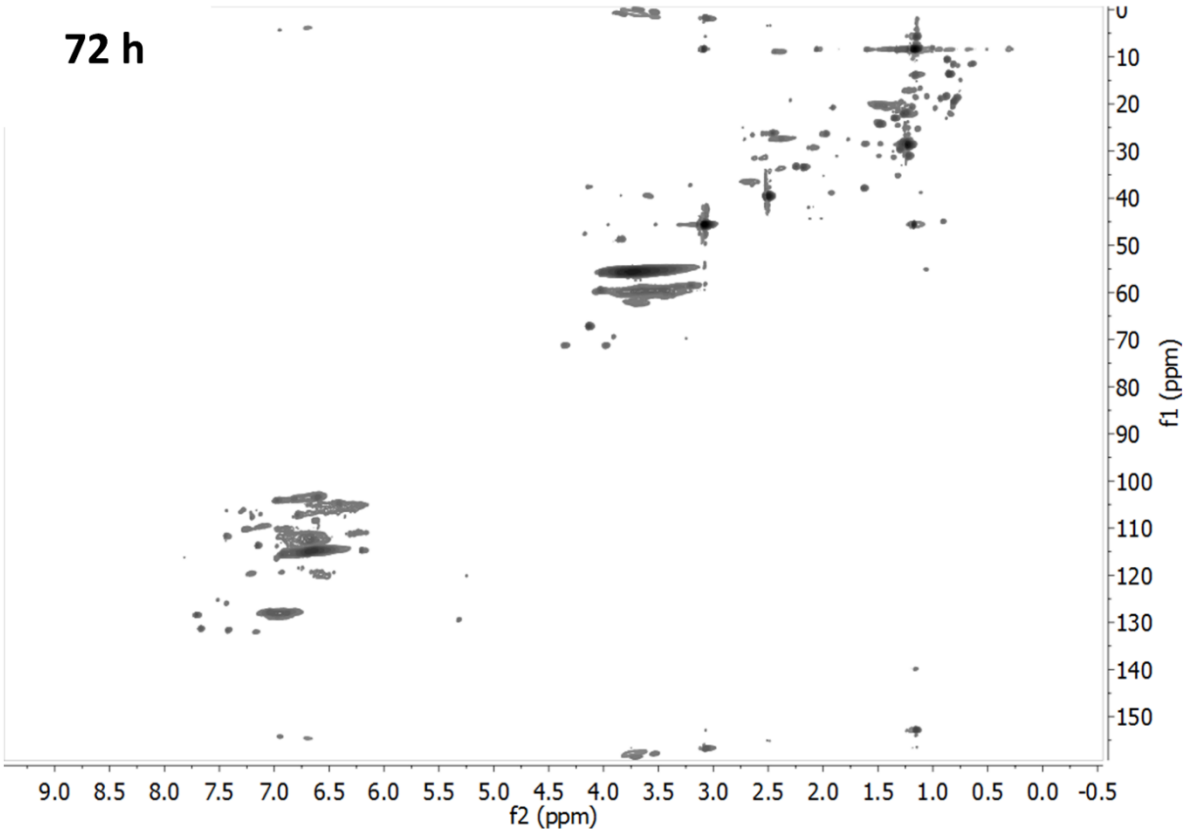
72 h
f1 (ppm)
f2 (ppm)

Miscanthus [TEA][HSO_4], 150-180°C

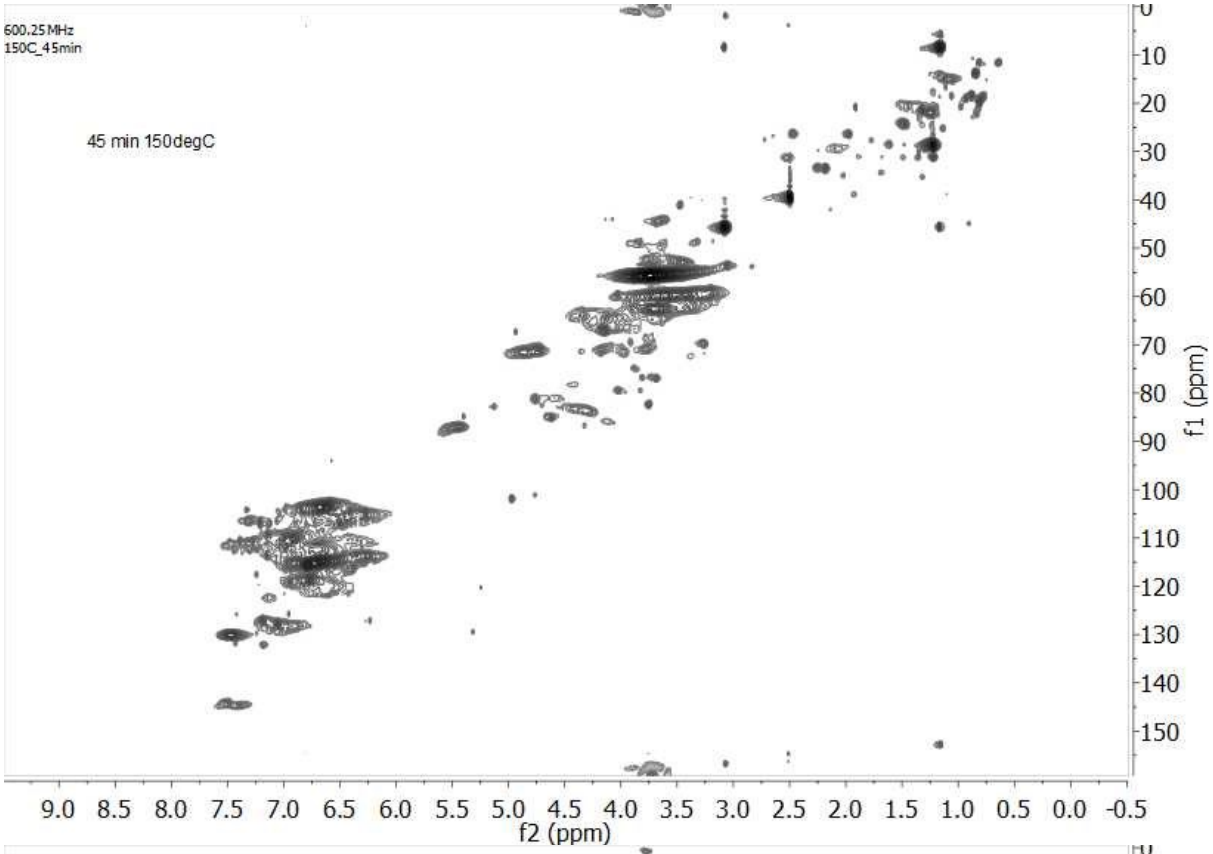

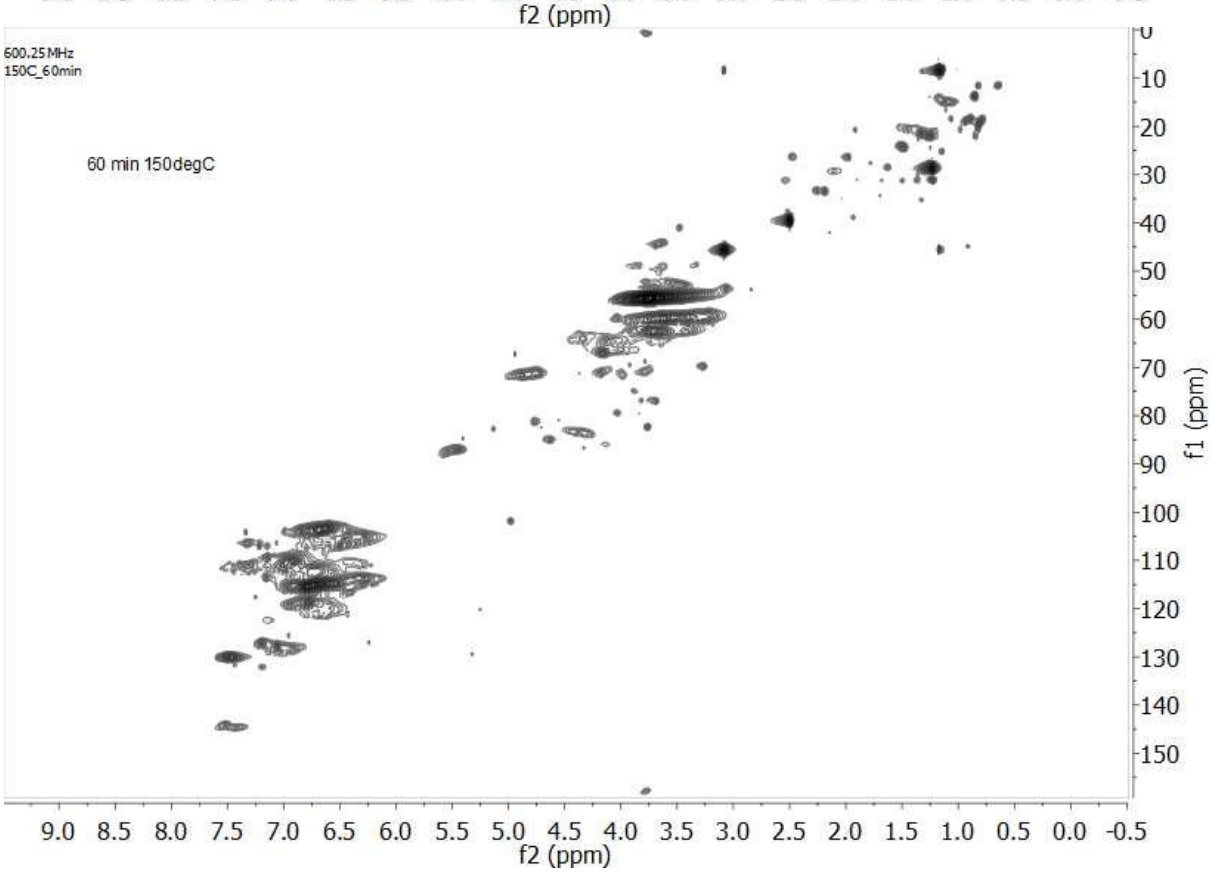

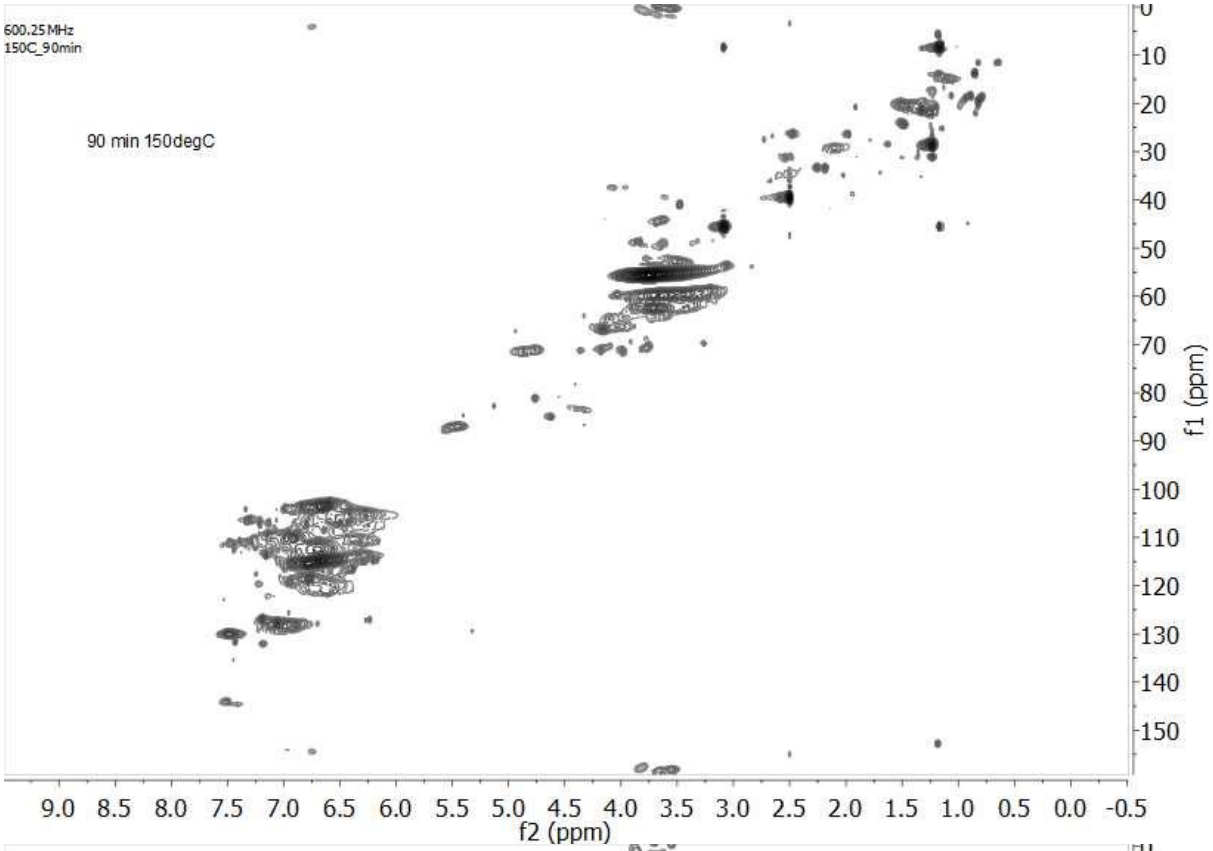
600.25 MHz
150C_90min
90 min 150degC
f1 (ppm)
f2 (ppm)

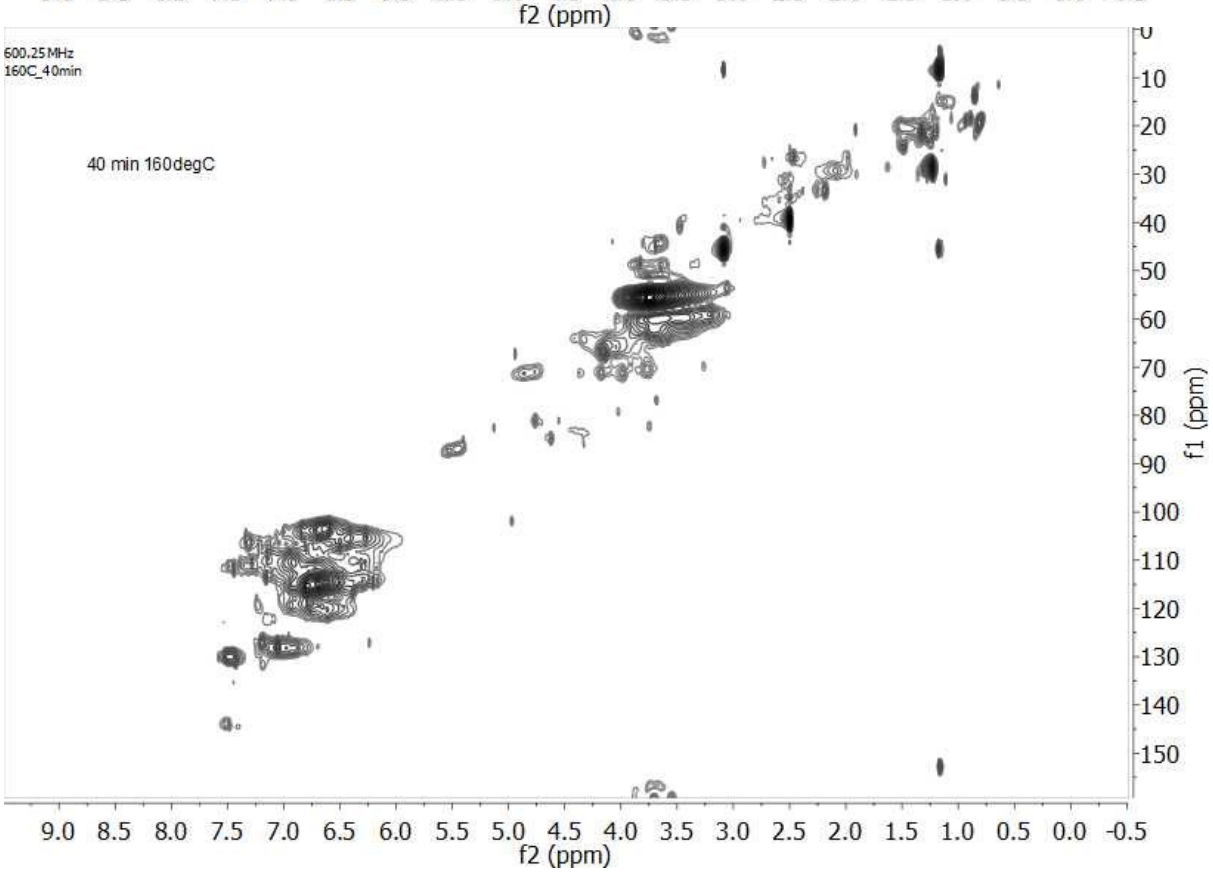
600.25 MHz
160C_40min
40 min 160degC
f1 (ppm)
f2 (ppm)

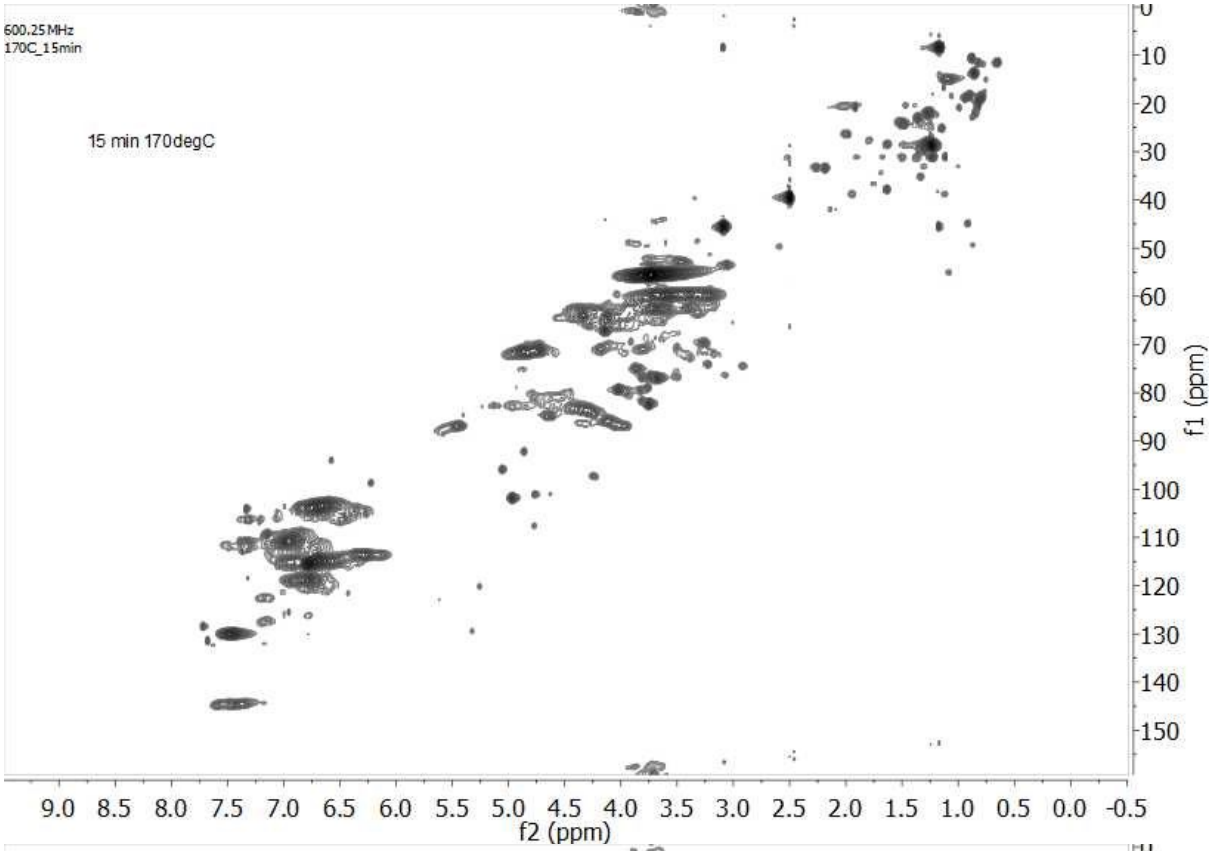
600.25 MHz
170C_15min
15 min 170degC
f1 (ppm)
f2 (ppm)

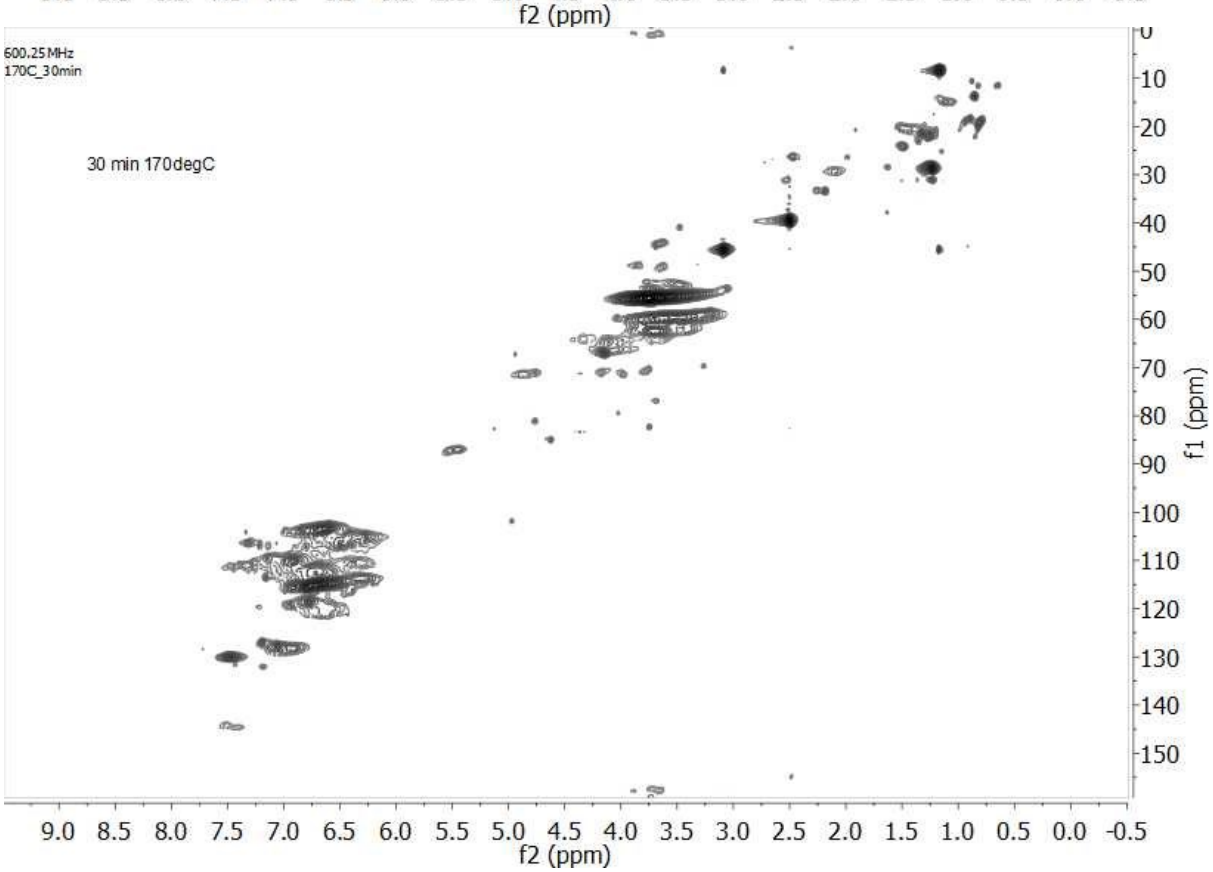
600.25 MHz
170C_30min
30 min 170degC
f1 (ppm)
f2 (ppm)

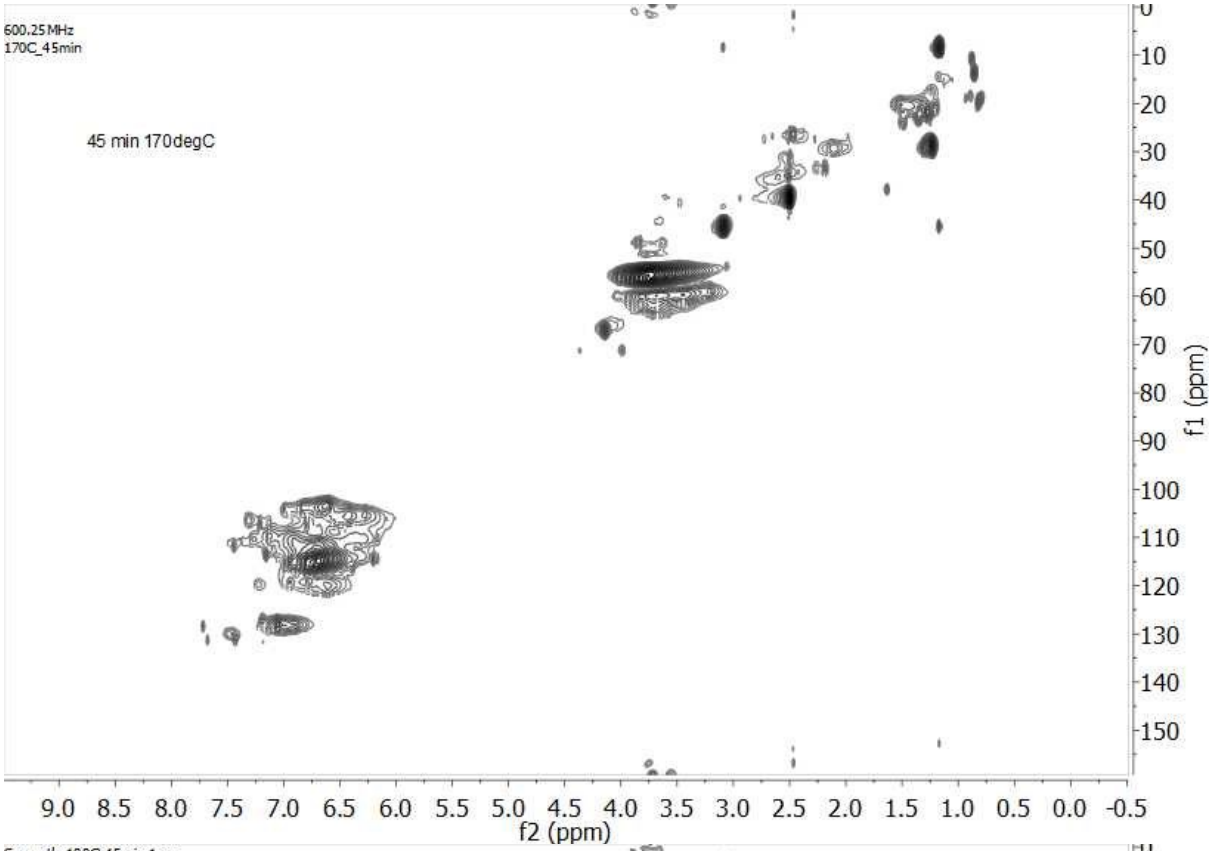
600.25 MHz
170C_45min
45 min 170degC
f1 (ppm)
f2 (ppm)

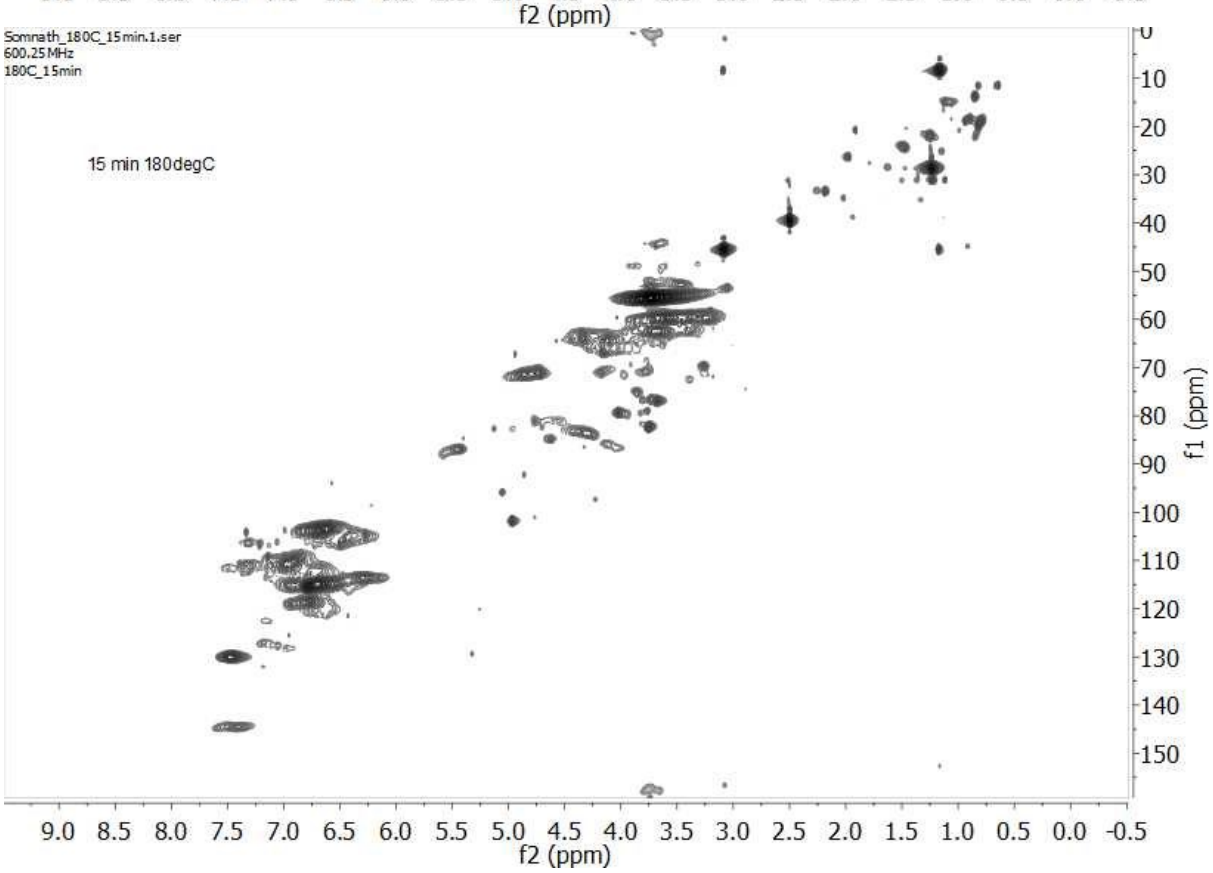
Somnath_180C_15min.1.ser
600.25 MHz
180C_15min
15 min 180degC
f1 (ppm)
f2 (ppm)

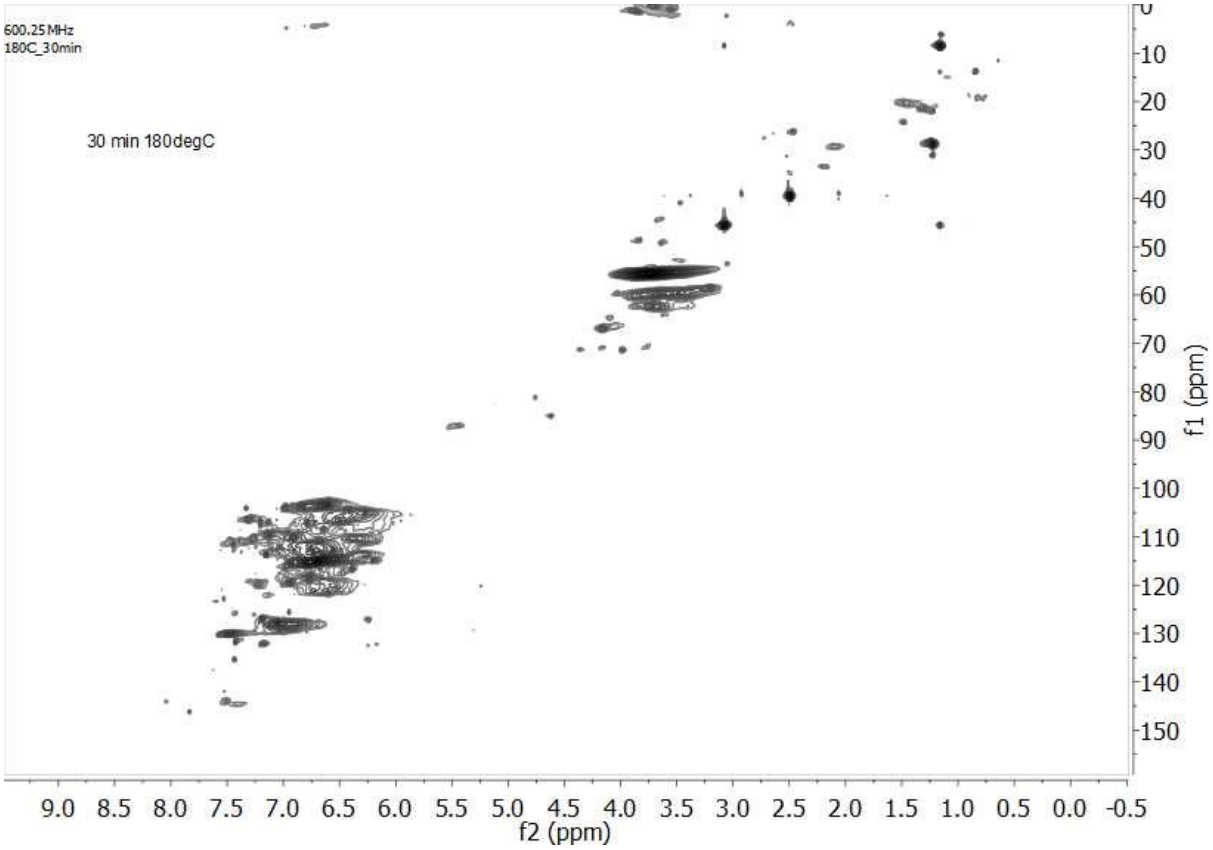

Pine [HC_4im][HSO_4], 10% biomass loading

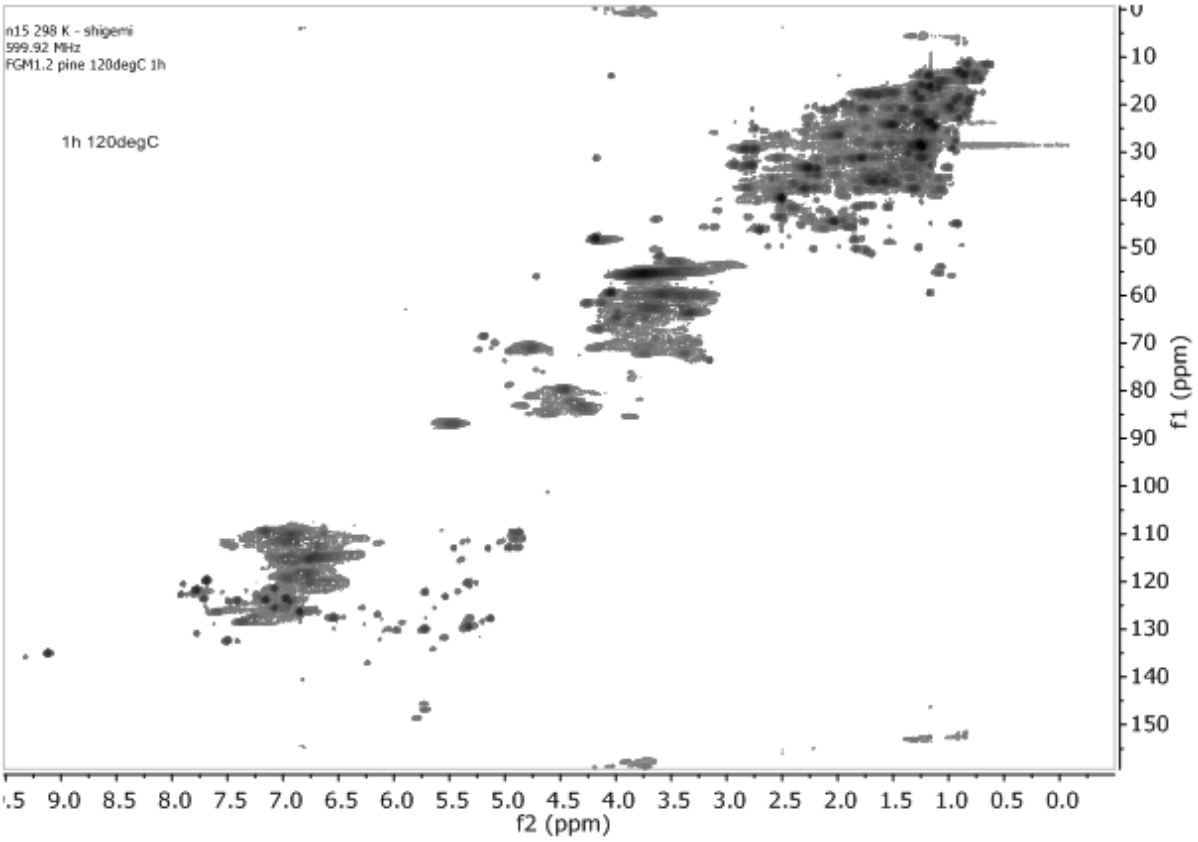

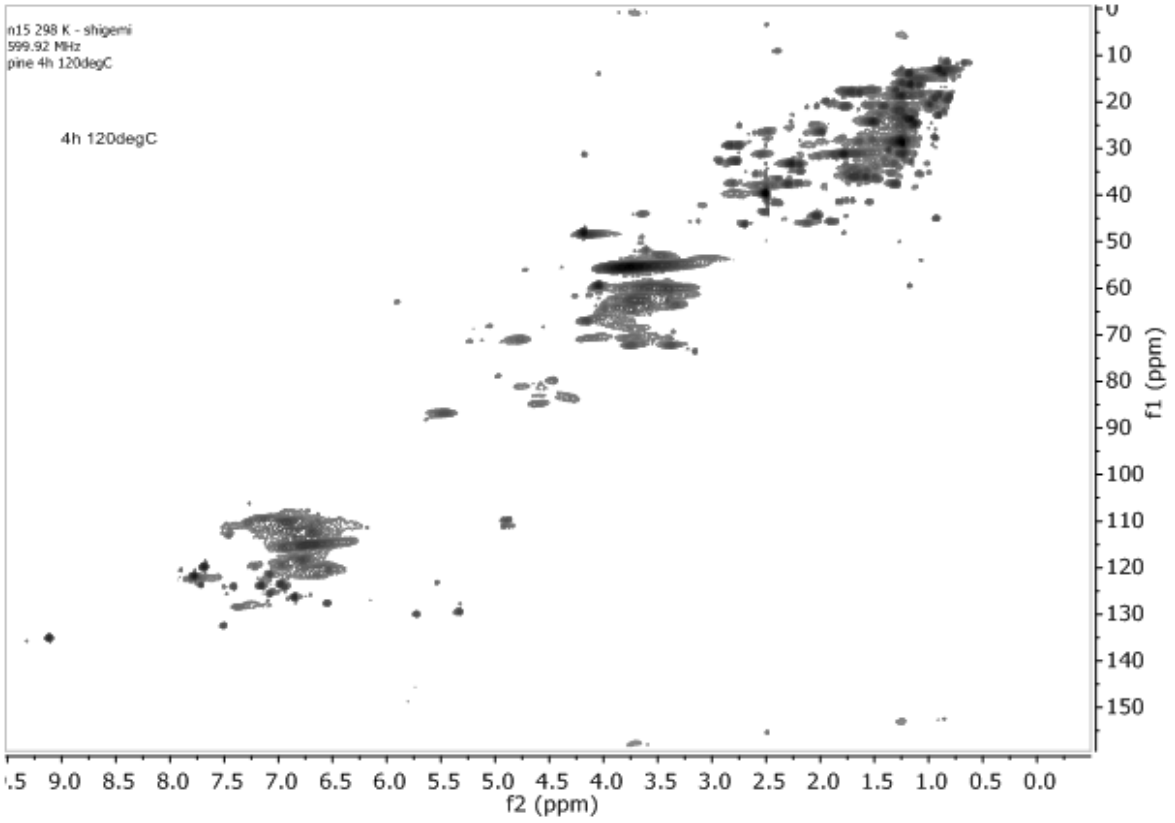
n15 298 K - shigemi
599.92 MHz
pine 4h 120degC
4h 120degC
f1 (ppm)
f2 (ppm)

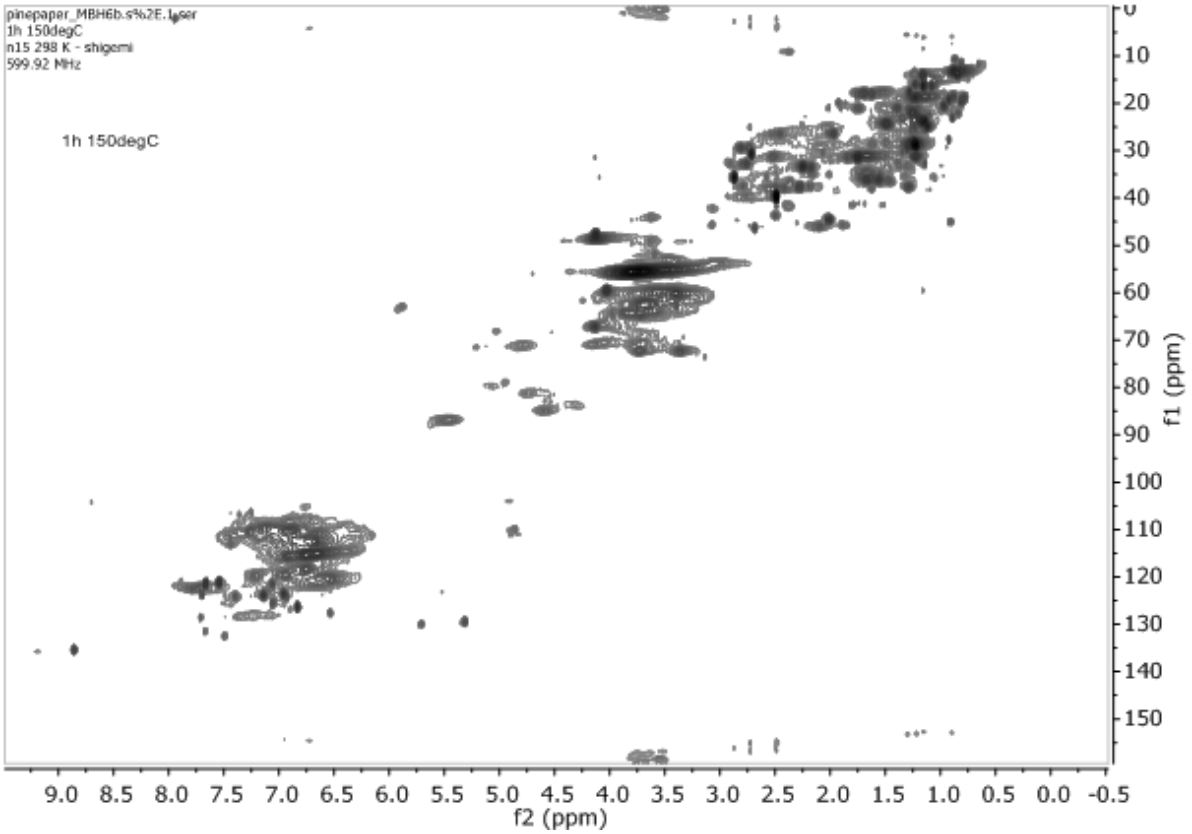
pinepaper_MBH6b.s%2E.ser
1h 150degC
n15 298 K - shigemi
599.92 MHz
1h 150degC
f1 (ppm)
f2 (ppm)

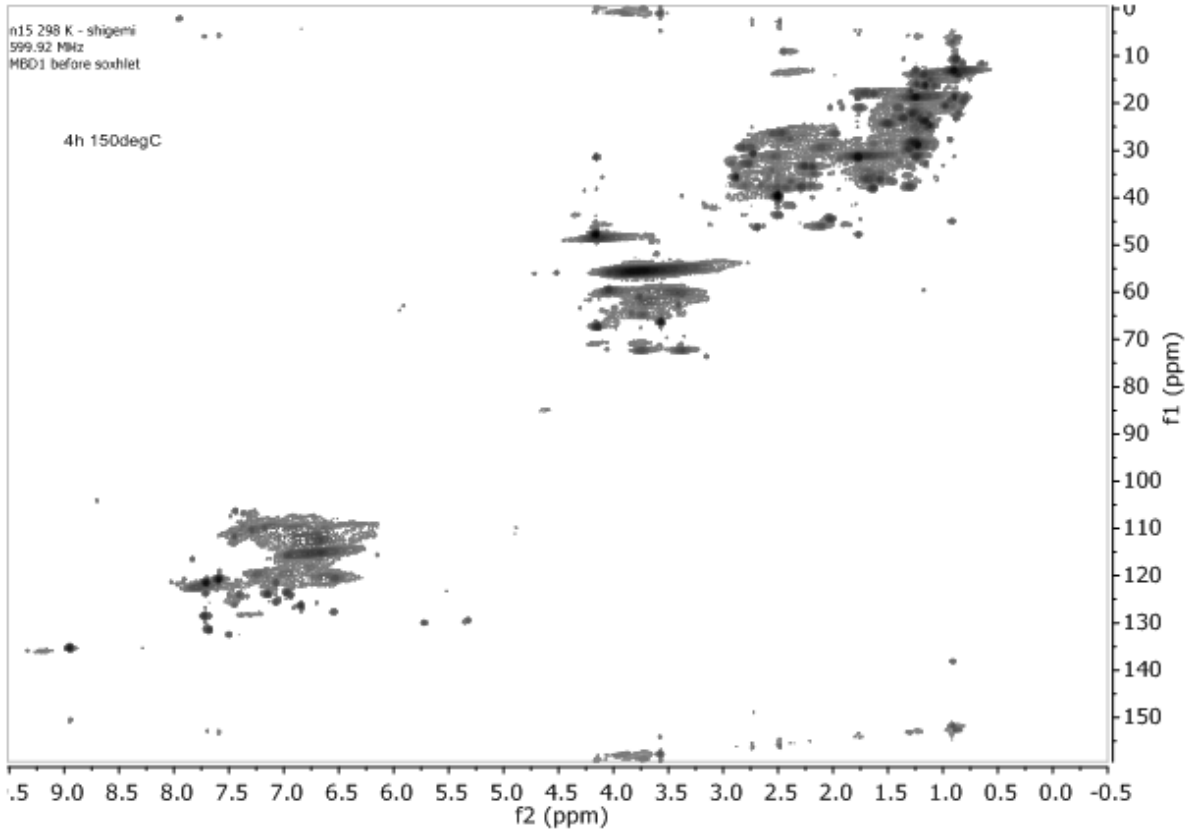
n15 298 K - shigemi
599.92 MHz
MBD1 before soxhlet
4h 150degC
f1 (ppm)
f2 (ppm)

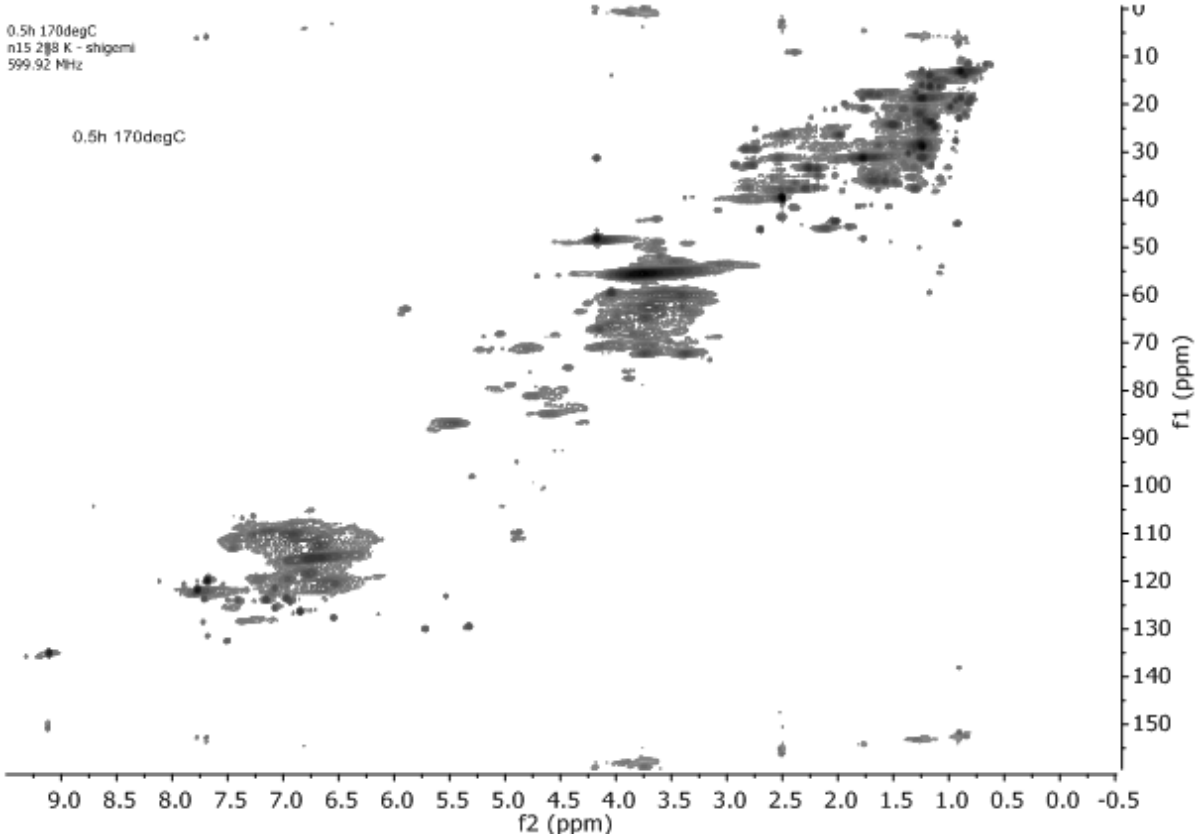
0.5h 170degC
n15 298 K - shigemi
599.92 MHz
0.5h 170degC
f1 (ppm)
f2 (ppm)

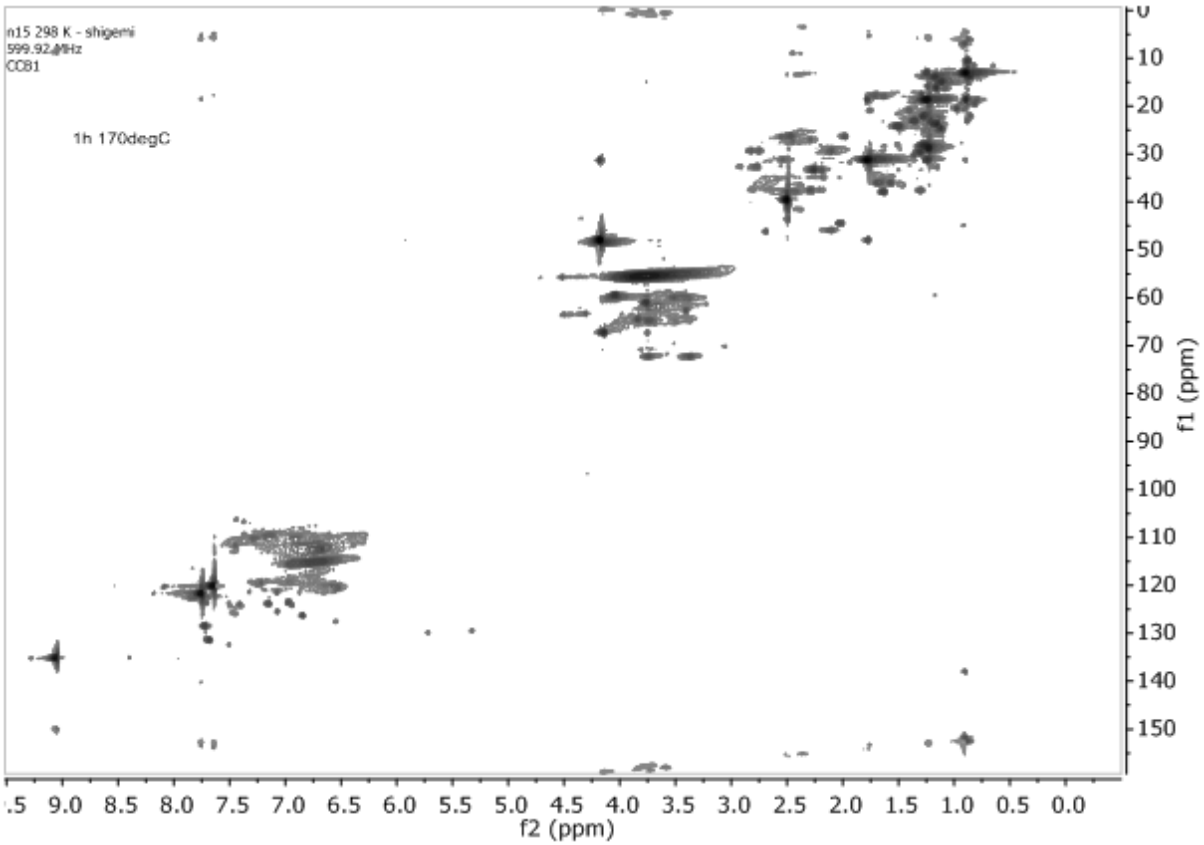

Pine [HC_4im][HSO_4], 5-50wt% loading

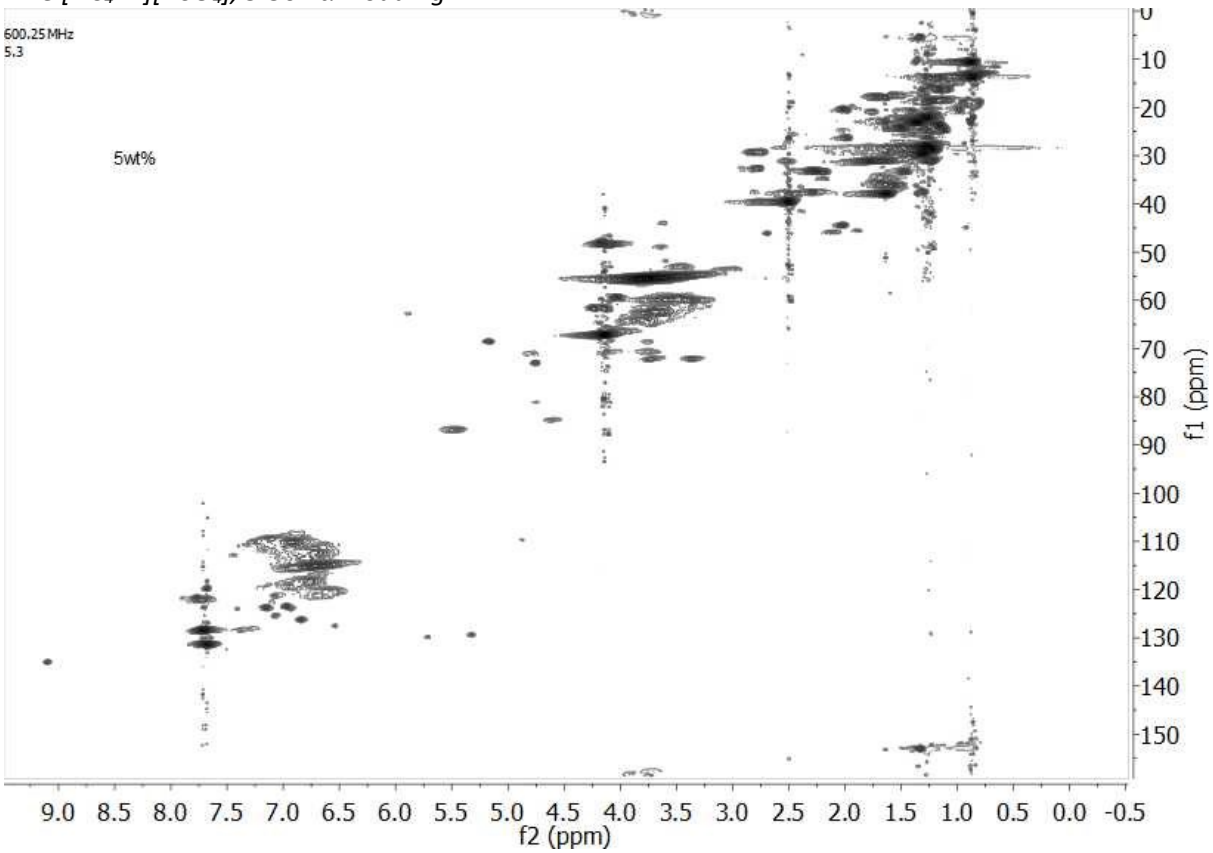

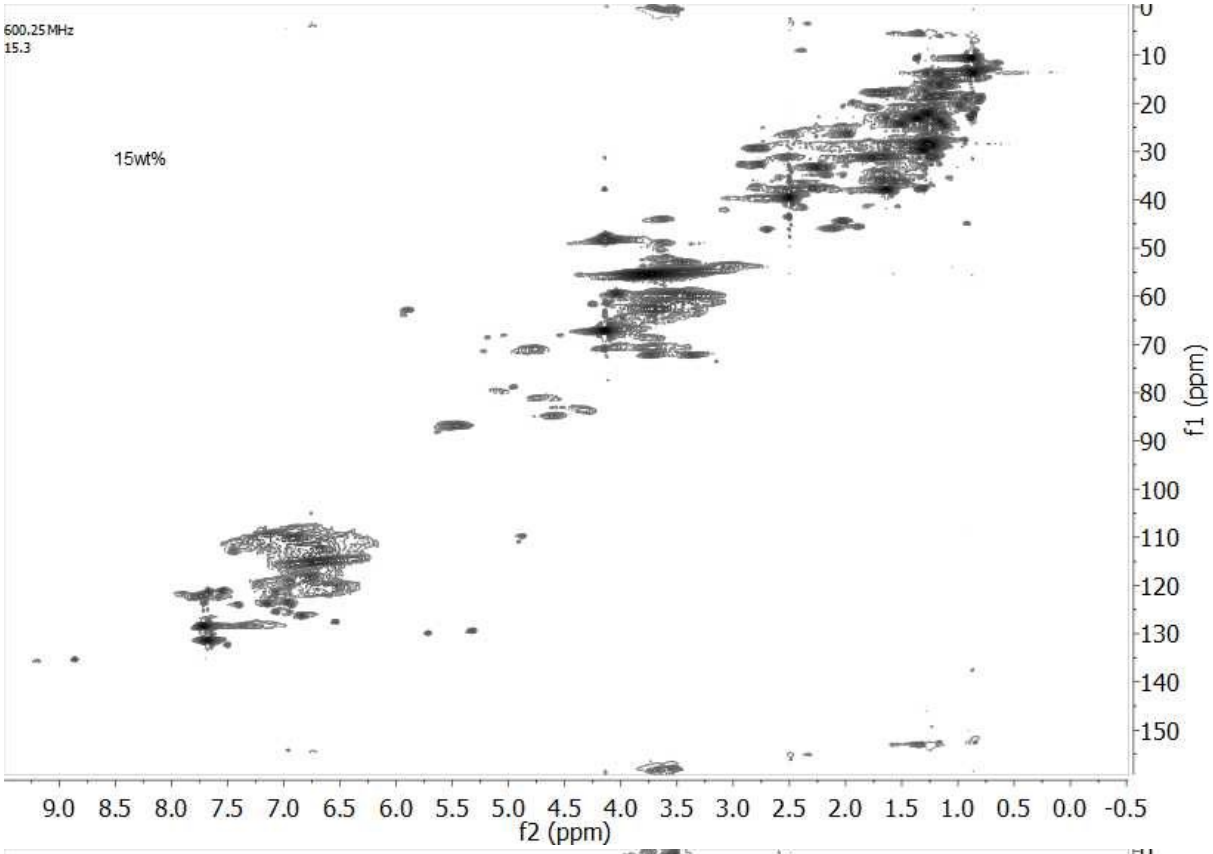
600.25 MHz
15.3
15wt%
f1 (ppm)
f2 (ppm)

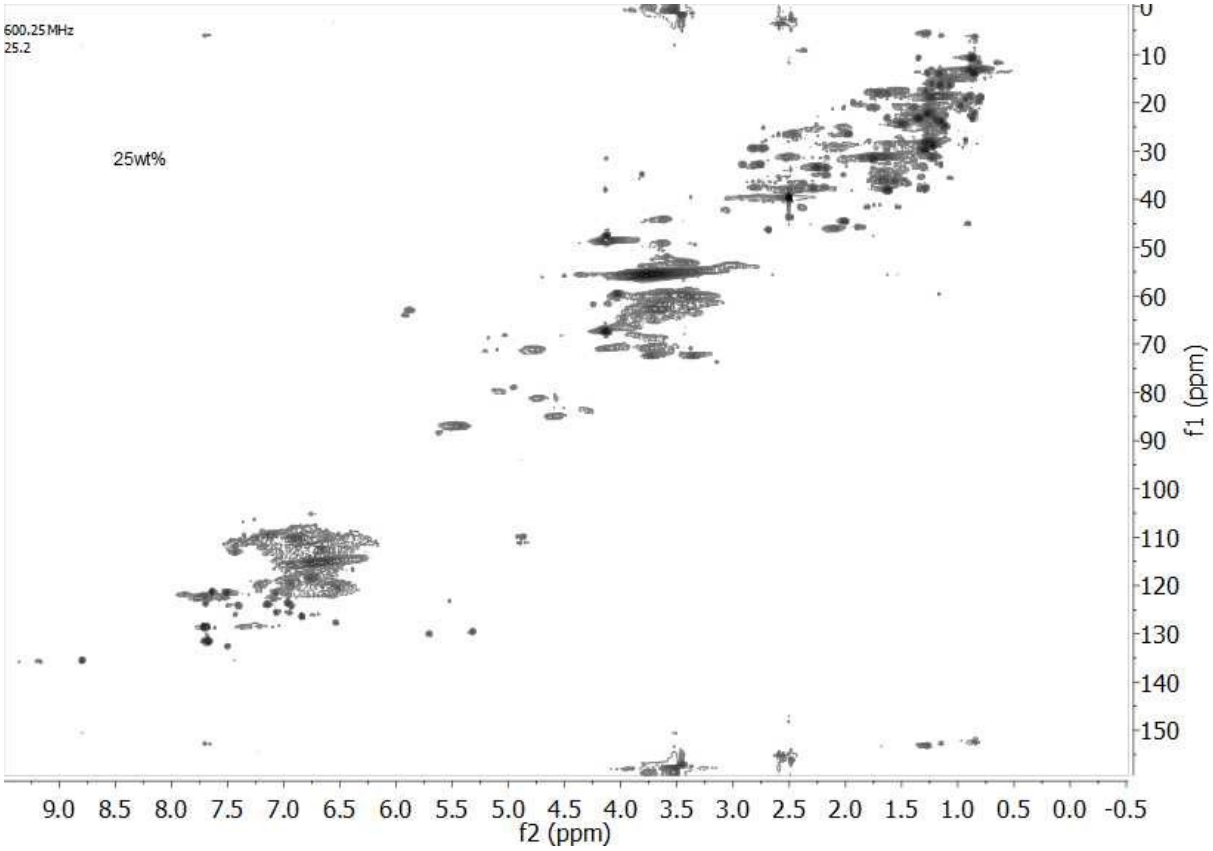
600.25 MHz
25.2
25wt%
f1 (ppm)
f2 (ppm)

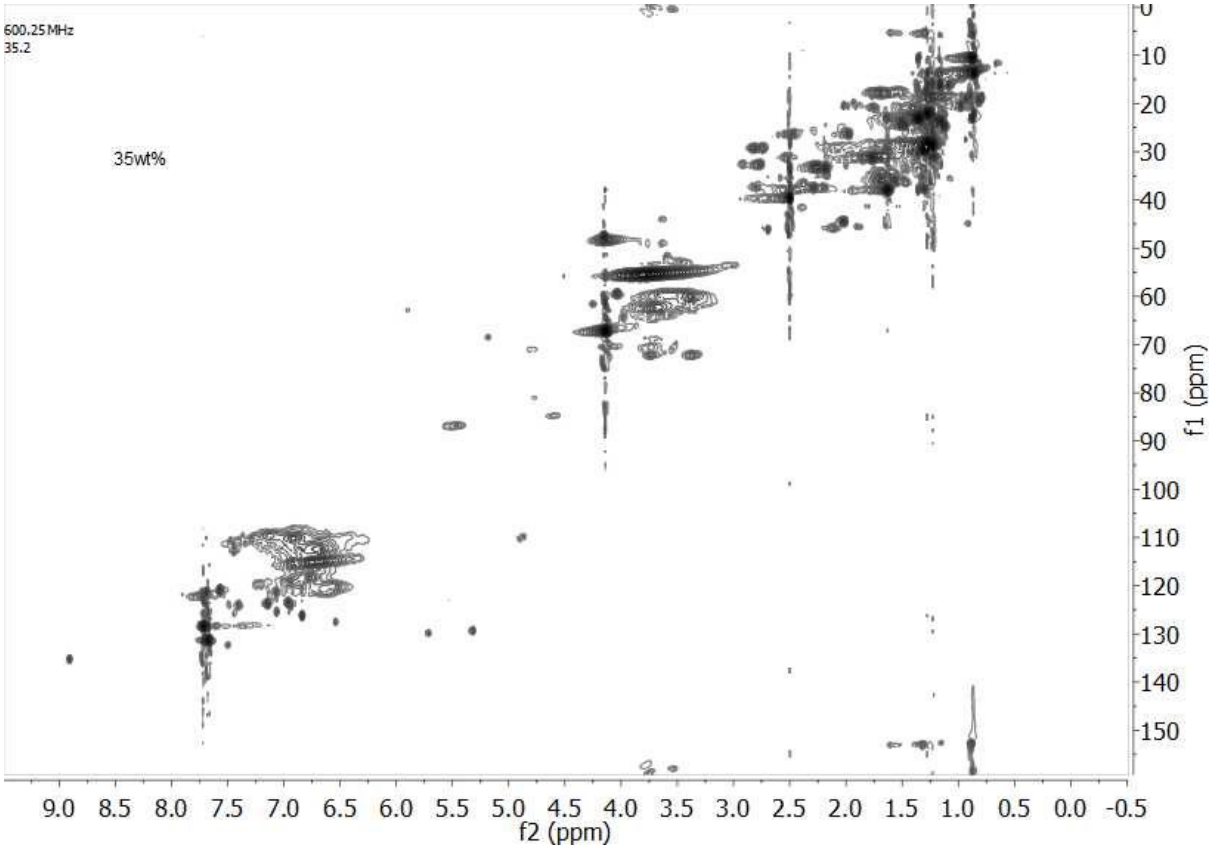
600.25 MHz
35.2
35wt%
f1 (ppm)
f2 (ppm)

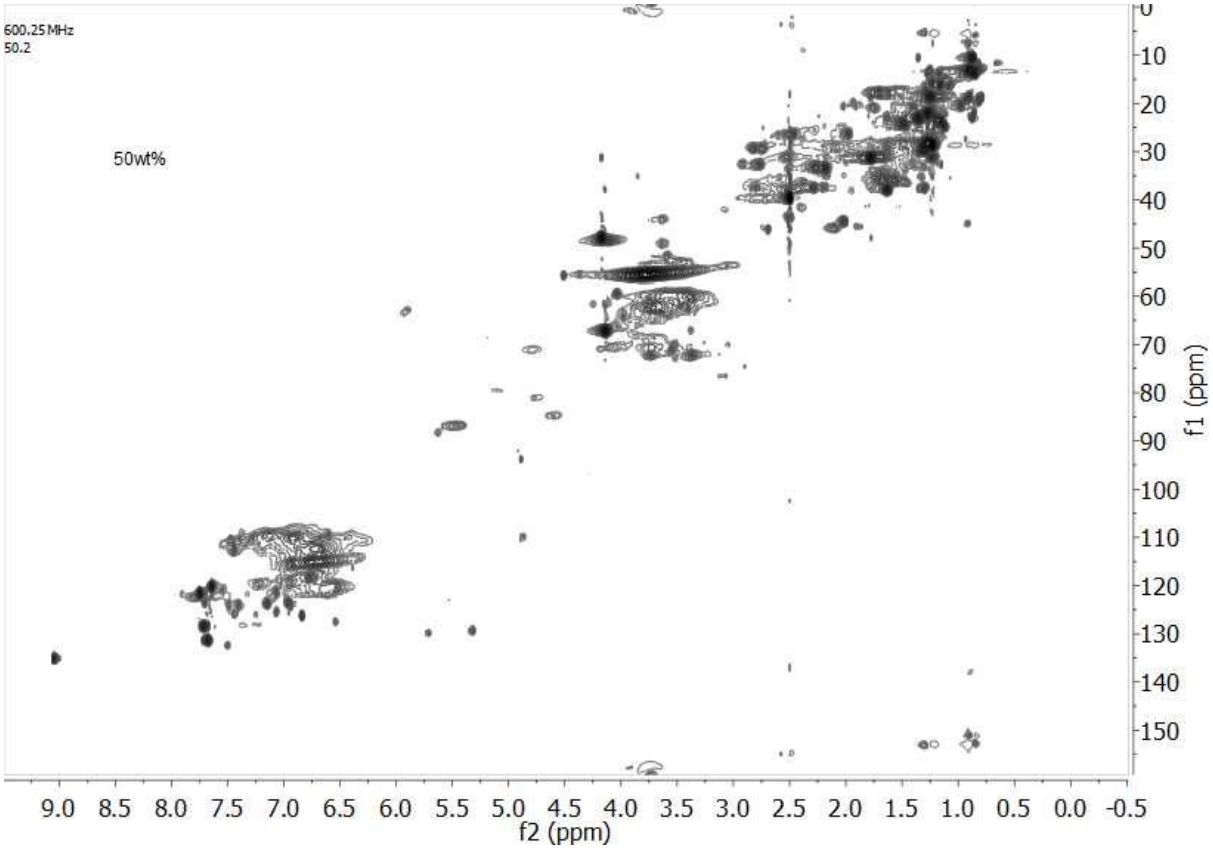
600.25 MHz
50.2
50wt%
f1 (ppm)
f2 (ppm)

Pine, IL Comparison

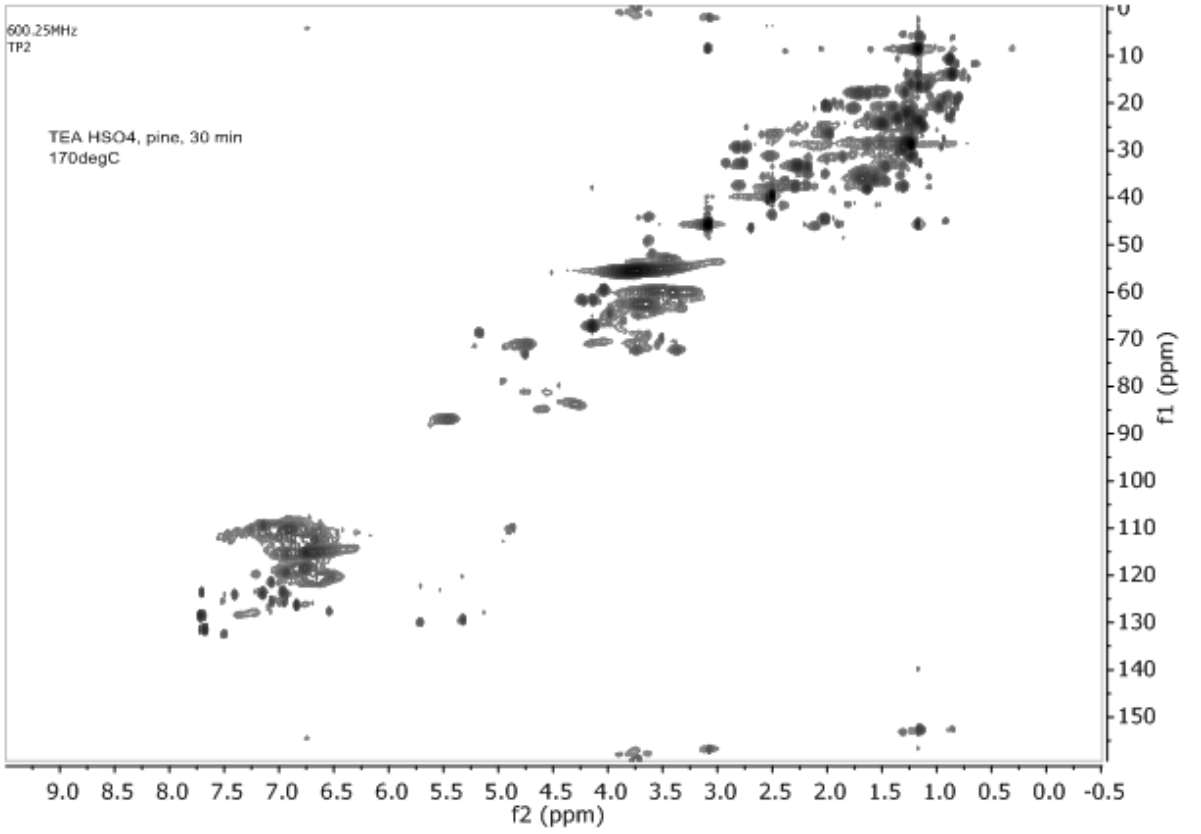

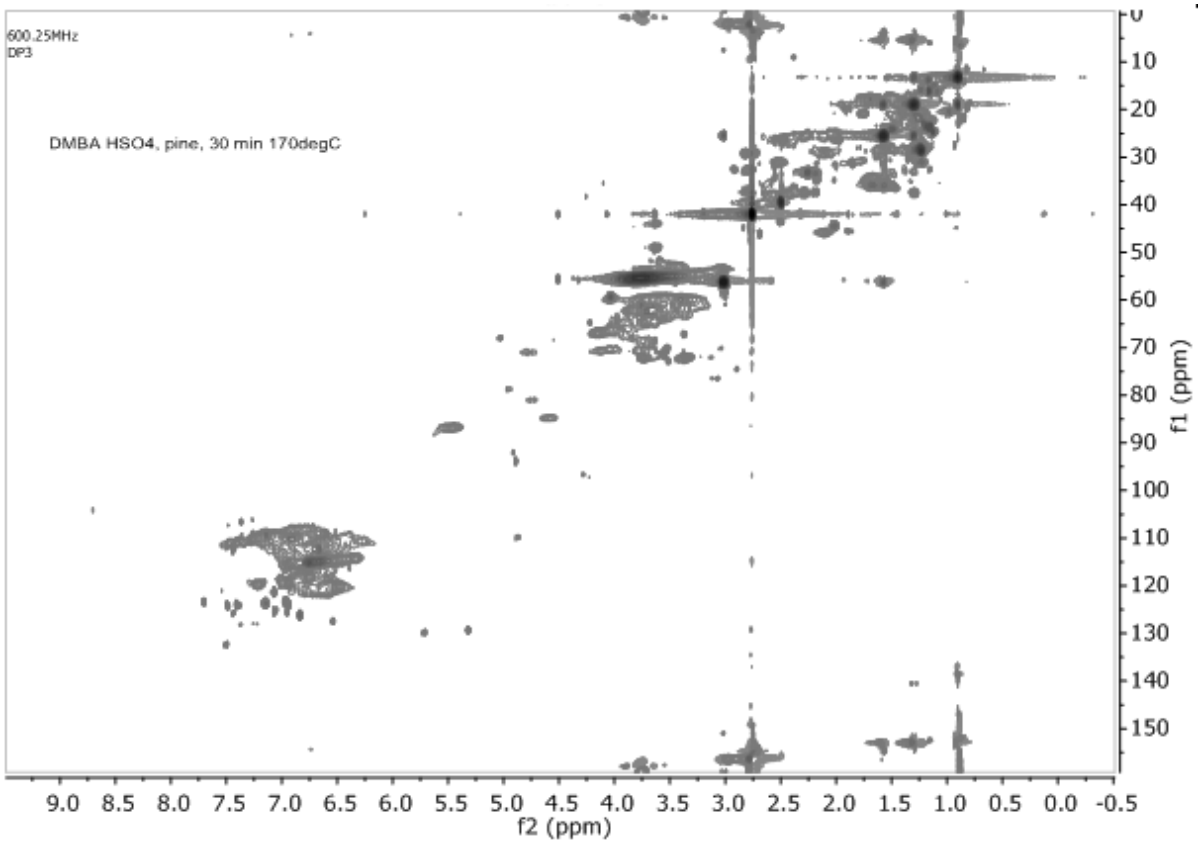

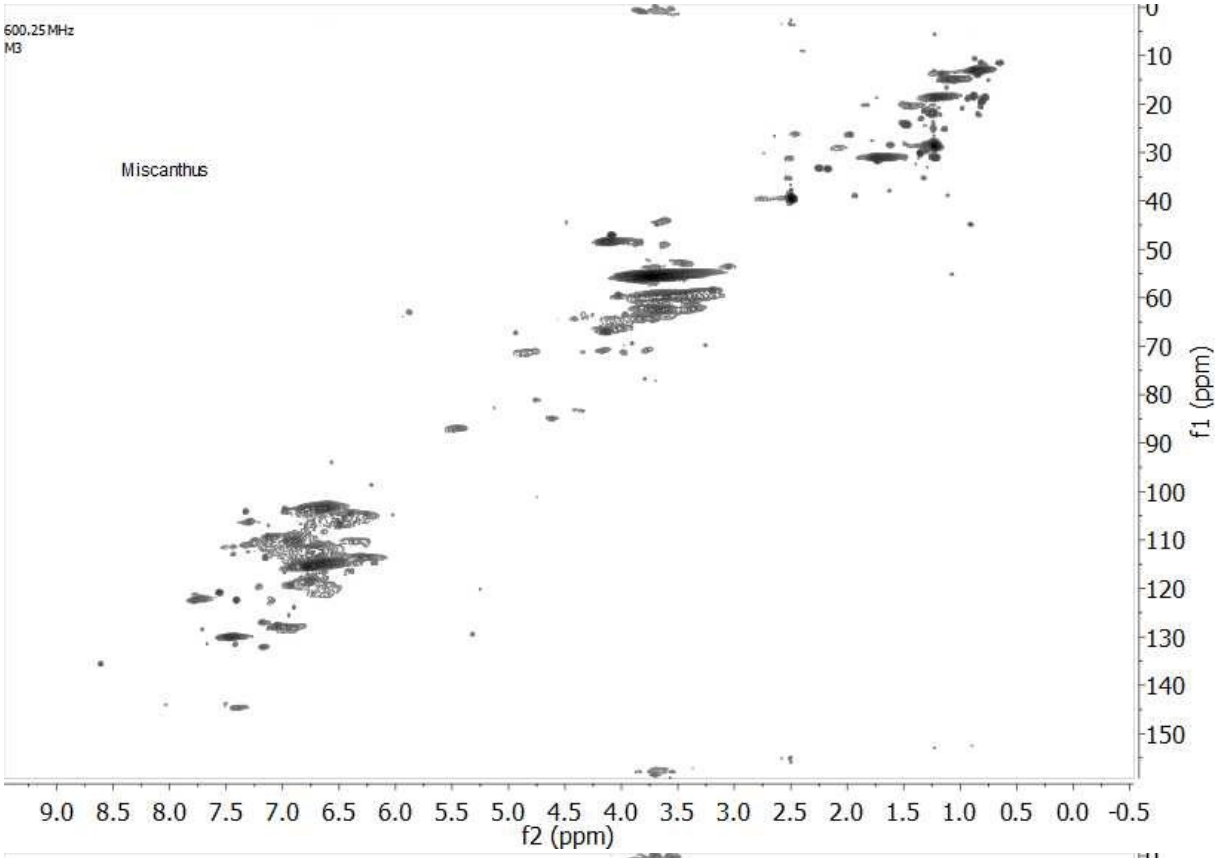
600.25 MHz
M3
Miscanthus
f1 (ppm)
f2 (ppm)

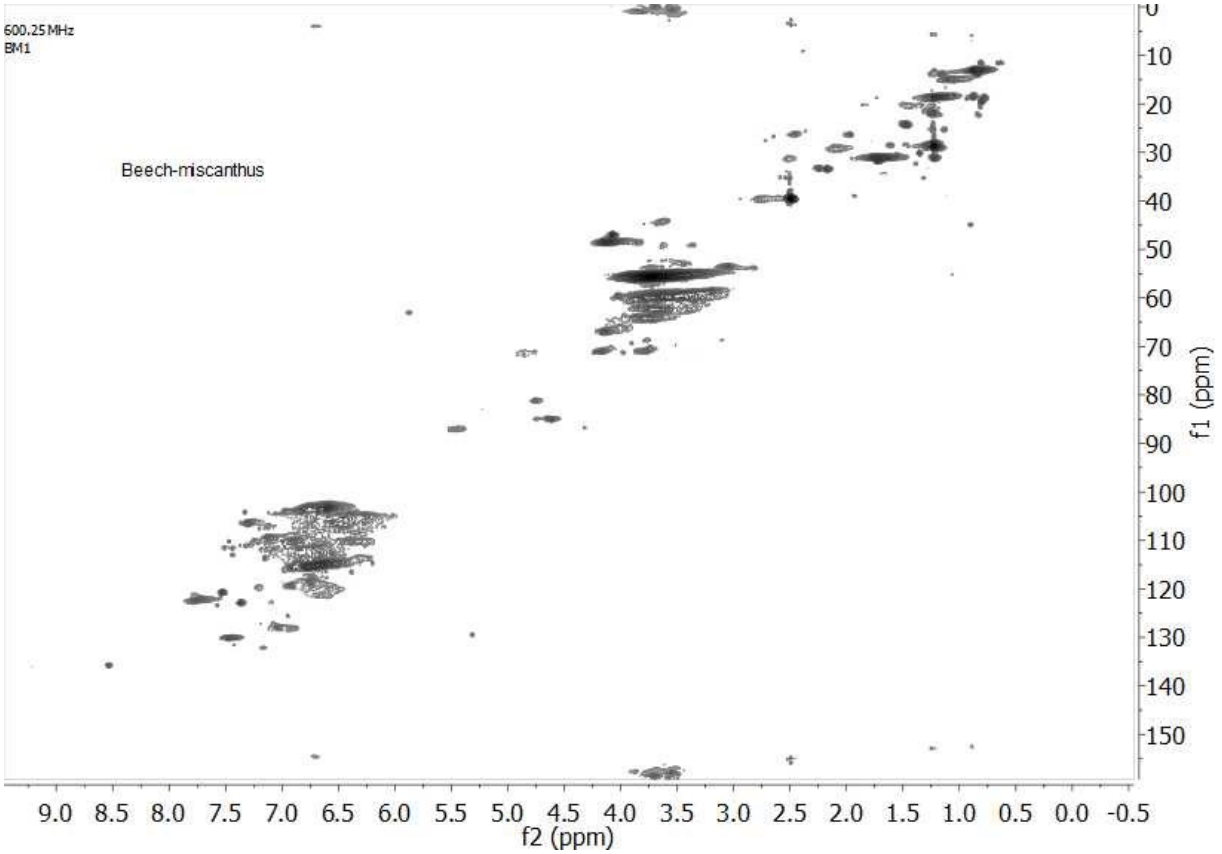
600.25 MHz
BM1
Beech-miscanthus
f1 (ppm)
f2 (ppm)

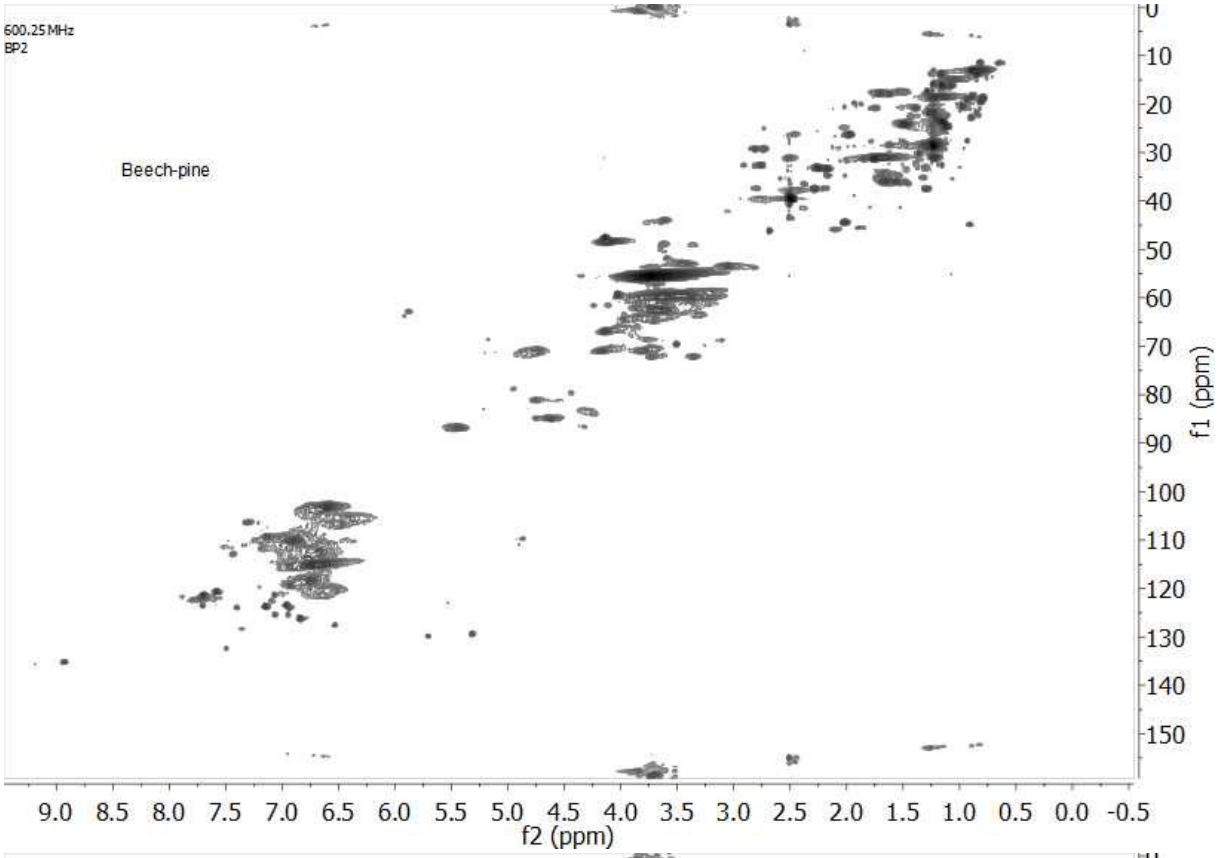
600.25 MHz
BP2
Beech-pine
f1 (ppm)
f2 (ppm)

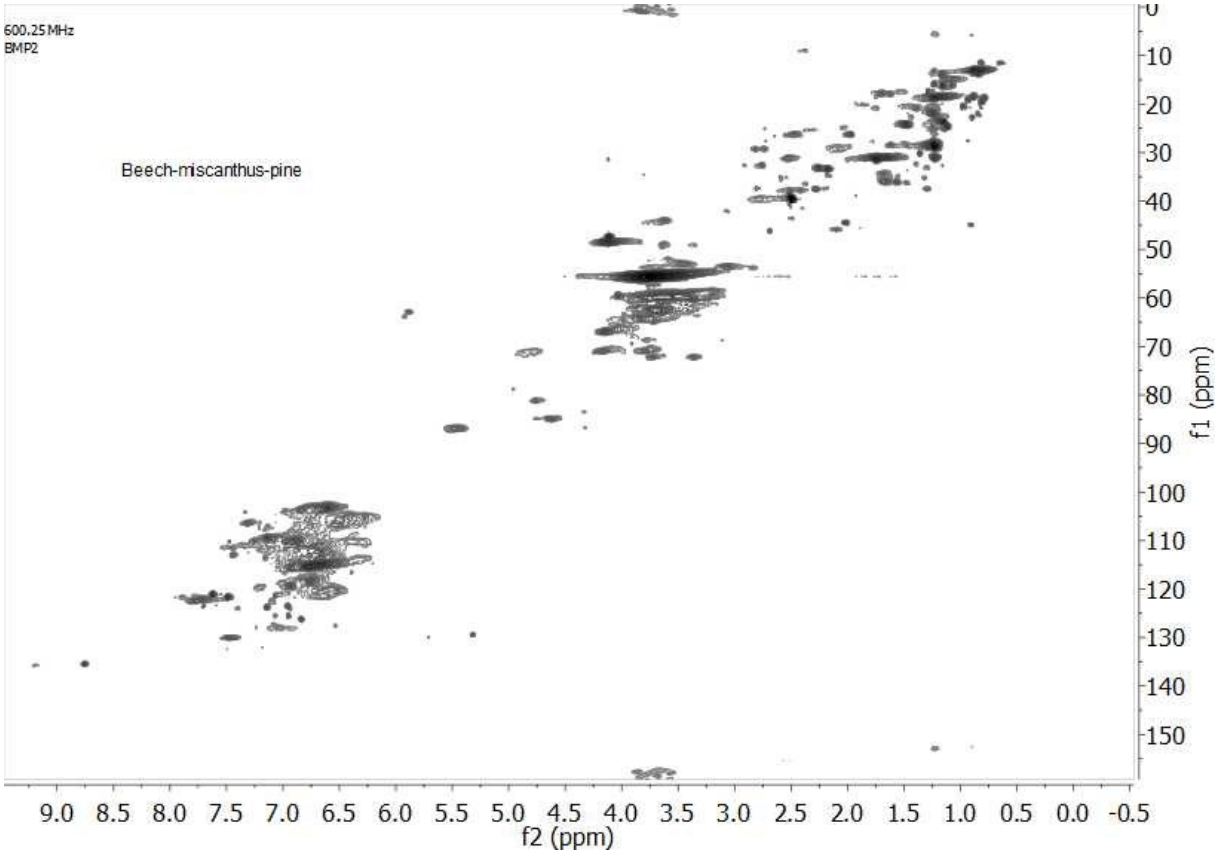
600.25 MHz
BMP2
Beech-miscanthus-pine
f1 (ppm)
f2 (ppm)

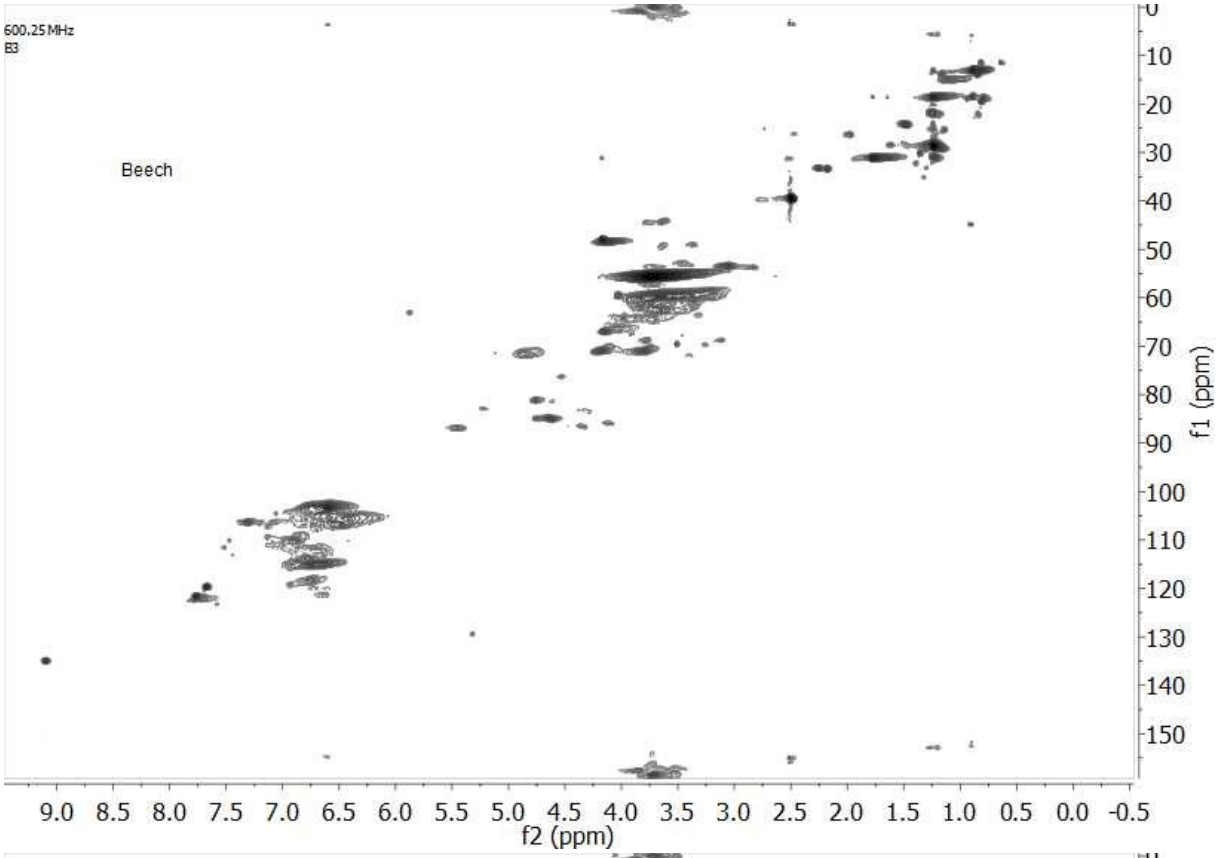
600.25 MHz
B3
Beech
f1 (ppm)
f2 (ppm)

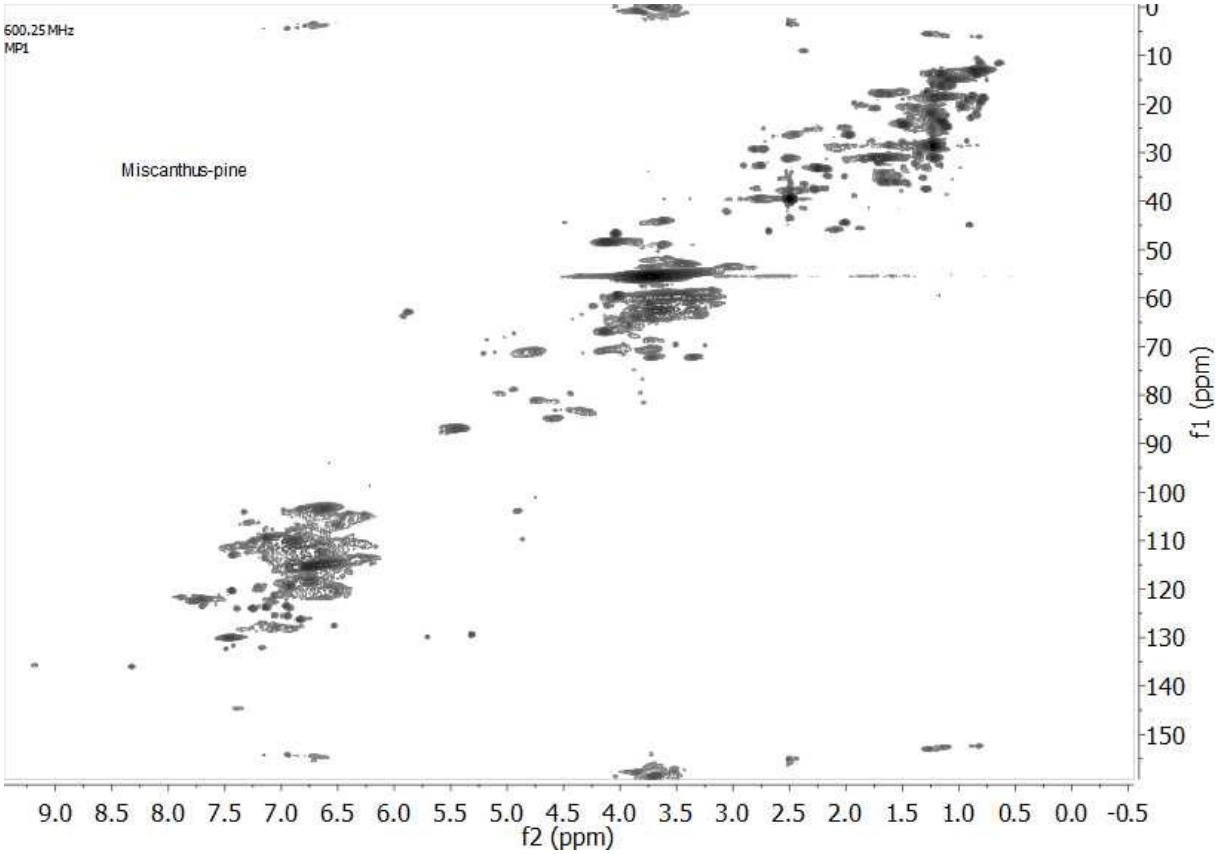
600.25 MHz
MP1
Miscanthus-pine
f1 (ppm)
f2 (ppm)

Lignin from recycling

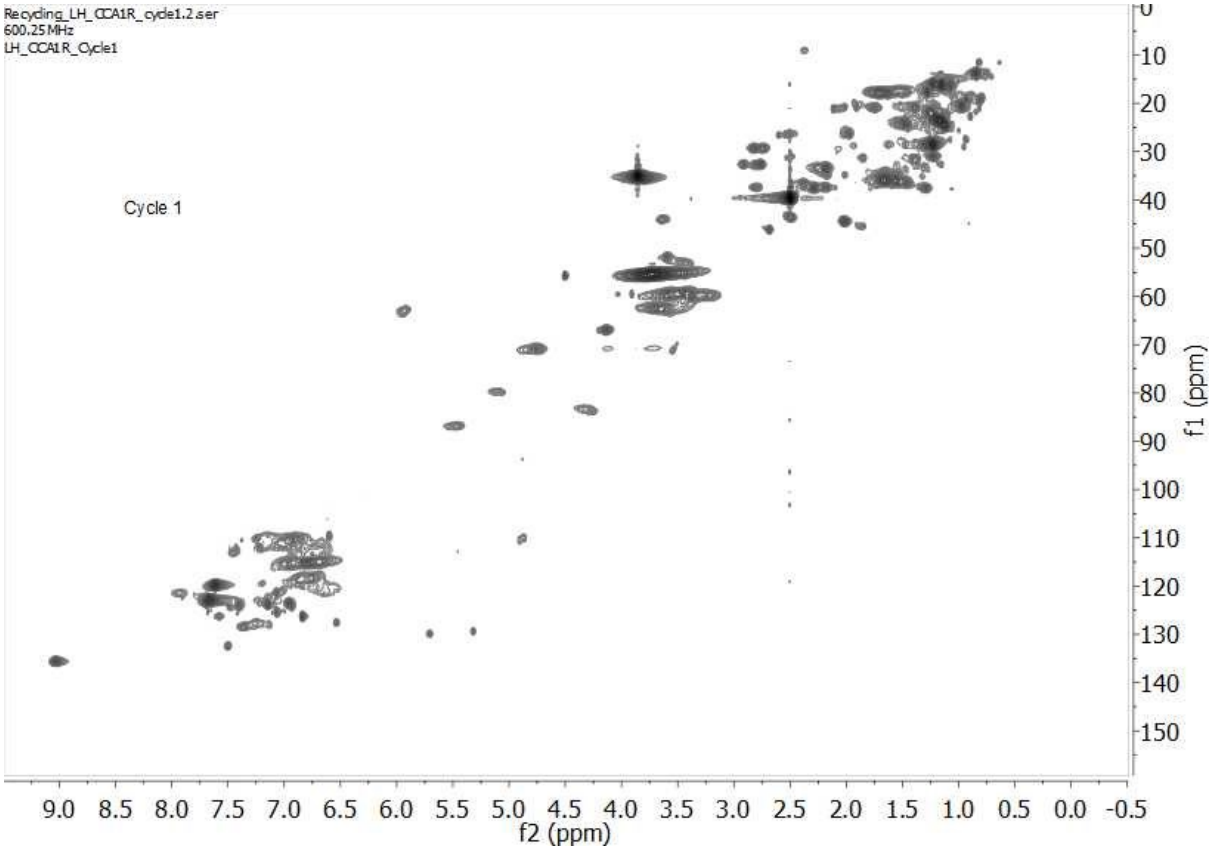

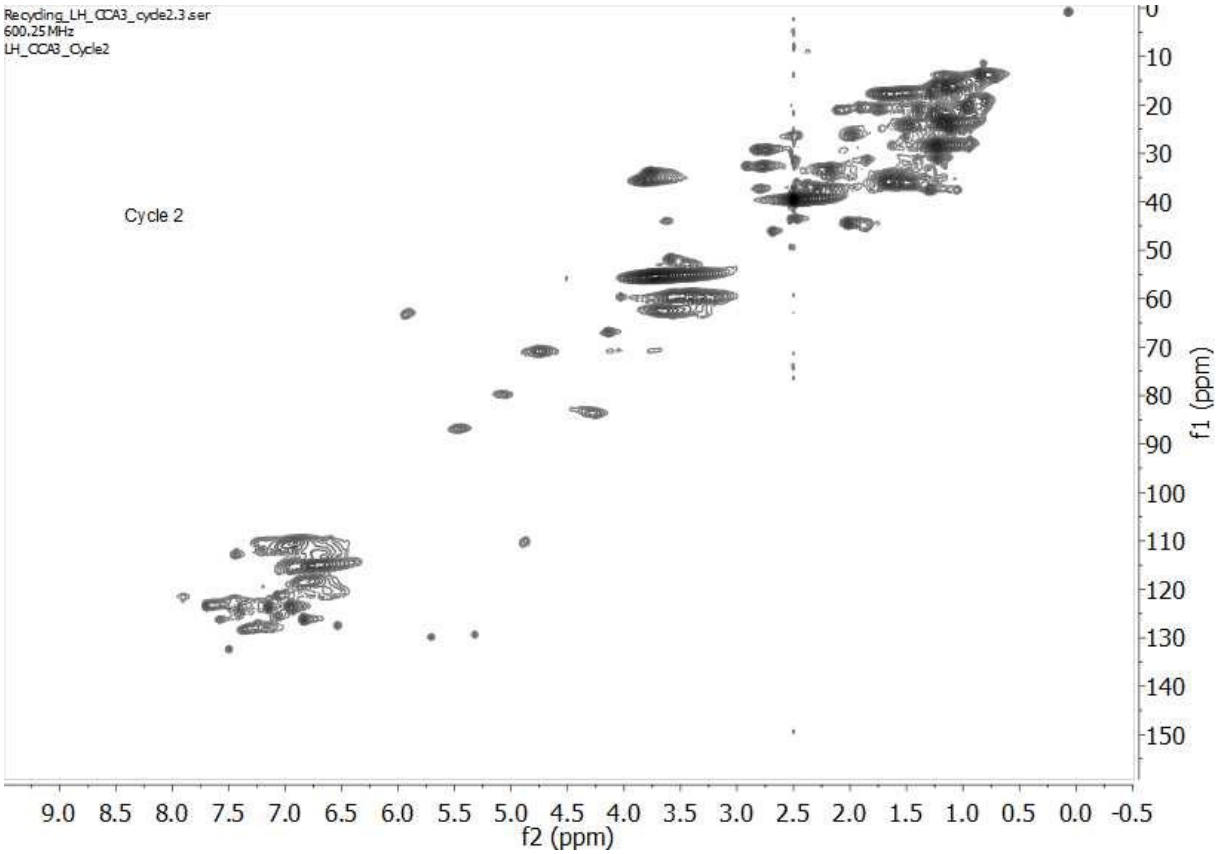

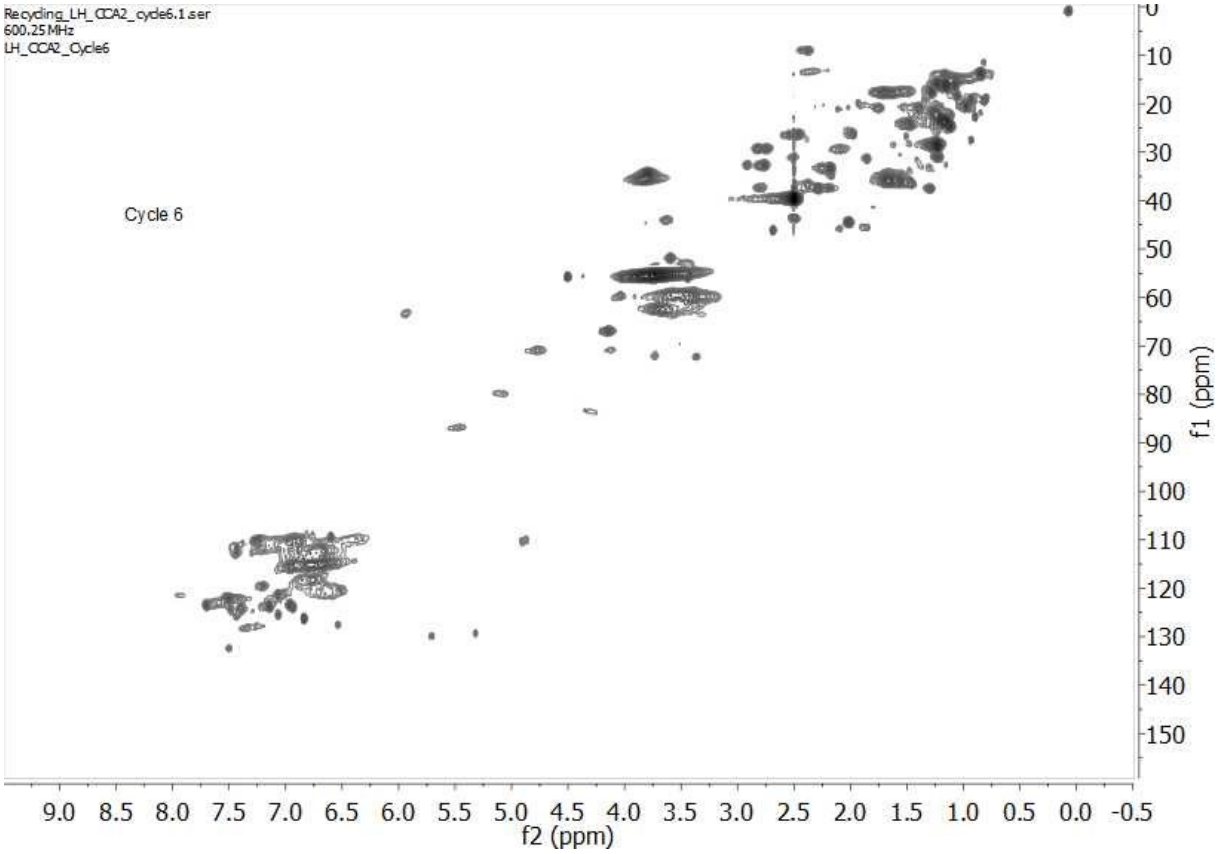
Recycling_LH_CCA2_cycle6.1.ser
600.25 MHz
LH_CCA2_Cycle6
Cycle 6
f1 (ppm)
f2 (ppm)

31P NMR

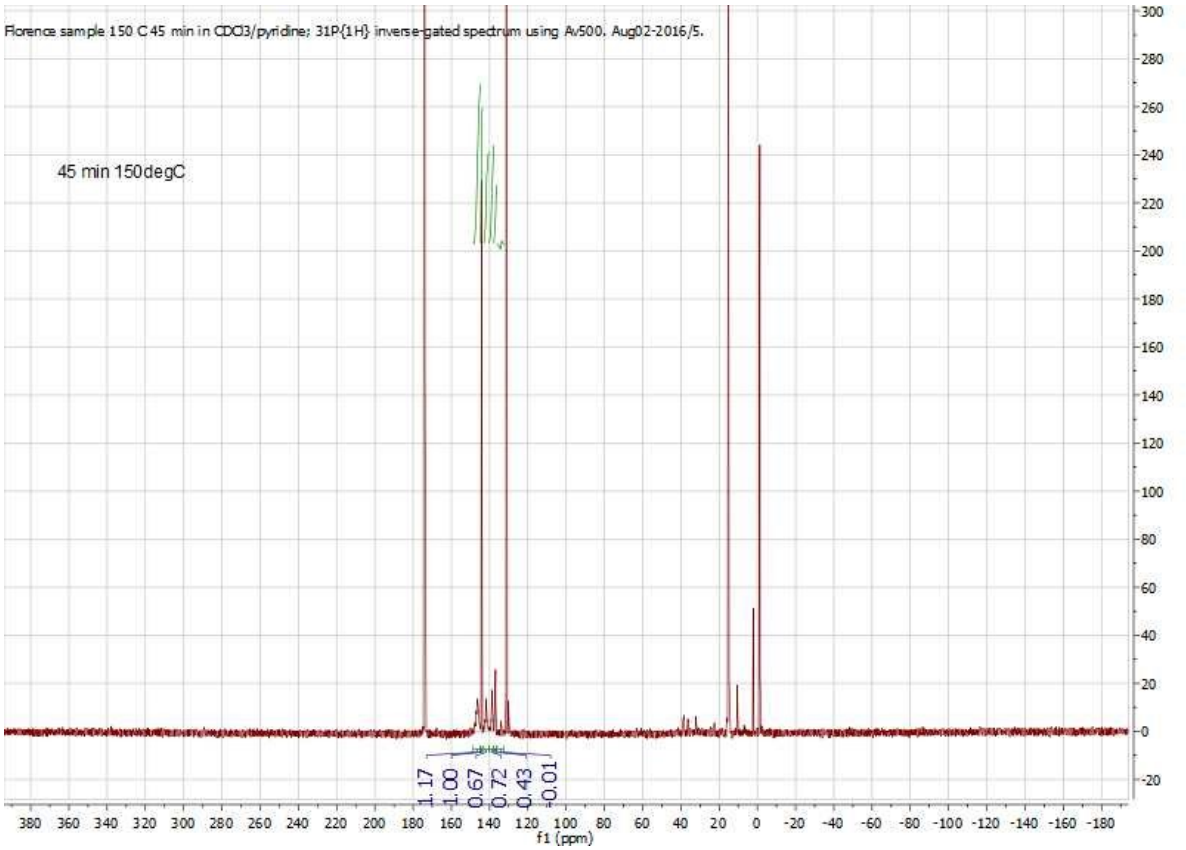
Florence sample 150 C 45 min in CDCl3/pyridine; 31P{1H} inverse-gated spectrum using Av500. Aug02-2016/5.
45 min 150degC
1.17
1.00
0.67
0.72
0.43
0.01
f1 (ppm)

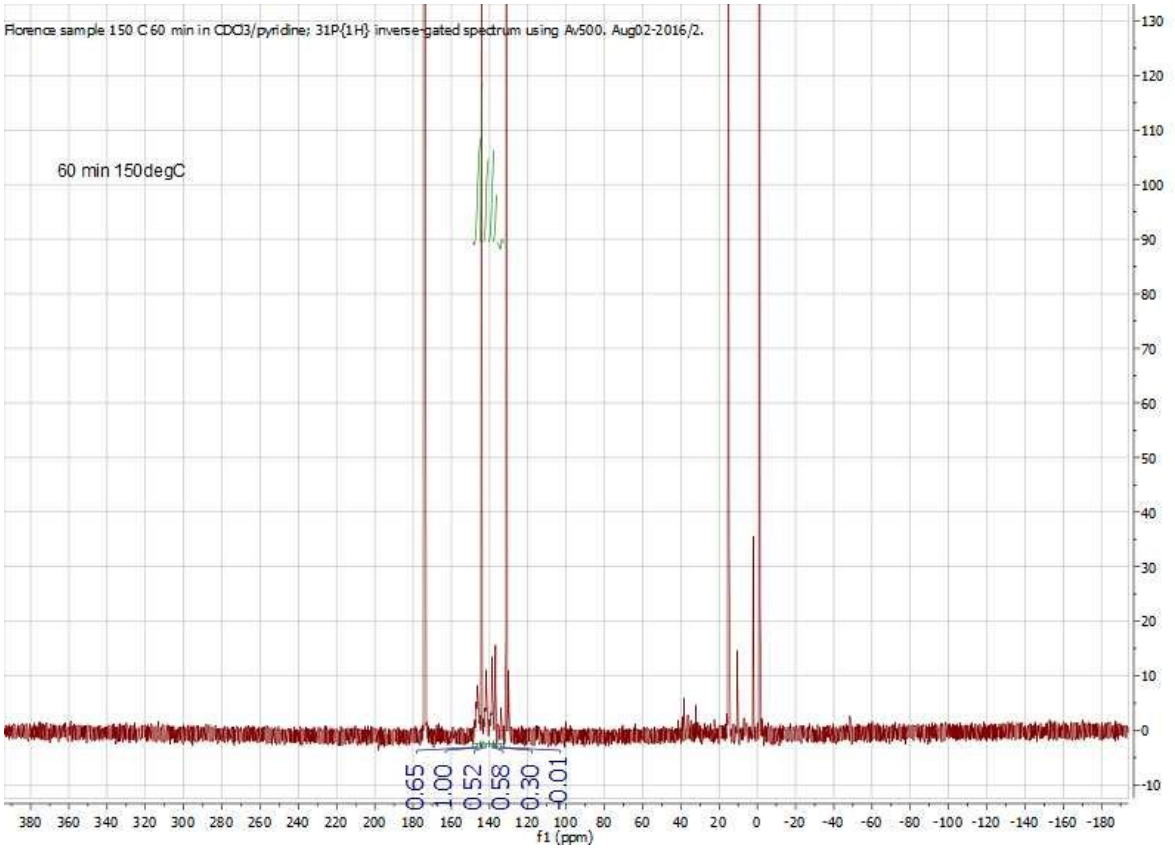
Florence sample 150 C 60 min in CDCl3/pyridine; 31P{1H} inverse-gated spectrum using Av500. Aug02-2016/2.
60 min 150degC
0.65
1.00
0.52
0.58
0.30
0.01
f1 (ppm)

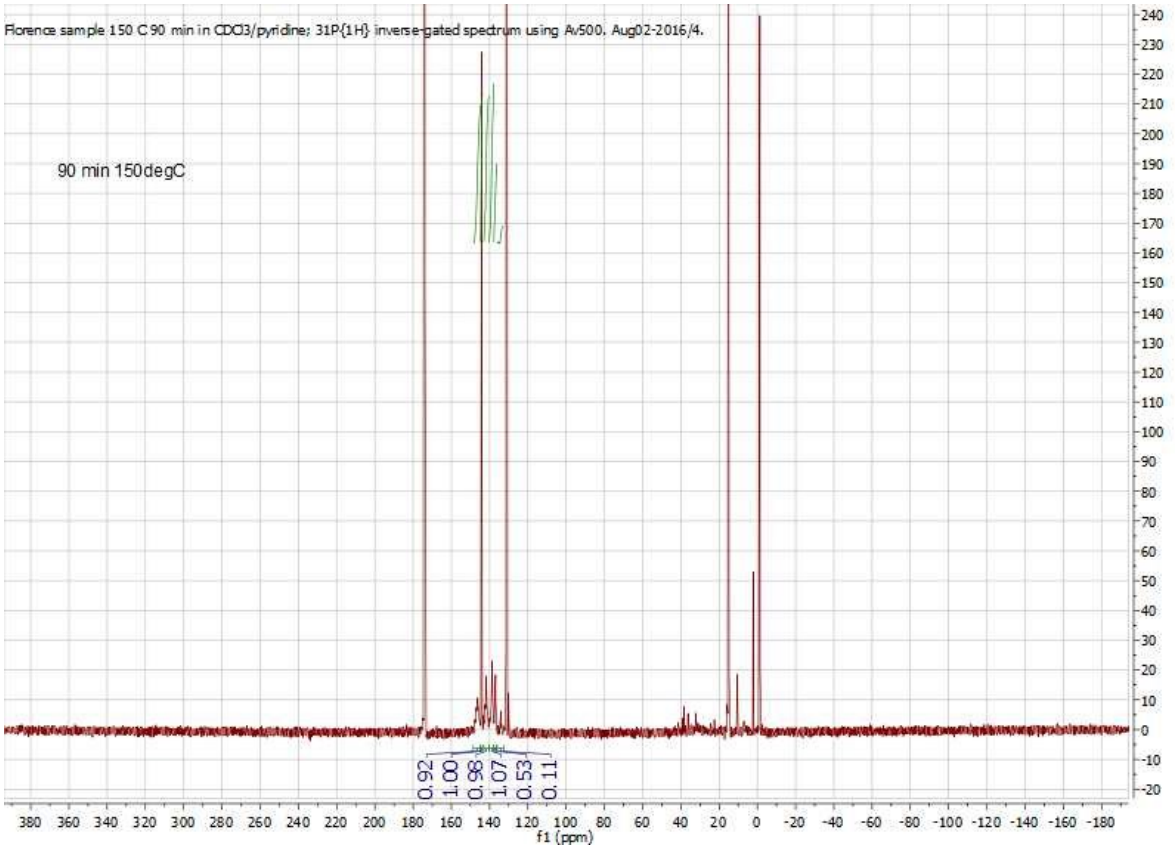
Florence sample 150 C 90 min in CDCl3/pyridine; 31P{1H} inverse-gated spectrum using Av500. Aug02-2016/4.
90 min 150degC
0.92
1.00
0.98
1.07
0.53
0.11
f1 (ppm)

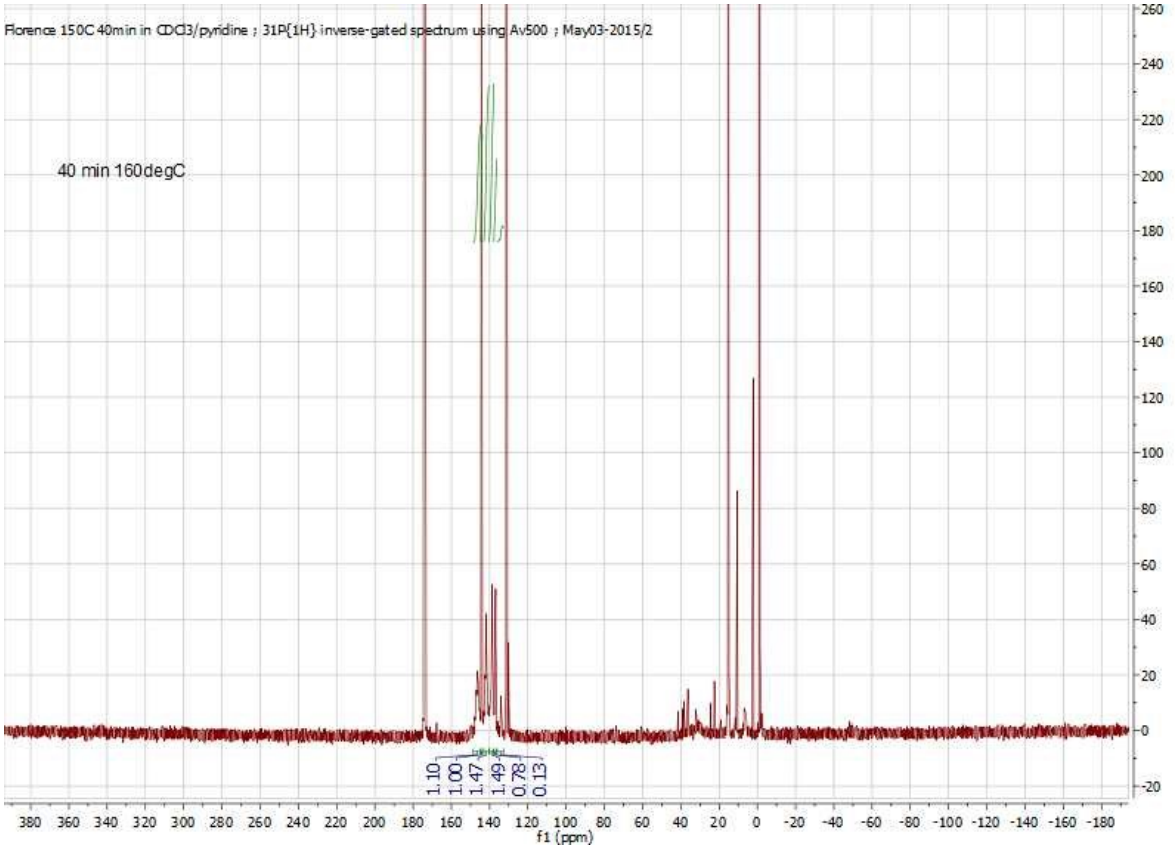
Florence 150C 40min in CDCl3/pyridine ; 31P{1H} inverse-gated spectrum using Av500 ; May03-2015/2
40 min 160degC
1.10
1.00
1.47
1.49
0.78
0.13
f1 (ppm)

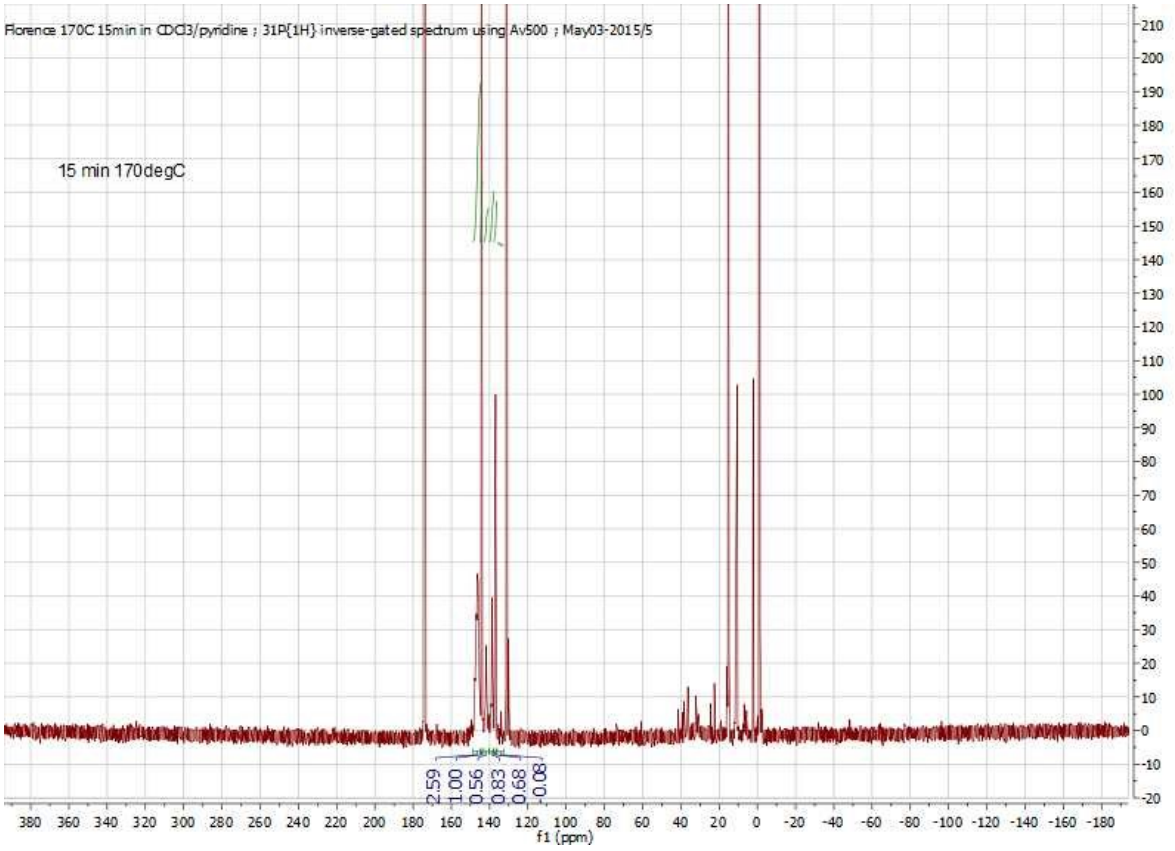
Florence 170C 15min in CDCl3/pyridine ; 31P{1H} inverse-gated spectrum using Av500 ; May03-2015/5
15 min 170degC
2.59
1.00
0.56
0.83
0.68
0.08
f1 (ppm)

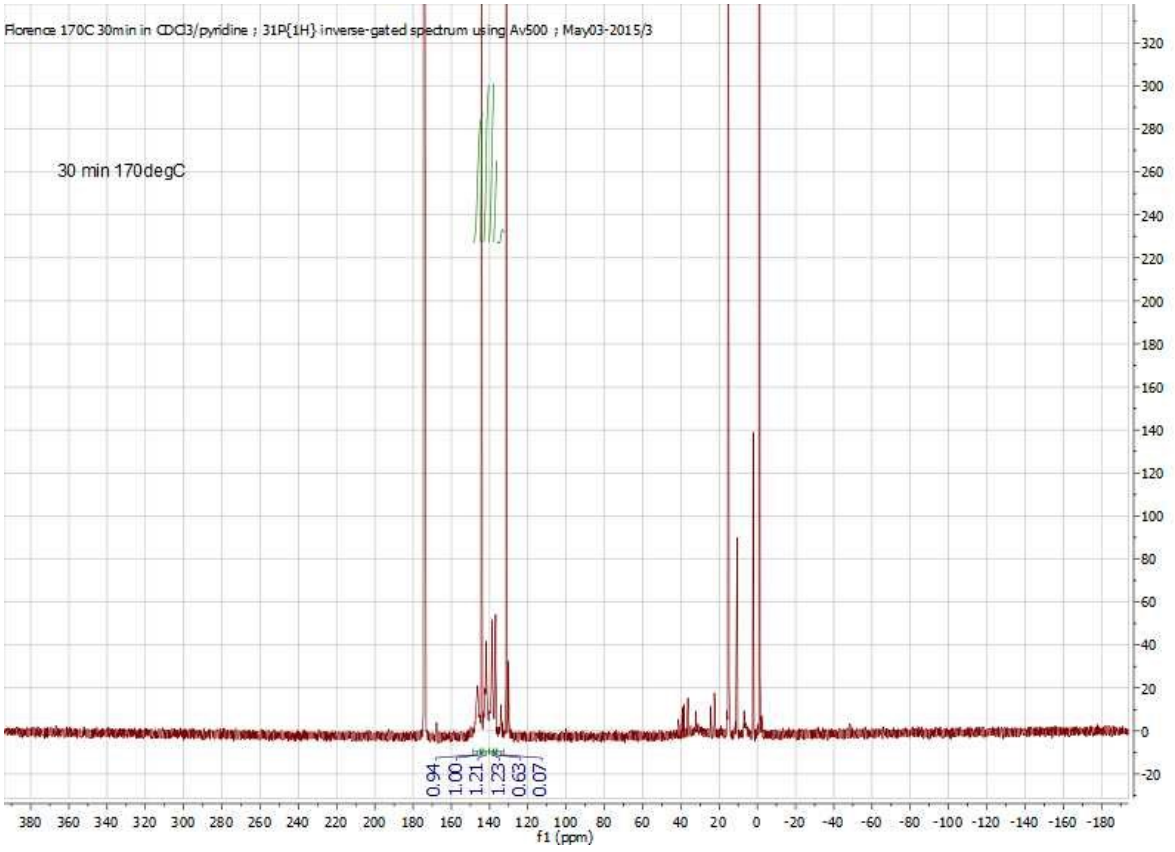
Florence 170C 30min in CDCl3/pyridine ; 31P{1H} inverse-gated spectrum using Av500 ; May03-2015/3
30 min 170degC
0.94
1.00
1.21
1.23
0.63
0.07
f1 (ppm)

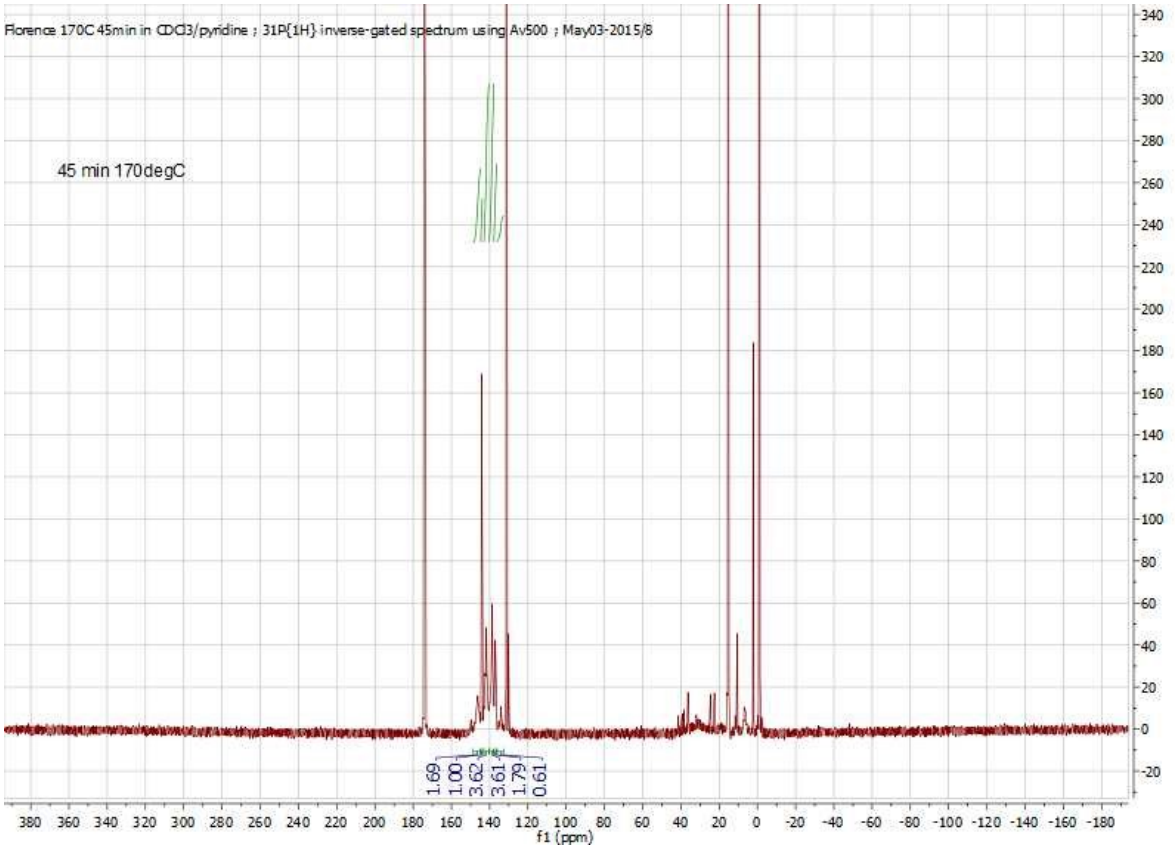
Florence 170C 45min in CDCl3/pyridine ; 31P{1H} inverse-gated spectrum using Av500 ; May03-2015/8
45 min 170degC
1.69
1.00
3.62
3.61
1.79
0.61
f1 (ppm)

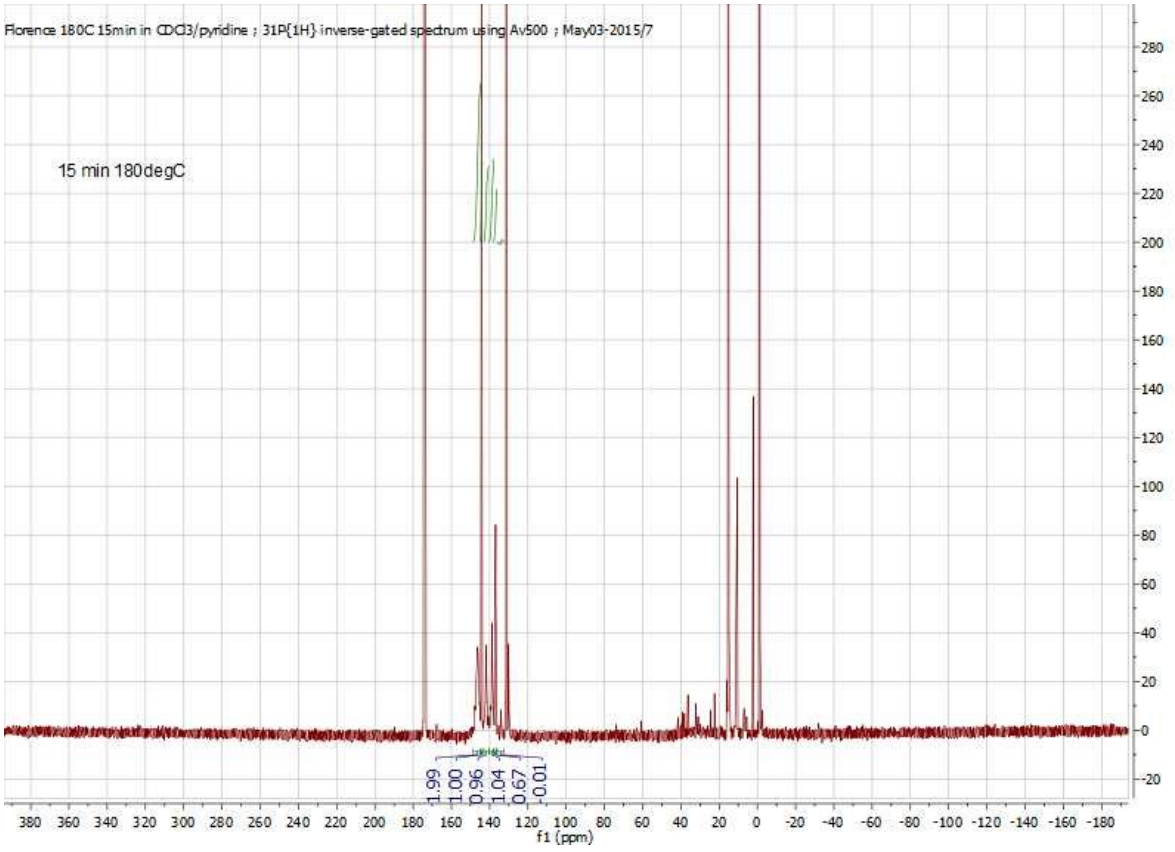
Florence 180C 15min in CDCl3/pyridine ; 31P{1H} inverse-gated spectrum using Av500 ; May03-2015/7
15 min 180degC
1.99
1.00
0.96
1.04
0.67
0.01
f1 (ppm)

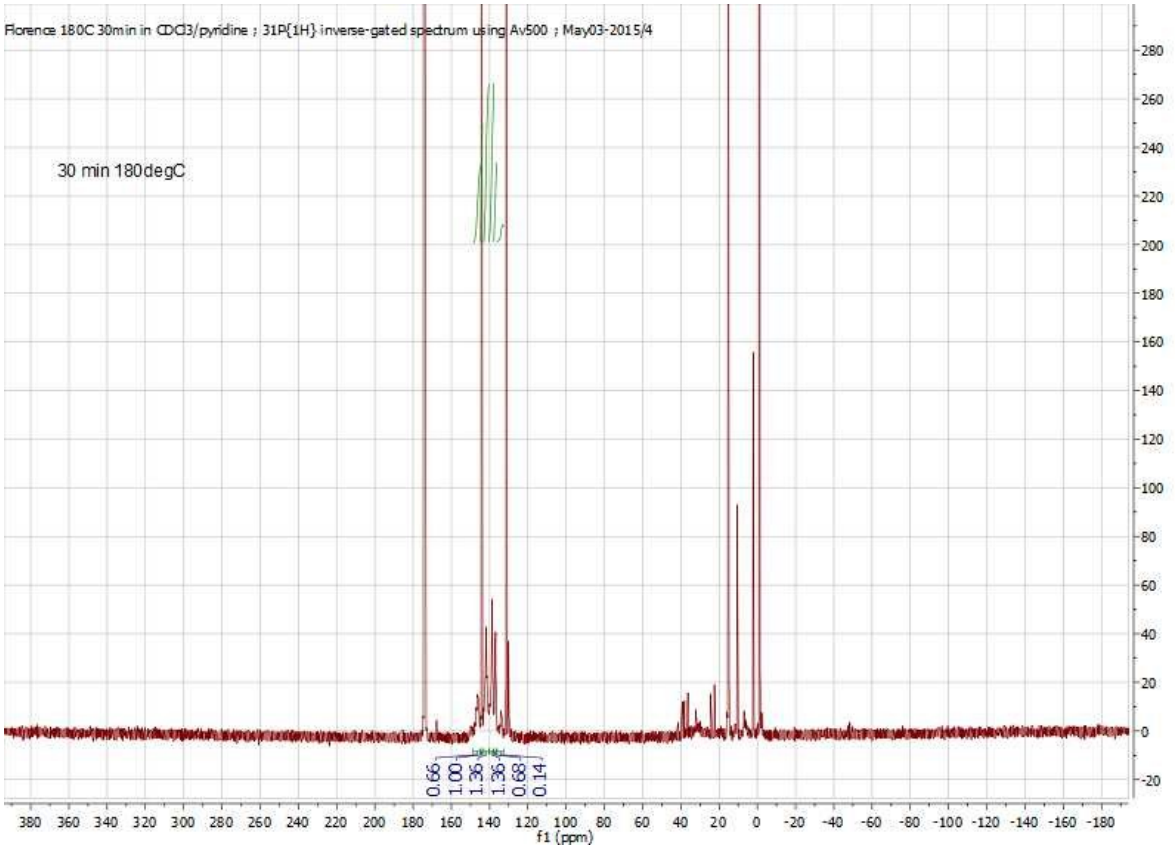
Florence 180C 30min in CDCl3/pyridine ; 31P{1H} inverse-gated spectrum using Av500 ; May03-2015/4
30 min 180degC
0.66
1.00
1.36
1.36
0.68
0.14
f1 (ppm)

Representative chromatograms

Saccharification

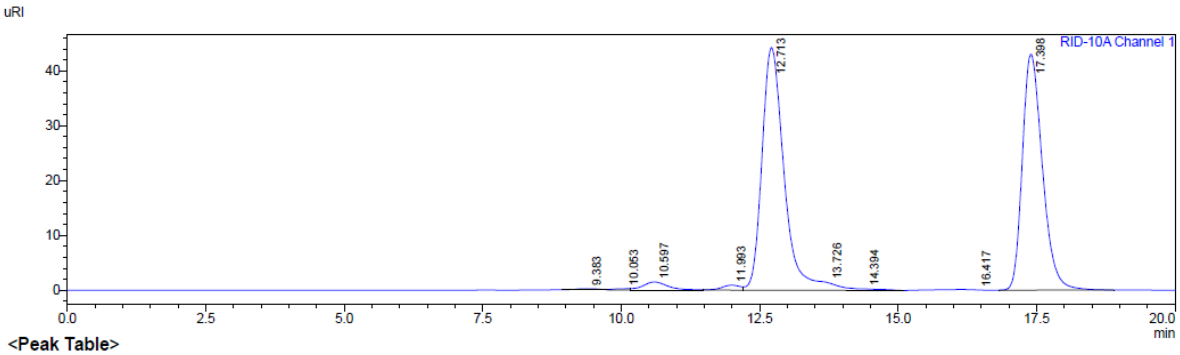

<Peak Table>

RID-10A Channel 1

Peak#	Name	Ret. Time	Area	Height	Conc.	Unit
1		9.383	5959	207	0.000	
2		10.053	4697	227	0.000	
3		10.597	45606	1461	0.000	
4		11.993	21173	907	0.000	
5	Glucose	12.713	1250067	44233	61.526	mg/mL
6	Xylose	13.726	0	0	0.000	mg/mL
7	Galactose	14.394	0	0	0.000	mg/mL
8	Arabinose	16.417	0	0	0.000	mg/mL
9	Mannose	17.398	1083383	43027	5.031	mg/mL
Total			2410884	90063		

ıbSolutions\Data\People's data\FG_7d_DM2_06092016_1125_004.lcd

Compositional Analysis

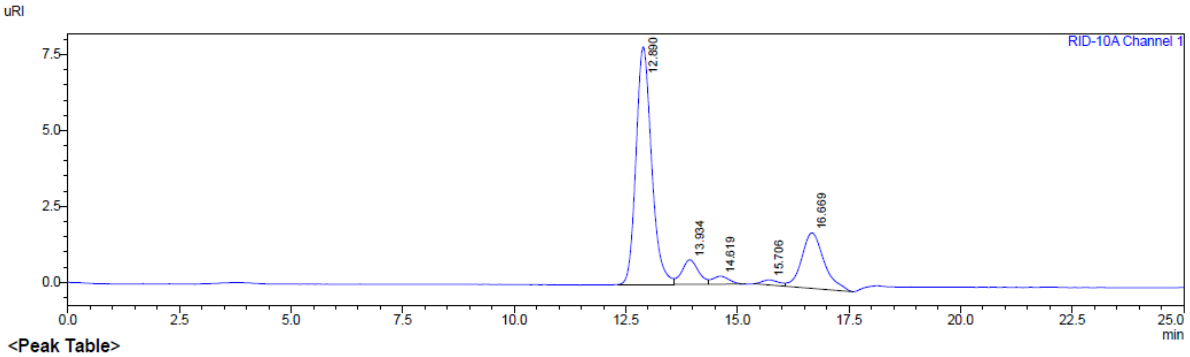

<Peak Table>

RID-10A Channel 1

Peak#	Name	Ret. Time	Area	Height	Conc.	Unit
1	Glucose	12.890	189701	7812	1.471	mg/mL
2	Xylose	13.934	20945	806	0.155	mg/mL
3	Galactose	14.619	6764	262	0.115	mg/mL
4	Arabinose	15.706	4391	164	0.020	mg/mL
5	Mannose	16.669	63697	1825	0.476	mg/mL
Total			285497	10868		

PDA Ch1 254nm

Peak#	Name	Ret. Time	Area	Height	Conc.	Unit
Total						

Solutions\Data\People's data\Flo TT01 rerun_16062014_1422_014.lcd

Liquor Analysis

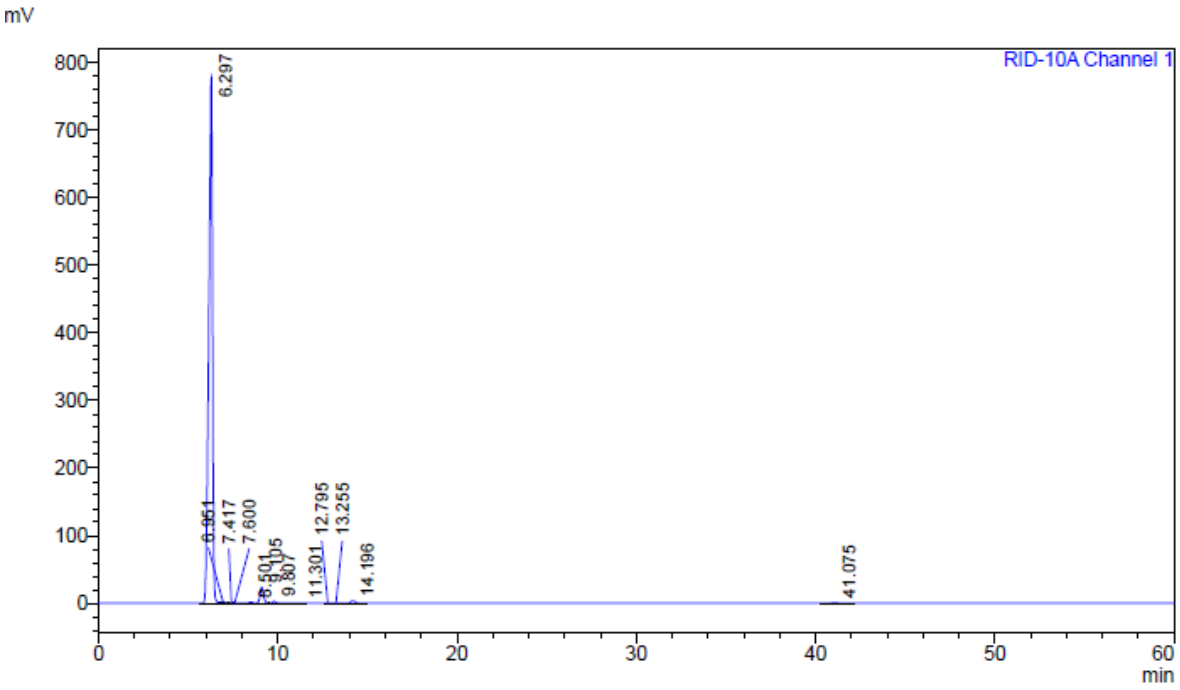

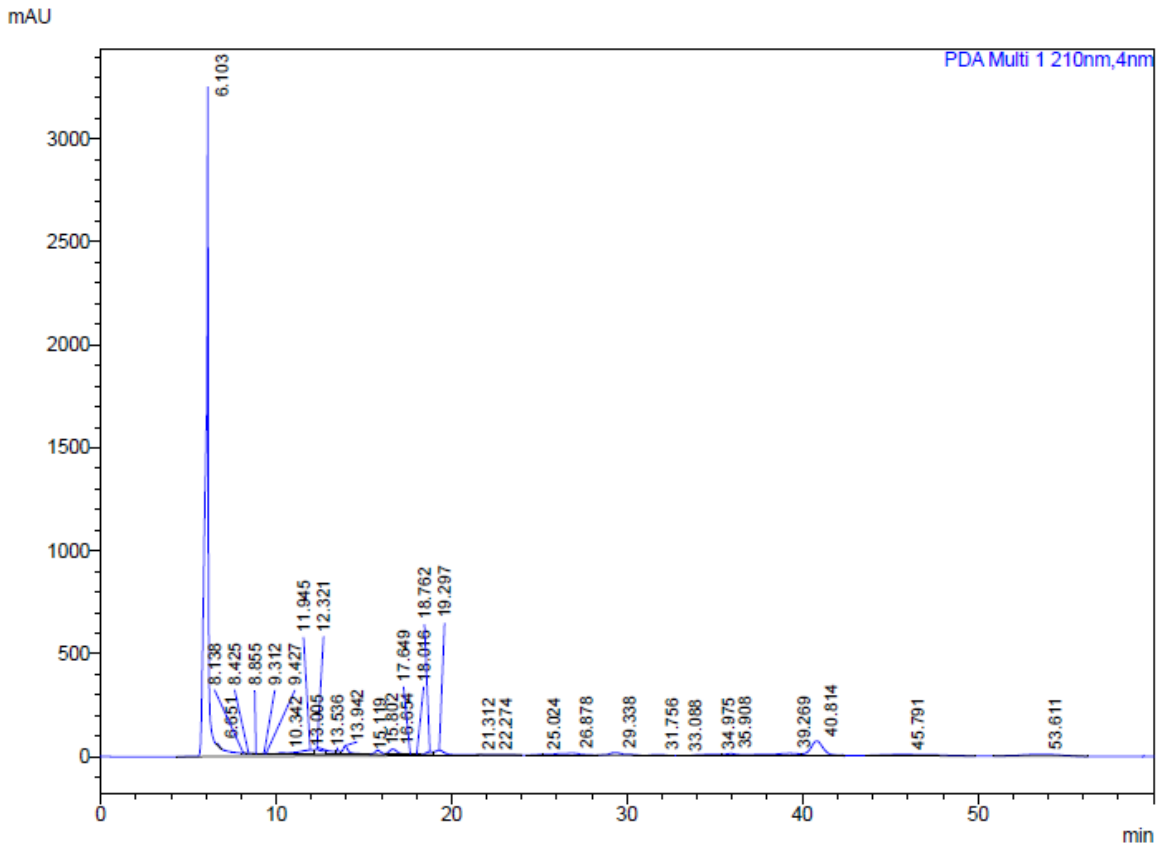

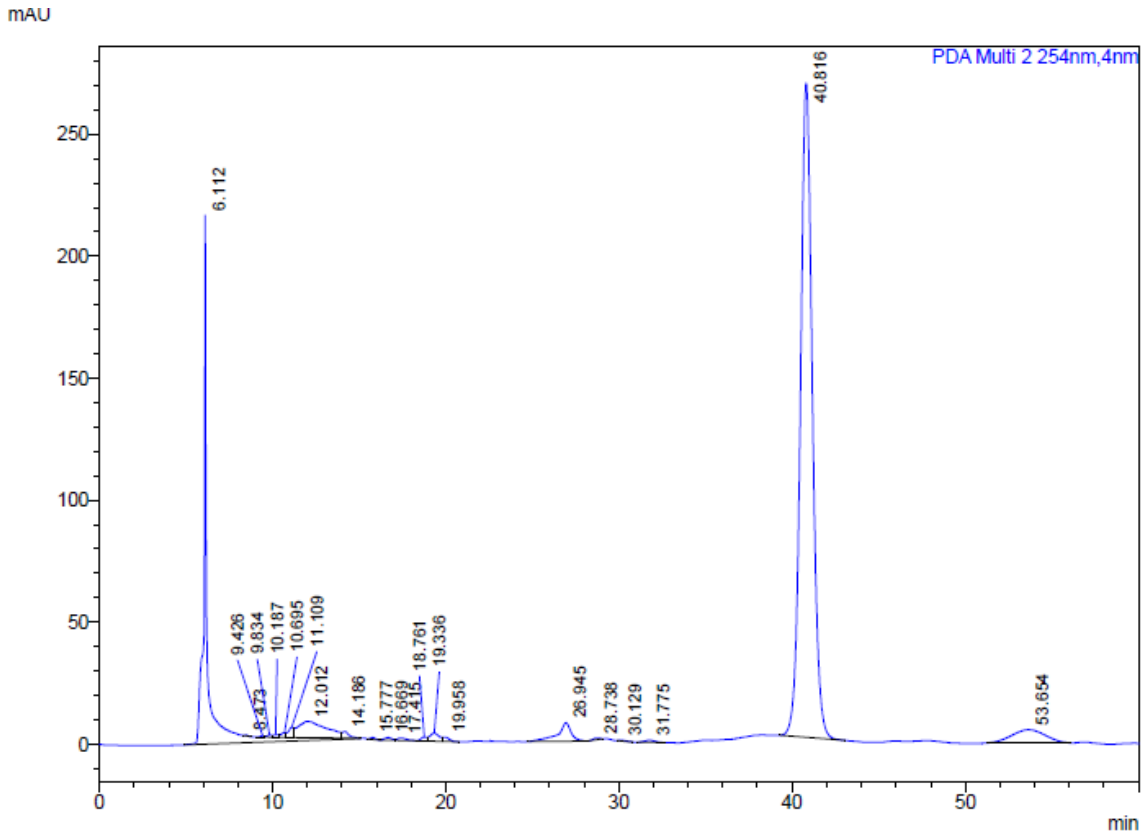

Fermentation

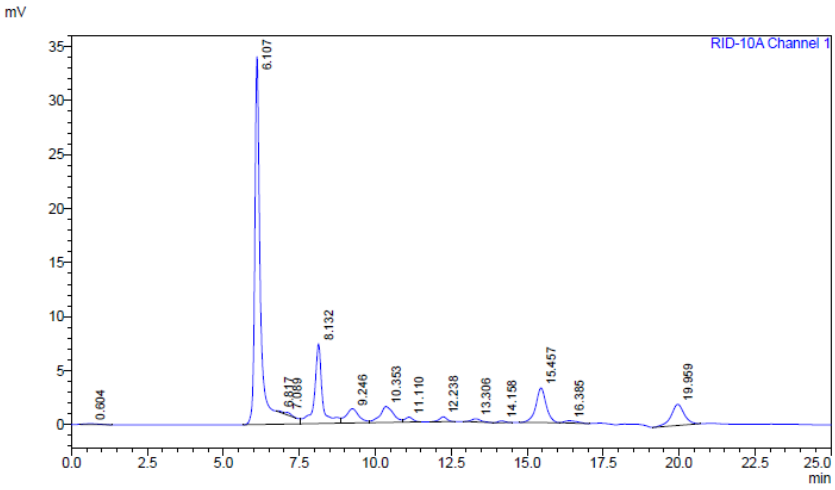

<Peak Table>

RID-10A Channel 1

Peak#	Ret. Time	Area	Height
1	0.604	2240	76
2	6.107	457467	34086
3	6.817	1206	87
4	7.089	3115	213
5	8.132	130399	7352
6	9.246	38165	1312
7	10.353	44582	1471
8	11.110	8093	448
9	12.238	8187	456
10	13.306	6628	299
11	14.158	2582	168
12	15.457	75467	3198
13	16.385	5910	211
14	19.959	59367	1960
Total		843409	51337